

Berichte

zur Polar-
und Meeresforschung

649
2012

Reports
on Polar and Marine Research



The Expedition of the Research Vessel "Polarstern"
to the Arctic in 2011 (ARK-XXVI/3 - TransArc)

Edited by
Ursula Schauer
with contributions of the participants



ALFRED-WEGENER-INSTITUT FÜR
POLAR- UND MEERESFORSCHUNG
in der Helmholtz-Gemeinschaft
D-27570 BREMERHAVEN
Bundesrepublik Deutschland

ISSN 1866-3192

Hinweis

Die Berichte zur Polar- und Meeresforschung werden vom Alfred-Wegener-Institut für Polar- und Meeresforschung in Bremerhaven* in unregelmäßiger Abfolge herausgegeben.

Sie enthalten Beschreibungen und Ergebnisse der vom Institut (AWI) oder mit seiner Unterstützung durchgeführten Forschungsarbeiten in den Polargebieten und in den Meeren.

Es werden veröffentlicht:

- Expeditionsberichte
(inkl. Stationslisten und Routenkarten)
- Expeditions- und Forschungsergebnisse
(inkl. Dissertationen)
- wissenschaftliche Berichte der
Forschungsstationen des AWI
- Berichte wissenschaftlicher Tagungen

Die Beiträge geben nicht notwendigerweise die Auffassung des Instituts wieder.

Notice

The Reports on Polar and Marine Research are issued by the Alfred Wegener Institute for Polar and Marine Research in Bremerhaven*, Federal Republic of Germany. They are published in irregular intervals.

They contain descriptions and results of investigations in polar regions and in the seas either conducted by the Institute (AWI) or with its support.

The following items are published:

- expedition reports
(incl. station lists and route maps)
- expedition and research results
(incl. Ph.D. theses)
- scientific reports of research stations
operated by the AWI
- reports on scientific meetings

The papers contained in the Reports do not necessarily reflect the opinion of the Institute.

The „Berichte zur Polar- und Meeresforschung“
continue the former „Berichte zur Polarforschung“

* Anschrift / Address

Alfred-Wegener-Institut
für Polar- und Meeresforschung
D-27570 Bremerhaven
Germany
www.awi.de

Editor:
Dr. Horst Bornemann

Assistant editor:
Birgit Chiaventone

Die "Berichte zur Polar- und Meeresforschung" (ISSN 1866-3192) werden ab 2008 als Open-Access-Publikation herausgegeben (URL: <http://epic.awi.de>).

Since 2008 the "Reports on Polar and Marine Research" (ISSN 1866-3192) are available as open-access publications (URL: <http://epic.awi.de>)

The Expedition of the Research Vessel "Polarstern" to the Arctic in 2011 (ARK-XXVI/3 - TransArc)

**Edited by
Ursula Schauer
with contributions of the participants**

**Please cite or link this publication using the identifier
hdl: 10013/epic.39934 or <http://hdl.handle.net/10013/epic.39934>**

ISSN 1866-3192

ARK-XXVI/3 - TransArc
5 August - 6 October 2011
Tromsø - Bremerhaven

Fahrtleiter / Chief Scientist
Ursula Schauer

Koordinator / Coordinator
Eberhard Fahrbach

Contents

1.	Zusammenfassung und Fahrtverlauf Summary and Itinerary	3 8
2.	Weather Conditions	11
3.	Sea Ice Physics	17
3.1	Airborne sea ice thickness surveys	18
3.2	Optical measurements	24
3.3	Ice station work and ice cores	36
3.4	Deployment of drifting buoys	48
3.5	Routine sea ice observations	50
3.6	References	56
4.	Physical Oceanography	57
5.	Geochemistry	85
5.1	The carbonate system	85
5.2	Radium and Thorium isotopes	87
5.3	Tracing terrestrial carbon across the Arctic shelf and slope	90
5.4	^7Be as tracer for determining atmospheric deposition of trace elements	91
5.5	Net community productivity using dissolved $\text{O}_2/\text{Ar}/^{222}\text{Rn}$	92
5.6	Mercury cycling in the Arctic	96
5.7	Distribution of ^{236}U and of Cs isotopes	97
6.	Biogeochemistry	98
7.	Marine Biology	101
7.1	Biology of sea-ice and related ecosystems	101
7.2	Plankton Ecology and Biogeochemistry in a Changing Arctic Ocean (PEBCAO)	109
7.3	Zooplankton investigations	113

8.	Marine Geology	119
8.1	Multi-beam bathymetry	120
8.2	Marine sediment echosounding using Parasound	124
8.3	Sediment cores	130
 Appendix		143
A.1	Beteiligte Institute / participating institutes	144
A.2	Fahrtteilnehmer / participants	146
A.3	Ship's crew	148
A.4	Stationsliste /station list PS78	150

1. ZUSAMMENFASSUNG UND FAHRTVERLAUF

Ursula Schauer
Alfred-Wegener-Institut

Die *Polarstern*-Expedition ARK-XXVI/3 „TransArc“ (Trans-Arctic survey of the Arctic Ocean in transition) diente dem übergeordneten Ziel, den physikalischen, biologischen und chemischen Zustand des Arktischen Ozeans im Klimawandel zu erfassen. Während der Rückgang der Meereisausdehnung kontinuierlich durch Satellitenfernerkundung überwacht werden kann, müssen Veränderungen aller anderen Parameter wie der Dicke und weiterer Charakteristiken des Meereises, der Eigenschaften und der Zirkulation von Wassermassen sowie der chemischen Substanzen und der Ökosysteme durch wiederholte Expeditionen mit dem Schiff oder durch autonome Plattformen erfasst werden. Vor diesem Hintergrund fand mit „TransArc“ vier Jahre nach dem Internationalen Polarjahr (IPY 2007/2008) die erste umfassende Aufnahme der Bedingungen im zentralen Arktischen Ozean statt.

Die Abnahme des mehrjährigen Eises hat Auswirkungen auf die Ozeanzirkulation und damit auf die Eigenschaften der Wassermassen und die Stabilität des Arktischen Ozeans. Diese werden durch den Einstrom aus dem Atlantik und dem Pazifik, sowie durch die immensen Festlandsabflüsse bestimmt. Die Variabilität dieser Komponenten, wie etwa die Erwärmung des Einstroms aus dem Atlantik und dem Pazifik und die starke Akkumulation von Süßwasser in den letzten beiden Dekaden beeinflussen zusammen mit der Eisabnahme den Gasaustausch mit der Atmosphäre, chemische Flüsse sowie Ökosysteme und die mit ihnen verknüpften biogeochemischen Kreisläufe im Eis und in der gesamten Wassersäule. Die Zirkulationsänderungen wirken sich auch auf den Nordatlantik aus.

Die Wirkung der Advektion und die Eisbedingungen bedingen große räumliche Kontraste. Um mehrjährige oder dekadische Veränderungen zu erkennen, müssen räumliche und zeitliche Signale klar voneinander getrennt werden, was im schwer zugänglichen Arktischen Ozean eine größere Herausforderung ist als in eisfreien Meeren.

Während TransArc beprobten wir auf multidisziplinären Stationen Eis- und Ozeaneigenschaften und die entsprechenden Ökosysteme entlang von Gradienten von den Eurasischen Schelfmeeren bis ins Kanadische Becken. Dabei wurden die Atlantischen Einstromzweige durch die Framstraße und die Barentssee ebenso abgedeckt wie die Ausbreitung des Süßwassers aus sibirischen Flüssen und die Verteilung des einströmenden Pazifikwassers. Gleichzeitig erstreckten sich die Schnitte vom offenen Wasser über einjähriges bis ins dichte mehrjährige Eis. Während der 1990er und der 2000er Jahre wurden Vorläufer dieser Schnitte auf Expeditionen mit der *Oden* und der *Polarstern* schon einmal beprobt. Um den Beobachtungsradius räumlich und zeitlich zu erweitern, wurden physikalische und biologische Messungen durch eine Reihe von eisgetragenen Bojen und

Bodenverankerungen ergänzt. Bei vielen Arbeiten wurden Hubschrauber eingesetzt: für Messflüge mit der Eisdickensonde, zum Personentransport zur Beprobung von entfernteren Eisschollen und zur Eiserkundung für nautische Zwecke.

Zwei Ereignisse verliehen dieser Expedition eine besondere Note: Das Erreichen des Nordpols am 22. August und der Besuch der russischen Driftstation NP-38. Beide Ereignisse wurden durch die günstigen Eisbedingungen sehr erleichtert. *Polarstern* erreichte auf dieser Reise den Nordpol zum dritten Mal, nachdem dies bereits 1991 während ARK-VII/3 und 2001 während ARK-XVII/2 erfolgt war. Im Gegensatz zu den ersten beiden Malen fuhren wir nun ohne Begleitung durch ein anderes Schiff zum Nordpol, ein deutlicher Hinweis auf die schon jetzt erheblich erleichterte Schiffbarkeit der Arktis.

Bedauerlich war, dass wir innerhalb der russischen ausschließlichen Wirtschaftszone (EEZ), und damit am Kontinentalhang und in den Schelfmeeren nur sehr eingeschränkt arbeiten durften. Lediglich die Messung physikalischer Parameter und der Konzentration einiger gelöster Gase sowie die Beprobung von Plankton und Aerosolen war zugelassen worden.

Polarstern lief pünktlich am 5. August 2011 aus Tromsø aus. Es waren 54 Wissenschaftler aus zehn Instituten aus sieben Ländern und 43 Besatzungsmitgliedern an Bord. Nach dem Passieren der Barentssee erreichten wir am 9. August nördlich von Franz-Josef-Land den Eisrand und begannen unsere Arbeit mit CTD- und Netzstationen auf einem Schnitt nach Norden entlang von 60° E. Am Kontinentalabhang bargen wir eine Verankerung des russisch-amerikanischen Programms NABOS (Nansen and Amundsen Basins Observational System). Keiner der beiden akustischen Auslöser funktionierte, aber mit einem ausgeklügelten Dredgeverfahren konnten wir im lockeren Eis Verankerungsmaterial und zwei Jahre wertvoller Daten bergen. Am 11. August gab es die erste Eisstation für Eisdicken- und optische Messungen, gefolgt vom ersten Einsatz eines Untereis-ROVs (Remotely Operated Vehicle) am 17. August. Den Gakkelrücken überquerten wir in einem Gebiet, wo vor 20 Jahren schon einmal Sedimentproben genommen worden waren; an diesen Lokationen nahmen wir wieder Sedimentproben, um eventuelle Veränderungen im Benthos zu erfassen.

Das mürbe Eis machte es schwer, geeignete Schollen für die Eisarbeit zu finden. Aber es ermöglichte uns, unseren Kurs nach Norden fast ungehindert fortzusetzen. So erreichten wir am 22. August den Nordpol und feierten dieses Ereignis. Ermutigt durch das gute Fortkommen setzten wir unseren Kurs fort und überquerten den Lomonossowrücken. Wir wagten uns sogar noch weiter nach Osten, um auf dem wenig erkundeten Alpharücken bathymetrische Aufnahmen durchzuführen und Sedimentkerne zu ziehen. Allerdings kamen wir hier im dicken Packeis nördlich von Ellesmere Island bald nicht mehr weiter und bei 88° 55' N, 115° W beschlossen wir am 25. August unseren Kurs nach Westen ins Makarowbecken zu nehmen. Schnell besserten sich die Eisbedingungen und so bogen wir ein weiteres Mal nach Süden ab, um weit ins Kanadische Becken vorzudringen. Nach dem Passieren des magnetischen Pols am 31. August nahe 85°04' N, 137° 14' W überquerten wir den Mendelejewrücken und erreichten das Kanadische Becken. Dort beprobten wir auf etlichen Eis- und Wasserstationen den pazifisch beeinflussten Teil des Arktischen Ozeans. Unsere südlichste Station in diesem Gebiet erreichten wir am 3. September. In lockerem Eis dampften wir anschließend nordwestwärts, um am 6. September die russische Eisstation NP-38 zu treffen. Dort übernahmen wir Ausrüstungsmaterial einer früheren deutschen Beteiligung und nutzten das

Treffen zu gegenseitigen Besuchen. Wir waren sehr beeindruckt von dem guten Mut und der herzlichen Gastfreundschaft unserer russischen Kollegen, die das Beobachtungsprogramm von ihrem kleinen Camp aus immerhin bereits seit einem Jahr ununterbrochen durchführten.

Von NP-38 aus ging es weiter nach Westen für einen zweiten langen Schnitt zum sibirischen Schelf. Dieser Schnitt bot uns eine letzte Chance, Eisbojen auszubringen. Aber die Suche nach geeigneten stabilen, d.h. hinreichend dicken und großen Schollen gestaltete sich zunehmend schwierig, da es kaum noch mehrjähriges Eis im östlichen Sektor der eurasischen Arktis gab. Am 8. September fanden wir eine passende Scholle für das, was wir die „Super Buoy Station“ nannten. Hier installierten wir eine Kombination verschiedener Bojen, die unterschiedlichste Sensoren trugen, um eine möglichst multidisziplinäre Aufnahme im Eis und im Ozean am gleichen Ort zu ermöglichen. Nebenbei wurde natürlich auch das übliche umfangreiche Eisstationsprogramm durchgeführt, aber das mürbe Eis, schneebedeckte Schmelztümpel und ein starker Schneesturm wiesen uns die Grenzen für Arbeiten in der Arktis auf, die selbst im Sommer bestehen.

Zurück im Eurasischen Becken verankerten wir zwei Gruppen von Bodenverankerungen für Aufnahmen ozeanographischer und biologischer Parameter. Die Verankerungen sollen 2012 während der Polarsternexpedition „IceArc“ wieder aufgenommen werden. Obwohl wir auf unserem Weg in Richtung Severnaja Zemlja schon nahe des Eisrands entlangfuhren, ließen uns Informationen über die Eisbedeckung, die wir täglich aus Bremen erhielten, noch einmal auf ein Gebiet mit konsolidiertem Eis hoffen. In der Tat konnten wir am 16. September unsere letzte Eisstation durchführen.

Der lange Schnitt endete an der Schelfkante. Er wurde noch durch drei weitere kurze Schnitte über den Kontinentalabhang mit Hydrographie und Netzfängen – und außerhalb der russischen EEZ auch mit Sedimentproben – ergänzt, so dass wir insgesamt den Randstrom vom Zusammenfluss des atlantischen Wassers aus der Framstraße mit dem aus der Barentssee bis zur abermaligen Verzweigung des Randstroms nördlich der Laptewsee aufgenommen haben. Am 21. September wurden zwei weitere Verankerungen des NABOS-Programms aufgenommen; eine davon enthielt Daten über vier Jahre. Bei beiden versagte wieder die Auslösertechnik und wieder machten nur höchstes nautisches und mannschaftliches Geschick die Bergung möglich.

Den Abschluss des Forschungsprogramms bildeten Schnitte in der flachen Laptewsee, die vorangegangene Arbeiten eines deutsch-russischen Programms ergänzten. Die letzte Station erfolgte am 26. September bei 77° 12' N, 112° 51' E. Nach der Rückfahrt durch die eisfreie Nordostpassage und die stürmische Norwegische See und die Nordsee lief *Polarstern* am 6. Oktober 2011 in Bremerhaven ein.

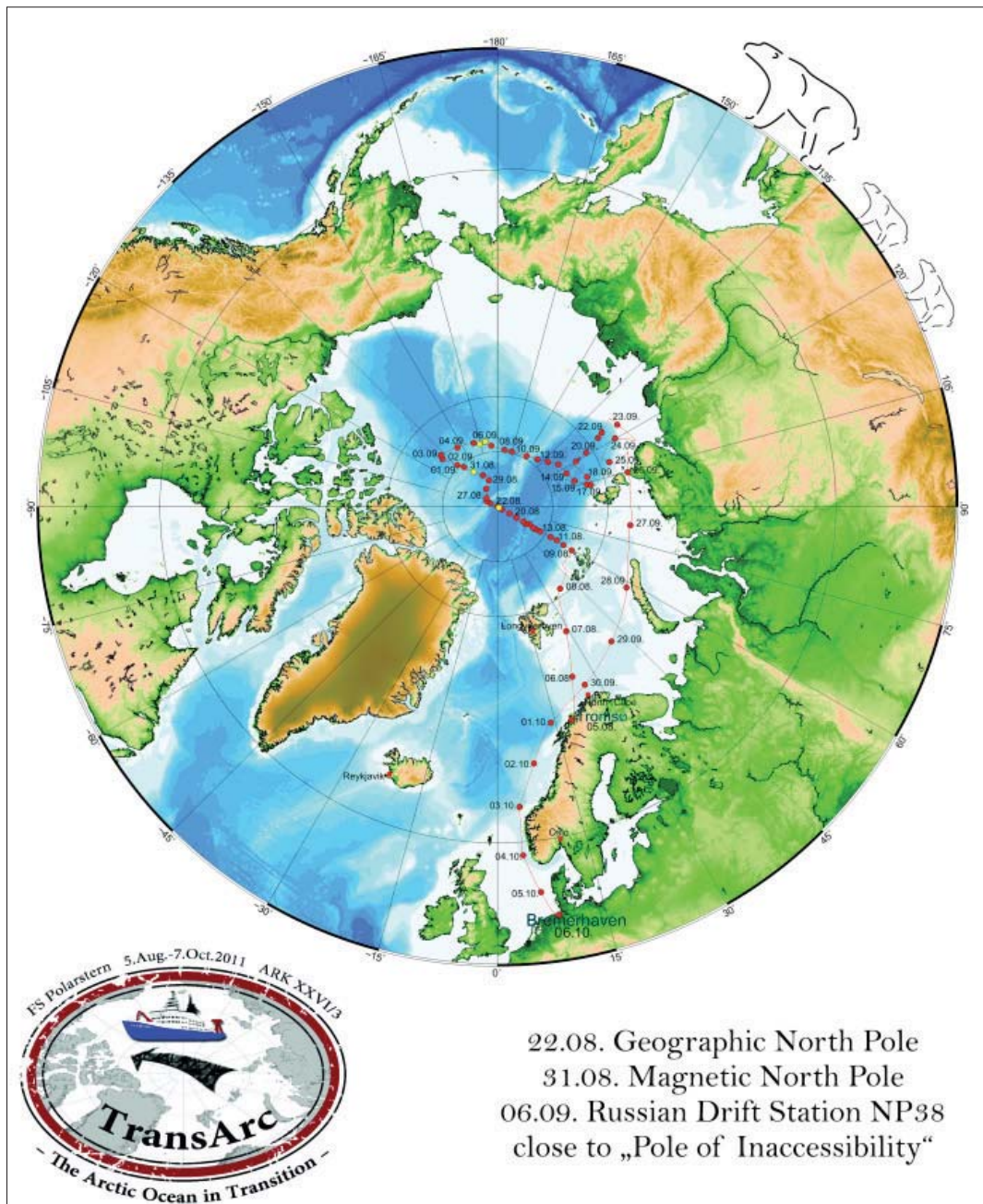


Fig. 1.1: Cruise track during "TransArc"

Abb. 1.1: Fahrtroute von „TransArc“

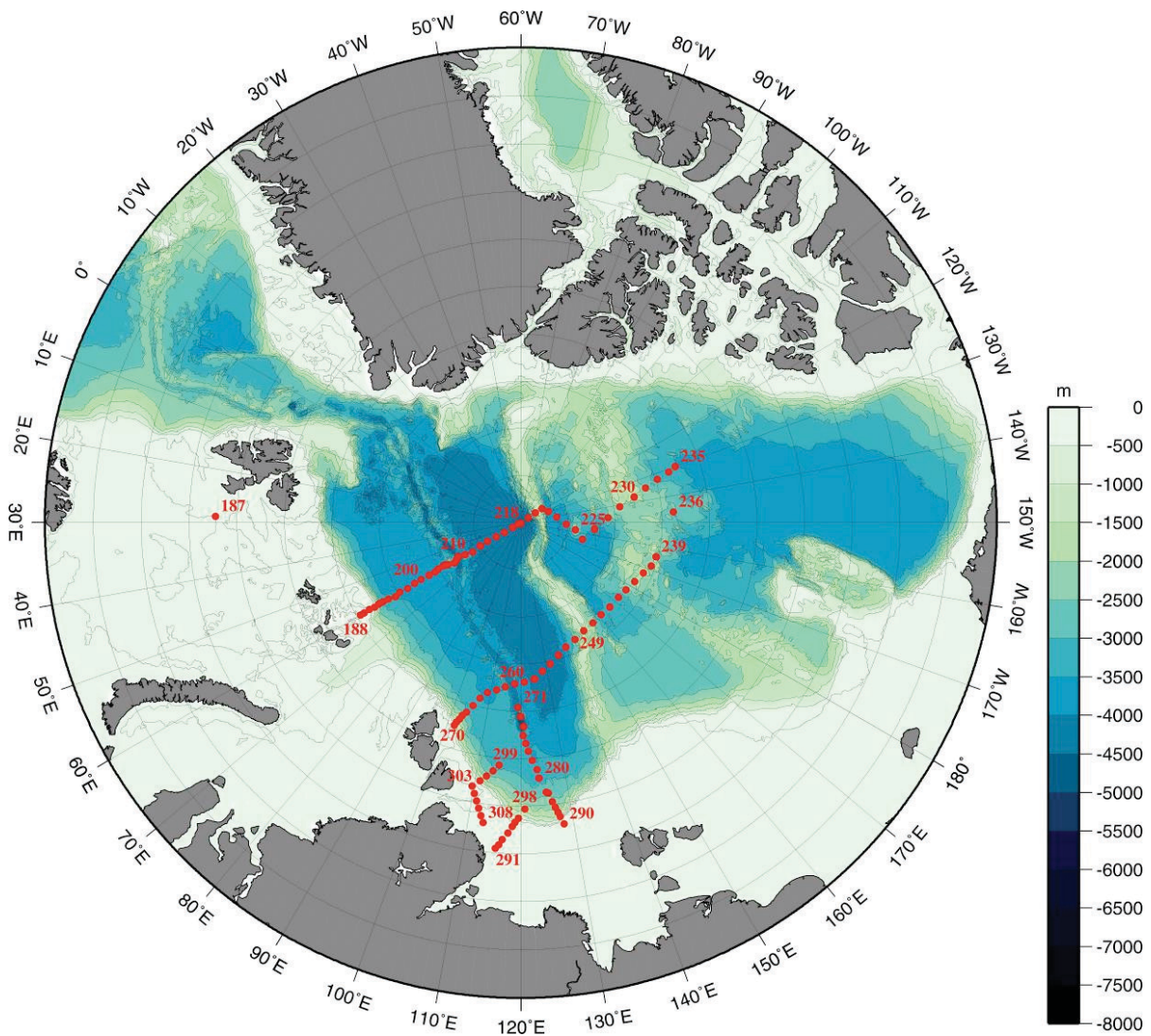


Fig. 1.2: Map of stations taken during "TransArc". Bottom topography from U.S. Department of Commerce, National Oceanic and Atmospheric Administration, National Geophysical Data Center, 2006. 2-minute Gridded Global Relief Data (ETOPO2v2.)

Abb. 1.2: Karte der Stationspositionen von „TransArc“. Bodentopographie von U.S. Department of Commerce, National Oceanic and Atmospheric Administration, National Geophysical Data Center, 2006. 2-minute Gridded Global Relief Data (ETOPO2v2.)

SUMMARY AND ITINERARY

The *Polarstern* expedition ARK-XXVI/3 "TransArc" (Trans-Arctic survey of the Arctic Ocean in transition) served the overarching goal to capture the physical, biological and chemical state of the Arctic Ocean in a changing climate. While the decrease of the sea ice extent can be monitored by satellite remote sensing, changes of all other oceanic parameters in the Arctic, such as thickness and other characteristics of sea ice, water mass properties and circulation as well as chemical constituents and biota need to be measured during repeated ice breaker cruises or from autonomous platforms. Hence, four years after the International Polar Year (IPY 2007/2008), "TransArc" constituted the first repeat survey of the central Arctic Ocean.

The water masses and the stability of the Arctic Ocean are largely conditioned by the inflow of waters from the Atlantic and Pacific Oceans and of huge amounts of fresh water from land. The ocean circulation and the shrinking of the multiyear ice are closely linked. Variations of these components, such as the accumulation of fresh water in the central Arctic and the warming of the Atlantic and Pacific inflows in the last decade, will affect also substance distribution and ecosystems. Together with the ice retreat they affect the gas exchange with the atmosphere, chemical fluxes as well as the ecosystems and the related biogeochemical cycling in the sea ice and in the entire water column. The Arctic circulation changes have also impact on the North Atlantic.

Due to advection and the ice cover significant spatial gradients are present in the Arctic Ocean. To distinguish between decadal or shorter term variability and long-term change one has to ensure a separation between spatial and temporal variations which is more difficult in the sparsely observed Arctic than in open oceans.

During TransArc we sampled the ocean and ice properties and their ecosystems along gradients from the Eurasian shelf edge to the Canadian Basin. This multidisciplinary effort captured the Atlantic water inflows through both Fram Strait and Barents Sea, as well as the spreading of Siberian river-runoff and of Pacific Water. At the same time the sections occupied the transition from the ice-free ocean through first-year ice to the multi-year pack ice and back again. The expedition repeated large-scale sections that were captured in the 1990s and early this century by e.g. *Oden* and *Polarstern*, thus permitting comparability. To extend the observation range and to obtain year-round observations of physical and biological parameters of ice and ocean a number of ice-tethered buoys and bottom-mounted moorings were deployed and recovered respectively. Many tasks were carried out or supported by helicopter flights, like missions with the ice thickness sensor, transfer of researchers for sampling at remote ice floes and ice reconnaissance flights for nautical purposes.

Two events made this cruise a special one: One was the visit of the North Pole on 22 August, the other was the visit of the Russian drifting station NP38. Both events were facilitated by the very favorable ice conditions. The visit of the North Pole was the third time for *Polarstern* after her first visit in 1991 (ARK-VIII/3) and a second visit in 2001 (ARK- XVII/2). It was however the first North Pole visit without any accompanying vessel, accentuating the transition towards easier shipping conditions in the Arctic Ocean.

Unfortunately, within the Russian Exclusive Economic Zone (EEZ), i.e. at the continental slope and in the shelf seas, the investigations were considerably restricted and sampling was only possible for physical parameters, some dissolved gas compounds, phyto- and zooplankton content of the water column and of the sea ice, and the aerosol content of the near-surface atmosphere.

Polarstern left Tromsø on August 5, 2011, with 54 scientists from 10 institutes of 7 countries and 43 crew members on board. After passing the Barents Sea, we reached the ice edge north of Franz Josef Land on August 9 and started our work with a northward transect along 60°E taking water property and plankton net casts. At the continental slope of the Nansen Basin we recovered a mooring belonging to the Russian-American program NABOS (Nansen and Amundsen Basins Observational System). Both acoustic releasers of the mooring failed, but, fortunately, the ice conditions were moderate so that the mooring could be recovered with a sophisticated dredging maneuver. On August 11 the first ice station was carried out for thickness and optical measurements which was followed on August 17 by the first deployment of a ROV for under ice observations. At the Gakkel Ridge, a couple of sites were revisited where surface sediment has been sampled 20 years ago during *Polarstern* cruise ARK-VIII/3, and now replicate cores were taken to study benthos variability.

The crumbled state of the ice, making it, on one hand, difficult to find suitable floes for ice stations, enabled us on the other hand to continue steaming and working along 60°E up to the North Pole, which was reached on August 22 and prompted a celebration. Encouraged by the good progress we continued the transect across the Lomonosov Ridge and even turned east to survey and take sediment cores in the poorly charted regions of the Alpha Ridge. However, we did not get very far before finally reaching heavy pack ice so that we decided on August 25 at 88°55'N, 115°W to turn westward into the Makarov Basin. Soon the ice became smoother and we turned once more south to get far into the Canadian Basin. Passing the Magnetic Pole on 31 August near 85° 4' N, 137° 14' W, we crossed the Mendelejev Ridge into the Canada Basin and, capturing several water and ice stations in the Pacific Water regime, reached our south-easternmost station on September 3. In moderate ice conditions we then sailed westward to meet the Russian drifting station NP-38 on September 6, where material from a former German participation was taken over. The day was used for visits in both directions and we were very much impressed by the good mood and the great hospitality of the Russian colleagues who have been carrying out observations in their little camp throughout a whole year.

From NP-38, located then at the Mendelejev Ridge, we headed westward to conduct a second long cross-basin section towards the Siberian shelf. This section brought us a last chance to deploy various ice buoys; yet, the search for appropriate, i.e. large and thick, ice floes became more and more difficult, because hardly any multiyear ice was left in eastern Eurasian Arctic. On September 8, we found a suitable floe for what we called our "Super buoy station" where we installed

a multitude of buoys carrying various sensors for sea ice, ocean and biooptical properties. There, of course, we also carried out extensive sea ice investigations. However, the mushy ice surface, snow-covered melt ponds and a heavy snow storm made this station a challenge for everybody working on the ice and on the bridge.

Back in the Eurasian Basin, two ensembles of moorings for year-round oceanographic and biologic recordings were deployed on either side of the Gakkel Ridge which will be recovered in 2012 with *Polarstern* during "IceArc". Although we had already passed the ice edge on our way towards Severnaya Zemlya, information of the sea ice concentration that we obtained daily from the University Bremen indicated a patch of consolidated multi-year sea ice ahead of us. This enabled us to plan and conduct the last ice station of the cruise on September 16.

The long section was conducted up the continental slope, and three additional short cross-slope sections with CTD stations, plankton net casts and, outside of the Russian EEZ, also sediments samples completed a series of transects, capturing the boundary current of Atlantic Water from the confluence of the Fram Strait and the Barents Sea branches up to the re-splitting of the boundary current off the Laptev Sea. In between, two more moorings of the NABOS program were recovered on September 21, both requiring once again highest dredging skills because of identical technical failure of the releasers. The last part of the working program augmented a hydrographic survey in the Laptev Sea of the German Russian program "Laptev Sea system".

The station work finished on September 26 at 77° 11.69' N, 112° 50.61' E. After passing the ice-free Northern Sea Route to the western Barents Sea and the stormy Norwegian and North Seas, *Polarstern* returned to Bremerhaven on 6 October 2011.

2. WEATHER CONDITIONS

Harald Rentsch, Hartmut Sonnabend Deutscher Wetterdienst

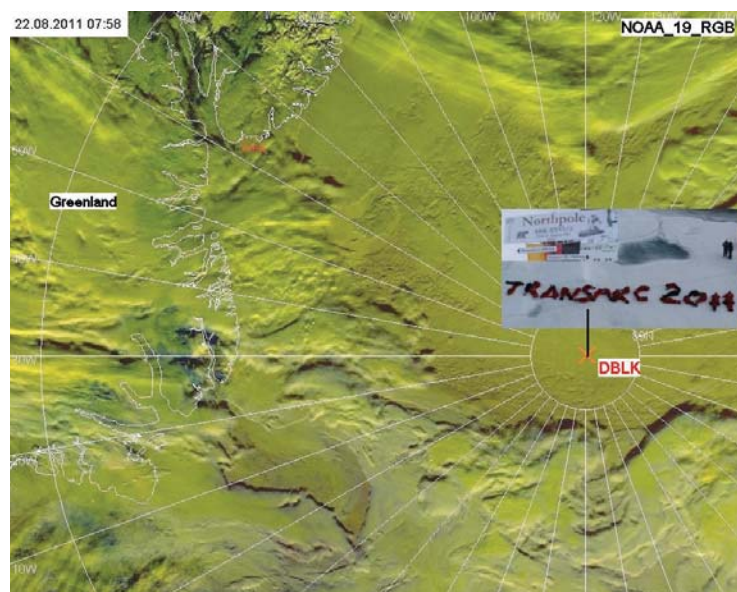
On August 5 (18:00 ship's time) RV *Polarstern* left the port of Tromsø at a nearly calm sea and broken skies. After leaving the fjords we got northerly winds of force 6 Beaufort (Bft) and a sea of 2 to 3 m. This was caused by the pressure field with an anticyclone over Greenland (maximum pressure around 1020 hPa) and a low east of Novaya Zemlya which moved westward. A covered sky and north-easterly winds of Bft 6-7 accompanied us up to the first working-station north of Franz Joseph Land where we also reached the ice edge on the fourth day of our journey.

During our transect along 60°E which we started on August 10, 2011, we passed a cyclone which moved from the Kara Sea towards Svalbard. Thereafter the wind reached 6-7 Bft. The associated rain, snow and fog did not affect the ship-based work but prevented helicopter flights for two days. Only on August 12 stronger winds coming from the lee side of Franz Joseph Land mountains provided us with good flight conditions.

Before the ship entered the region of the dynamical Arctic anticyclone near the North Pole, weak low pressure systems (polar lows) dominated with fog, precipitation (mostly rain) and low clouds and inhibited helicopter-flights with the EM-Bird. However, despite very low ceiling and visibility, flights for ice reconnaissance could be realized. Occasionally, on August 16, 17 and 18 we got sunny periods at the back side of fronts in connection with nearly 100% sea ice cover. These short time spans were used for flights with EM-Bird and X-CTD-launches. Before we reached the North Pole the flight conditions were usually bad (see Fig. 2.3 and 2.4).

Fig. 2.1: NOAA-19 satellite picture during crossing North Pole of Polarstern (ship's call sign DBLK), August 22, 2011, 7:58 utc.

When we reached the North Pole at August 22, 2011, 07:42 UTC (see Fig. 2.1), a high-pressure system over the Barents Sea brought moist, warm and stably layered air towards our cruise track. This caused fog and often very low



clouds with icing conditions preventing long-range helicopter flights. Only short (40 miles) flights for ice reconnaissance were possible.

A trough on the surface passing the North Pole on August 23, 2011 changed the general weather situation completely. Further on, north-easterly winds advecting moist, cold air from the Laptev Sea brought often snow showers. Helicopter flights for scientific purposes could be done.

During the next four days an anticyclone near the North Pole caused a stable stratification in the lower atmosphere. Supported was this state by a nearly closed sea-ice cover and dryer air flow from northeast of wind force 5 Bft.

The precipitation-free period ended on August 27 with the arrival of a polar low which brought light snowfall. During the following days low clouds, snow and fog patches reached us together with weak fronts that developed in the Laptev Sea and spread northward. At calm north winds and low clouds helicopter flights were restricted.

Between August 30 and September 1, we met the first complex low pressure system on this expedition (lowest pressure 1005 hPa) bringing snowfall and low-level clouds. The system moved from Chuckchi Sea towards Greenland passing our operation area. Icing in combination with rain and snow inhibited again helicopter flights. Changing wind directions near the centre of the low and bad visibility did not make it easier for navigation of the research vessel through compact multi-year ice.

On September 2 we reached the back side of the low and got westerly winds, low clouds and temperatures below 0 °C and most helicopter-based tasks could be carried out.

On September 6 when we met the Russian ice-drifting station NP38, a nearby front caused weak snowfall and easterly wind of force 4 Bft.

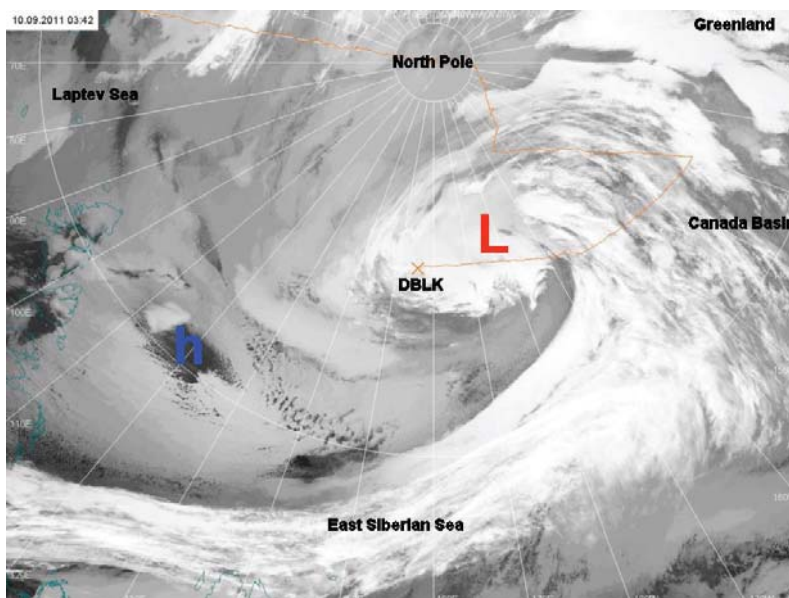


Fig. 2.2: NOAA-16 satellite picture, September 10, 2011, 03:42 utc; Extended gale force low (L) nearby Polarstern (DBLK), course Laptev Sea; maximum gusts 90° cross from stern port side: 47 Knots.

This weather enabled numerous shuttle flights per helicopter between the ship and "NP38". After a weak polar low had crossed our ship's track on September 7,

a well structured front of a low centred at 86°N 80°W brought us strong south-westerly winds of force 6 to 7 Bft and snowfall due to gliding of warmer over colder air masses, which prevented flights for that day.

From September 9 to 11 a low (lowest pressure 980 hPa, Fig. 2.2) situated over the Lomonosov Ridge and moving towards the Canada Basin caused continuous snowfall and brought us one of the rare occasions of high wind speed (force 8 to 9 Bft from stew port side) and with -10°C the lowest temperatures of our cruise (see the statistics in Fig. 2.5). The strong wind and the low temperatures caused a wind-chill temperature of -35°C . Due to the bad visibility without any contrast and horizon, called "white out", which is typical for overcast skies and snow-covered sea ice, all helicopter flights had to be cancelled. The northerly winds pushed the ice towards south, and the more open ice-cover enabled easier sailing for the ship.

At September 12, a ridge of high pressure with weak and dry wind spread into our working area and brought us very good flight conditions. This situation caused, at 14:51 ship's time, the greatest sunset of this cruise. However, on September 13 a new low and its snowfall moving from the New Siberian Islands towards southeast reached our ship's track.

From September 14 to 16 we passed the edge of a ridge of high pressure and had cold north-westerly, later north-easterly wind at force 5 Bft and large fields of low clouds but also some sunny spells, conditions which again restricted helicopter flights. Only in the night from September 16 to 17, at our the last sea-ice station, southerly winds caused by lee-effects from mountains of Severnaya Zemlya produced clear sky and enabled last flights with the EM-Bird.

After that, warm air with temperatures above 0°C arrived from Laptev Sea which caused fog when it met the ice. This situation prevented helicopter flights. Later a well structured cold front from the central Arctic brought cold air and light snow showers but also good visibility. Northerly wind on the eastern side of a strong high pressure system over Barents Sea led the temperatures drop to -5°C . Some upper troughs raised the wind velocity for short time so that a swell up to 2 m was observed at our passage of the Gakkel Ridge.

When we arrived in the open Laptev Sea, the sea-surface temperatures were up to 3°C . At the same time cold air was pushed from the central Arctic towards south causing intense snow showers until September 25. Until the end of our work one day later we remained under the influence of a high-pressure system over Barents Sea bringing north-westerly wind and wave heights up to 2.5 m.

On our way through the ice-free Kara and Barents Sea we faced weak westerly winds near a ridge of high pressure and at times fog until September 29.

When we passed the North Sea heading for Bremerhaven our weather was dominated by storms. With the help of the exact forecasts for our planned ship track we were able to circumnavigate the highest waves and the windiest situations and thus reached Bremerhaven safely one day earlier than planned.

The wind and temperature conditions during the cruise are displayed in figures 2.5 to 2.7.

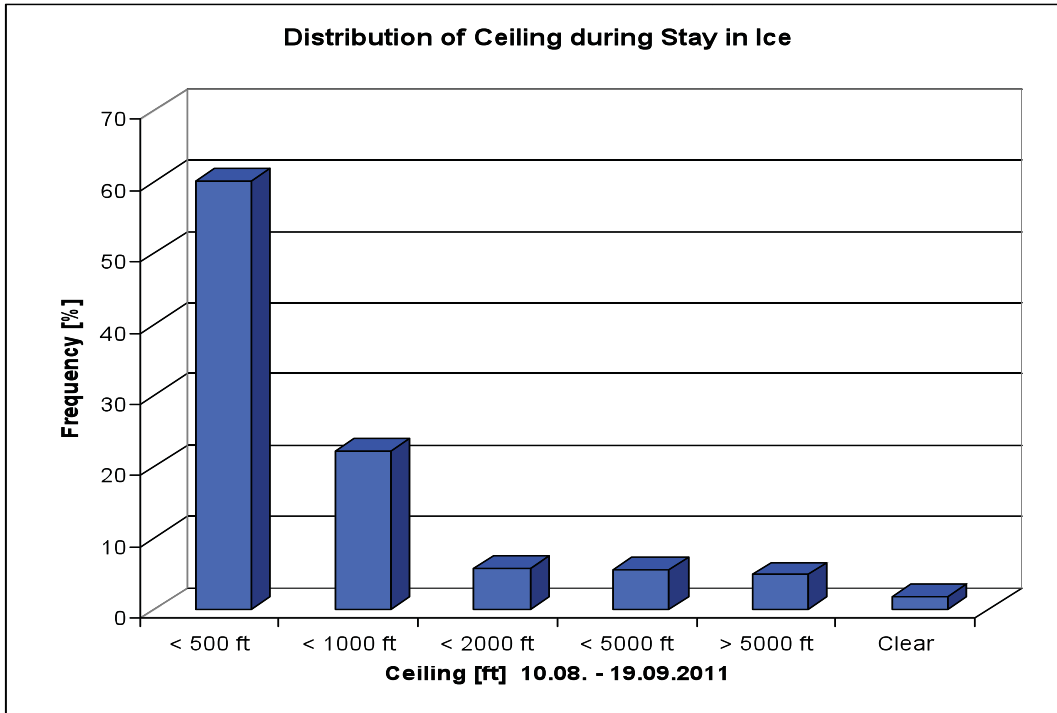


Fig. 2.3: Distribution of ceiling, August 10 to September 19, 2011, along Polarstern's (DBLK) cruise track in ice covered seas.

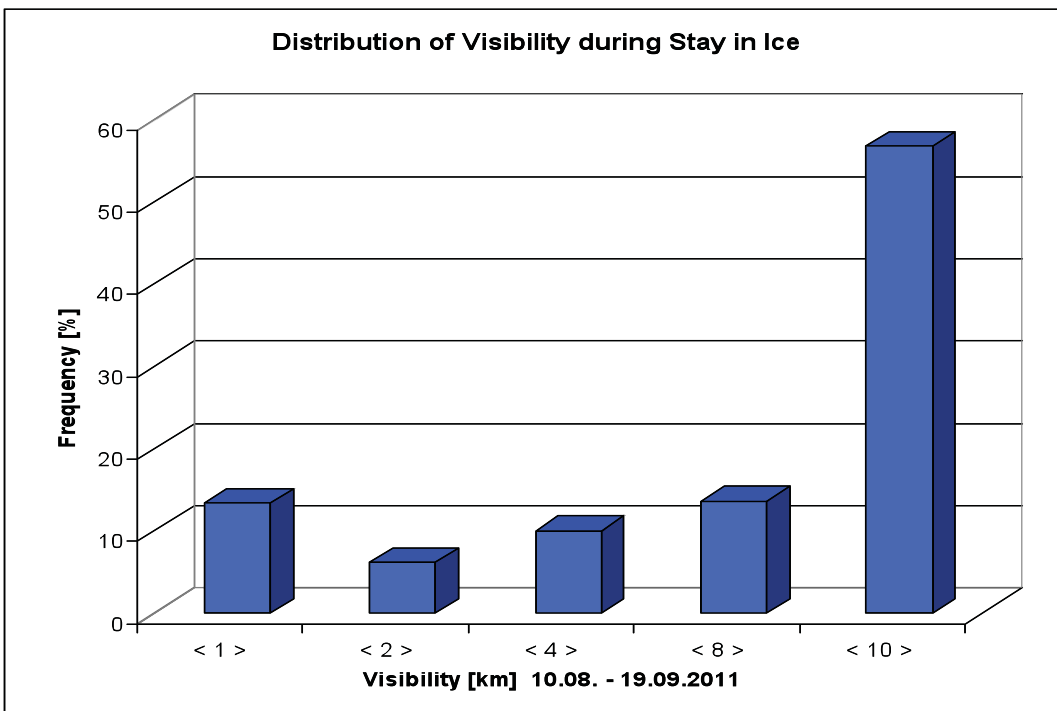


Fig. 2.4: Distribution of visibility, August 10 to September 19, 2011, along Polarstern's (DBLK) cruise track in ice covered seas.

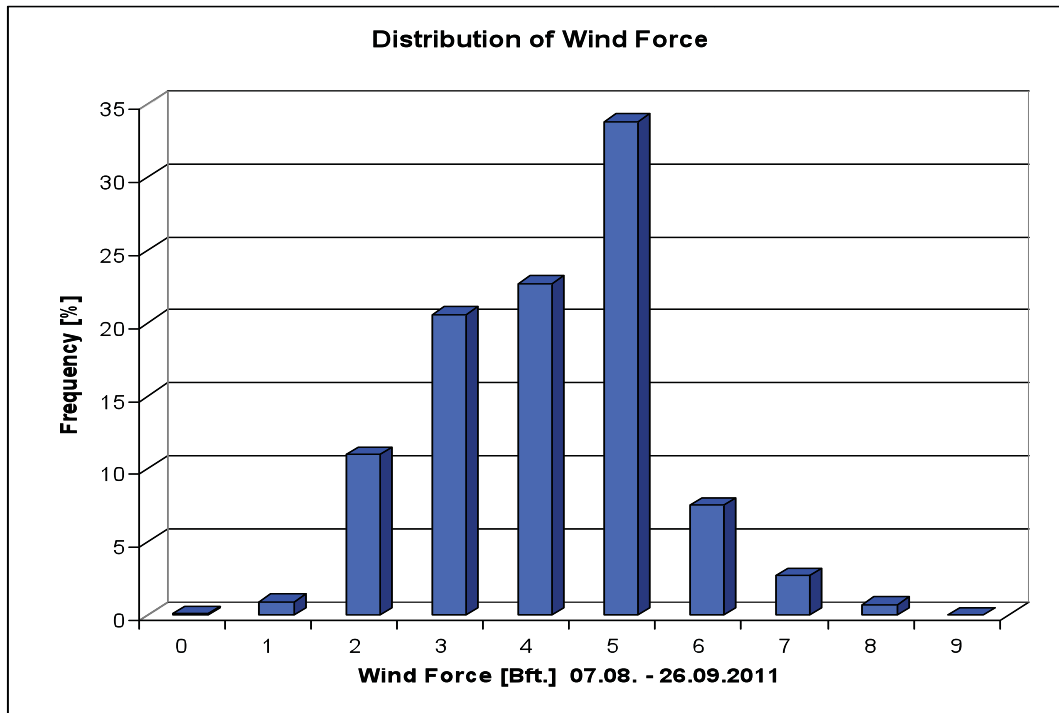


Fig. 2.5: Distribution of wind force along Polarstern's (DBLK) cruise track during scientific station work from August 07 to September 26, 2011.

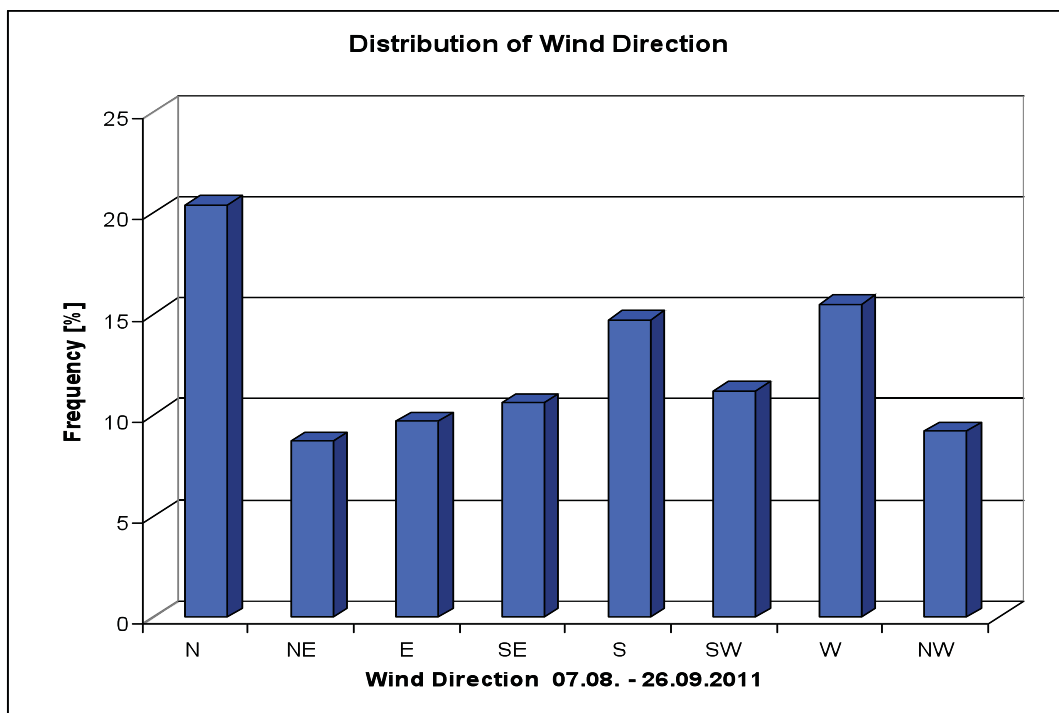


Fig. 2.6: Distribution of wind direction along Polarstern's (DBLK) cruise track during scientific station work from August 07 to September 26, 2011.

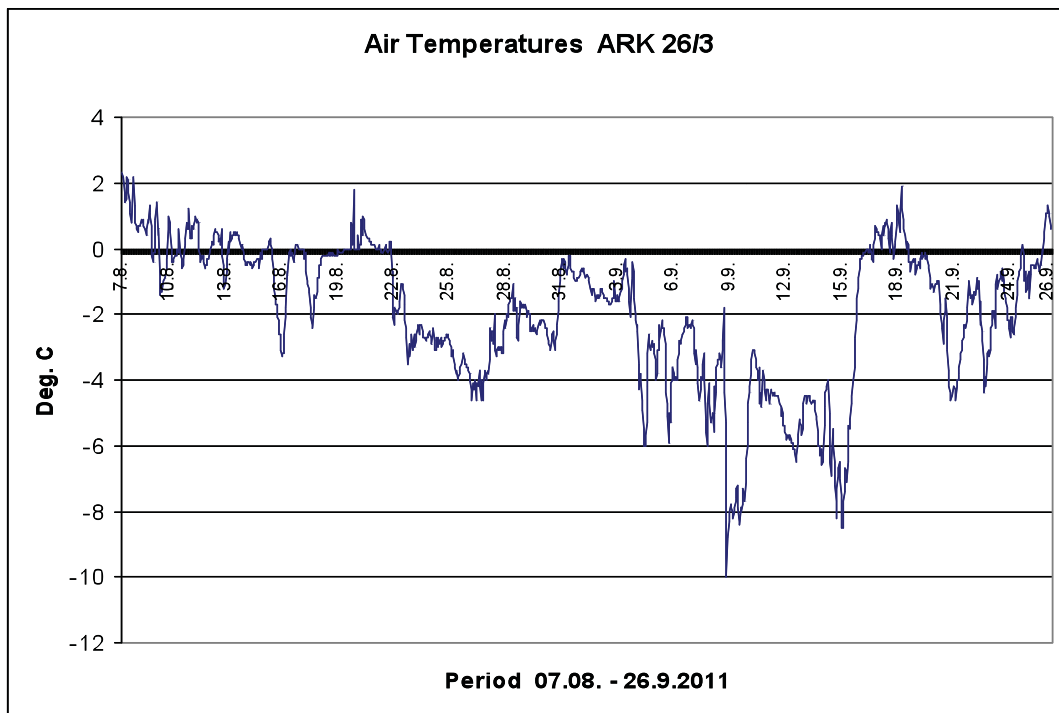


Fig. 2.7: Time series of air temperature along Polarstern's (DBLK) cruise track during scientific station work from 07 August to 26 September 2011.

3. SEA ICE PHYSICS

Stefan Hendricks, Marcel Nicolaus,
Robert Ricker, Mario Hoppman, Priska
Hunkeler, Christian Katlein

Alfred-Wegener-Institut

Introduction

Satellite observations reveal a reduction of Arctic summer sea ice extent in the order of 8% per decade. This reduction is accompanied by a decrease of ice age, leaving a smaller, younger and subsequently thinner ice cover at the end of the annual melting cycle. The critical factor to assess these changes is the sea ice thickness distribution. However, satellite based ice thickness monitoring does not yield reliable results in the summer season, due to unfavourable surface conditions such as melt ponds. Therefore, we estimated the regional sea ice thickness distribution along the cruise track with helicopter surveys with an airborne electromagnetic induction sensor (EM-Bird). The assessment of the ice thickness distribution was accompanied by hourly visual observations of sea ice conditions from the bridge. While the airborne ice thickness surveys revealed a snapshot of the Arctic sea ice thickness distribution, an Ice Mass Balance (IMB) buoys was deployed to monitor the ice thickness evolution at a selected location throughout the Arctic winter. Besides the IMB, a total of 11 ice drifting buoys were deployed in coordination with the International Arctic Buoy Program (IABP) along the cruise track, which measure ice drift and meteorological parameters.

The observed thinning demonstrates a shift of sea ice regimes in the central Arctic, which has consequences for the physical and biological properties of sea ice and the upper ocean layer. To assess and quantify these changes towards a younger and thinner sea ice cover we measured the physical properties of sea ice, such as ice texture and spatial and spectral distribution of light transmission through sea ice. The optical measurements were carried out with a Remotely Operated Vehicle (ROV) during ice stations and from the deck of *Polarstern*. The work on the ice stations was completed by ice coring at selected sites and high resolution ground EM ice thickness measurements.

This report presents the work of the sea ice physics group in individual chapters for sea ice thickness data acquisition, ROV optical measurements, ice station work, buoy deployment and visual sea ice observations. An overview of these activities is given in Figure 3.1.

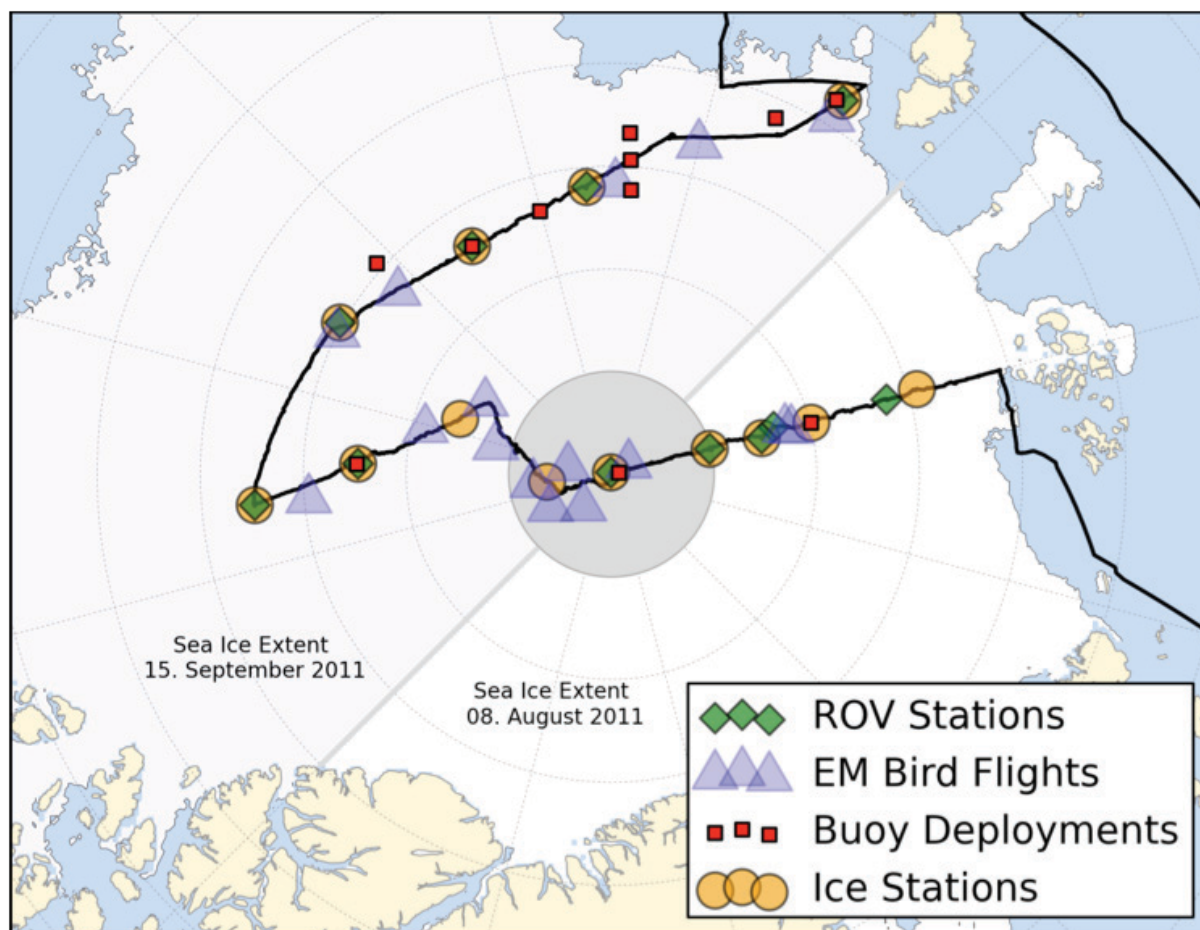


Fig. 3.1: Overview of activities of the sea ice physics group during ARK-XXVII/3. Sea ice thickness data was acquired during helicopter surveys (blue triangles) along the cruise track. Optical measurements of spectral light transmissivity through sea ice and upper ocean layer were carried out during several ice stations and from the working deck of Polarstern. Several drifting buoys were deployed. Not shown here: Hourly visual sea ice observations from the bridge.

3.1 Airborne sea ice thickness surveys

Stefan Hendricks, Priska Hunkeler,
Robert Ricker

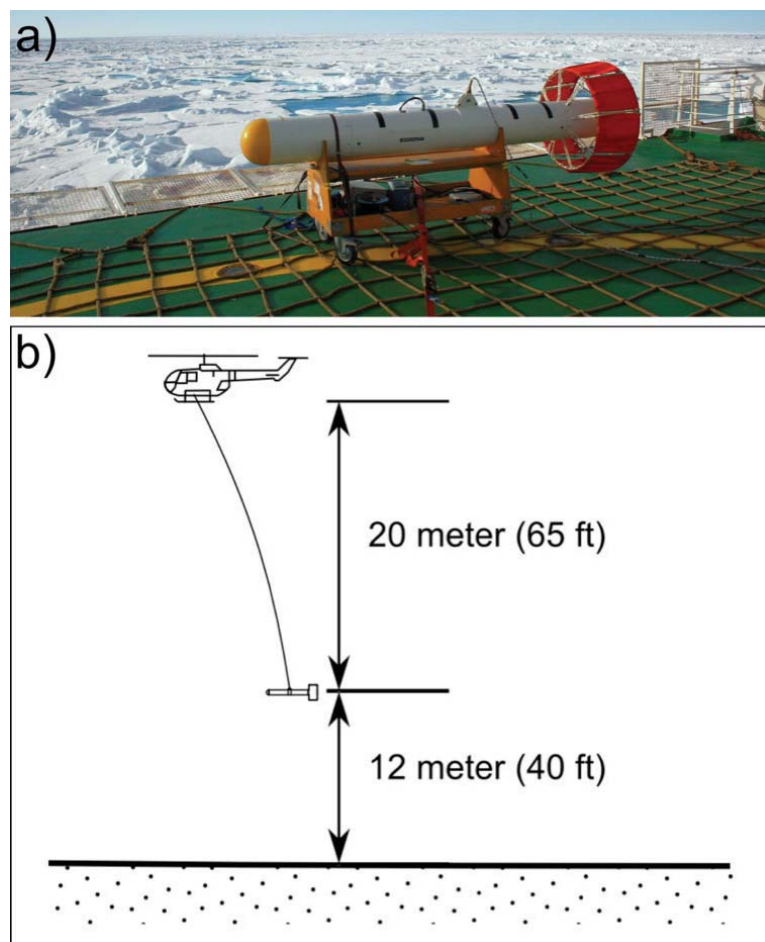
Alfred-Wegener-Institut

Objectives

Airborne electromagnetic (AEM) inductions soundings of sea ice thickness during ARK-XXVI/3 extend the existing time series of ice thickness surveys in the Transpolar Drift during the Arctic summer. This geophysical method is based on the contrast of electrical conductivity between sea ice and ocean water layers and presents the only method of direct airborne sea ice thickness measurements. The surveys are typically carried out by sensors, so called EM-Birds, which are towed by a helicopter or fixed-wing aircraft above the ice surface. As an alternative,

ground-based induction sensors can be used for high resolution but lower coverage EM ice thickness estimates on ice stations. The time series of AEM ice thickness measurements in central Arctic extends back to 1991 in irregular intervals. This dataset is of particular importance since sea ice thickness products from spaceborne platforms are not available during the summer season, when the ice surface is covered by melt ponds. Therefore, we used AEM to estimate the sea ice thickness distribution in the central Arctic Transpolar Drift in summer in order to help understand the sea ice mass balance in the complete annual cycle.

Fig. 3.2: (a) EM-Bird on the helicopter deck of *Polarstern*. (b) The sensor is towed by a helicopter in an altitude of around 12 m over the ice surface.



Work at sea

In total, 16 helicopter flights with more than 2500 km of sea ice thickness profiles were conducted during ARK-XXVI/3. Each flight track followed a triangular pattern with a side length of 40 nautical miles (74.2 km). The EM-Bird is typically operated in an altitude of 40 feet (12 m) above the sea ice surface (Fig. 3.2). Every 15 to 20 minutes, the helicopter ascends to an altitude of 500 feet for system calibration and radio contact with the bridge of *Polarstern*. Two operators were involved in the surveys for control of the EM-Bird and additional sea ice observations with geolocated aerial photography. The oblique aerial images were taken approximately every one or two minutes from front seat of the helicopter facing in flight direction with a GPS-capable digital camera (Ricoh Caplio 500SE).

3.1 Airborne sea ice thickness surveys

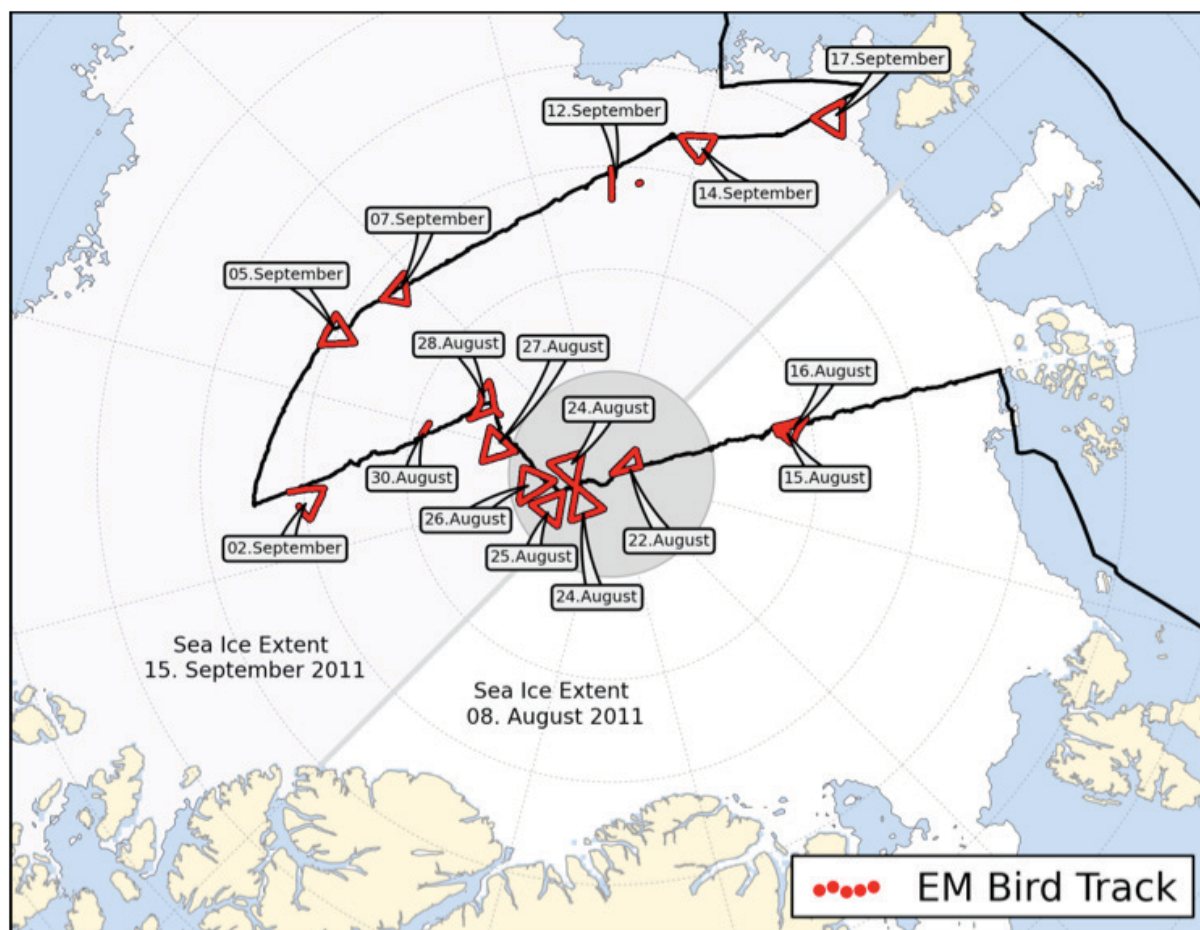


Fig. 3.3: Overview of the location and dates of all airborne EM sea ice thickness surveys during ARK-XXVI/3. The survey flights are given by triangular shaped and roughly 200 km long profiles.

Throughout the cruise, helicopter operations were significantly hampered by unfavourable weather conditions such as low visibility caused by fog or low clouds. Therefore, data from only two flights exist on the 60°W transect to the north pole. The weather situation improved after August 24, resulting in daily helicopter surveys. After August 30 flight conditions worsened again, allowing only 6 additional flights until *Polarstern* left the sea ice covered region.

The list of all available flight is given in Figure 3.3 and Table 3.1. Several flights had to be aborted early because of weather conditions, leaving a mean track length of 156 km per survey. During the end of the cruise some surveys were shifted to night (ship time), when weather and light condition were more favourable.

The processing of the EM data requires the knowledge of the electrical conductivity of the sea water. This information was obtained by the ships thermosalinograph. The conductivity values were determined for each flight in steps of 100 ms/m (Tab. 3.1). In addition, the sea ice thickness data of each flight was calibrated on sites of open water, which were marked by the EM operator during the surveys.

Tab. 3.1: List of all airborne EM sea ice thickness surveys during ARK-XXVI/3 with thickness statistics

Date	Flight	Conductivity [mS/m]	Length [km]	Modal Thickness [m]	Mean Thick- ness [m]	Standard Deviation [m]	Median Thickness [m]
2011/08/15	#1	2600	77,6	0,8	1,24	0,60	1,09
2011/08/16	#1	2600	156,7	0,9	1,29	0,60	1,14
2011/08/22	#1	2600	155,4	0,8	1,21	0,66	1,03
2011/08/24	#1	2500	186,0	1,1	1,56	0,87	1,33
2011/08/24	#2	2500	191,5	1,1	1,61	0,97	1,34
2011/08/25	#1	2500	214,5	0,9	1,34	0,80	1,13
2011/08/26	#1	2500	204,7	0,9	1,58	0,90	1,35
2011/08/27	#1	2500	217,2	0,9	1,60	1,27	1,23
2011/08/28	#1	2500	182,2	0,9	1,43	0,79	1,20
2011/08/30	#1	2500	29,3	1,1	1,61	0,86	1,37
2011/09/02	#1	2400	149,9	0,9	1,26	0,68	1,08
2011/09/05	#1	2300	203,3	0,7	1,14	0,96	0,92
2011/09/07	#1	2400	195,2	0,6	1,02	0,57	0,84
2011/09/12	#1	2400	63,3	0,6	0,99	0,60	0,85
2011/09/14	#1	2400	169,0	0,1	0,34	0,36	0,22
2011/09/17	#1	2500	191,2	0,0	0,78	0,87	0,54

Preliminary results

Exemplary sea ice thickness results of typical first-year and multiyear sea ice floes can be seen in Figure 3.4. Typical first year level sea ice shows a thickness of less than 1 m and very few ridges with thicknesses larger than 4 m. It has to be mentioned however, that the airborne EM underestimates maximum thickness of pressure ridges by as much as 50%, due to footprint effects. While the amount of thick ice (> 6 m) is generally low for first-year ice, multiyear sea ice can easily exceed thicknesses of 8 m or more at a length of 1 km, as can be seen in the lower part of Figure 3.4.

In general, typical first-year sea ice thickness distributions dominate the dataset, with only very few multiyear floes. Consequently, the modal thicknesses of the individual flight range between 0.6 m and 1.1 m in the central ice zone and 0.0 to 0.1 m close to the ice edge (Tab. 3.1). The highest modal and mean thicknesses were found between August 24 and August 30 in the area close to the North Pole, which coincides with the highest density of multiyear ice floes. The rare amount of multiyear sea ice is confirmed by the visual observations of the ice surface during the surveys (Example: Fig. 3.5). Multiyear and first-year sea ice

3.1 Airborne sea ice thickness surveys

surfaces show distinct characteristics with respect to surface features and melt pond concentration, however quantitative results are difficult to obtain from the oblique aerial imagery.

The average sea ice thickness distribution from all datapoints is shown in Figure 3.6. The modal thickness of 0.9 m matches the result from 2007 (*Polarstern* cruise leg ARK-XXII/2) in the region of the Transpolar Drift Stream. However, not only the modal thickness, but also the entire shape of the ice thickness distributions from summer 2007 and 2011 are very similar. Regional differences do exist in the different surveys, but the comparison reveals, that the general ice conditions were very comparable in the two years of 2007 and 2011.

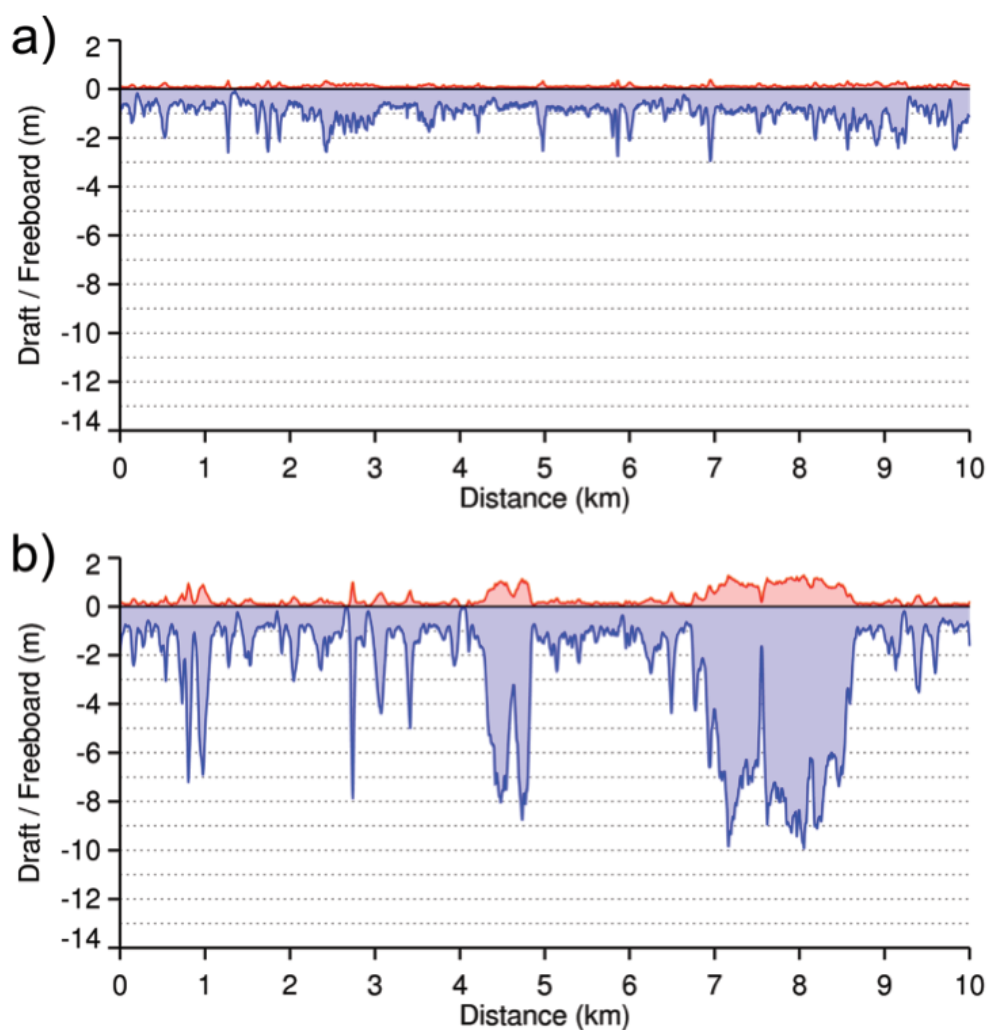


Fig. 3.4: Sea ice thickness examples from the EM-Bird system. The top panel (a) shows typical summer first year ice as found during ARK-XXVI/3 and the lower panel (b) shows thicker multi-year sea ice, which was occasionally found during the surveys.



Fig. 3.5: Exemplary sea ice observation photo. The photos were acquired by sea ice observers in the front passenger seat of the helicopter and are automatically written with a UTC timestamp and GPS position.

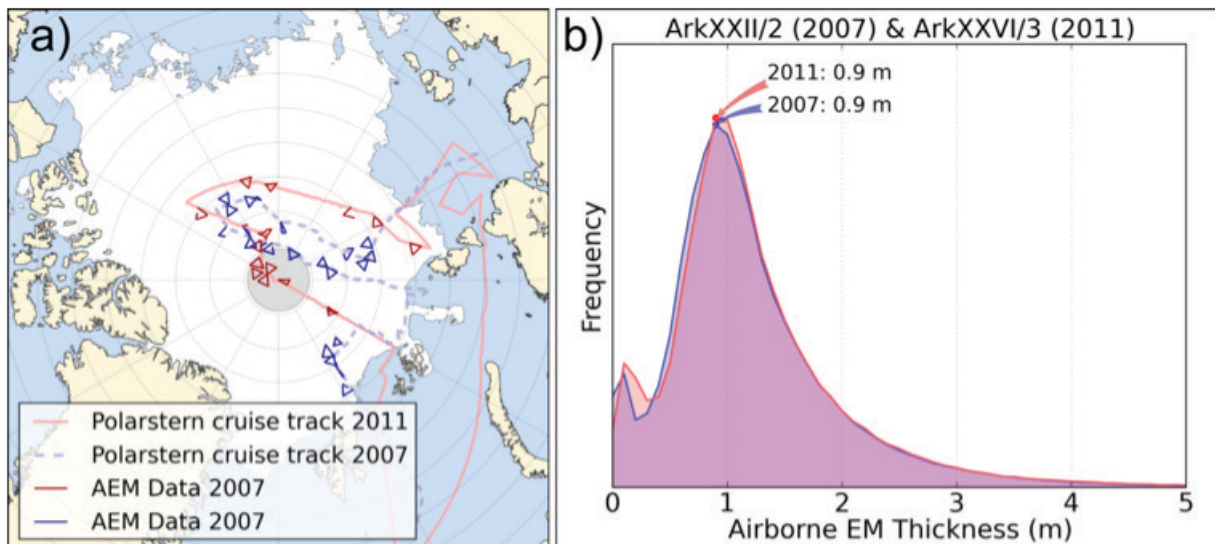


Fig. 3.6: a) Locations of all EM-Bird sea ice thickness surveys of 2007 (ARK-XXII/2, red) and 2011 (ARK-XXVI/3, blue). b) Sea ice thickness distributions of all EM data points in 2007 and 2011. Marked are the modal thicknesses (maximum of the ice thickness distribution) for the respective years.

3.2 Optical measurements

Marcel Nicolaus, Christian Katlein

Alfred-Wegener-Institut

Objectives

The amount of solar light transmitted through snow and sea ice plays a major role for the energy budget of ice-covered seas. Thus it is of critical importance for formation and melt of sea ice. In addition, the horizontal and vertical distribution of light under sea ice impacts biological processes and biogeochemical fluxes in the sea ice and the uppermost ocean. Due to their different absorption spectra, snow, sea ice, sea water, biota, sediments, and impurities affect the spectral composition of the light in its way from the atmosphere into the ocean. During the last years, the number of studies of spectral light measurements under sea ice has increased. However, observations that allow insight into the spatial variability of under-ice irradiance and radiance are still sparse, and little is known about how light conditions change on different scales from meters to kilometres. In addition, there are only very few data on the total energy budget under sea ice as well as on relating biomass estimates to radiation measurements. Therefore, we have performed comprehensive measurements of spectral radiation over and under sea ice during ARK-XXVI/3.

Work at sea

We have measured spectral irradiance and radiance of visible light (wavelength range from 350 to 920 nm with 3.3 nm resolution) above and beneath sea ice with Ramses spectral radiometers (Trios GmbH, Rastede, Germany), using different setups in order to gain different kind of data sets related to different objectives. Radiance measurements (7° field of view) are best suited for studying the spatial variability of optical properties of sea ice, because the measured signal originates from a comparably small area. Irradiance measurements (cosine receptor) are best suited for studying the energy budget at the point of measurement, integrating all incident energy (from above) at this point. Optical measurements have been performed during each ice station (Fig. 3.7, 3.8 and Tab. 3.2).

ROV measurements

We operated two radiometers synchronously on a Remotely Operated Vehicle (ROV, Ocean Modules V8ii, Åtvidaberg, Sweden) under the sea ice with one reference sensor at the ice surface. From these measurements, we obtained horizontal transects and vertical profiles of under-ice irradiance (Edw) and radiance (Idw). In total, the ROV was operated successfully during two tests from the working deck of *Polarstern* and directly from the sea ice during nine ice stations (Fig. 3.7, 3.8, and Tab. 3.2). In addition, two ROV operations were not successful due to problems with the power supply (August 14) and with the magnetic compass (August 26). The data quality from measurements on September 11 strongly suffered from very low solar irradiance (local time night hours). All other data sets look most promising.

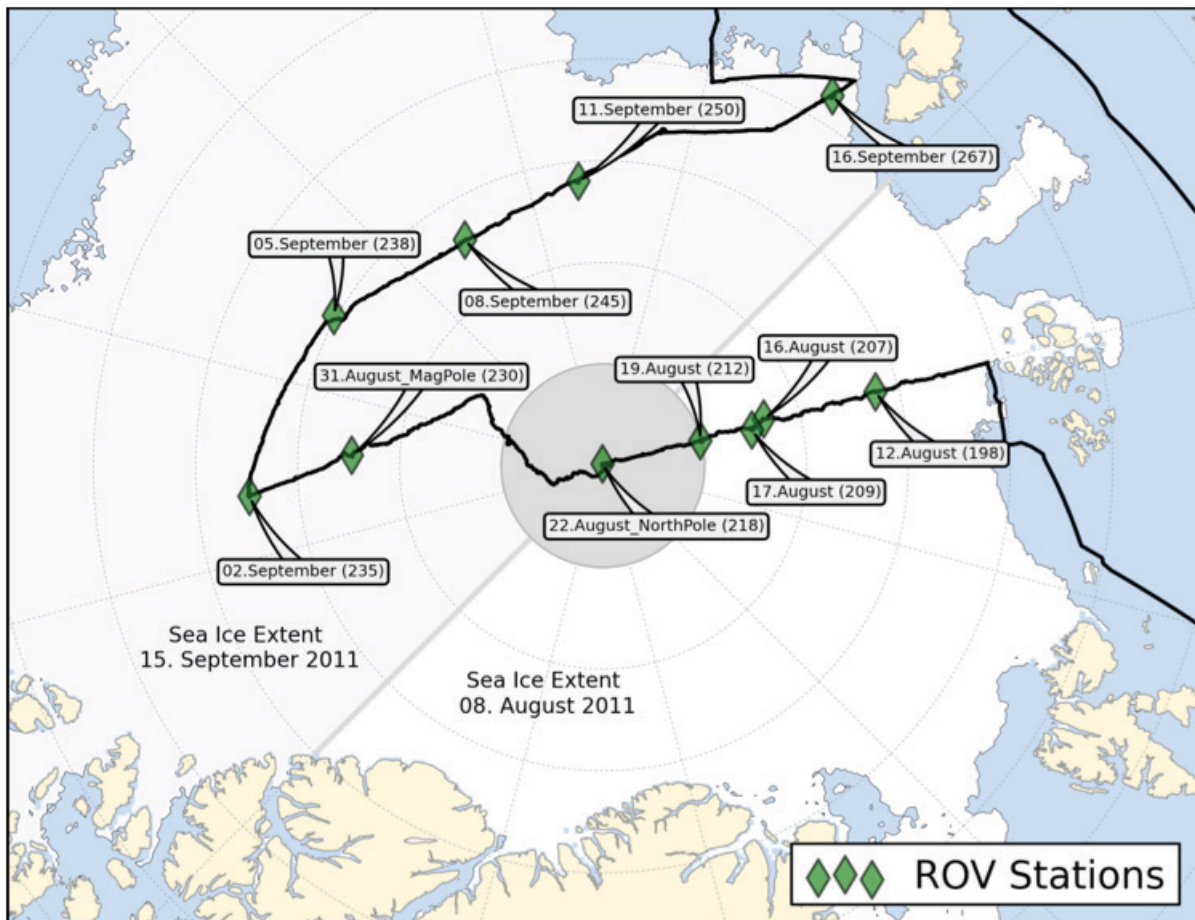


Fig. 3.7: Overview of all ROV stations. The background image gives sea-ice concentration on August 8, 2011 for the first part and September 15, 2011 for the second part of the cruise. Numbers in brackets give Polarstern station numbers. The Magnetic Pole was almost reached with the ice station on August 31 (78-230).

3.2 Optical measurements

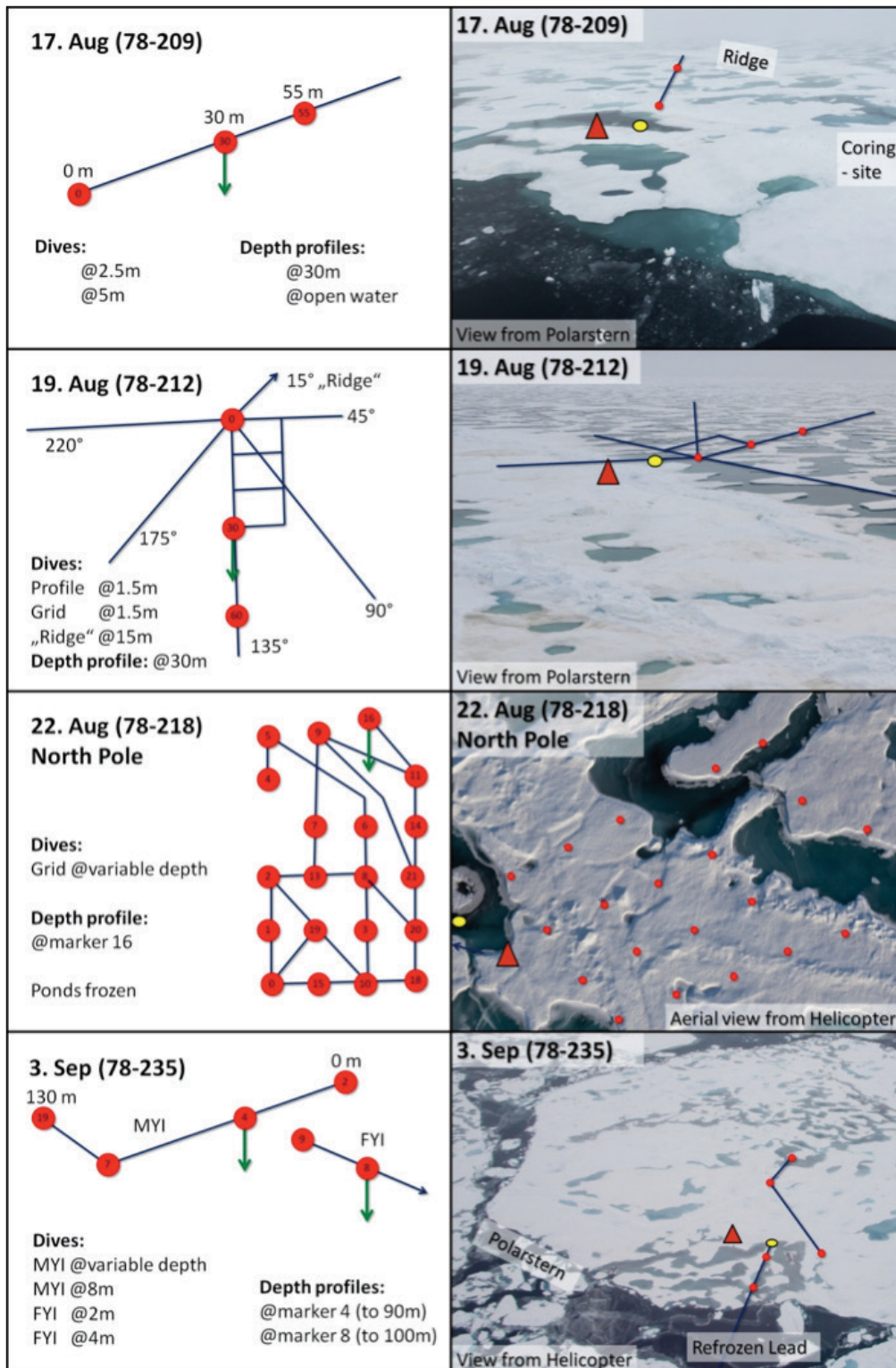


Fig. 3.8a: Sketches and Overview images of ROV sea-ice stations with profile lines (dark blue), selected markers with according numbers (red dots), depth profiles (green arrows), biooptical cores (light green cylinders), and the depths of main dives. The yellow ellipse indicates the ROV launch hole and the red triangle the location of the pilot tent.

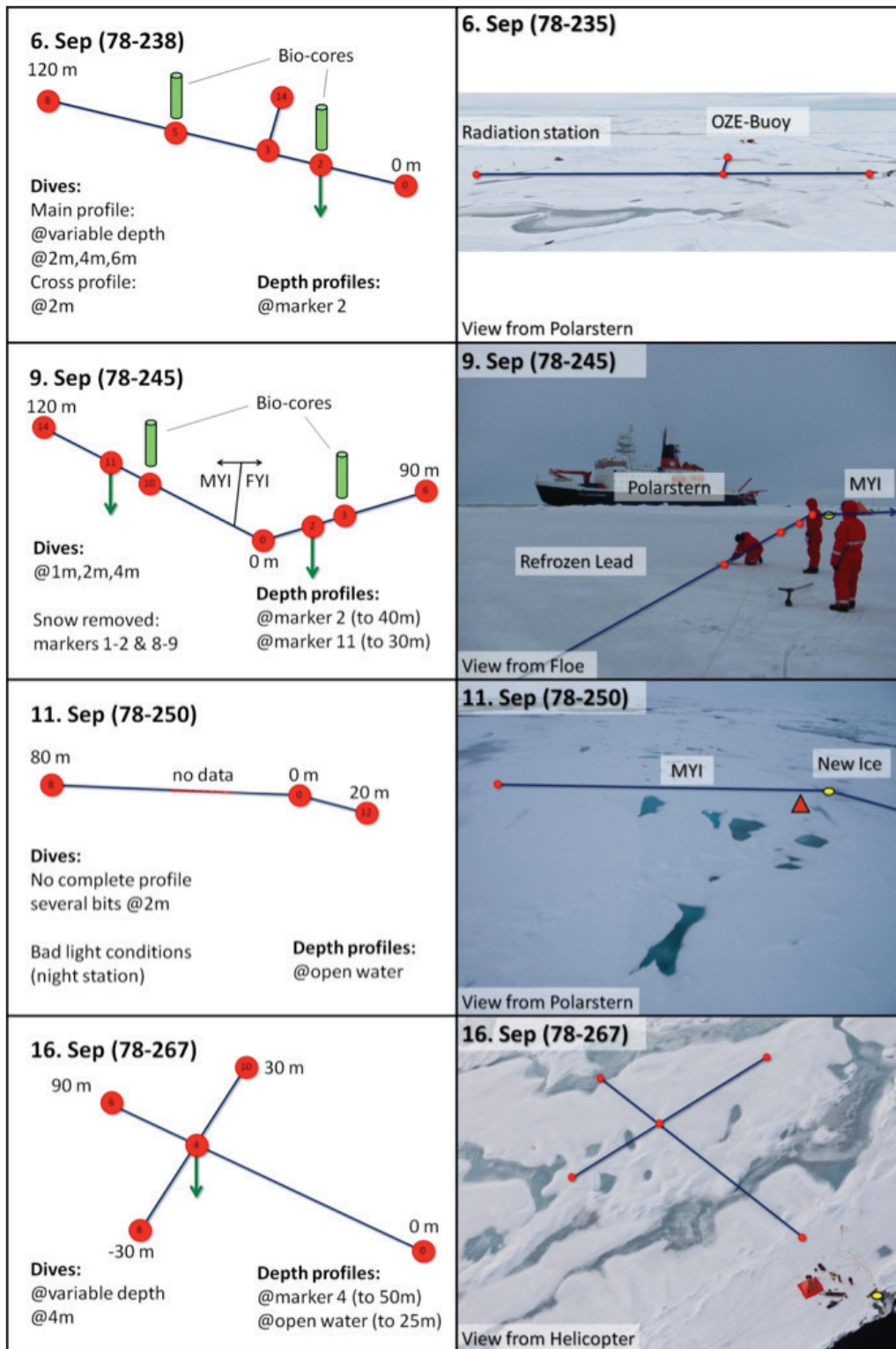


Fig. 3.8b: Sketches and Overview images of ROV sea-ice stations with profile lines (dark blue), selected markers with according numbers (red dots), depth profiles (green arrows), biooptical cores (light green cylinders), and the depths of main dives. The yellow ellipse indicates the ROV launch hole and the red triangle the location of the pilot tent.

3.2 Optical measurements

Tab. 3.2: All ROV profiles where data were recorded. Dates (UTC) refer to the ROV measurements (not station beginning). Markers are named with "M" and their number, e.g. M6 for marker number 6. Abbreviations: MYI: multi year sea ice, FYI: first year sea ice.

Date PS station	Profile (@ ROV depth)	Length/Depth (m)	Sea ice and thickness	Surface conditions Pond status	Comments
12.08.11 78-198	Profile @ 2.0m Profile @ 5.0m	ca. 110 ca. 110	Mostly FYI Mostly FYI	No snow, open ponds	ROV test from <i>Polarstern</i> Irradiance only
16.08.11 78-207	Depth under ice	20		No snow, open ponds	ROV test from <i>Polarstern</i> Profile at floe edge
17.08.11 78-209	Profile @ 2.5m Profile @ 5.0m Profile @ ice bottom Profile @ ice bottom Depth @ M30 Depth	100 50 30 no data 50 13	FYI 1.1m FYI 1.1m FYI 1.1m FYI 1.1m FYI 1.1m Open water	No snow, open ponds	"Stop and go" mode Continuous, bad positioning
19.08.11 78-212	Profile 000° @1.5m Profile 045°, @1.5m Profile 095°, @1.5m Profile 175°, @1.5m Profile 220°, @1.5m Profile ridges, @15m Grid @1.5m Depth @ M30	120 60 120 120 150 points 30x15 50	FYI 1.2m FYI 1.2m FYI 1.2m FYI 1.2m FYI 1.2m MYI < 8.0m FYI 1.2m FYI 1.2m	No snow, open ponds	
22.08.11 78-218	Grid @ variable depth Depth @ M16	30x50 10	MYI 1.5-3.5m MYI 1.5-3.5m	Frozen sur- face and ponds, no snow	Only radiance sensor
31.08.11 78-230	Profile @ variable depth		FYI 1.1m	2-3 cm new snow, ponds fro- zen (7cm)	ROV in Deck mode, no pressure sensor, bad data quality
03.09.11 78-235	Profile 1 @ 4-8m Profile 1 @ 8m Profile 1 @ variable depth Profile 2 @ 2m Depth @ M4 Depth @ M8 Surface depth profile	2x130 2x130 120 2x80 90 100 5	MYI 2.0-3.8m MYI 2.0-3.8m MYI 2.0-3.8m FYI 1.2m MYI close FYI FYI close water MYI/FYI	2-3 cm new snow, ponds fro- zen (10cm)	

Date PS station	Profile (@ ROV depth)	Length/Depth (m)	Sea ice and thickness	Surface conditions Pond status	Comments
06.09.11 78-238	Profile @ 1.2m Profile @ 2.0m Profile @ 4.0m Profile @ 6.0m Profile @ variable depth Cross profile @ 3.0m Depth @ M2 Depth	30 120 120 105 120 70 50 5	FYI 0.8m FYI 0.8 (to 2.0) FYI 0.8 (to 2.0) FYI 0.8 (to 2.0) FYI 0.8 (to 2.0) FYI 0.8 FYI 0.8 (to 2.0) FYI 0.8 (to 2.0)	Snow 3 cm, ponds frozen	Bad positioning
09.09.11 78-245	Profile @ 1.0m Profile @ 1.2m Profile @ 2.0m Profile @ 4.0m Profile @ 1.0m no snow Profile @ 2.0m no snow Profile @ 2.0m no snow Depth @ M2 Depth @ M11	120 90 2x210 210 15 15 15 40 25	FYI 1.2m New ice 0.3m FYI + new ice FYI + new ice New ice 0.3m New ice 0.3m FYI 1.2m New ice 0.3m FYI 1.2m	Snow 10cm, ponds frozen	New ice = frozen lead Snow removed M8-M9 Snow removed M8-M9 Snow removed M1-M2
11.09.11 78-250	Profile @ 2.0m Depth Depth	Ca. 4x30 10 3	New ice + MYI Open water Open water	Ponds frozen, snow covered	Low light level, bad data quality (night station), Bad positioning
16.09.11 78-267	Profile @ 4.0m Profile @ variable depth Depth @ M4 Depth	Total 450 Total 240 50 25	MYI 1.7 to 2.9m MYI 1.7 to 2.9m MYI 1.7 to 2.9m Open water	Ponds frozen, snow covered	

The ROV system consisted of a surface unit (incl. power supply, control unit, monitor), a 300-m long tether cable, and the ROV itself. The ROV is controlled and moved by eight thrusters allowing diving speed of up to 1.0 m/s. The standard measurement speed (using 25% thruster gain) was about 0.25 m/s for horizontal and vertical profiles. The speed varied from profile to profile and depended on under-ice currents as well. The ROV was equipped with two standard VGA video cameras, one looking forward and one looking backward (Fig. 3.9). Both cameras were used for navigation (orientation) and to document the dives. One video signal, usually the forward one, was recorded always. An altimeter (DST Micron Echosounder, Trittech, Aberdeen, UK) and a sonar (Micron DST MK2, Trittech, Aberdeen, UK) were mounted to support navigation and measure the distances to obstacles and markers (see below). The altimeter was particularly used to measure the distance between the radiometers (ROV) and the sea ice. In addition, the ROV measured its depth, heading, roll, pitch, and turns and displayed this as an overlay together with a time stamp on the control monitor (Fig. 3.10). After it was found that the designated 5-kW generator was not able to power the ROV system under full load (August 14), ship's power was used on all stations. For this, 100 to 150 m of cable had to be laid out from the vessel to the ROV site (tent). This also restricted the choice of the launch site to a distance smaller than the cable length. The ROV was balanced in a pool on the working deck of *Polarstern* with actual sea water. Doing so, it was balanced slightly heavy in order to make it sink down, finally hanging straight under the launch hole, in case of any failure. Similarly the tether was slightly negatively buoyant, too. Salinity variations between the stations due to sea ice melt led to slightly varying balancing throughout the cruise.

3.2 Optical measurements

The irradiance sensor (type SAMIP) was directly implemented into the ROV, meaning its communication was led through the tether, using (the last) unused twisted pair. The radiance sensor (type SAM) was connected through a separate 150-m long cable, which was strapped to the tether and dragged along. This limited the operation radius to 150 m when both sensors were used (standard setup). At the surface, both sensors were connected to one interface box (type PS 100 or IPS 400) each. All data were directly recorded into a PC running the sensors' software MSDA_xe. An additional reference irradiance sensor (type SAMIP) was mounted on a tripod on the sea-ice surface measuring incident solar radiation (E_d). All sensors were triggered synchronously in intervals of 2 to 10 s, depending on light conditions under the ice. Integration times of the sensors varied depending on ice conditions between 512 and 4048 ms, with longer times for the irradiance sensor due to the lower light transmittance of the opaque cosine receptor. The overall point-to-point distance was approx. 1.0 m for irradiance and 2.0 m for irradiance measurements.

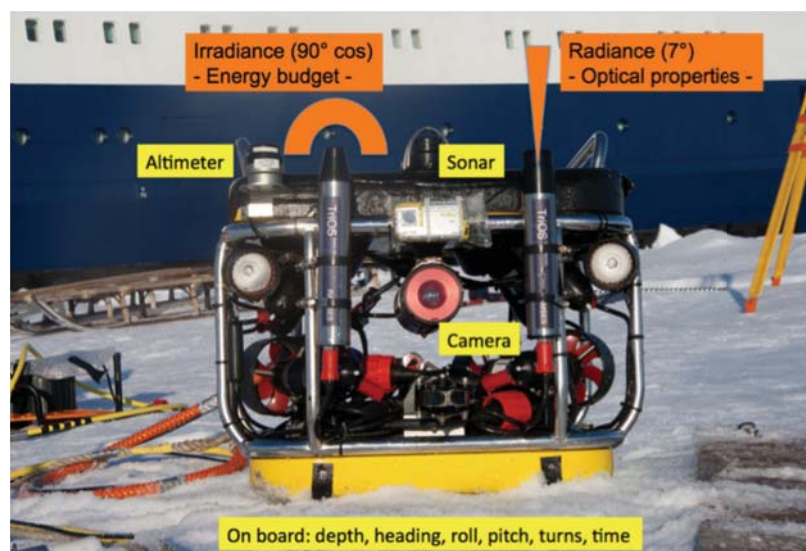


Fig. 3.9: Photograph of the Ocean Modules V8ii ROV equipped with two Ramses radiometers, one measuring irradiance (left) and one measuring radiance (right). An additional rear-looking camera is not visible in this photograph.

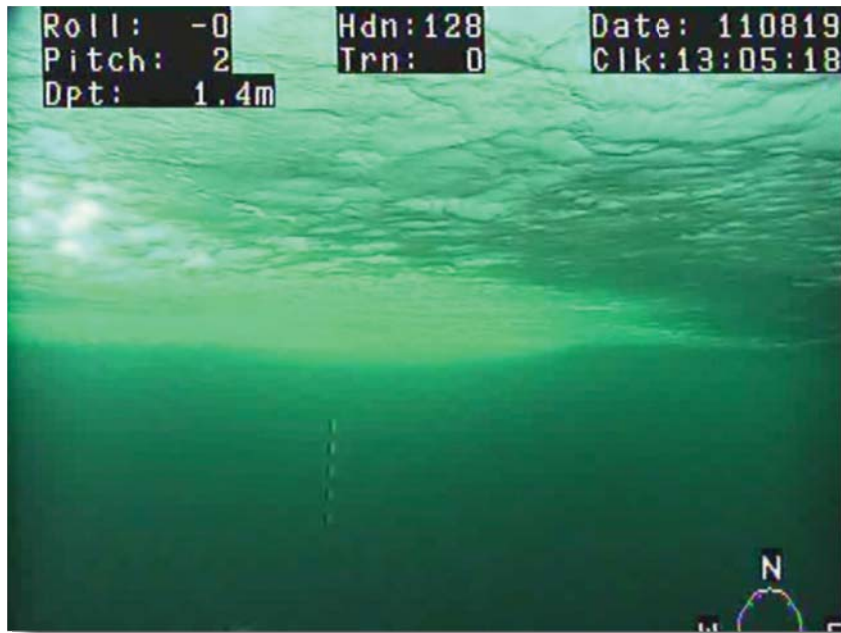


Fig. 3.10: Under-sea-ice photograph extracted from the ROV (front) camera video record (Station August 19, 78-212). It shows the smooth ice bottom and a marker stake (1-m long, 0.1-m sections). Differences in brightness indicate differences in light transmission. In addition, navigational information is overlaid. Abbreviations [and units]: pitch and roll [deg], Dpt: depth [m], Hdn: heading [deg], Trn: turns, Date [yymmdd], Clk: clock/time [UTC].



Fig. 3.11: Photograph of the ROV site taken from board Polarstern during the ice station on September 2 (78-235). The main picture shows the deployment hole in a frozen (surface) melt pond, the yellow tether, and the pilot tent. The inset picture shows two ROV pilots, one controlling the ROV and one controlling the sensors and documenting all operations.

3.2 Optical measurements

All electronics were set up in a pilot tent (Fig. 3.11), which was heated when necessary. The ROV operations always needed four persons: one pilot controlling the ROV, one co-pilot controlling the optical sensors and documenting the dive, one tether handler, and one polar-bear guard. The ROV was launched through melt ponds (preferably melted all the way through) or over floe edges in order to reduce the amount of work for an access hole to a minimum. We found that this worked out nicely under the given summer conditions. After an initial system check and test dive, the profiles (grids) were marked with numbered, red-white colored poles, hanging under the ice through drill holes. Sea-ice thickness, snow thickness / surface layer thickness / pond depth, and freeboard were measured at each hole. Additional measurements of total sea-ice thickness were performed by EM31-measurements (see other section) over the profiles (not all stations). Furthermore, surface features, such as pond distributions along the profiles, were noted to support later analyses. Over all, such an ROV station (setup, measurements, packing) took six to eight hours.

The preferred mode of operation for the ROV is "normal horizon" mode. In this mode, the ROV keeps its own position in the water stable whenever no other command is given. This mode was used on the first two ROV ice-stations (until August 22) without any problems. Closer to the magnetic pole (137.3°W, 85.25°N) this mode did not work anymore, because it requires a stable compass information, which was not given since the field strengths of the horizontal component of the magnetic field was too low (<2000 nT). On August 31 the ROV was operated in "deck mode", meaning no stabilization at all. Additionally, the depth sensor did not work and ROV depth had to be read from the SAMIP module of the irradiance sensor. With this, we managed to fly one 50-m long profile, but the quality of optical data is much lower than on all other stations. From September 3 onwards, the ROV was operated in "normal horizon" again, but it was not possible to use the compass (heading information) for orientation any longer. The compass signal was strong enough to prevent the ROV from crazily spinning, but still highly variable and drifting.

Standard profiles were dives of constant depth, mostly on 2, 4, or 6 m depth. Additional tests were also performed with flights following topography or simulating point measurements by diving up to the ice bottom for each measurement. But these routines were found to be more difficult to handle and analyse later on. Depending on flight depth and marker depth, it was found to be difficult to position the ROV precisely under the ice. In general, orientation and positioning were quite difficult and caused most problems for the ROV operation. Depth profiles were found to be best when following a long line hanging under the ice in order not to lose orientation and drift too far off the profile due to currents.

Stationary setup

Time series of solar irradiance (no radiance measurements) over and under sea ice (e.g. albedo and transmittance) were measured with a stationary setup of a radiation station (Fig. 3.12). This radiation station was set up in different configurations of three to five radiometers during four ice stations for up to 12 hours (Fig. 3.7 and Tab. 3.2). The station at the North Pole on August 22 did not record any data due to an operational mistake. An additional radiation station was deployed on the Peildeck of *Polarstern* from September 21 to 23. This station consisted of three irradiance sensors and one radiance sensor, all measuring incident solar radiation in order to inter-compare the sensors and to enable comparisons with the standard short-wave measurements of the meteorological station on board *Polarstern*.



Fig. 3.12: Photograph of the radiation station. Two sensors are mounted above the surface for albedo measurements (left rack), one mounted on an l-arm held by the yellow stand, and two hanging under the ice at the position of the l-arm. Station on September 5 (78-238).

Each station on the sea ice consisted of two sensors at the surface (downward and upward, E_d and E_u) mounted on a horizontal bar between two tripods and one upward looking sensor mounted on an L-Arm (see below) adjusted directly at the sea-ice bottom (E_{di}). On September 5 and 8, two additional under-ice sensors were added hanging in the water in a depth of 6.0 m. One sensor was installed in a small frame looking upward (E_{dw}) and one was hanging on its cable looking downward (E_{uw}). These sensors were added to get a more comprehensive idea of the energy budget under the ice, including upward irradiance.

All data were recorded in a customized version of a Tribox2 (Trios GmbH, Rastede, Germany) with an additional interface box to enable synchronous recording of up to five sensors. Logging interval was 1 min. The station was powered using two 75 Ah car batteries. All electronics was placed in a white isolated box (Fig. 3.12).

Point measurements (L-Arm)

Point measurements of spectral radiance and irradiance directly at the bottom of the sea ice (E_{di} and I_{di}) were performed using a foldable holder, so called L-Arm (Fig. 3.13), through core holes of 10 cm diameter. This arm was pushed straight through the hole before the bottommost section was folded up by pulling a rope. This resulted in the sensor being upright right at the ice-water interface, 80 cm away from the centre of the core hole. An additional irradiance sensor was set up close to the measurement to measure E_d . L-arm measurements were

3.2 Optical measurements

mostly performed using an irradiance sensor. Only on August 29, comparison measurements were made, using a radiance sensor on the L-Arm and measuring at the same positions. Mostly, the core from the access hole was used as texture core (TEX) for this site.

L-arm measurements were performed at all four stationary setups and during three additional stations independently of station measurements (Fig. 3.7 and Tab. 3.3). On August 19, these measurements were also performed directly in a melt pond. For stationary measurements, the L-Arm was mounted in a tripod, for other stations, the L-Arm was operated and held by a person. Such it was also possible to perform multiple measurements from one access (core) hole by rotating the L-Arm, e.g. in 45° steps.



Fig. 3.13: Photograph of under-ice radiation measurements using a foldable holder, so called l-arm. Station on August 29 (78-227).

Tab. 3.3: All optical stations and l-arm measurements, where data were recorded. Dates (UTC) refer to the optical measurements (not station beginning). Abbreviations for irradiance sensors: Ed / Eu: Downward / upward (reflected) at surface; Edi: Downward at sea-ice bottom; Edw / Euw: Downward / upward in water under sea ice at 6 m. Abbreviations for radiance sensor: Id: Downward at sea-ice surface, Idi: Downward at sea-ice bottom

Date PS station	L-arm	Station (Sensors)	Ice / snow	Comments
11.08.11 78-195	Site 1: 5 angles		MYI 1.5m, no snow	
14.08.11 78-203		Ed, Eu, Edi	Ed + Eu on MYI, no snow Edi under FYI 1.2m, no snow	6.5 h data
19.08.11 78-212	Site 1: 5 angles Site 2: 5 angles Site 3: 5 angles		FYI 1.0m, no snow FYI 1.0m, no snow Pond	
29.08.11 78-227	Site 1: 5 angles Site 2: no data Site 3: 6 angles Site 4: 6 meas.		FYI 1.4m, surface layer 3 cm FYI 1.4m, surface layer 3 cm MYI 3.3m	At pond edge Transect to pond edge
06.09.11 78-238		Ed, Eu, Edi, Edw, Euw	MYI 2.1m, snow covered	19 h data
09.09.11 78-245		Ed, Eu, Edi, Edw, Euw	FYI 1.2m, snow covered	9.5 h data
21.09.11 to 23.09.11		4x Ed (Id)	Peildeck	Sensor comparison

L-arm measurements were recorded either directly into a standard PC (see also ROV measurements) or using a handheld PC (TBS Nomad, Trimble / Tripod Data Systems, Corvallis, USA), connected via Bluetooth to the IPS box, and running Pocket MSDA software (Trios GmbH, Rastede, Germany). Under-ice and above-ice measurements were triggered manually and synchronously.

Bio-optical ice cores

During the cruise, 14 bio-optical cores (named "OPT") were obtained from the sea ice. These cores were obtained to study correlations between bio-optical sea-ice parameters (pigment content, particular absorption, dissolved organic matter) and the light measurements (spectral optical properties). All cores were drilled at points where under-ice irradiance was measured before. The cores were segmented into (mostly) three pieces: topmost 20 cm, bottommost 20 cm, and the remaining middle part. For further treatment and analyses see Sea Ice Biology section of this report.

Preliminary results

During the cruise, all radiation measurements (spectra) were processed from measured raw data to calibrated fluxes. However, results from sensor inter-comparisons and additional calibration and plausibility tests were not applied yet. In addition, most work was done to georeference all measurements, in particular to localize the under-ice ROV data. Station and L-Arm data were not processed any further and no preliminary results can be given in this report.

Exemplary ROV result (Station on August 22, North Pole Grid)

ROV measurements of under-ice radiance were performed along a 30x50-m grid on MYI on August 22. The grid was marked in a 10x10-m grid with markers in advance (red

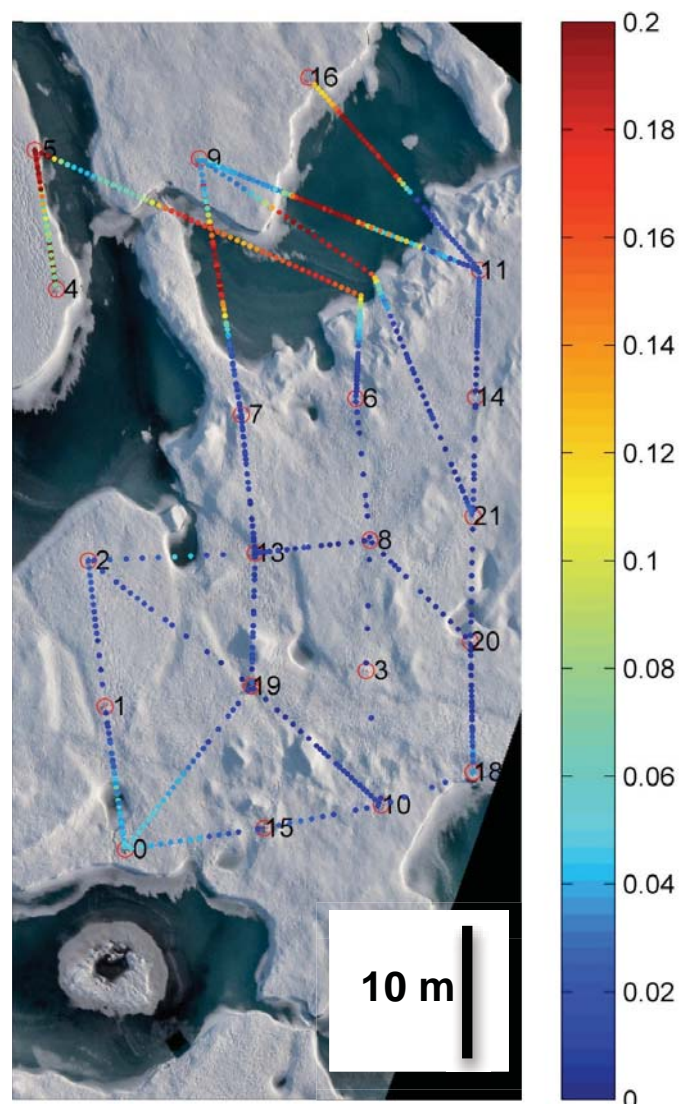


Fig. 3.14: Overlay of an aerial photograph and preliminary results of under-ice transmittance (derived from the radiance sensor) at the North-Pole station on August 22 (78-218). The scale is in fraction, e.g. 0.2 means 20% of solar irradiance reach the bottom of the ice.

3.3 Ice station work and ice cores

circles in Fig. 3.14), except pond locations in order not to destroy the thin new ice crust on top of the freshly frozen pond surfaces. Due to navigational problems, the resulting data grid is not entirely matching the designated grid. However, all points were reached. Measurements with uncertainties in localization are not shown and used for analyses. The aerial photograph was taken during a designated helicopter flight, and distorted to match the marker positions (GPS referenced). Figure 3.14 shows the fraction of incident light reaching the bottom of the sea ice. This result is based on radiance measurements, showing distinct differences of white ice (lower transmittance of about 2-3%) and ponded ice (higher transmittance of 10 to 20%). In addition, the result points to a strong variability of light transmission also within one category (white or ponded ice).

General summary of ROV measurements

Spectral radiometers were operated for the first time under Arctic sea ice on an ROV, which was launched through the ice during ice stations. A comprehensive dataset was gathered from 42 dives on 11 stations. The core data set consists of 11 depth profiles (> 10 m) and 51 horizontal transects (4.4 km of data). In total, 3100 irradiance and 6700 radiance spectra (after quality control and localization) were recorded, resulting in a data set with a spatial resolution better than 1 m in horizontal transects and depth profiles under various sea-ice conditions. Most optical measurements were co-located with physical, biological, and biogeochemical sampling of sea ice and water.

Our results show a broad range of light conditions that can be related to ice and water conditions as functions of sea-ice and snow thickness, melt-pond coverage, and biomass. Although these data are not analysed in any detail, the data set shows that light regimes differ strongly between multi- (MYI) and first-year sea ice (FYI), as well as between ponded and white ice of each ice type. In addition, comparing Atlantic and Pacific water masses also shows strong differences with much more light penetrating much deeper in Pacific than in Atlantic waters.

3.3 Ice station work and ice cores

Mario Hoppmann, Robert Ricker Alfred-Wegener-Institut

Objectives

The goal of the ice station work was to characterize the physical state of the sea ice such as ice temperature and salinity, texture and high resolution ice thickness distribution. This data complements the large-scale aerial thickness surveys in terms of ice type classification with additional parameters than thickness. The analysis of sea ice cores at each station reveals the ice age and the stage of melting and can be used to describe the history of the sampled ice station. High resolution ice thickness data reveals the local ice thickness distribution and shows the representativeness of the ice cores on the ice station. The main objective is therefore to assess the state of different types of sea ice along the cruise track and compare the results with those of earlier cruises and to answer the scientific question of how the basic physical parameters of sea ice have changed in the Arctic Ocean becoming dominated by first-year ice.

Work at sea

The work at sea can be divided into 12 ice stations where several cores were retrieved. Table 3.4 and Figure 3.15 give an overview about the several ice stations and ice cores. On each ice station salinity (SAL) and temperature (ARC) cores were drilled. In addition to that texture cores (TEX) and North Pole cores (POL) were taken at some stations. We choose for each ice station a coring site that covered an area of about 4 m². The salinity and temperature cores were always retrieved in direct vicinity. Afterwards a half pipe was used for cutting and analysing.

Tab. 3.4: List of all sea ice cores with their length and assigned names

Date	Core Name	Length [cm]
11.08.2011	110811-ARC	164
	110811-TEX1	196
14.08.2011	110814-ARC	200
	110814-TEX	
	110814-SAL	190
17.08.2011	110817-ARC	140
	110817-SAL	170
19.08.2011	110819-ARC	135
	110819-SAL	140
	110819-TEX1b	
	110819-TEX2	
22.08.2011	110822-SAL	243
23.08.2011	110823-ARC	280
	110823-POL1	
	110823-POL2	
	110823-POL3	
26.08.2011	110826-ARC	164
	110826-SAL	170
	110826-MAJO	
29.08.2011	110829-ARC	151
	110829-SAL	153
	110829-TEX1	
	110829-TEX2	
31.08.2011	110831-ARC	198
	110831-SAL	153
03.09.2011	110903-ARC	215
	110903-SAL	240
06.09.2011	110906-ARC	181
	110906-SAL	179
	110906-TEX1	
09.09.2011	110909-ARC	116
	110909-SAL	116
	110909-TEX1	
11.09.2011	110911-ARC	156
	110911-SAL	158

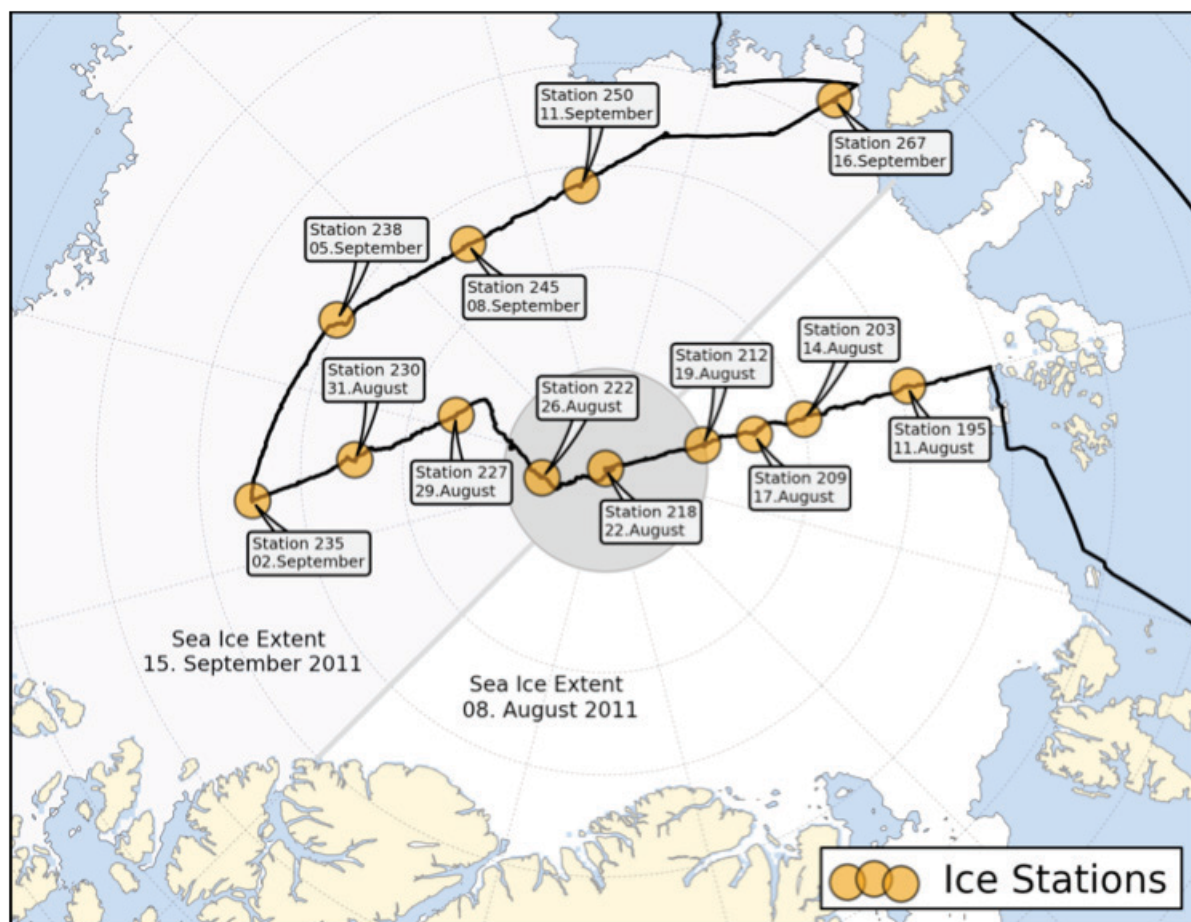


Fig. 3.15: Overview of ice station locations, dates and the corresponding Polarstern station numbers.

In addition, the thickness distribution of each station was mapped by a survey with a hand-held EM ice thickness (EM31 MkII, Geonics Ltd.). The surveys were motivated by general ice type classification but also to provide near real-time ice thickness maps, which were used to identify suitable locations for buoy deployments.

3.3.1 Temperature and salinity

Salinity and temperature of sea ice are two important parameters for describing its properties. The salinity profile of young and first year ice usually shows a characteristic C-shape due to brine movement (Fig. 3.16). The difference in salinity between brine that leaves the sea ice and brine that enters the ice is responsible for the net desalination of sea ice and thus leads to the characteristic bulk salinity profiles in Fig. 3.17. However, environmental conditions exist, which can lead to variability in the salinity. The curve of the August profile shows a very low surface salinity. This can be explained with the surface warming during summer and the resulting snow melt that flush salt downwards through the ice cover.

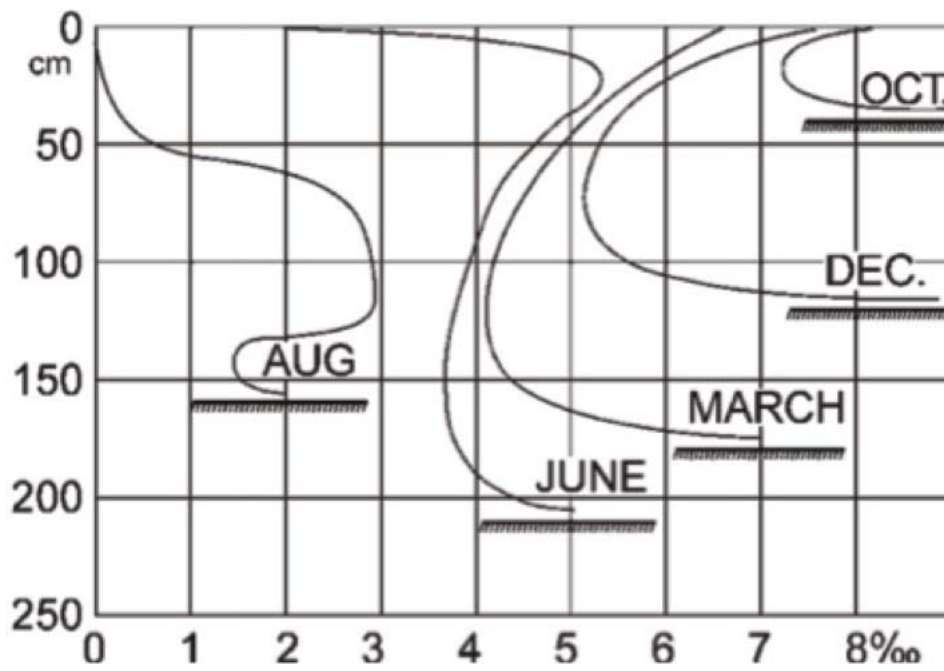


Fig. 3.16: Sea-ice salinity profiles from August to October (after Petrich & Eicken, 2010).

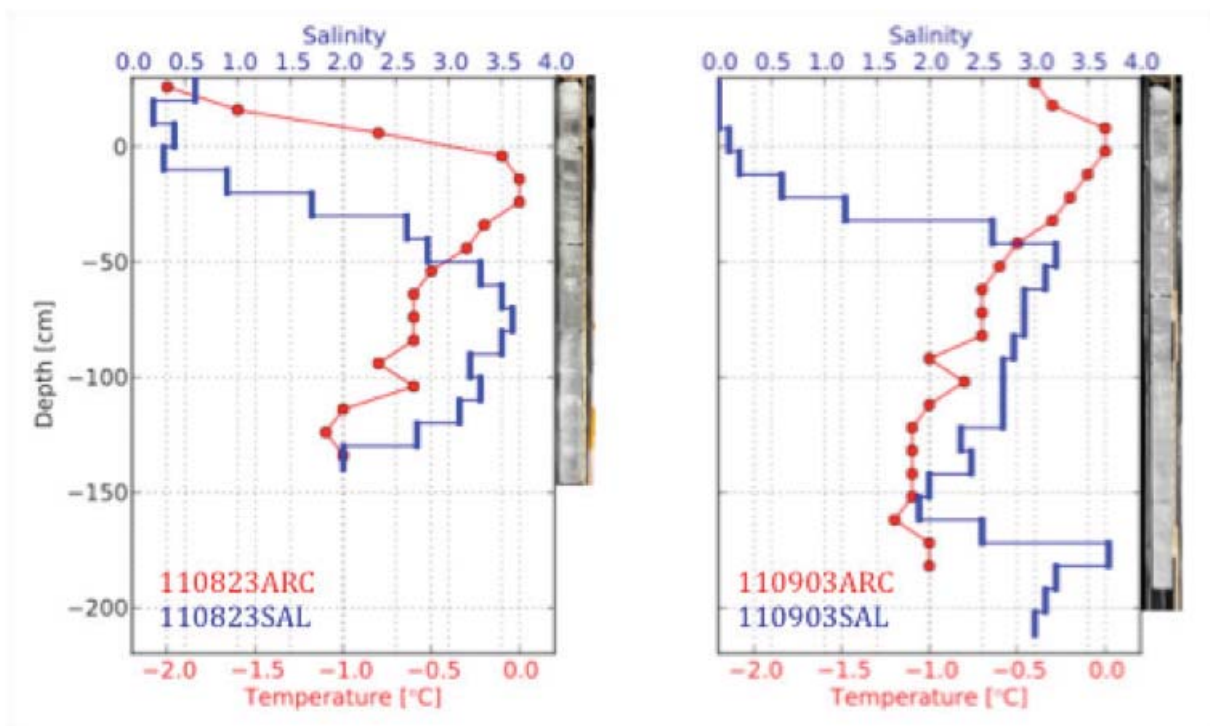


Fig. 3.17: Example of temperature and salinity profiles of two ice stations. Note that the zero in Depth refers to the local freeboard. The difference in length between the 110909ARC and 110903SAL shows that there has to be a kind of roughness at the bottom side of the sea ice because the drill holes were not more than 1 m away from each other



Fig. 3.18: Drilling of small holes in a sea ice core in preparation for temperature measurements every 10 cm

The temperature was measured while in 10 cm steps small holes were drilled into one core to place the rod thermometer (Fig. 3.18). The measurements were made directly after drilling to avoid a change in temperature of the ice. The core was immediately packed into one or several labeled plastic bags and was carried into the ice laboratory to store it at a temperature of -20 °C.

The salinity core was sawed in slices of 10 cm and packed into boxes. After melting of the samples, the salinity was measured onboard with a salinometer of type „WTW Cond 3151“. Afterwards small samples were filled up for biological studies.

Sea ice thickness and draft at the coring sites was measured with a thickness gauge. Furthermore snow or rotten ice at the surface that layer was measured with a ruler stick when present. The slush at the top of the core segments was always thrown away. Sometimes the core length did not fit to the measured thickness that was mainly caused by voids in the ice sample.

Preliminary results

We took the cores during August and September within the melting period of the sea ice, although in September it already started to freeze at the surface. The measurements show a low salinity throughout the cores (Fig. 3.17).

In addition to that the drilled cores exhibit a high porosity. This led to the effect that during sawing the core into slices and also shortly after drilling an unknown amount of brine got lost. That is why some salinity profiles have an irregular shape near zero.

10823ARC and 110903ARC have a similar temperature profile (Fig. 3.17). The top of the profile is ruled by an almost linear increase from the air temperature to the warmest segment of the core, which is always near the freeboard. This is followed by an almost linear decrease down to circa $-1.0\text{ }^{\circ}\text{C}$, which corresponds to the temperature of the underlying ocean. 110823SAL shows a typical C-shaped profile with a very low salinity at the surface above the freeboard, caused by flushing of surface melt water. Core 110903SAL shows another increase in salinity at the bottom of the core that might be due to rafting or multiyear ice.

3.3.2 Ice core texture analysis

On the scale of 100 to 10^{-4} m, sea ice reveals a complex internal structure. Crystals can assume a multitude of shapes, orientations and sizes, depending on the growth conditions of the sea-ice sheet. Brine is included within the ice matrix both between and within crystals. The amount of air and brine inclusions, their orientation, as well as crystal morphology all affect the bulk properties of sea ice. Figure 3.19 shows the different textures that are commonly found in sea ice.

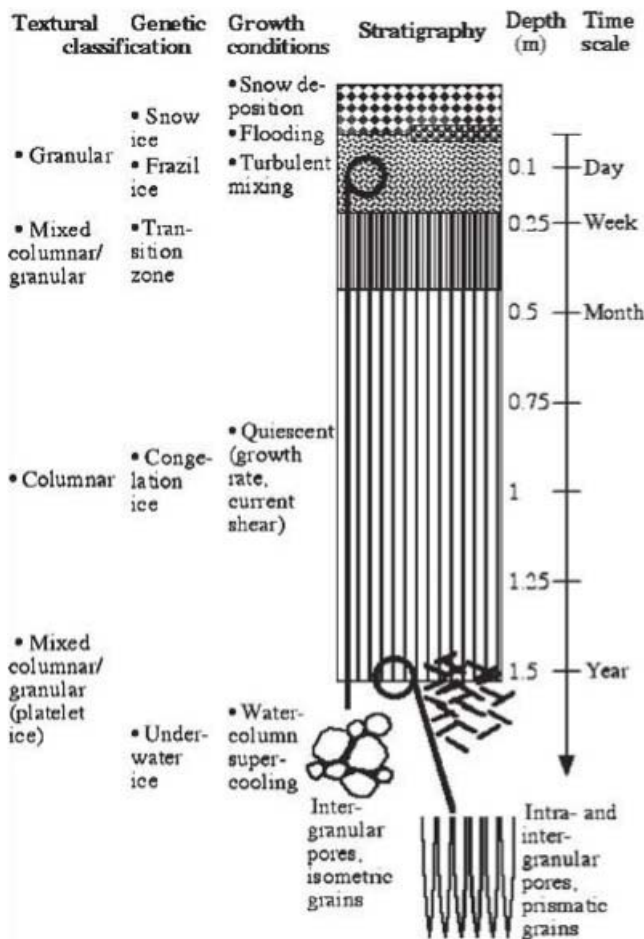


Fig. 3.19: Overview of main ice textures (after Petrich & Eicken, 2010).

The crystal structure of a core taken in the field can reveal information about the growth history of the ice floe and for example help to distinguish between first-year and multi-year ice. Before further processing, each sea-ice core was photographed with a scale on a black background (Fig. 3.20). For the texture analysis, the stored temperature core (ARC) was cut vertically with the help of a band saw, and a thick section of a few millimetres in thickness was prepared and placed on a light table (Fig. 3.21, Tab. 3.5). By sliding a set of crossed polarizer over the thick section, the texture of the core was highlighted and the different crystal structures and sizes, as well as

the amount of bubbles and holes, were documented. Afterwards, the core was photographed to later determine the fraction of brine channels.

3.3 Ice station work and ice cores

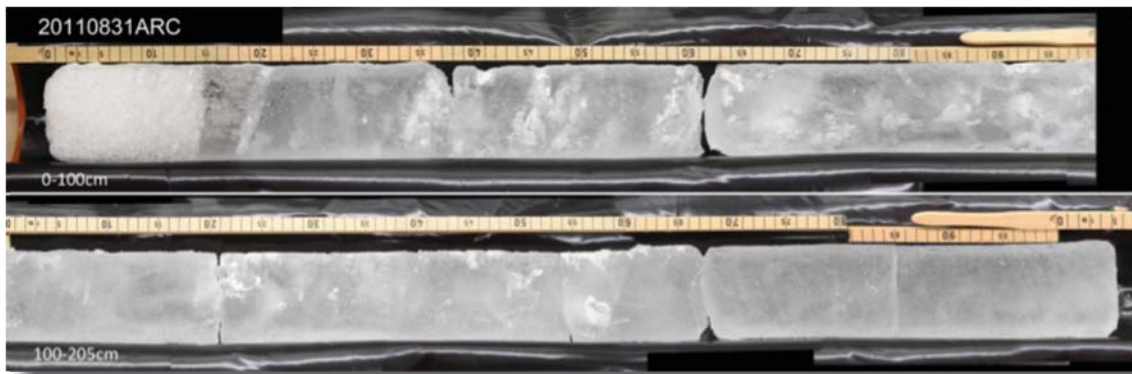


Fig. 3.20: Example photo of archive core taken on August 31, 2011.



Fig. 3.21: Equipment for texture analysis of sea-ice cores. a) Kolbe K200 Band Saw; b) Light table with crossed polarizers; c) Microtome; d) Universal Stage.

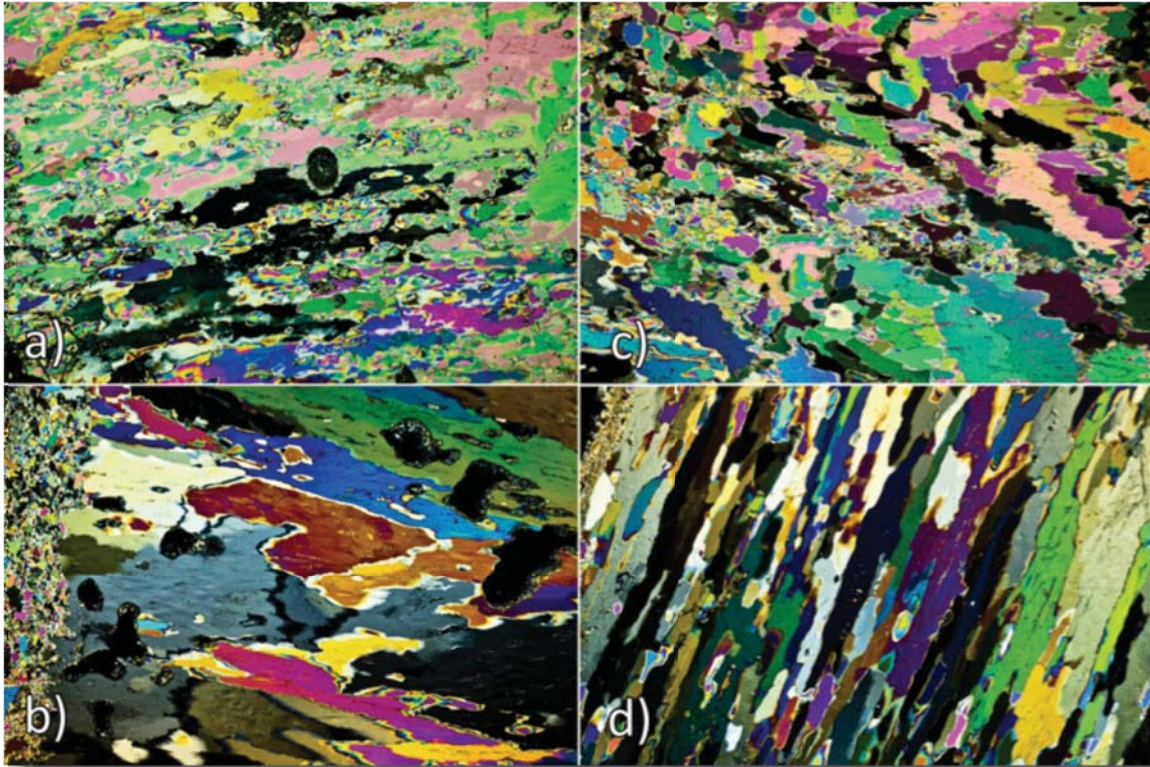


Fig. 3.22: Thin sections of different segments of sea-ice core 20110831ARC. a) 12-24cm; b) 62-74cm; c) 122-134cm; d) 166-174cm.

Depending on the crystal shapes and the overall porosity of the ice core, vertical thin sections were prepared with the help of a microtome, but this was not done systematically. These were afterwards photographed between crossed polarizers on a universal stage (Fig. 3.22).

Tab. 3.5: List of ice core thin sections. The sections are taken from 8 ice cores (see Tab. 3.4 for respective ice stations) in different depth levels.

Core Name	Thin sections
110819TEX1b	054-064 cm
	lowermost 10 cm
110823ARC	110-120 cm
	132-142 cm
	151-161 cm
	185-195 cm
110826MAJO	35 cm horizontal
	139 cm horizontal
110829ARC	140-150 cm
110831ARC	012-024 cm
	024-038 cm
	062-074 cm
	074-086 cm
	086-098 cm

3.3 Ice station work and ice cores

Core Name	Thin sections
	098-110 cm
	110-122 cm
	122-134 cm
	134-146 cm
	146-156 cm
	156-166 cm
	166-175 cm
	175-185 cm
110903ARC	075-087cm
110909ARC	000-010 cm
	010-020 cm
110911ARC	042-054 cm
	072-084 cm
	084-094 cm

Tab. 3.6: Exemplary texture description of ice core 110831ARC

from	to	type	comment
0,0	14,0	columnar	old columnar, small crystals, many small bubbles, crack at 12cm, big holes at 9cm
14,0	22,0	columnar	crystals 5-6cm, pieces missing
22,0	53,0	columnar	crystals 2-4cm, very big hole at 35cm, crack at 38cm
53,0	61,0	columnar	crystals 5-10cm, few big holes at 35cm
61,0	63,0	granular	granular, very small crystals
63,0	95,0	columnar	very big crystals 5-10cm, several cm wide, big holes
95,0	105,0	columnar	elongated crystals 5-10cm
105,0	120,0	columnar	old columnar, crystals 1-4cm, small bubbles, crack at 120cm
120,0	135,0	columnar	crystals 2-4cm, not aligned, various forms
135,0	145,0	columnar	old columnar, small crystals
145,0	153,0	polygonal granular	crystals 2-3cm, crack at 153cm
153,0	166,0	polygonal granular	crystals 1-2cm,
166,0	204,0	columnar	elongated crystals diagonal 5-10cm

Preliminary results

Generally, thick sections from all cores show characteristic columnar growth, with crystal sizes varying between 1 and 15 cm. In the top 20 cm of most cores, the crystal outlines are blurry as signs of ongoing decay. In the detailed texture description (Tab. 3.6), these sections are called "old columnar". In addition, the first 10 cm of each core show a significant amount of small bubbles, originating from the strong summer surface melt. Throughout all cores, brine channels of different sizes are visible, again due to melting processes.

3.3.3 Ground-Based EM ice thickness surveys

High-resolution sea ice thickness data is a standard parameter for the characterization of an ice floe. We used a ground-based EM device (EM31 MkII Geonics Ltd.) for mapping of the sea ice thickness distribution on every ice station (Tab. 3.7). This instrument is based on the same principles, that are used to estimate sea ice thickness from the air (See section: Airborne sea ice thickness surveys), however the application directly on the ice surface allows higher resolution thickness measurements than with the EM-Bird.

Tab. 3.7: List of all EM31 ice thickness surveys with number of measurement points per survey, resulting mean thickness and standard deviation.

Date	Number of Points	Mean Thickness [m]	Std. Dev. Thickness [m]
2011/08/26	2048	2.05	0.54
2011/08/23	4001	1.98	0.47
2011/09/11	7040	2.00	0.57
2011/08/29	10190	2.38	1.34
2011/09/16	14851	2.56	1.31
2011/09/05	18961	2.47	1.32
2011/08/11	19145	2.46	1.32
2011/08/17	21403	2.38	1.28
2011/09/02	25683	2.42	1.22
2011/08/14	30141	2.28	1.19
2011/08/19	31500	2.26	1.18
2011/09/08	36417	2.20	1.14

During the surveys, the EM31 is placed inside a canoe (Fig. 3.23), which is then towed by a person over the ice surface. The canoe is free of metal, which might disturb the electromagnetic signal and allows ice thickness measurements in open melt ponds. The EM data (apparent subsurface conductivity) is stored in an external data logger at 1 Hz. The data logger is connected to a handheld GPS system, which provides UTC timestamp and position. Since the latitude/longitude positions are of limited use on the dynamic sea ice, the positions are corrected for floe drift and rotation by the GPS position and heading of *Polarstern* in post-processing. The result is a Cartesian reference frame in meter, which is centered at the GPS antenna (Trimble1) of *Polarstern*. An example of a data in this reference frame is shown in Figure 3.24. The EM surveys were carried out in the beginning of each ice station, and graphical maps were created shortly after the end of the survey. Therefore, print-outs were available for other ice station work and were used e.g. for the identification of suitable buoy deployment sites.

3.3 Ice station work and ice cores



Fig. 3.23: Ground-based sea ice thickness survey with an EM31 Mk II (Geonics Limited). The instrument was towed over the sea ice in a canoe, which also allowed ice thickness measurements in melt ponds (Photo: Estelle Kilias).

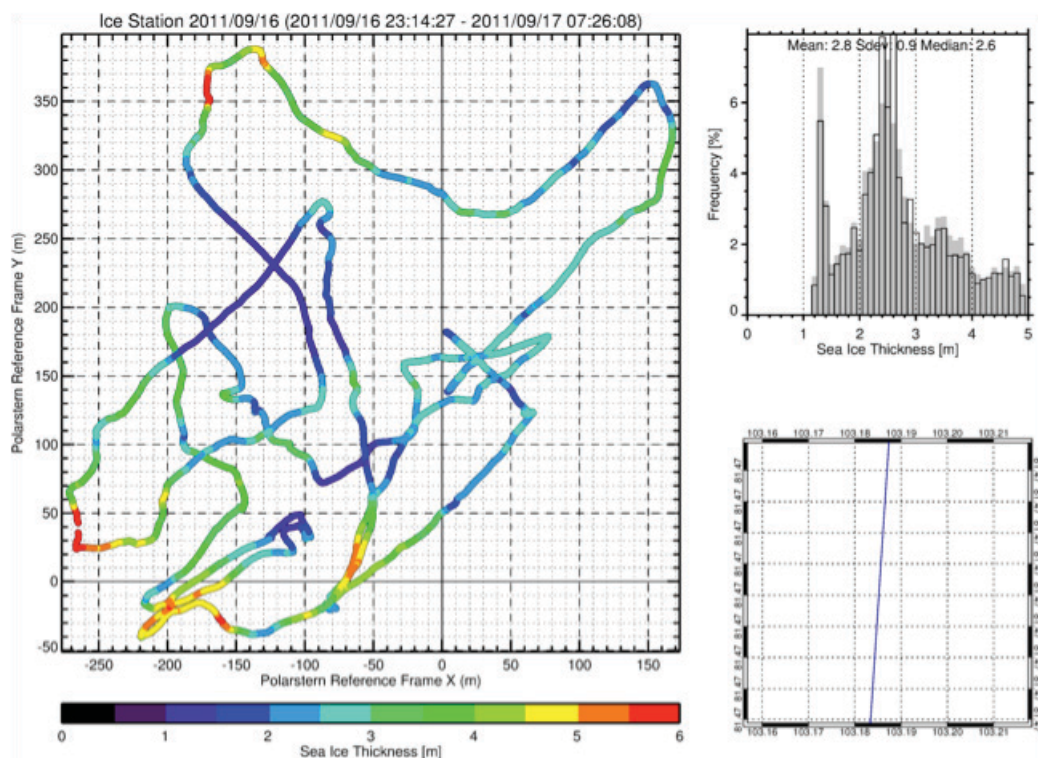


Fig. 3.24: Example of sea ice thickness survey (Ice station 2011/09/16). Coordinates are given in a Cartesian reference frame in meter, where the origin is the GPS antenna of Polarstern (Trimble1).

Preliminary results

From analytical calculation it is known that ice thickness can be reliably retrieved, if the electrical conductivity of the sea water is known with an uncertainty of approx. 100 mS/m. For all the ice stations it is assumed that the conductivity of the sea ice plays no role despite the fact that a lot of brine channels were present during the cruise. Therefore, all calibration results of different ice station were used to construct one relation between apparent conductivity and ice thickness which was used for all ice stations (Fig. 3.15). The relation has the following form:

$$z = -1/a_2 \cdot \ln \left((s_a - a_0) / a_1 \right) - h_0$$

The calibration procedure consists of lifting the sensor and measuring the response at different distances to the ice water interface (instrument height plus ice thickness) in a spot of level sea ice. Since the conductivity of the sea ice is negligible, it is practically the same medium as air. Thus, lifting the sensor is identical to an increase of ice thickness and the readings at different height can be used to calibrate the apparent conductivity (s_a) – ice thickness (z) relation. From the calibration procedures we found the following calibration factors: a_0 : 1026.69, a_1 : -0.797, a_2 : 12.486. The offset $h_0 = 0.14$ m describes the offset of the instrument in the canoe from the top of the ice surface and has to be subtracted from any ice thickness estimate.

The resulting ice thickness distributions of all combined surveys are shown in Figure 3.25. If compared to the results of the airborne surveys, ground-based EM data shows significantly thicker sea ice. This can be related to a selection bias of the ice station work, because only the thickest floes were suitable candidates. More typical floes did not have the structural strength to withstand the manoeuvres of *Polarstern* and their high density of open melt ponds and cracks made safe working with heavy equipment impossible. However, if compared to the ground-based EM surveys from 2007 (*Polarstern* cruise ARK-XXII/2), the thickness distributions are very similar again with identical modal thicknesses of 1.3 m (Airborne survey: 0.9 m).

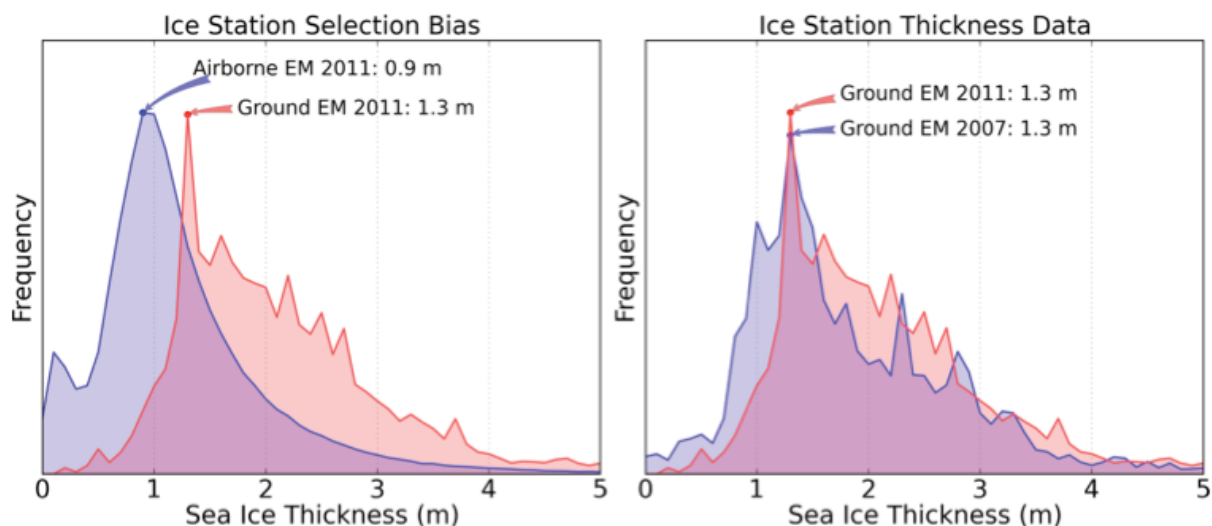


Fig. 3.25: Resulting sea ice thickness distribution from all ground-based EM surveys in comparison to the airborne EM surveys (left) and ground-based surveys from 2007 (right).

3.4 Deployment of drifting buoys

Stefan Hendricks

Alfred-Wegener-Institut

Objectives

Continuous measurements of basic physical parameters, such as air temperature and pressure, ice drift and ice thickness, are sparse in the vast area of the sea ice covered Arctic Ocean. One method to close this data gap is the use of autonomous drifting stations, which report their data over a satellite communication network in near real-time and thus do not need to be recovered. Such measurements are especially rare in the Siberian Arctic, where the predominant drift patterns export drifting stations with the Transpolar Drift Stream in the central Arctic and ultimately into Fram Strait or the Beaufort Gyre. In addition, drifting stations may be destroyed by sea ice deformation events and by activities of polar bears. Therefore cruises into the Siberian Arctic, like ARK-XXVI/3, provide key opportunities to repopulate this region with drifting ice buoys. The main objective of these buoy deployments, which are coordinated by the International Arctic Buoy Program (IABP), is to obtain time series of physical parameters of the air-sea ice interface as input dataset for modelling efforts and remote sensing data products.

Work at sea

Deployments were carried out during regular ice stations, by dedicated landings with the helicopter on ice floes up 40 miles to the side of the cruise track and on ice floes, which were accessed by the mummy chair of *Polarstern*.

We deployed 11 drifting buoys of different design with a special regional emphasis on the Siberian Arctic (Fig. 3.26 and Tab. 3.8). Surface Velocity Profilers (SVP) from MetOcean Data Systems transmits GPS positions and surface temperatures. All buoys were deployed on the ice surface. The temperature recording however, either represents the ice, snow or air temperature, depending on the orientation of the sphere-shaped buoy body. In total, 7 SVPs were deployed for Meteo France and the Norwegian Polar Institute.

The second buoy type (Ice Beacon, MetOcean Data Systems) was deployed on three locations towards the end of the cruise. The IceBeacon (ICEB) transmits position, surface temperature and air pressure, where the sensors are mounted on a mast in a height of 1.2 m above the ice surface. The buoys are anchored in the ice in a roughly 1 meter deep hole. Ice Beacons are equipped with flotation collars, which allows the buoy to survive even total ice melt.

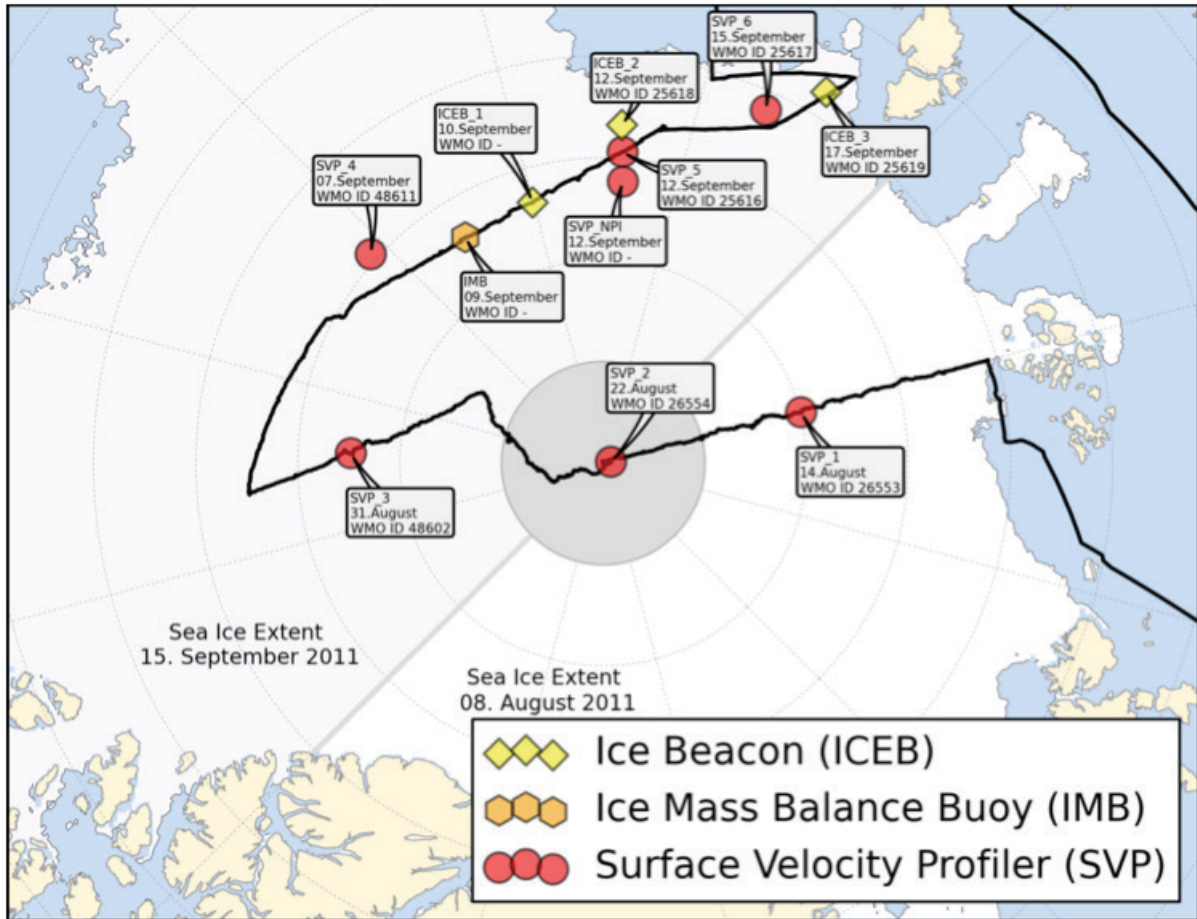


Fig. 3.26: Location and date of deployments and WMO ID's of sea ice buoys. The three buoy types are marked by different symbols.

Tab. 3.8: Type, date and position of buoy deployments during the ARK-XXVI/3. Sea ice thickness was not measured on all deployment sites. ID of the World Meteorological Organization and International Mobile Equipment Identity (IMEI) is given if provided.

Buoy Type	Argos ID	WMO ID	IMEI	Date	Longitude	Latitude	Ice Thickness
SVP	-	26553	300234010826150	14.08.2011	59,4167	85,9833	> 2m
SVP	-	26554	300234010828610	22.08.2011	55,5500	89,8500	2.9 m
SVP	-	48602	300234010826110	31.08.2011	-137,2690	85,0348	-
SVP	-	48611	300234010826630	07.09.2011	-176,9375	83,8559	-
SVP	-	25616	300234010824160	12.09.2011	131,4783	83,8703	-
SVP	-	25617	300234010829160	15.09.2011	110,2440	82,3671	-
SVP (NPI)	-	-	300034013353520	12.09.2011	131,0500	84,4519	-
ICEB	-	-	300034013409520	10.09.2011	150,1830	84,6900	-
ICEB	57009	25618	-	12.09.2011	131,8713	83,3456	-
ICEB	57010	25619	-	17.09.2011	103,1983	81,3543	-
IMB	-	-	-	09.09.2011	166,4240	84,7950	1.1 m

The third buoy type was an Ice Mass Balance Buoy (IMB), provided by the Norwegian Polar Institute. This buoy type requires the installation of three main components: 1) The central electronic, power and communication unit, 2) A mast with two ultrasonic pingers, which measure the range from the sensors to the top snow/ice surface from above and the lower ice surface from below and 3) One mast with air temperature and pressure sensors. With the measured initial sea ice thickness and snow depth values, this buoy type is able to monitor snow accumulation, ice growth as well as top and bottom melt in the following summer and link these measurements to local meteorological conditions. This installation was done during the ice station on September 9 on a piece of multiyear sea ice as part of a multi-buoy station with additional oceanographic buoys. EM31 ice thickness surveys were conducted prior to the deployment to identify a suitable site with a target thickness of less than 2 m. In addition and to protect the buoy from damage by ice deformation, the deployment site ideally had to be in a centre of a floe without any melt ponds or other weak ice structures. The only suitable place however was found on ice with a thickness of 1.1 m.

The buoy activities in the Arctic Ocean are linked together in the International Arctic Buoy Program (IABP). Science data as well as the operational range of buoys with a WMO Id can be obtained there.

3.5 Routine sea ice observations

Priska Hunkeler

Alfred-Wegener-Institut

Objectives

Hourly standardized visual ice observations from the bridge of *Polarstern* were carried in the ice covered part of the cruise track to characterize and document different states and specific features of the sea ice cover. Besides the visual observation photos for documentation were taken in three different directions. For comparison with other acquired data during this and prior cruises the routine visual observation of sea ice are essential. Furthermore, visual observation represents the longest time series of sea ice conditions in the Arctic. But also as database by its own the data acquired show interesting results as presented in this section.

Work at sea

Every hour during day and sporadically during night, depending on observers working shifts, the ice observation was carried out by 27 persons. A computer was installed on the bridge, where the observations directly could be entered by the observer. The observation followed the ASPeCt (Antarctic Sea Ice Processes and Climate) protocol as in 2007 (ARK-XXII/2). The recording software was taken from Worby (1999).

General data (date, UTC time, ship coordinates) were copied from the general data display (DSHIP). Then total ice concentration and the state of open water (e.g. "narrow breaks 50-200 m") were filled into the protocol. Maximal three different ice types (e.g. "first-year 0.3-0.7 m" or "multi-year floes") were then described, starting with the thickest one. For each of the ice types ice concentration, ice thickness, floe size, topography (e.g. "level ice" or "consolidated ridges") with

areal coverage and average sail heights, snow type (e.g. "cold old snow") and snow thickness were chosen from a drop-down list. By convention the comment line was used for melt pond concentrations, since no dedicated melt pond classifications exist in ASPECT.

The spatial variability was taken into account by taking the average between observation to port side, ahead and to starboard side. Ice thicknesses of tilted floes were estimated by observing a stick attached to the ships starboard side (Fig. 3.27).

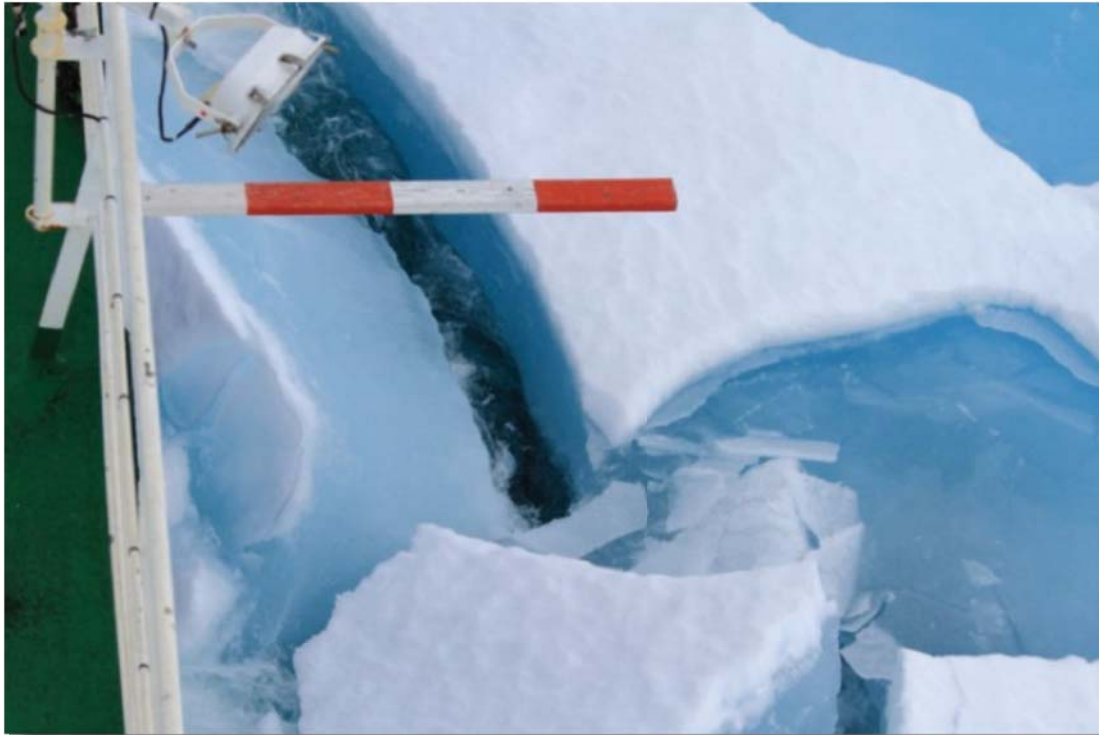


Fig. 3.27: Observation from the bridge: Ruler to obtain the thickness of tilted sea ice when the ship is breaking ice. This broken floe has a thickness of approximately one meter.

Meteorological data (sea temperature, air temperature, true wind speed, true wind direction, visibility) were also copied from the bridges computer and filled into the protocol. Cloud cover and actual weather were estimated by the observer. Three photos were then taken (view to port side, ahead and to starboard side, Fig. 3.28 and 3.30) and their numbers were filled into the protocol.

3.5 Routine sea ice observations

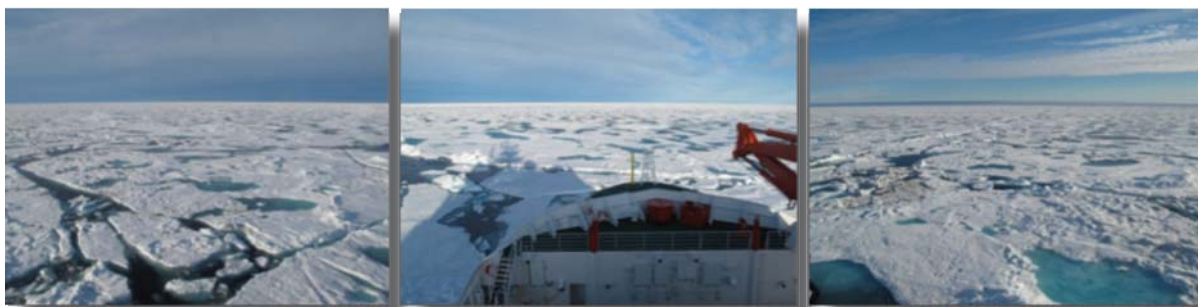


Fig. 3.28: Examples of ice observation photos: good visibility, snow-free sea ice (August 18, 2011 01:00 UTC) taken from the bridge of Polarstern. View to port side, ahead and to starboard side. Good visibility, snow-free melt ponds.



Fig. 3.29: Examples of ice observation photos: bad visibility, snow-covered sea ice <math>< 2</math> m (September 10, 2011 07:00 UTC) taken from the bridge of Polarstern. View to port side, ahead and to starboard side.

The software was developed for Antarctic sea ice, what caused some problems. Because there are no melt ponds in the Antarctic the comment line had to be used for that purpose, what resulted in some inconsistent entries. Further, thin multi-year ice (< 2 m) was observed. But as this not foreseen in the Antarctic, an error showed up in the software and a minimum of 2 m had to be entered.

Depending on the weather condition there was more or less space for interpretation. Snow on melt ponds complicated the observation, as Figure 3.31 and 3.32 are indicating. Also the personal view and estimation of the different observers has to be kept in mind.

Preliminary results

The ice observations were carried out between August 9, 2011 when *Polarstern* entered ice-covered waters in the North of Franz Joseph Land till September 19, 2011 passing last floes when *Polarstern* left the ice zone the Laptev Sea. The ice conditions were favourable for ship operation. Only after the North Pole, *Polarstern* turned westwards because of severe ice conditions. The Alpha Ridge couldn't be studied as planned and the ships track was relocated to the one of ARK-XXII/2 in 2007. In total 324 observations at 42 days were carried out, what are 7.7 observations per day. During station work under unchanging ice conditions no data was recorded, what gives a more representative distribution of observations.

Ice types

The mean total ice concentration was 86.5%. Total ice coverage could be observed mainly when refreezing started and new ice was built after August 23, 2011. As *Polarstern* went further south open water could be observed again more frequent. First multi-year ice was observed at August 14, 2011 on the way to North Pole. After September 5, 2011 the observation of multi-year ice was less frequent as *Polarstern* went to the west. In Figure 3.30 photos of new-built, brash, first-year and multi-year ice are illustrated and in Figure 3.31 the occurrence in per cent is shown.

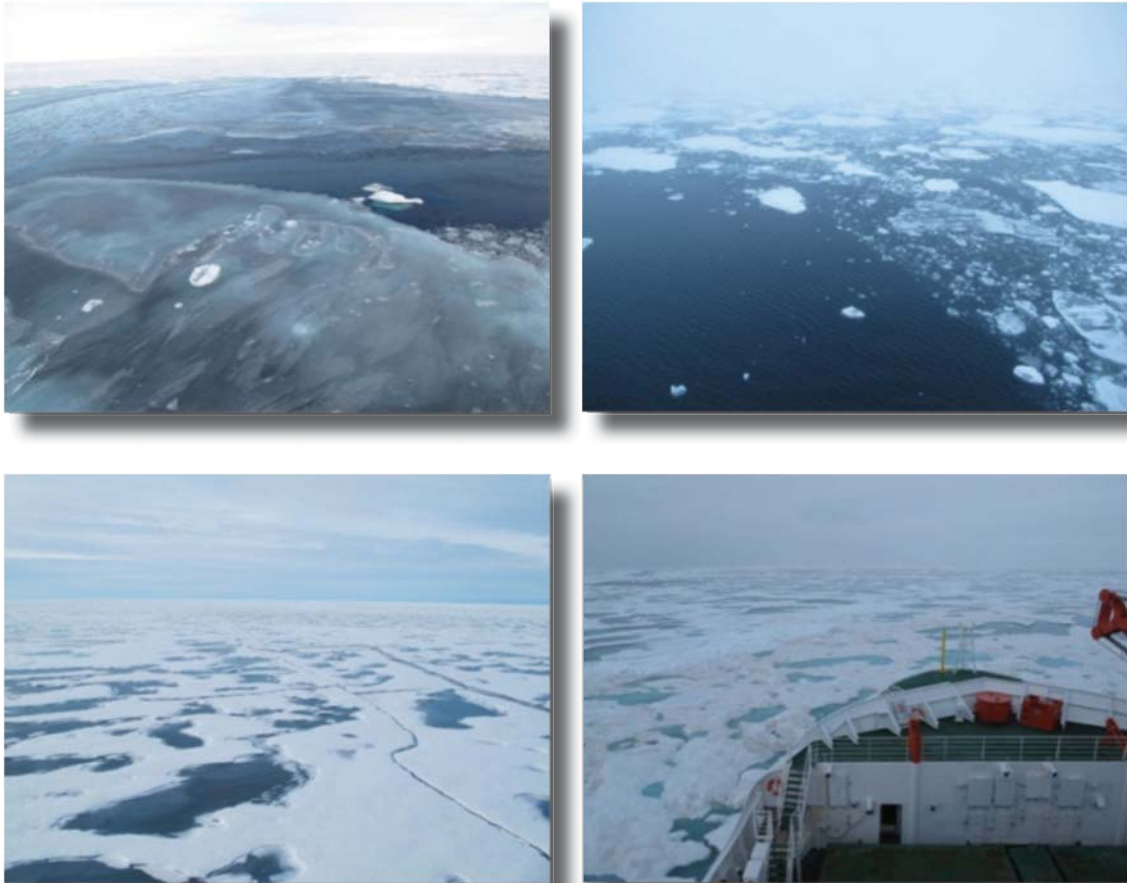


Fig. 3.30: Different ice types. Above: Left: New-built ice, finger rafting (August 24, 2011 08:00 UTC). Right: Brash ice and open water September 18, 2011 21:00 UTC. Below: Left: First-year ice August 23, 2011 19:00 UTC, Right: Multi-year ice August 14, 2011 10:00 UTC.

3.5 Routine sea ice observations

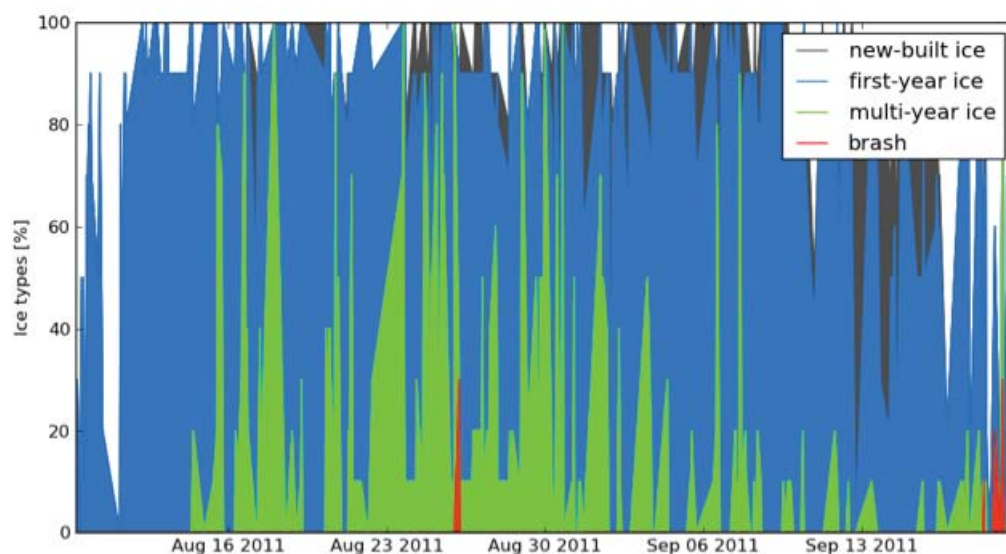


Fig. 3.31: Ice type occurrence of multi-year-ice (green), first-year ice (blue), young ice (grey), brash ice (red) and open water (white) observed from the bridge of Polarstern between August 9 and October 19 2011.

Ice thickness and topography

The average level ice thickness of multi-year ice was 230 cm and of first-year ice 96cm (Tab. 3.9), what is in good agreement with the EM-data. Multi-year ice thickness is overestimated due to the required 2 m (green in Fig. 3.32). Newly formed ice was mainly observed as nilas or thin young grey ice (Tab. 3.10).

Tab. 3.9: Sea ice thickness observation of first-year and multiyear ice classes in centimetres: Number of observations and thickness statistics.

Ice type	First-year 30-70cm	First-year 70-120cm	First-year >120cm	First-year all data	Multi-year >200cm	Brash ice
Number of observations	58	206	45	309	146	5
Minimum [cm]	30	70	120	30	200	10
Maximum [cm]	70	120	300	300	500	40
Average [cm]	54	95	157	96	230	30

Tab. 3.10: Sea ice thickness observation of thin ice classes in centimetres: Number of observations and thickness statistics.

Ice type	Frazil	Shuga	Grease	Nilas	Young grey ice (10-15cm)	Young grey white ice (15-30cm)
Number of observations	1	1	4	59	31	9
Minimum [cm]	2	2	1	1	10	15
Maximum [cm]	2	2	2	10	15	30
Average [cm]	2	2	2	6	12	22

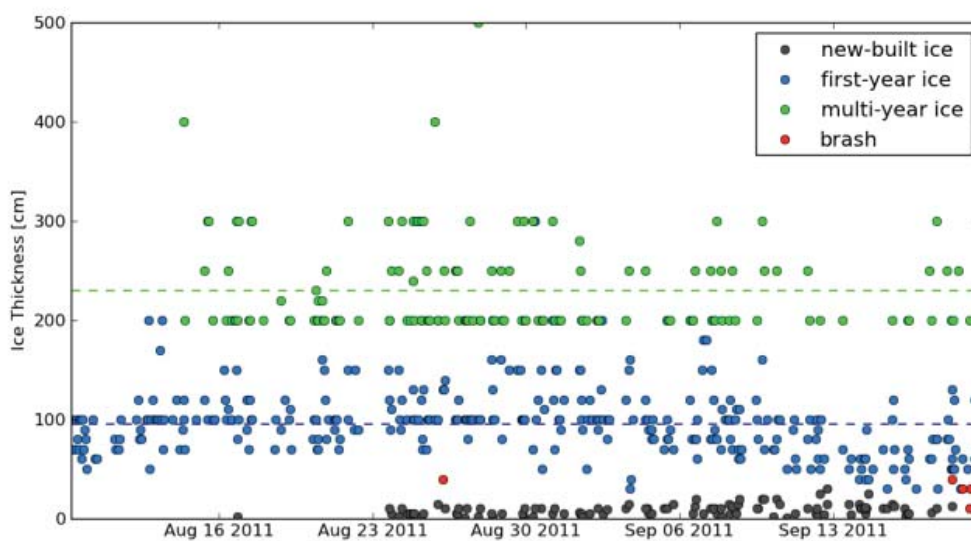


Fig. 3.32: Ice thickness of multi-year-ice (green), first-year ice (blue), young ice (grey) and brash ice (red) observed from the bridge of Polarstern between August 9 and October 19, 2011. Dashed lines show the mean first-year and multi-year ice of 96 and 230 cm.

The main topography type observed were "old, weathered ridges" with 43%, "level ice" with 32% and "consolidated ridges" with 17%. Only few per cent of "new unconsolidated ridges", "new ridges filled with snow" and "finger rafting" were observed. In general 52% of the ridges covered an ice floe with 0-10% and 21% with 10-20%. 45% of the ridges reached an average sail height of 0.5m, 36% of 1m and 14% of 1.5m. As the view was from above on the ice the sail height may be underestimated.

Melt ponds and snow coverage

Melt pond concentrations on ice floes of first-year and multi-year ice were estimated. Mean melt pond concentration on multi-year floes was 20% and on first-year floes

3.5 Routine sea ice observations

46% (green and blue lines in Fig. 3.33). Because not all observers divided between melt ponds on first- and multi-year ice, their estimated average values are shown in black. At the end there were fewer observations of melt ponds, because it was difficult to do an estimation of a floe covered with snow (Fig. 3.29). The amount of increased brash ice at the end of the cruise may also lead to fewer observations. Snow coverage on first-year ice is in average 3.7cm high, starting from first snow observation of August 13, 2011 the average snow thickness is 4.1cm.

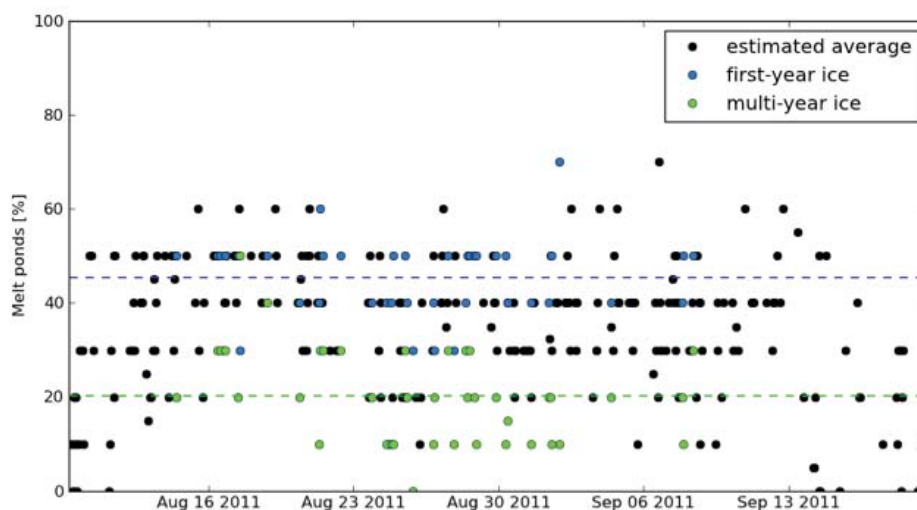


Fig. 3.33: Melt pond concentration of multi-year-ice (green), first-year ice (blue) and in average (black), observed from the bridge of *Polarstern* between August 9 and October 19, 2011. Dashed lines show the mean first-year and mean multi-year melt pond concentration of 46 and 20%.

3.6 References

Petrich, C., Eicken, H. 2010. Growth, Structure, and Properties of Sea Ice, in *Sea Ice*, edited by D. N. Thomas and G. Dieckmann, pp. 23-78, Blackwell Science, Oxford, UK.

Worby, A. P., 1999. Observing operating in the Antarctic sea ice: A practical guide for conducting sea ice observations from vessels operating in the Antarctic pack ice.

Acknowledgements

We thank the crew of the *Polarstern*, FIELAX, and the team of Heli-Service International for their excellent collaboration. The hourly sea ice observation data only exists, because of all the volunteers. Many thanks to Ursula Schauer who made this cruise possible.

4. PHYSICAL OCEANOGRAPHY

Ursula Schauer¹, Benjamin Rabe¹,
Bert Rudels², Sergey Pisarev³,
Andreas Wisotzki¹, Hiroshi
Sumata¹, Ian Waddington⁴, Oliver
Zenk⁵

¹ Alfred-Wegener-Institut

² Department of Physics, University of
Helsinki, and Finnish Meteorological
Research Institute

³ Shirshov Institute of Oceanology

⁴ International Arctic Research Institute

⁵ OPTIMARE Marine Messsysteme GmbH
& Co. KG

Background and Objectives

Not only sea ice coverage, but also the circulation and water mass properties of the Arctic Ocean have been changing considerably during the past decades. The waters advected from the Atlantic and the Pacific became much warmer and, for the Atlantic part, saltier and on the other hand much more fresh-water was stored recently in the Arctic Ocean than in the 1990s. To understand the underlying processes and the impact of these changes their further evolutions need to be observed. Therefore the aim of the oceanographic part of this cruise was to document and quantify the present state of the water mass distribution and circulation in the Eurasian and northern Canadian basins. In the context with appropriate modelling, the observations will be fundamental to distinguish between variability and long-term trends in the Arctic.

In the Arctic, the imported ocean waters are subject to transformations through cooling, freezing and melting. The pathways and properties of the two branches of warm Atlantic Water, flowing into the Arctic Ocean through the Fram Strait and the Barents Sea and travelling presumably in cyclonic loops along the continental slopes and ridges, however vary and so does the flow of Pacific Water.

In the central Arctic both inflows, even though getting warmer, are inhibited from releasing their heat to the atmosphere by the thick layer of fresh water, which is supplied by continental runoff and ice or meltwater. However, the variable distribution of the fresh water may facilitate some heat release in certain areas. E.g. the recent convergence of fresh water in the central Arctic may for dynamical reasons lead to a weakening of the stratification along the warm boundary current at the rim of the basins. Changes may also occur from the different wind mixing with and without ice cover and the fact that now large areas have longer seasons without sea ice.

There are also indications of a (recent) change of the pathways of the Atlantic Water. The warmer branch from Fram Strait seems to return already in the Nansen Basin back to the Atlantic sector and also the flow of Barents Sea water into the Canadian Basin may be reduced in the context with the strengthening of the Beaufort Gyre. Such changes will affect the properties of the water returning to the North Atlantic and hence directly or indirectly influence the Atlantic meridional overturning circulation.

To address these questions hydrographic sections were recaptured that were taken in the Eurasian Basin during the cruises with *Polarstern* and *Oden* since the early 1990s. To extend the observational range of the ship survey in space and time, autonomous, ice-based buoys as well as bottom-moored observatories were deployed. The ice-tethered buoys were deployed in upstream regions of the Transpolar Drift so that they would cross the Eurasian Basin. The moorings were deployed near the south-eastern end of Gakkel Ridge to obtain first year-round data of the return flow in the Eurasian Basin.

Work at sea

CTD casts and ship-borne ADCP measurements

Full-depth sections and several shallower casts of temperature and salinity were obtained by using three Conductivity Temperature Depth (CTD) systems (Fig. 4.1). Two of these systems, an XCTD-system and a newly developed light full-depth CTD-system, enabled profiles to be taken from ice floes far from the ship that were reached by helicopter. This extended the observational range. In total, 228 CTD profiles were taken.

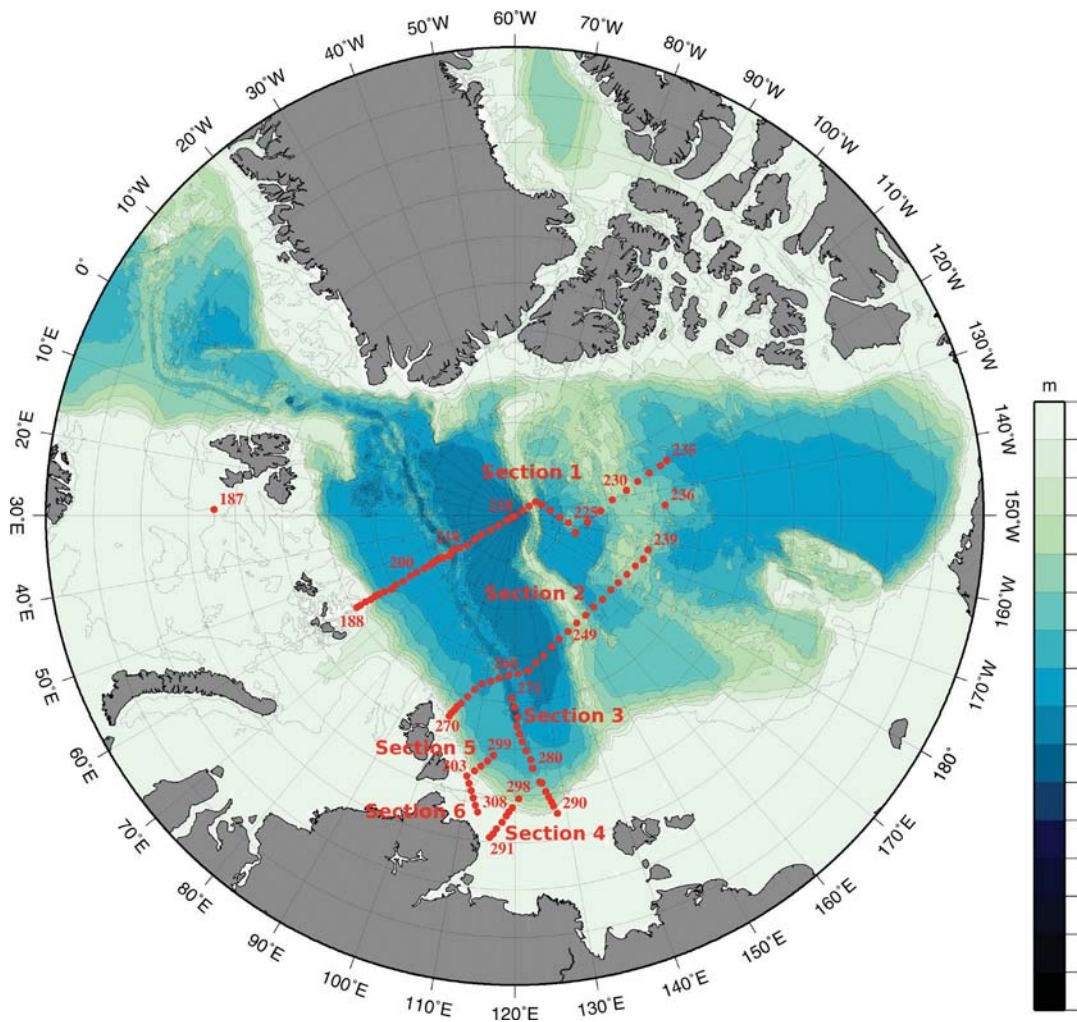


Fig. 4.1: Seafloor bathymetry with locations of CTD stations.

136 profiles were taken at 111 stations with a standard CTD/rosette water sampler system from Sea-Bird Electronics Inc. The SBE9+ CTD (S/N 937) was equipped with duplicate temperature (S/N 2929 and 1373) and conductivity (S/N 2470 and 3290) sensors and was connected to a SBE32 Carousel Water Sampler (S/N 718) with 24 12-liter bottles. Additionally, a Benthos Altimeter (S/N 46611 and 47768), a Wetlabs C-Star Transmissometer (S/N 1198), a Wetlabs FLRTD Fluorometer (S/N 1853) and an SBE 43 dissolved oxygen sensor (S/N 1834) were mounted on the carousel. The SBE 43 contains a membrane polarographic oxygen detector. The algorithm to compute oxygen concentration requires also measurements of temperature, salinity and pressure which are provided by the CTD system.

To calibrate the oxygen profiles water from CTD rosette bottles was measured onboard with Winkler titration; in addition, dissolved oxygen water samples were measured for other groups on-board, giving a total of 534 measurements.

208 salinity samples for the calibration of the conductivity sensors were taken from rosette bottles and analysed with a recently developed salinometer manufactured by Optimare Sensorsysteme AG (Bremerhaven, Germany) with Standard Water Batch p152. Further samples were taken by other groups on-board for chemical and biological analysis.

A XCTD-1, by Tsurumi-Seiki Co. Ltd. (Yokohama, Japan) was used to obtain 88 CTD casts up to 1100 m water depth while underway from the ship and from ice floes reachable by helicopter. The system consisted of a launcher for expendable CTD probes and a mobile deck-unit for data acquisition. The probe sinks down with constant velocity measuring temperature and conductivity.

A third system utilized a new light-weight, mobile winch with a thin rope. This winch has been developed by Gereon Budéus at AWI and was tested during this cruise for the first time. The winch was operated with a Seabird SBE-19 sensor package (S/N 6666) mounted together with a buoyancy package (ceramic spheres in plastic casing) to minimize the load for the winch motor. Four profiles were conducted successfully with this system.

One advantage of the mobile CTD system is that it can be used away from the influence of the ship that may destroy the original structure of the upper ca. 15 meters of the water stratification, particularly when using the thrusters during station work. Two profiles from the mobile CTD at the Gakkel Ridge showed mixed-layer depths of between 15 to 20 m, with a relatively uniform temperature and salinity structure of the layer below 4 m (Fig. 4.2). Layers shallower than 4 m, possibly containing melt water, could not be sampled as the system had to be deployed and recovered together with the buoyancy package above.

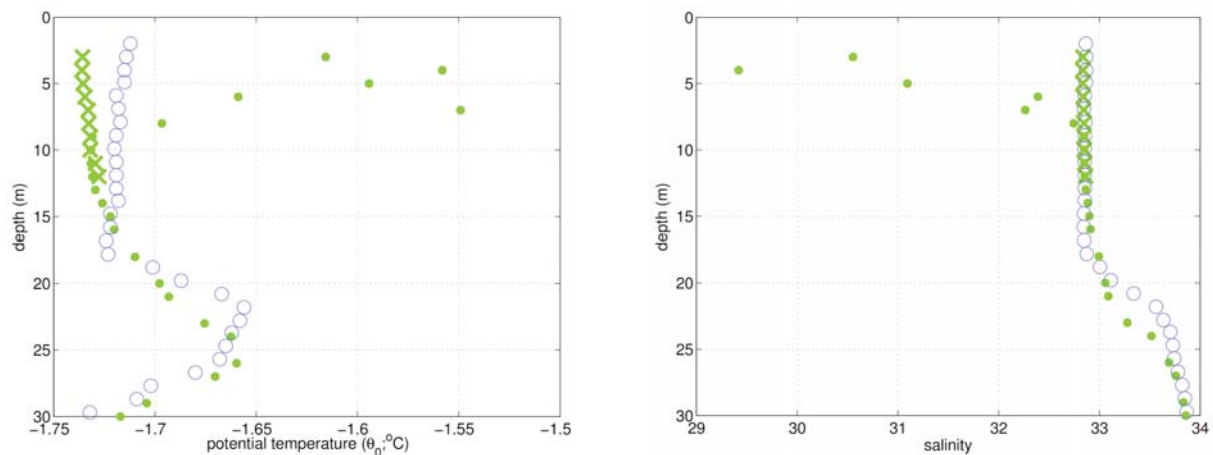


Fig. 4.2: Comparison of mobile CTD (on the ice floe, green) and ship CTD (blue) profiles taken at station 209-4. The crosses represent values from the mobile CTD upcast, otherwise downcasts are shown (dots).

Underway measurements with a vessel-mounted narrow-band 150 kHz ADCP from TRD Instruments and with two Sea-Bird SBE45 thermosalinographs were conducted to supply water current velocity and temperature / salinity data, respectively. The thermosalinographs are installed in 6 m depth in the bow thruster tunnel and in 11 m depth in the keel, although the bow system was switched off while the ship was crossing sea ice. The salinity of both instruments was controlled by taking water for calibration. The ADCP worked well throughout most of the cruise with very few data gaps.

Data from the ship rosette CTD, underway CTD and the ADCP will ultimately be available through the PANGAEA database (World Ocean Data Center #4). In order to provide year-round autonomous measurements, ice-tethered platforms with various instrumentation and several bottom mounted moorings were deployed, as detailed in the following sections.

Bottom moored arrays

During the cruise 3 moorings were recovered and 5 moorings were deployed.

Deployment of moorings near the Gakkel Ridge:

To obtain timeseries of velocity, temperature, salinity and ice thickness as well as samples of sinking particles in the Eurasian Basin return flow of Atlantic Water, five moorings were deployed at two locations near the Gakkel Ridge, one in the Amundsen Basin and one in the Nansen Basin. The recovery of these mooring is planned for the *Polarstern* expedition in 2012. The details of the moorings are given in Fig. 4.18 to 4.21.

Two mooring pairs with identical design and one extra mooring were deployed on either side of the Gakkel Ridge (Fig 4.3): One mooring of each pair carries a profiling CTD system, designed by Gereon Budéus at AWI, to give nearly full-depth profiles of temperature and salinity once a day. The other mooring has

several current meters. Two of them are TRD Instruments ADCP that measure the shear profiles of the upper 800 m. Due to close vicinity to the magnetic pole, the horizontal magnetic field intensity falls below the value required to obtain accurate measurements by the ADCP internal compass. However, the vertical shear will be accurate within each profile, as the data is recorded in instrument coordinates, and the ping interval was set to near minimum to minimize the influence of angular movement of the ADCP within each ensemble. Further instrumentation included two Aandera current meters to measure current speed at depths not covered by the ADCPs, three Seabird SM 37 for point measurements of salinity, temperature and depth and an upward looking sonar to measure ice draft. Sediment traps are located at 200 m depth and near the sea floor. Only on the Amundsen Basin side of the Gakkel Ridge, an additional profiler for temperature/salinity was deployed to measure the upper 200 m. The deployments were on fairly level sea floor, and the region of the deployments was ice-free.

Three moorings belonging to the Russian-US program Nansen and Amundsen Basins Observational System (*NABOS*, <http://nabos.iarc.uaf.edu>) were successfully recovered at the continental margin north of the Laptev Sea and north of Franz-Josef-Land. The recovery was extremely difficult, due to failure of the bottom releases (double at each mooring). Only the experience and skill of the *Polarstern* crew allowed exact location of the moorings using the fish finder (echosounder) and recovering them using a tugging method, whereby the mooring is encircled with a line between the ship and a dinghy and subsequently pulled toward the ship. The mooring north of Franz Josef Land was recovered in partial ice cover, whereas the two moorings north of the Laptev Sea were in ice-free waters. With the recovery, existing observation time series at the respective locations could be extended by up to 4 years.

Ice-tethered buoys

In order to obtain year-round measurements of ocean temperature, salinity, velocity, oxygen and bio-optical parameters as well as air temperature, pressure and wind velocity, ice-tethered platforms with various instruments were deployed. They consist of a sub-ice sensor system that is connected by a cable to a surface unit that transmits the data to shore via satellite. Since they drift with the host ice floe, they have the potential to provide observations over a substantial region of the Arctic Ocean. Five different types of ocean buoys were deployed, all of which record their geographic position at time of measurement:

3 ITPs (Ice-Tethered Profiler) equipped with Seabird CTDs that will sample temperature, salinity and dissolved oxygen profiles once per day between the surface and 760 m water depth,

1 Bio-ITP, equipped as the other ITPs, but with a bio-optical package, measuring Photosynthetically Active Radiation (PAR) and Chlorophyll Fluorescence,

2 POPS (Polar Ocean Profiling System) equipped with Seabird CTDs that will sample temperature and salinity profiles once per day between the surface and 800 m water depth, and meteorological sensors for surface air temperature and barometric pressure,

1 ITAC (Ice-tethered Acoustic Current profiler) consisting of a surface unit connected to an RDI ADCP (150 kHz, Quartermaster) that measures the velocity profile of the upper 300 m every two hours,

1 ITBOB (Ice-Tethered Bio-Optical Buoy) consisting of a surface unit with GPS and satellite communication, connected to three YSI probes with radiance (PAR) sensors, temperature and conductivity probes, an oxygen optode, a fluorescence probe, one 5 m long thermistor chain in and under the ice, and an additional PAR sensor.

Further autonomous buoys are described in the Sea Ice Physics section.

In total, 7 ocean buoy systems were deployed on 5 ice floes (crosses Fig. 4.3). One further POPS system was deployed but had to be subsequently recovered due to hardware problems (diamond in Fig. 4.3).

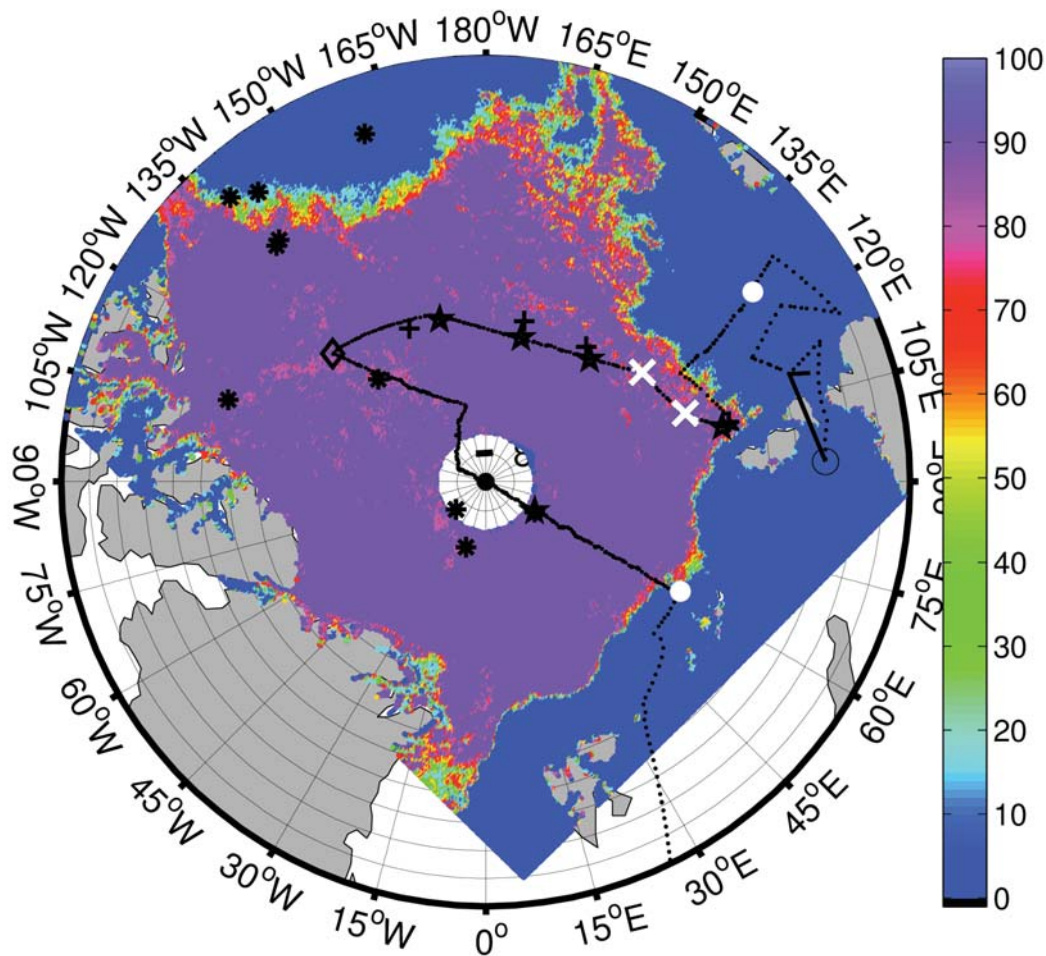


Fig. 4.3: Map of CTD-profiling buoy (ITP and POPS) locations at deployment (pentagons) and on September 24 (crosses). Asterisks show the locations of other ITP and POPS transmitting data in the Arctic Ocean at that time. The colour scale indicates the sea ice concentration (%; AMSRE). The black line represents the cruise track. The first ocean buoy deployment was a POPS. The diamond represents a further POPS that was recovered subsequent to deployment because of a technical failure. The locations of the bottom mounted moorings are shown by a white X (AWI mooring cluster) and a white circle (NABOS moorings).

Four ITP / Bio-ITP systems manufactured by Woods Hole Oceanographic Institution (WHOI) in Woods Hole (Massachusetts, USA) measure twice daily temperature/salinity/depth/oxygen profiles with 1 Hz (nominally 0.25 m) vertical resolution between 8 and 760 m using a profiling CTD unit (Seabird Electronics, Inc. model 41CP) on a wire tether and an inductive modem to communicate the data to a surface unit (SU). The ITP SU records GPS position and relays all data via an Iridium satellite modem connection to a server at WHOI. The ITPs are manufactured by WHOI with a profiler from McLane Research Laboratories (Falmouth, Massachusetts, USA). The Bio-ITP measures, in addition, photosynthetically active radiation and chlorophyll fluorescence throughout the profiles. Two ITP were provided by AWI and the remaining ITP and one Bio-ITP by WHOI.

Two systems similar to the ITP, Polar Ocean Profiling Systems (POPS) manufactured by MetOcean Data Systems (Dartmouth, Nova Scotia, Canada) were also deployed. The POPS were configured to measure temperature/salinity/depth profiles at the same vertical resolution as the ITP systems and surface atmospheric temperature and barometric pressure. The data sampling intervals for meteorological and ocean profiling data were set to be 3 hours and 1 day, respectively. However, it was found that the newly incorporated NOVA profiler shows about 4 m gaps at irregular intervals due to design limitations of the profiler controller.

An Ice Tethered Acoustic Current profiler (ITAC) by Optimare Sensorsysteme AG (Bremerhaven, Germany), measuring ocean current velocity profiles from 10 m under the ice to a depth of around 300 m, incorporates an ADCP mounted about 4 m from the top of the ice floe. The ADCP is rigidly connected via a stainless steel pole with a wooden beam on the surface. A cable provides the electrical connection to a surface unit with a GPS receiver and an Iridium modem. To allow the recording of the ADCP orientation even in regions of low horizontal magnetic field strength, two further GPS are positioned about 98 m in opposite directions from the surface unit and in line with the wooden beam and the ITAC SU. Data are relayed daily via the Iridium Short Burst Data (SBD) message service to an email address at Optimare. The communication is bi-directional and also allows setting of data sampling parameters via SBD messages, both for the ADCP and the ITAC SU (e.g. GPS sampling rate).

The ITBOB (Ice-Tethered Bio-Optical Buoy) consisted of a surface unit with GPS and satellite communication, connected to three YSI probes with radiance (PAR) sensors, temperature and conductivity probes, an oxygen optode and a fluorescence probe. The three packages were deployed in the ice, and 20 cm as well as 1m under the ice flow. In addition, a 5 m long thermistor chain was deployed in and under the ice, and a PAR sensor was connected to the surface unit. Results from the first 6 weeks of deployment showed a change in bio-optical parameters along with a rapid temperature decrease and diminishing PAR in mid-September. During the initial phase the freeze-in effect of the YSI 1 module into the ice floe showed in rapidly increasing salinities and changing oxygen concentrations. The PAR sensors showed strong daily variations in light availability. Already in mid-September only a limited amount of light is available in the ice and below the ice (max $2 \mu\text{mol photons m}^{-2} \text{ s}^{-1}$), which was further decreasing with time. First trends in oxygen, temperature and salinity were observed. Oxygen concentrations increased despite increasing salinity, probably dominated by the decreasing temperature. Thus already this short-term continuous sensor record provided valuable information on physico-chemical gradients and behaviour within the ice and in the transition zone between the sea ice and the open water.

All ocean buoys were distributed on six sites, of them on the section crossing the North Pole, but most on the section from the Canadian Basin to the Laptev Sea in order to maximise their expected drifting time and range (Fig. 4.3). One site was named a 'Super Buoy station' where an ITP, ITAC and ITBOB were deployed on the same ice floe. All ocean buoys were deployed while the ship was docked to the ice floe.

The search for suitable floes was often hampered by bad weather which made helicopter use impossible, so that several ice floe searches had to be carried out from the ship. Finally for all buoys multi-year ice floes with large ridges and ice thicknesses of more than 1 m were found.

Performance and failures

The autonomous ocean buoys drifted during the cruise since deployment (Fig.4.3). The POPS data will be processed in-house at AWI, but will be made available in public databases, either ARGO or PANGAEA, in the future. The ITP data can be downloaded from the WHOI ITP web site.

So far, one POPS sent profiles until September 17, but no profiles thereafter. One of the ITPs suffered a technical failure of the inductive modem and has not sent any profiles. Two further ITPs have stopped sending profiles toward the end of 2011, one due to grounding at shallow topography. The remaining ITP is still obtaining profiles into 2012.

The ITAC operated fine, but an initial configuration could not be optimized due to bad weather during the deployment, forcing people to go back to the ship before a final configuration and testing could be performed on the ice subsequent to deployment. Remote configuration is generally possible and was attempted during the cruise. However, so far technical problems have prevented the system from accepting the new configuration parameters.

One ITP system, deployed in the Makarov Basin, failed the final inductive modem test for communication between the surface unit and the profiler. However, the conditions and the lack of a motorised system prevented recovery. To date, the system has reported status and position but no ocean profiles.

One of the POPS systems had a similar inductive modem test failure but could be recovered using one of the ship's capstans, as the deployment site was only about 100 m from the ship's stern. The two POPS systems had been supplied with different mooring cables: one system had a wire with, presumably, a polypropylene or hard PVC jacket, the other system with, seemingly, a polyethylene jacket (the wire specification by Metocean stated PVC for all wire jackets). The wire of the second system showed problems coming off the drum, as it was only loosely reeled on, and the jacket was breaking in several places during the deployment. These parts of the wire jacket were fixed with tape, but the test for the inductive modem communication between the surface unit and the profiler failed after deployment.

Perliminary results

Sections of temperature, salinity and oxygen profiles are shown in Figures 4.4 to 4.17.

North of Franz-Josef-Land, the warm Atlantic Water, flowing into the Arctic Ocean via the Fram Strait, is clearly visible near the shelf break with temperatures up to

2.5 °C (Section 1, Fig. 4.10) and salinities around 34.96 (Fig. 4.11). The maximum temperature has decreased by about 0.5 °C, relative to measurements at this location in 2007. The cooling resumes a respective temperature drop observed after 2006 in the West Spitsbergen Current in Fram Strait where the inflow properties are recorded by a mooring array, maintained by AWI. In Fram Strait, subsequent to 2008, the Atlantic Water temperature increased again slightly until 2011. Hence, the observed cooling at the Eurasian continental margin appears to be an intermittent anomaly propagating with the boundary current from the subarctic Atlantic.

The cooling signal has already spread up to the eastern Nansen Basin north of the Laptev Sea, where near at the Gakkel Ridge maximum temperatures were around 1.5 °C (Section 3, Fig. 4.10), 0.5 °C cooler than at nearby stations in 2007. Also the salinity maximum has decreased north of the Laptev Sea since 2007 by about 0.05 (Section 3, Fig. 4.11).

If the low salinity observed north of the Laptev Sea is primarily due to intense mixing of the Barents Sea and Fram Strait branches of the AW inflow to the Arctic Ocean or if the warmer and more saline Fram Strait branch returns to the Fram Strait in the Nansen Basin before reaching the region north of the Laptev Sea is still an open question.

Deep layers

The deep water in the Nansen Basin was found to be about 10^{-3} °C warmer than in 2007. This is close to the accuracy of the temperature sensors and an order of magnitude less than the warming of 0.02 °C observed between 1996 and 2007.

The results of all CTD casts are still preliminary, as the final calibration using the salinity and temperature data was done after the cruise. The ADCP data will be processed after the cruise for further analysis in conjunction with the CTD data.

Integration to national and international programmes

The oceanographic work of the cruise was supported by the current HGF (Helmholtzgemeinschaft) Programme and by the project "The North Atlantic as Part of the Earth System: From System Comprehension to Analysis of Regional Impacts" funded by the German Federal Ministry for Education and Research (BMBF). Instrumental work was also supported by the Japan Agency for Marine Earth Science and Technology (JAMSTEC) and by the Woods Hole Oceanographic institution (WHOI). The ice-based platforms contribute to the Hybrid Arctic/Antarctic Float Observation System (HAFOS) and the "International Arctic Buoy Programme" (<http://iabp.apl.washington.edu/>).

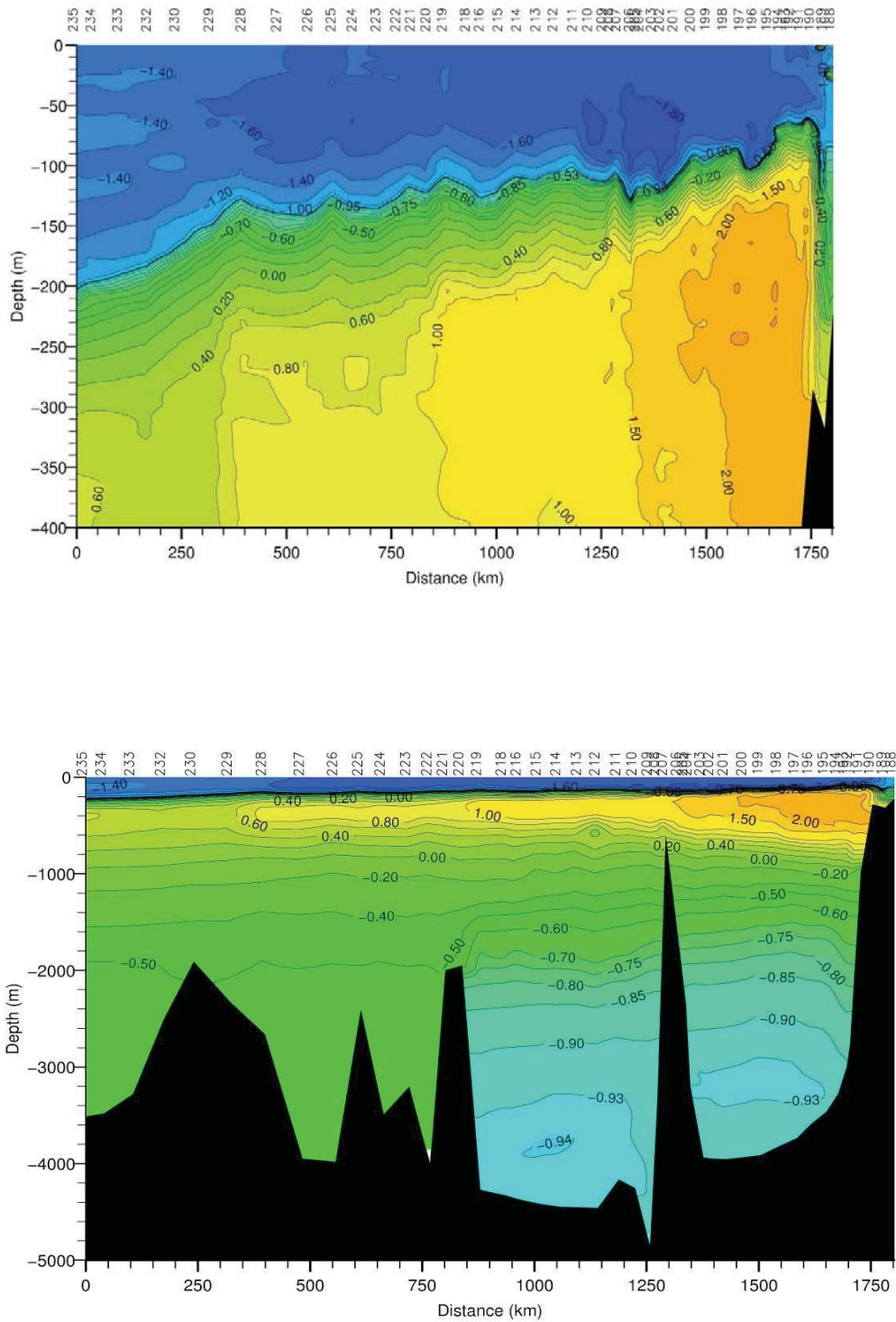


Fig. 4.4: Potential temperature (°C) along Section 1, station numbers on top. Plots for both full-depth and only the top 400 m are shown.

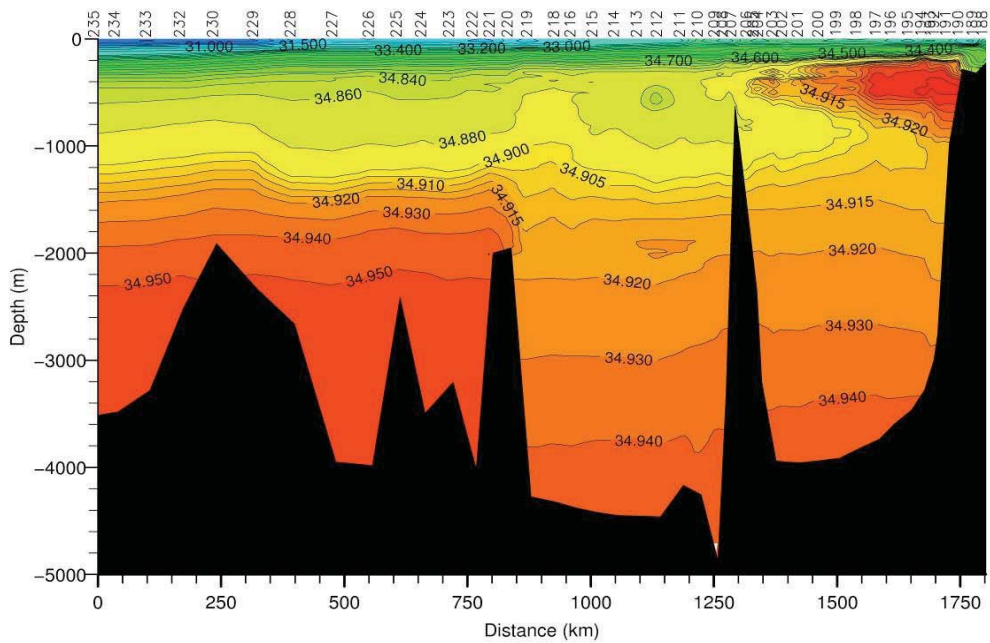
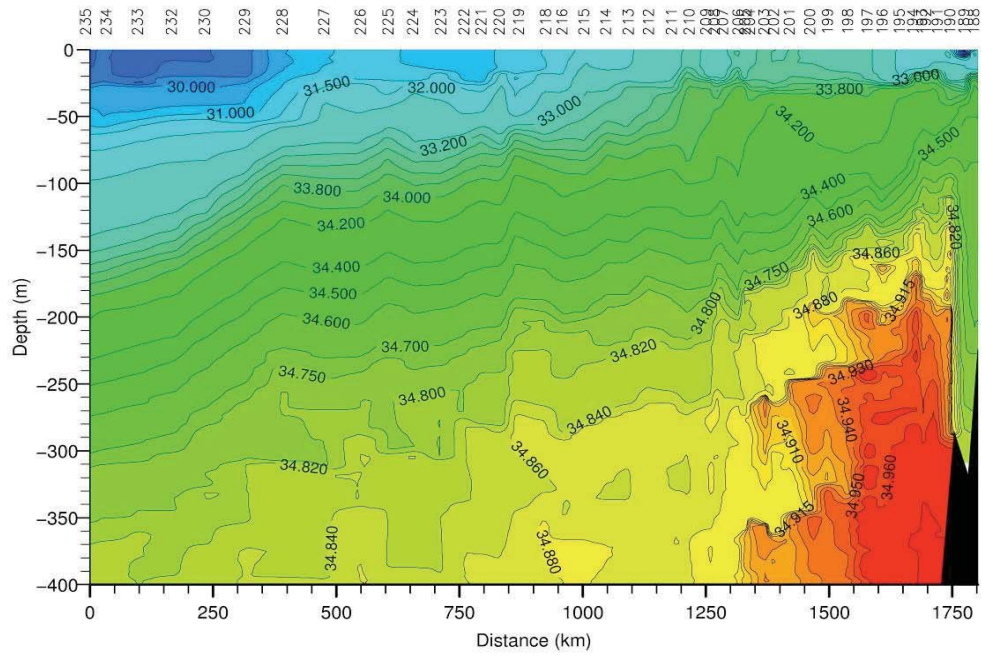


Fig. 4.5: Salinity along Section 1, station numbers on top. Plots for both full-depth and only the top 400 m are shown.

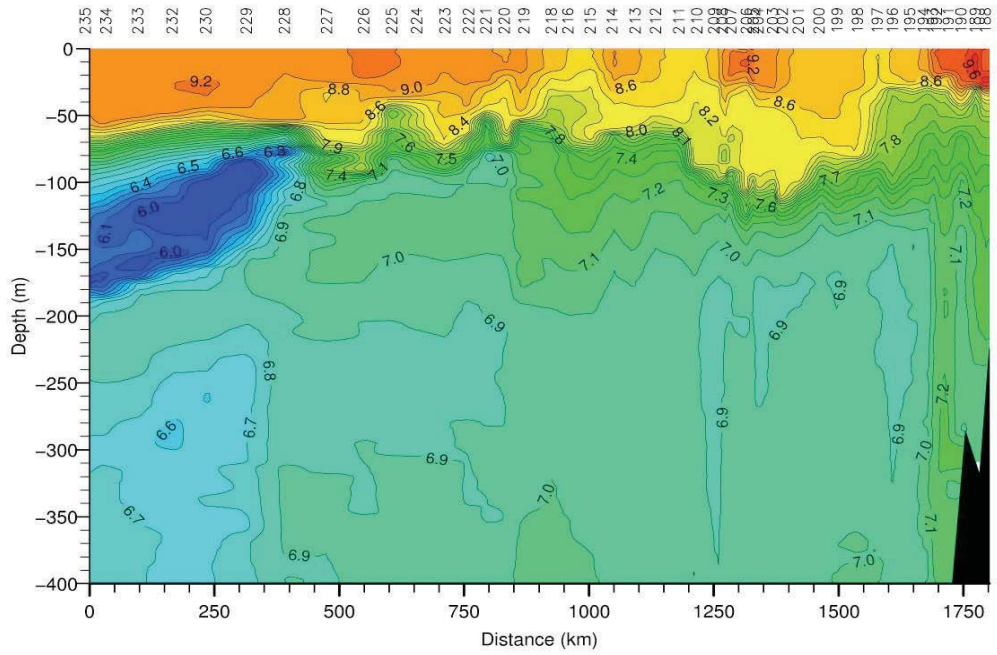


Fig. 4.6: Dissolved oxygen (ml/l) along Section 1, station numbers on top. Plots for both full-depth and only the top 400 m are shown.

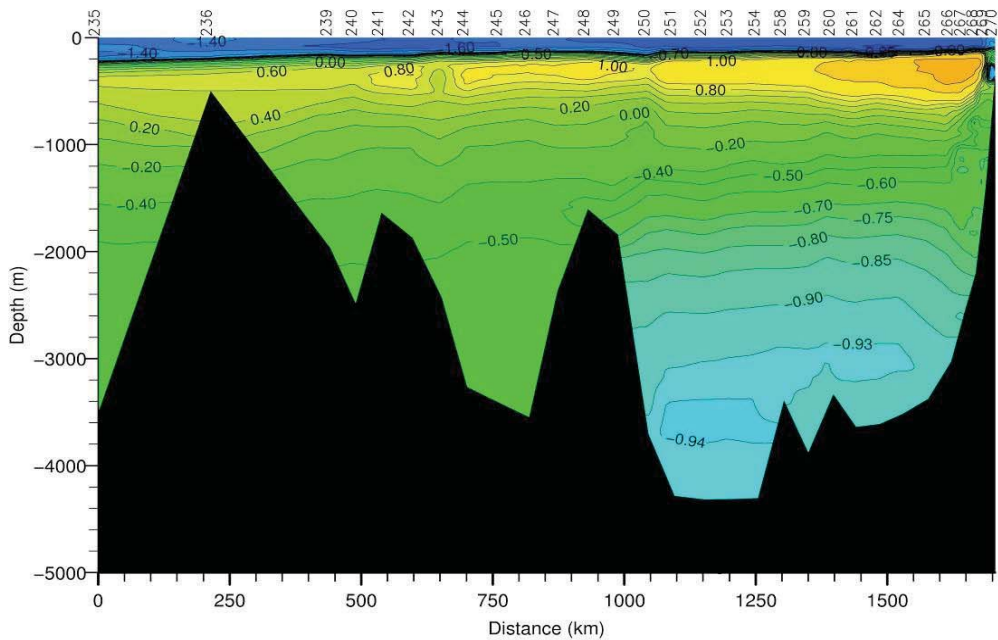
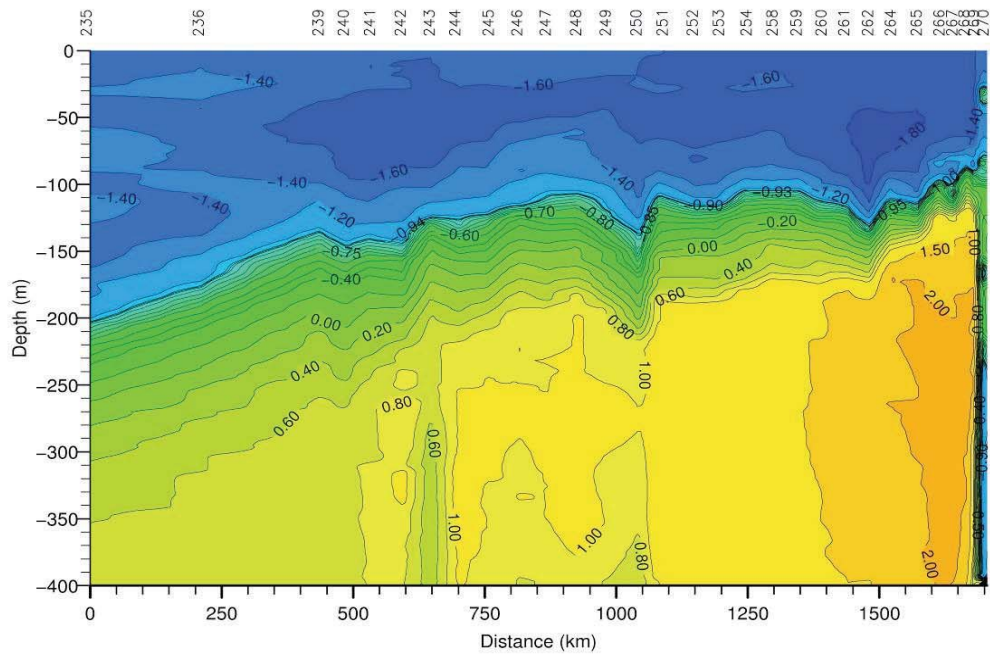


Fig. 4.7: Potential temperature ($^{\circ}\text{C}$) along Section 2, station numbers on top. Plots for both full-depth and only the top 400 m are shown.

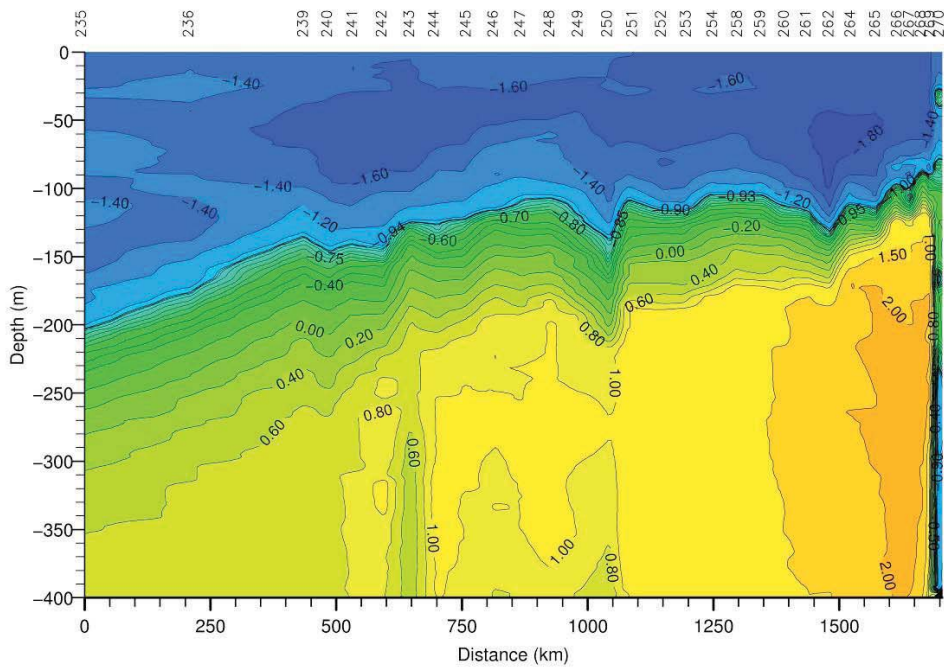
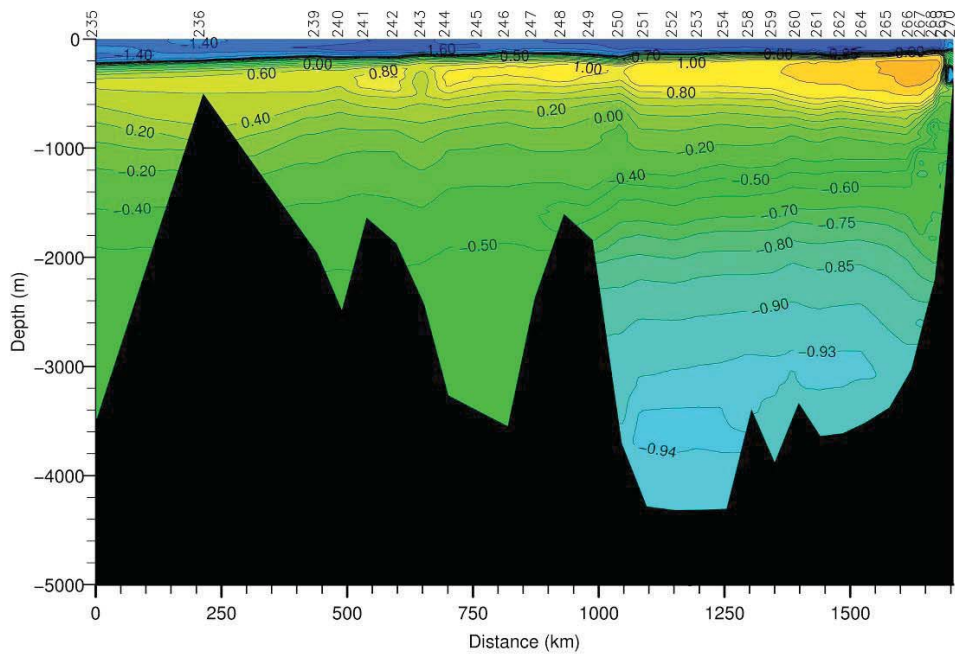


Fig. 4.7: Potential temperature (°C) along Section 2, station numbers on top. Plots for both full-depth and only the top 400 m are shown.

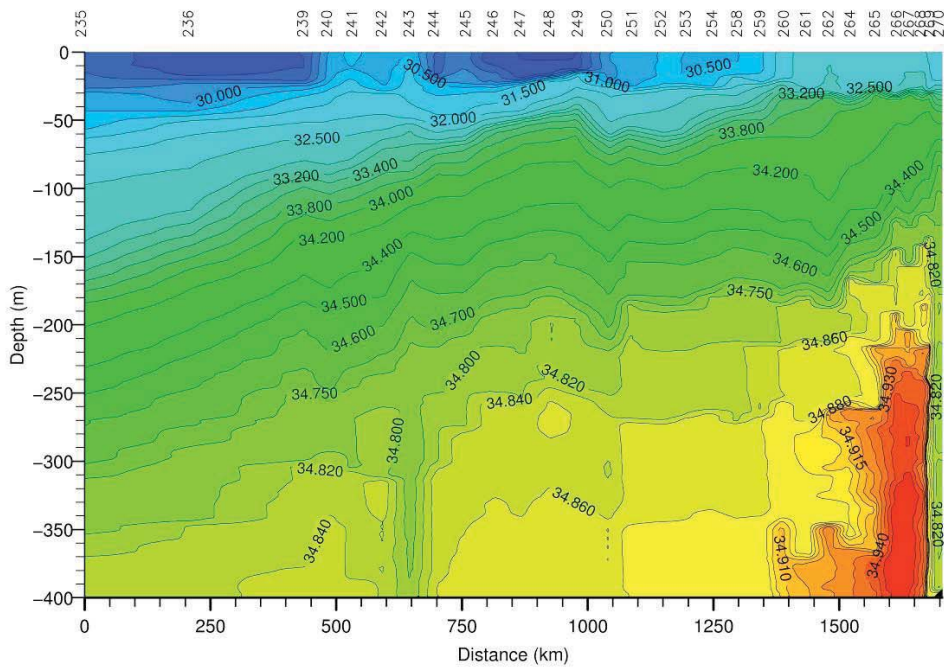
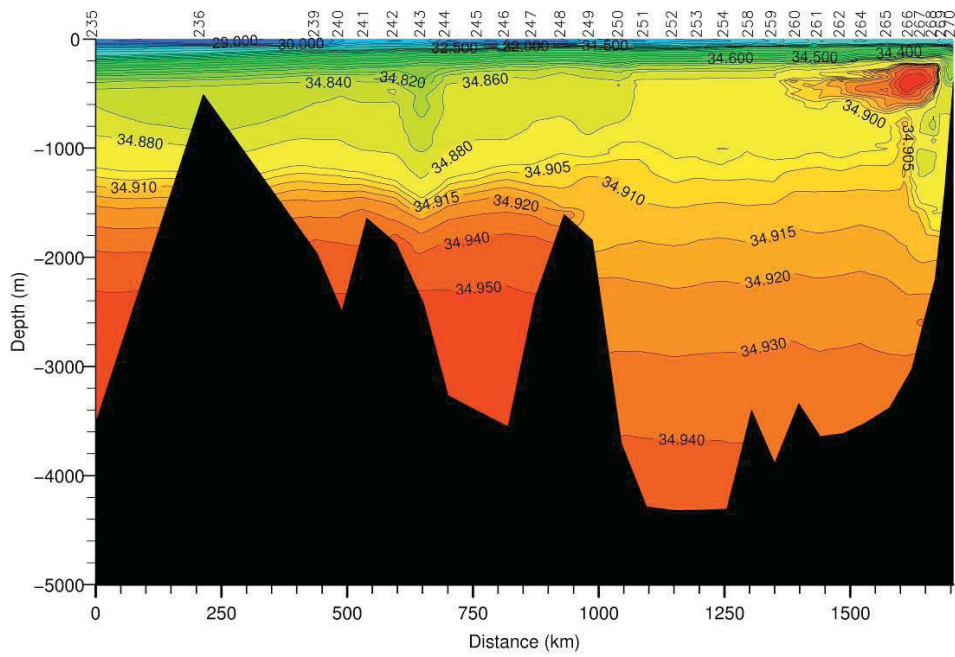


Fig. 4.8: Salinity along Section 2, station numbers on top. Plots for both full-depth and only the top 400 m are shown.

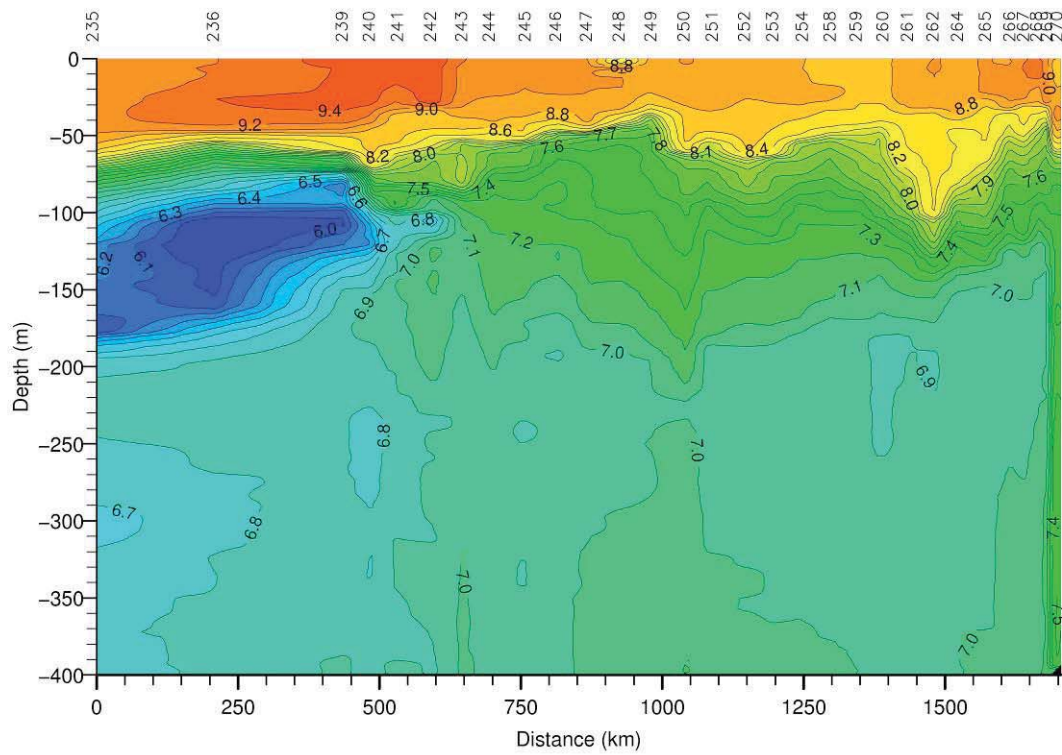


Figure 4.9: Dissolved oxygen (ml/l) along Section 2, station numbers on top. Only the top 400 m are shown.

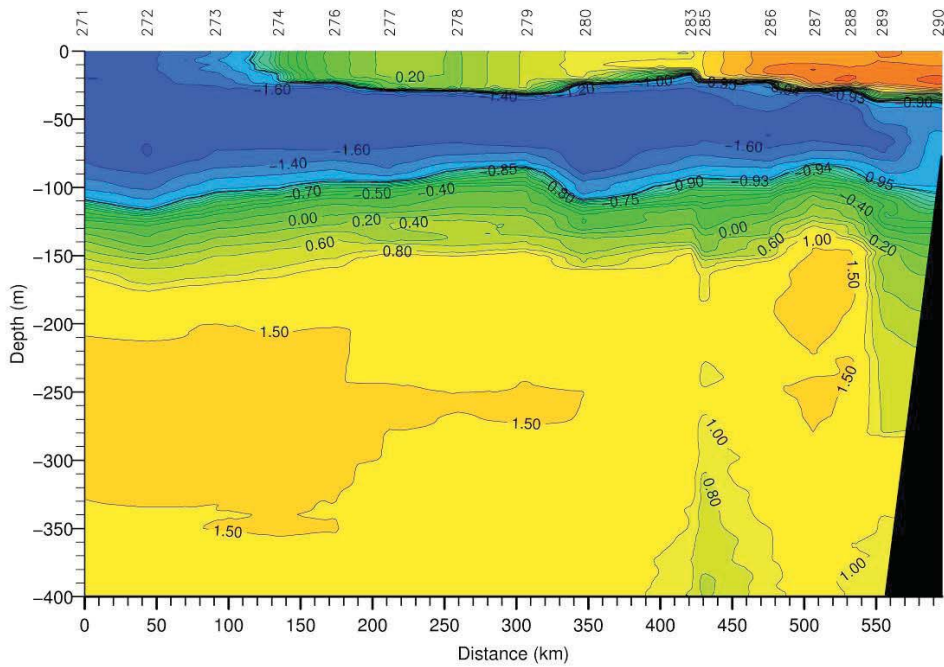
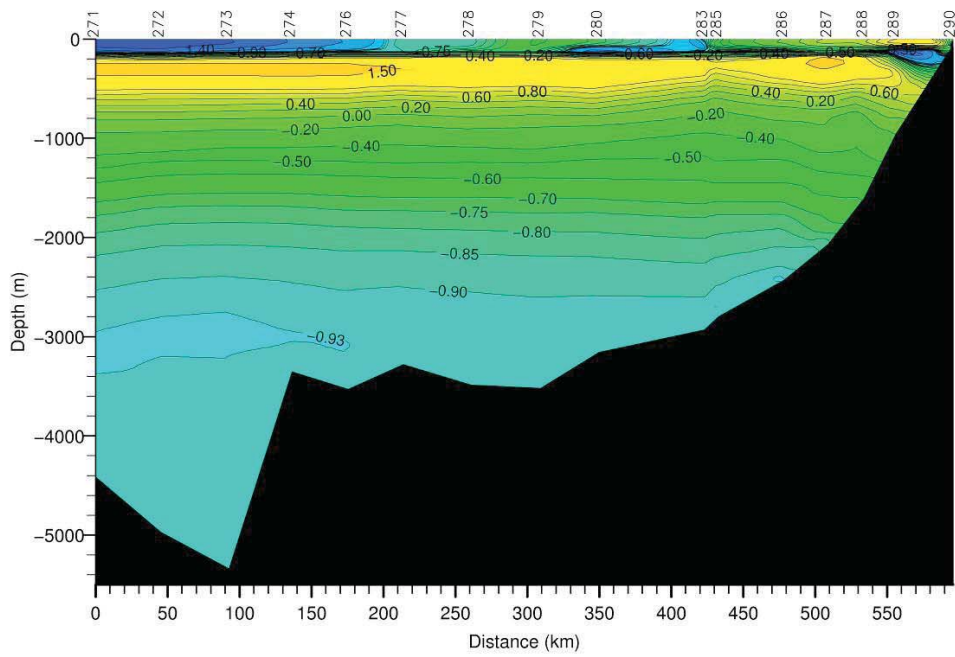


Fig. 4.10: Potential temperature (°C) along Section 3, station numbers on top. Plots for both full-depth and only the top 400 m are shown.

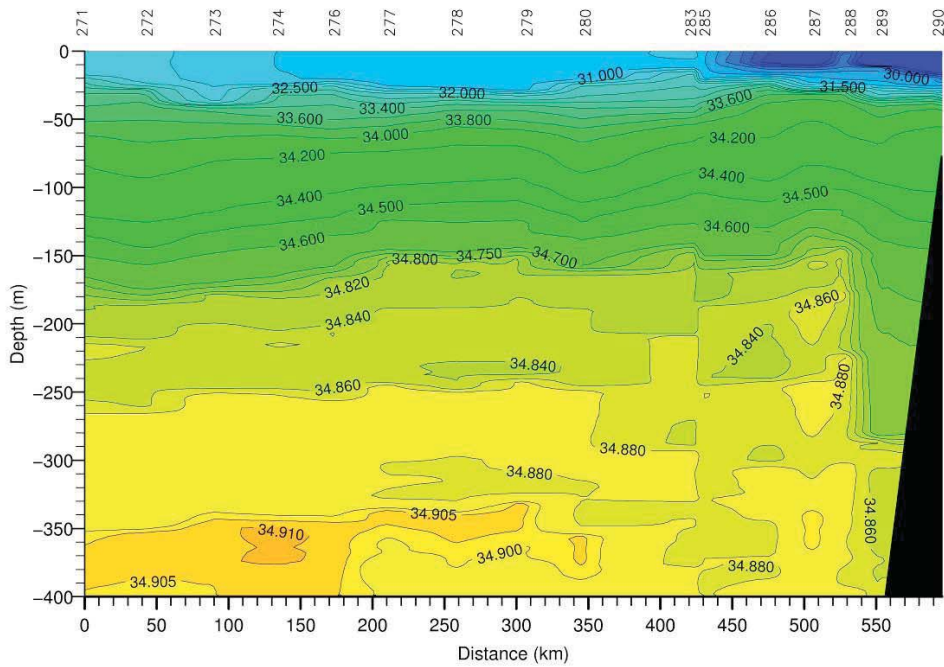
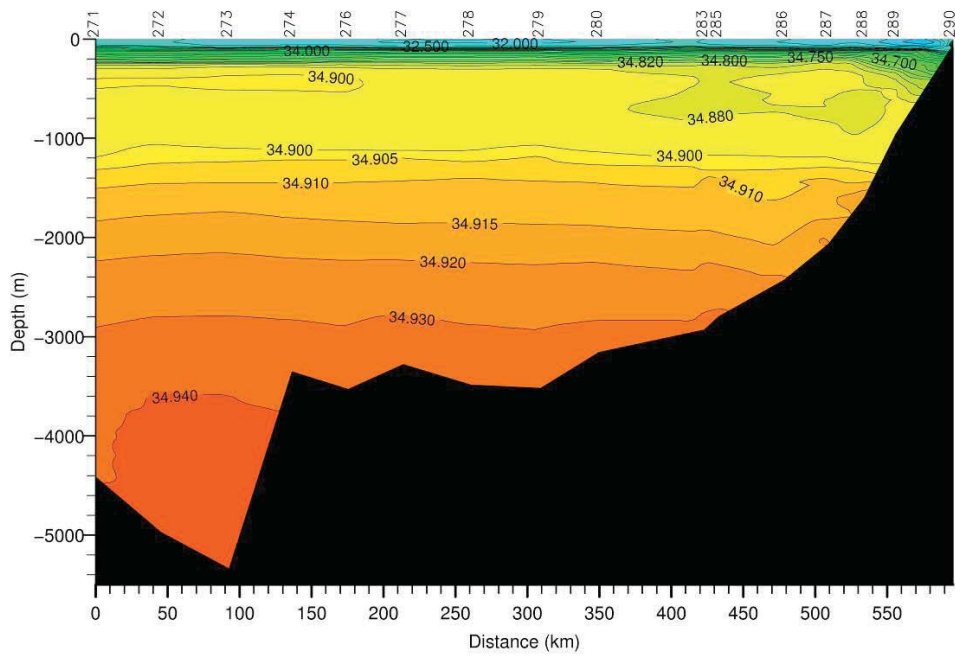


Fig. 4.11: Salinity along Section 3, station numbers on top. Plots for both full-depth and only the top 400 m are shown.

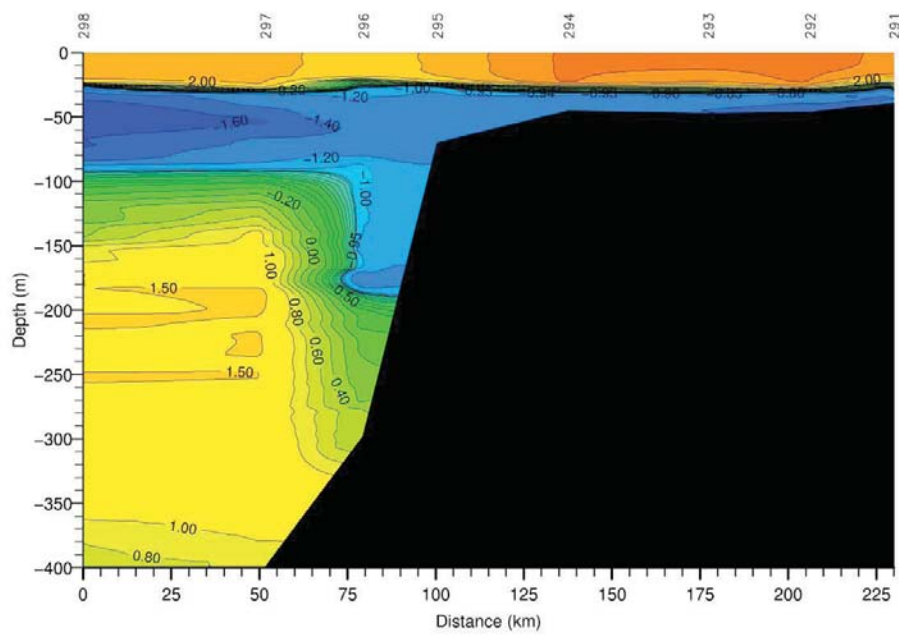
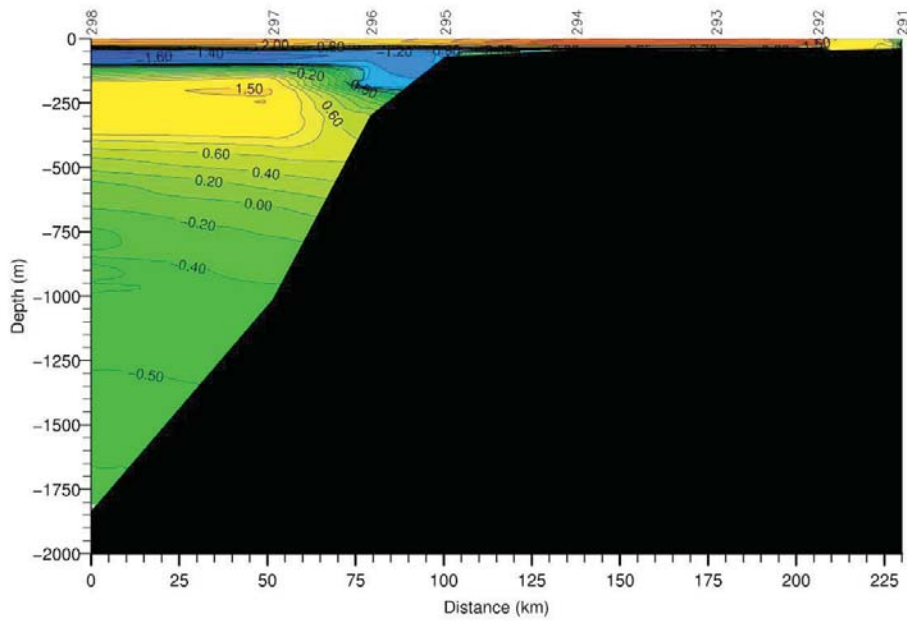


Fig. 4.12: Potential temperature ($^{\circ}\text{C}$) along Section 4, station numbers on top. Plots for both full-depth and only the top 400 m are shown.

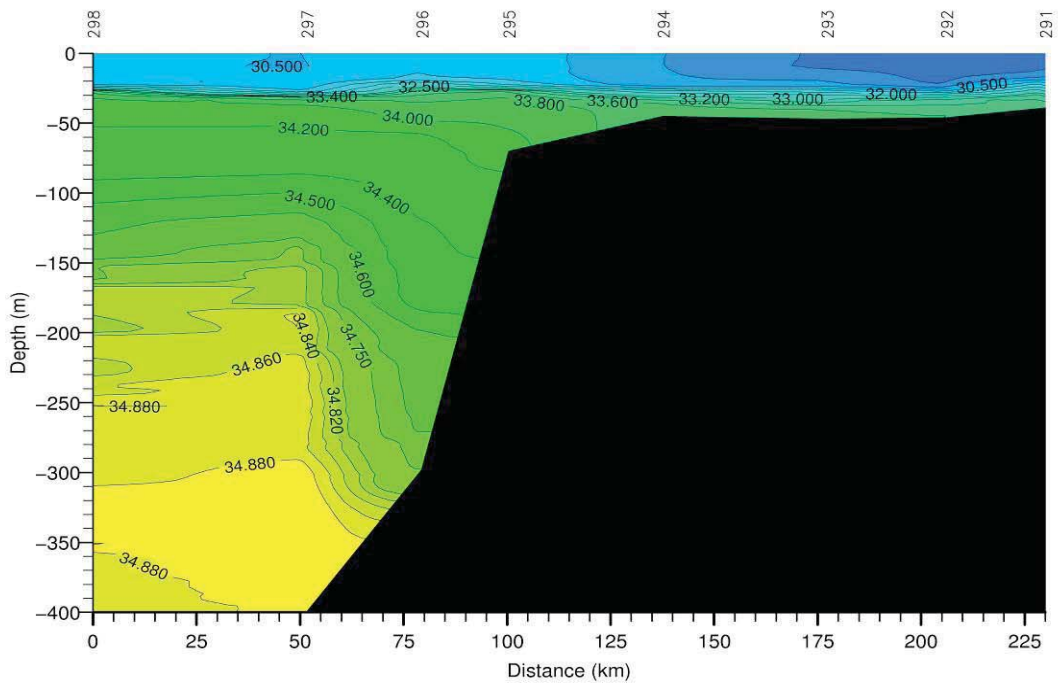
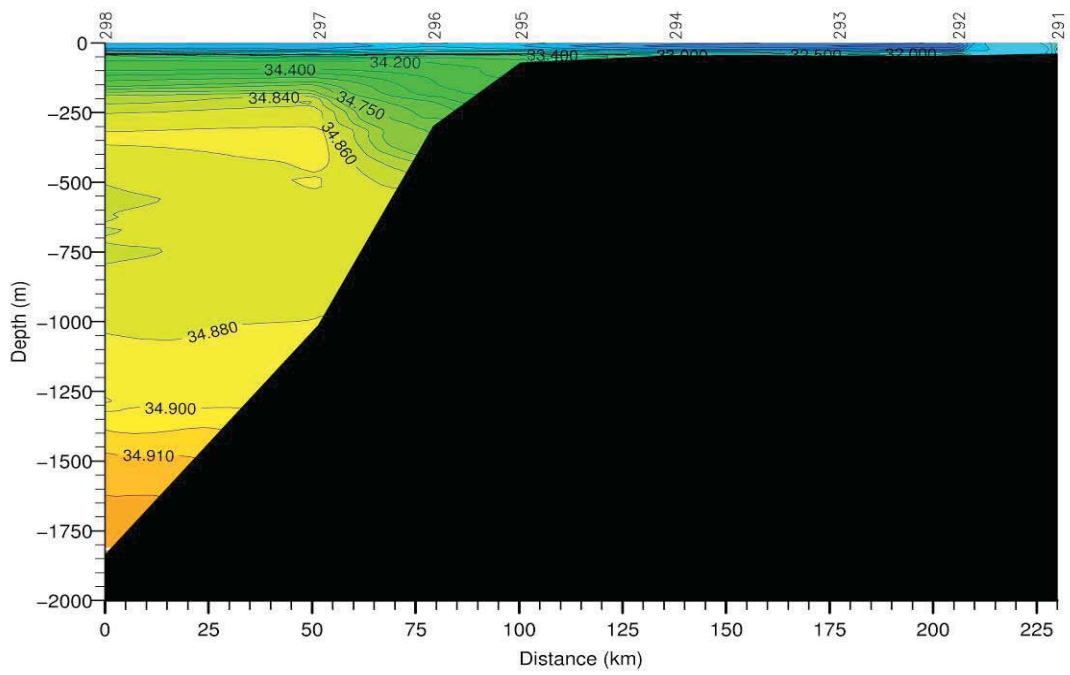


Fig. 4.13: Salinity along Section 4, station numbers on top. Plots for both full-depth and only the top 400 m are shown.

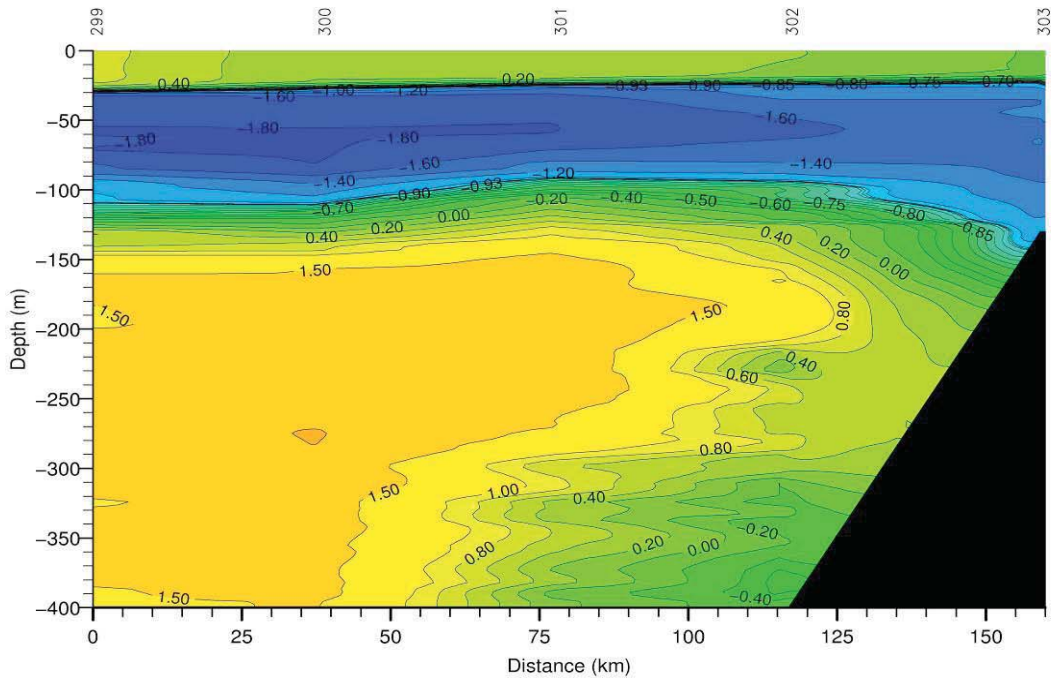
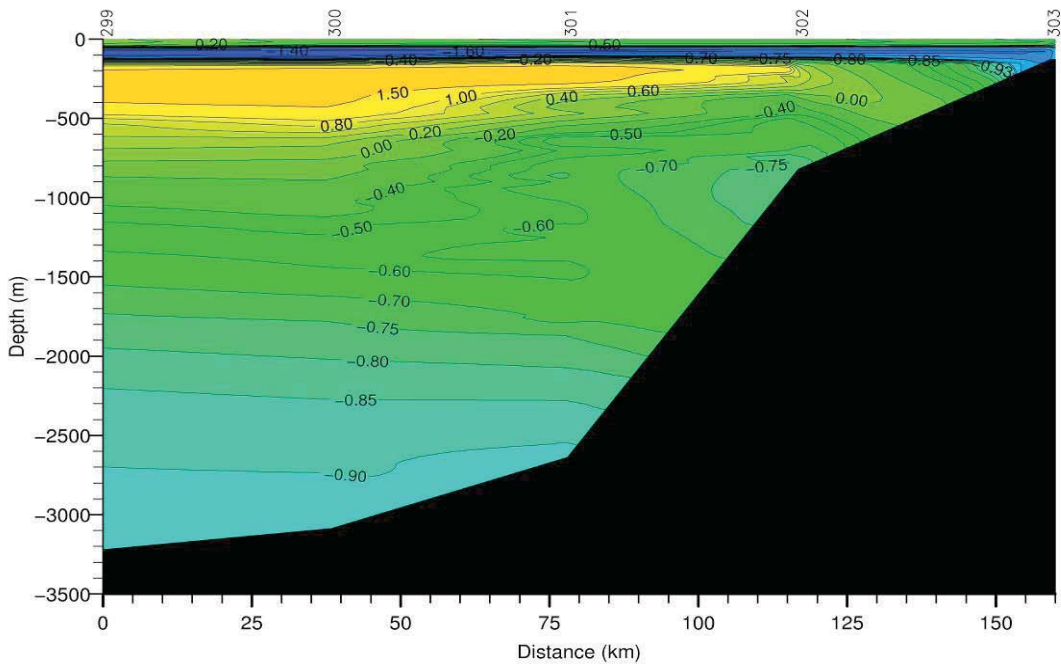


Fig. 4.14: Potential temperature ($^{\circ}\text{C}$) along Section 5, station numbers on top. Plots for both full-depth and only the top 400 m are shown.

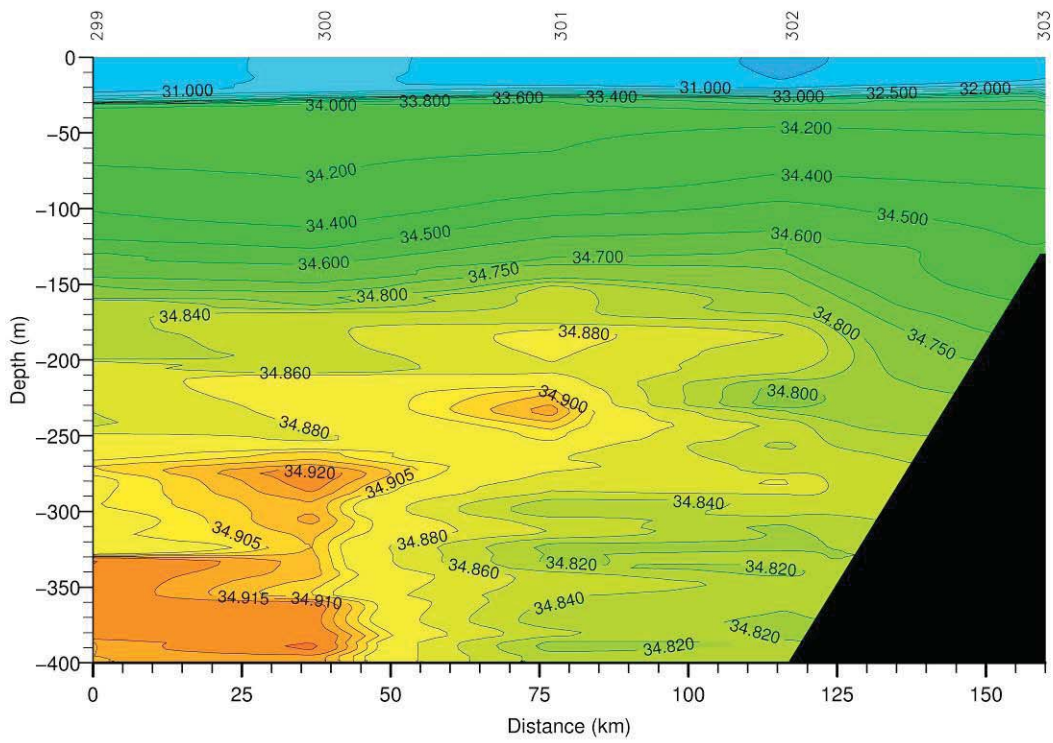
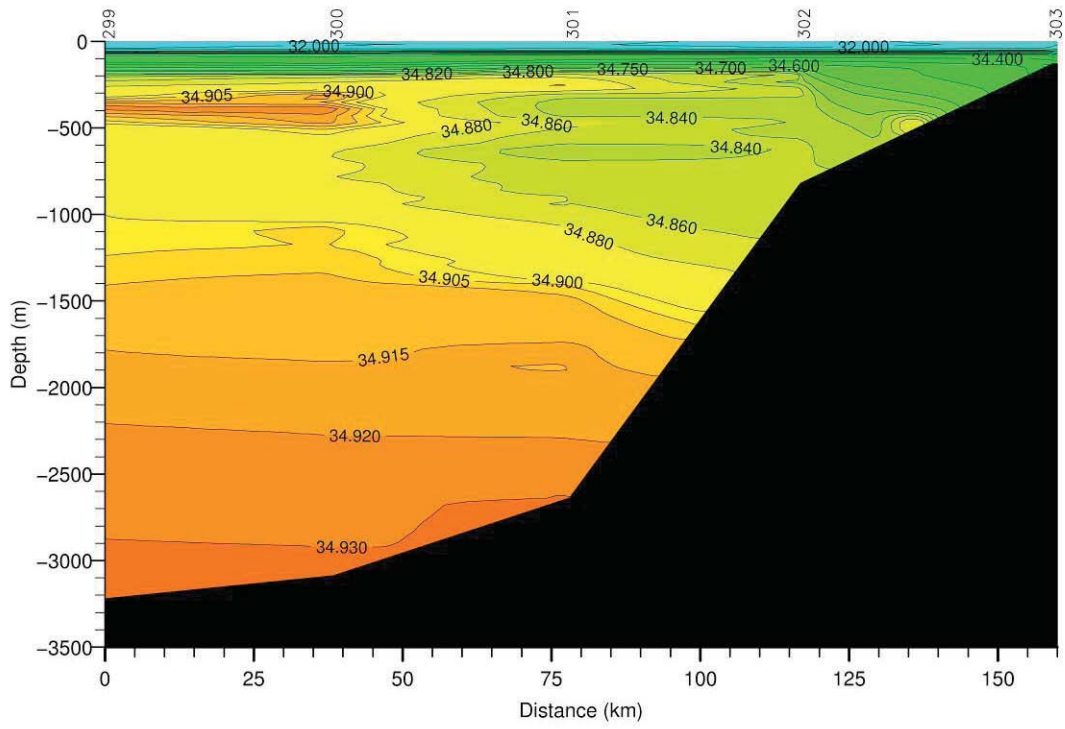


Fig. 4.15: Salinity along Section 5, station numbers on top. Plots for both full-depth and only the top 400 m are shown.

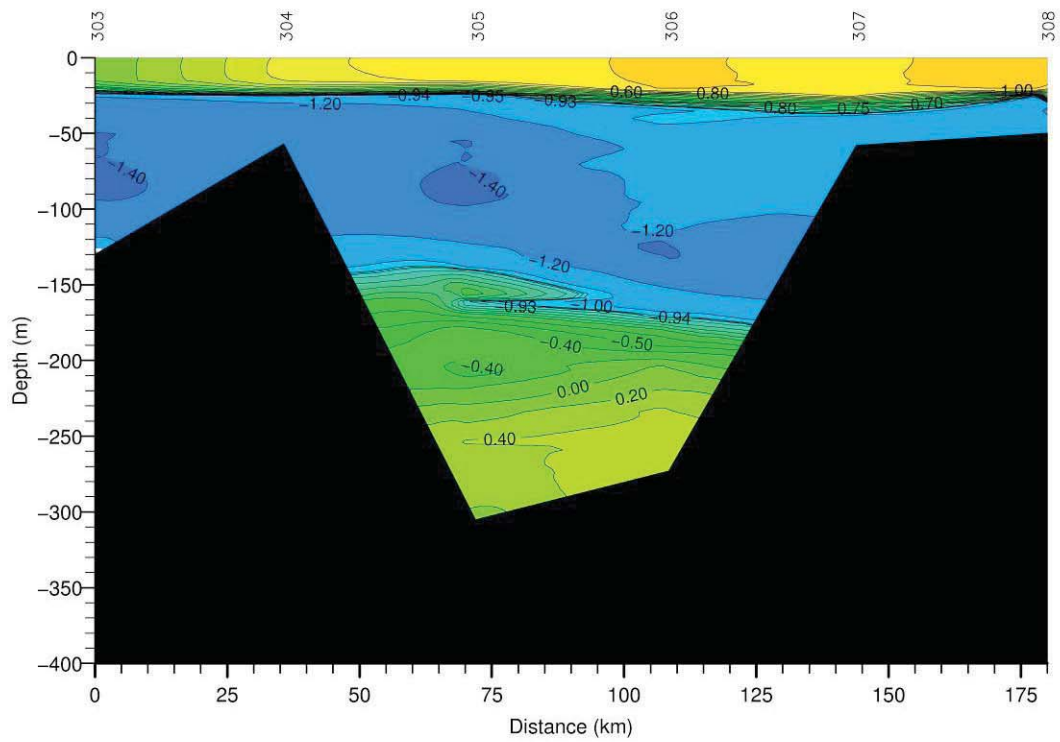


Fig. 4.16: Potential temperature ($^{\circ}\text{C}$) along Section 6, station numbers on top.

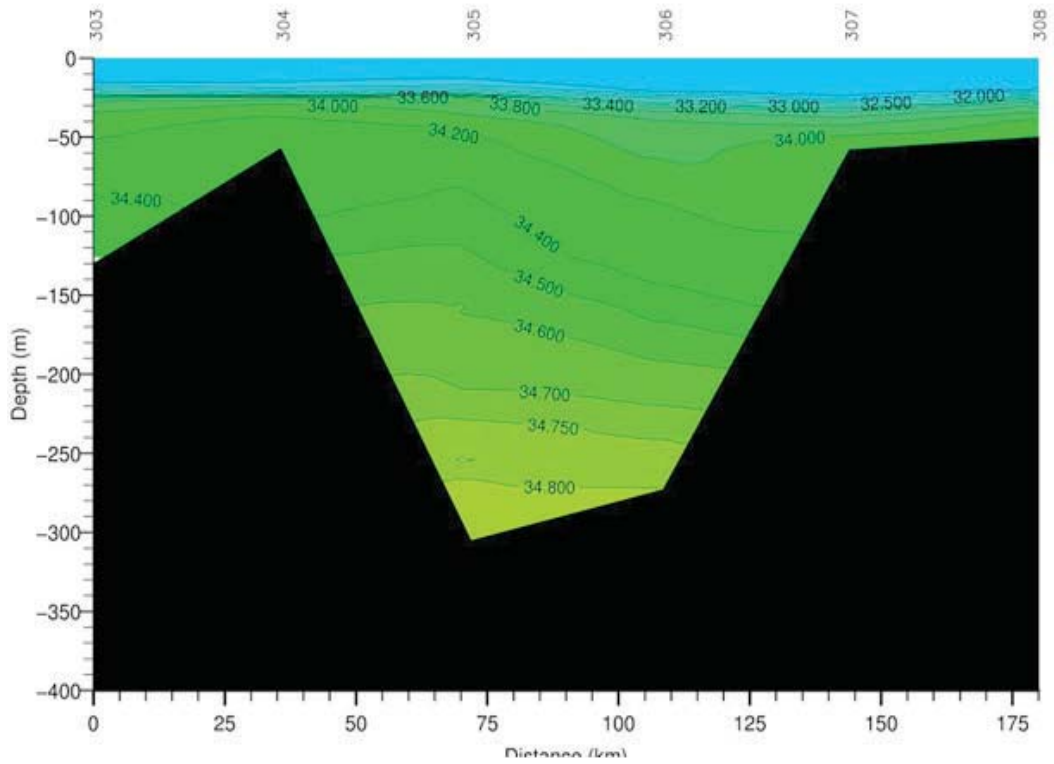


Fig. 4.17: Salinity along Section 6, station numbers on top. Plots for both full-depth and only the top 400 m are shown

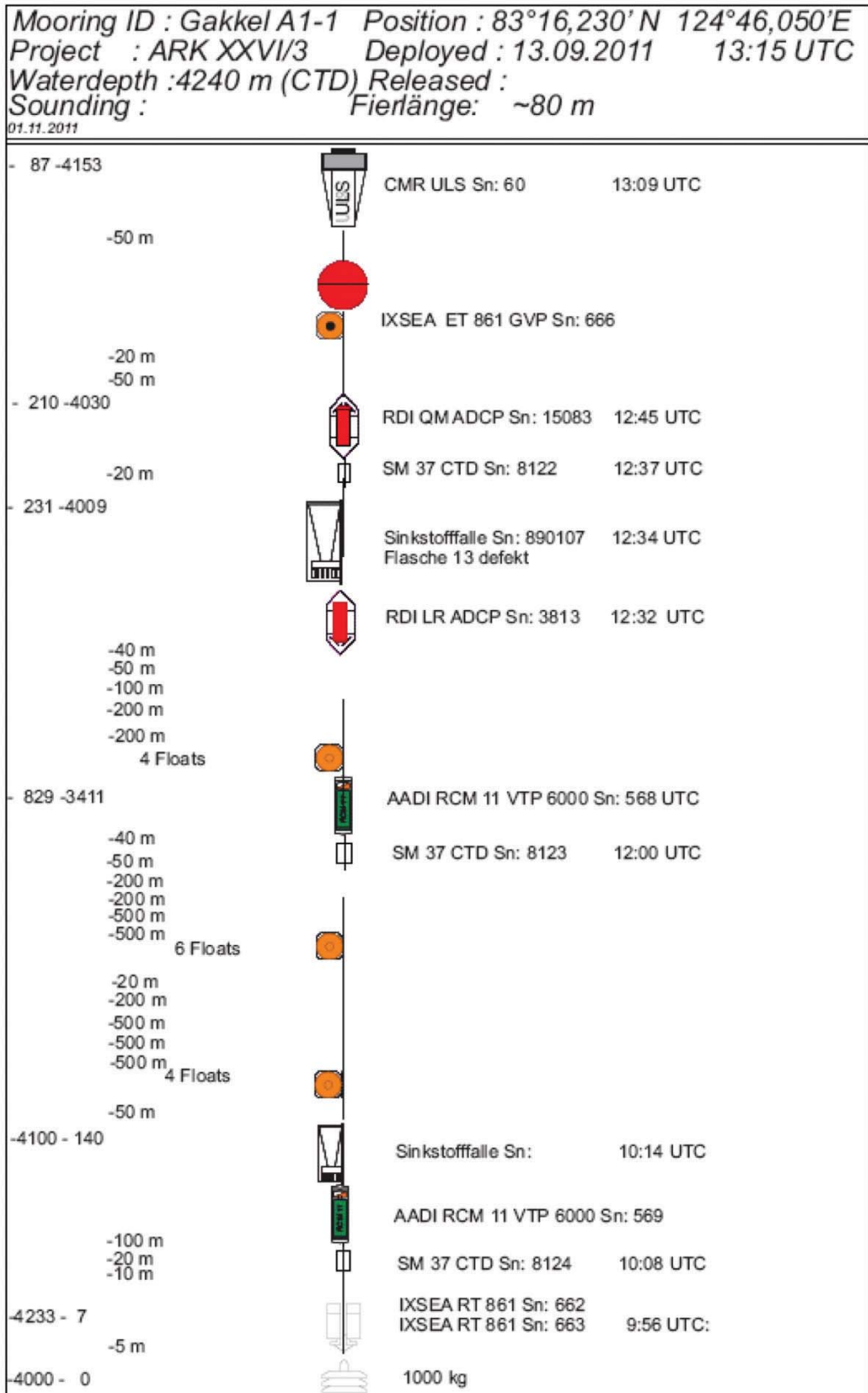


Fig. 4.18: Schematics of the mooring A1-1 deployed in the Amundsen Basin (north-eastern white cross in Fig. 4.3.)

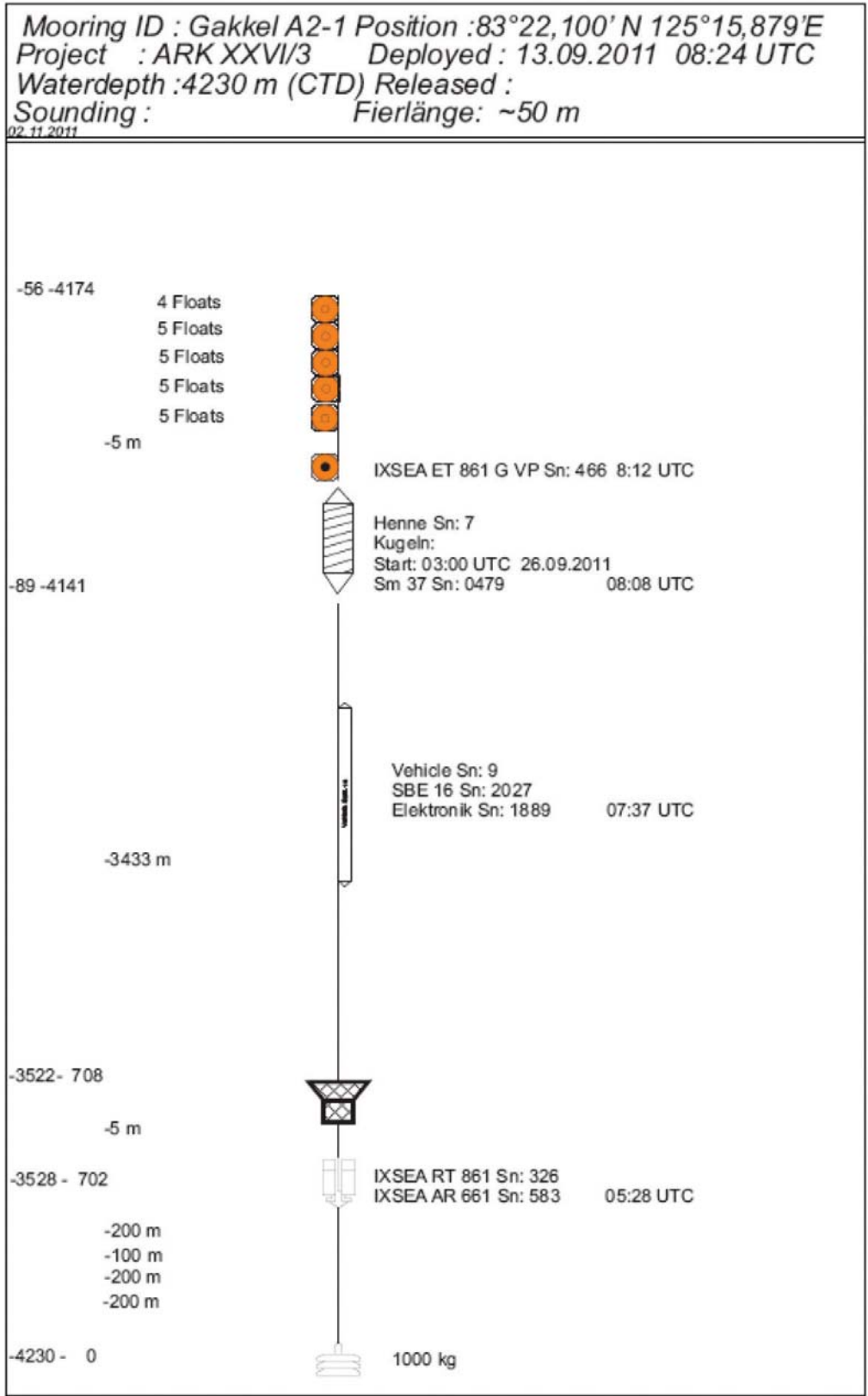


Fig. 4.19: Schematics of the mooring A2-1 deployed in the Amundsen Basin (north-eastern white cross in Fig. 4.3).

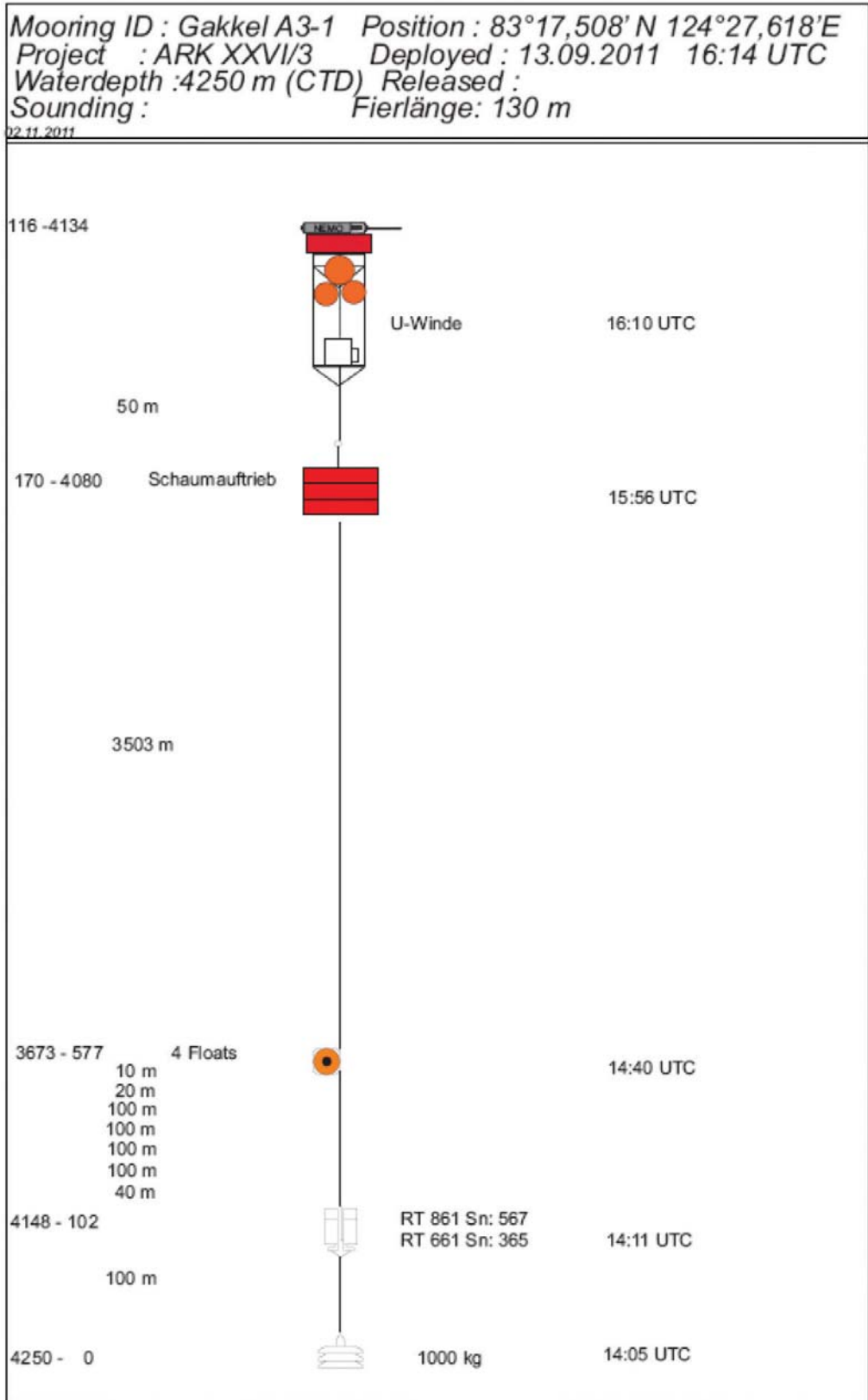


Fig. 4.20: Schematics of the mooring A3-1 deployed in the Amundsen Basin (north-eastern white cross in Fig.4.3).

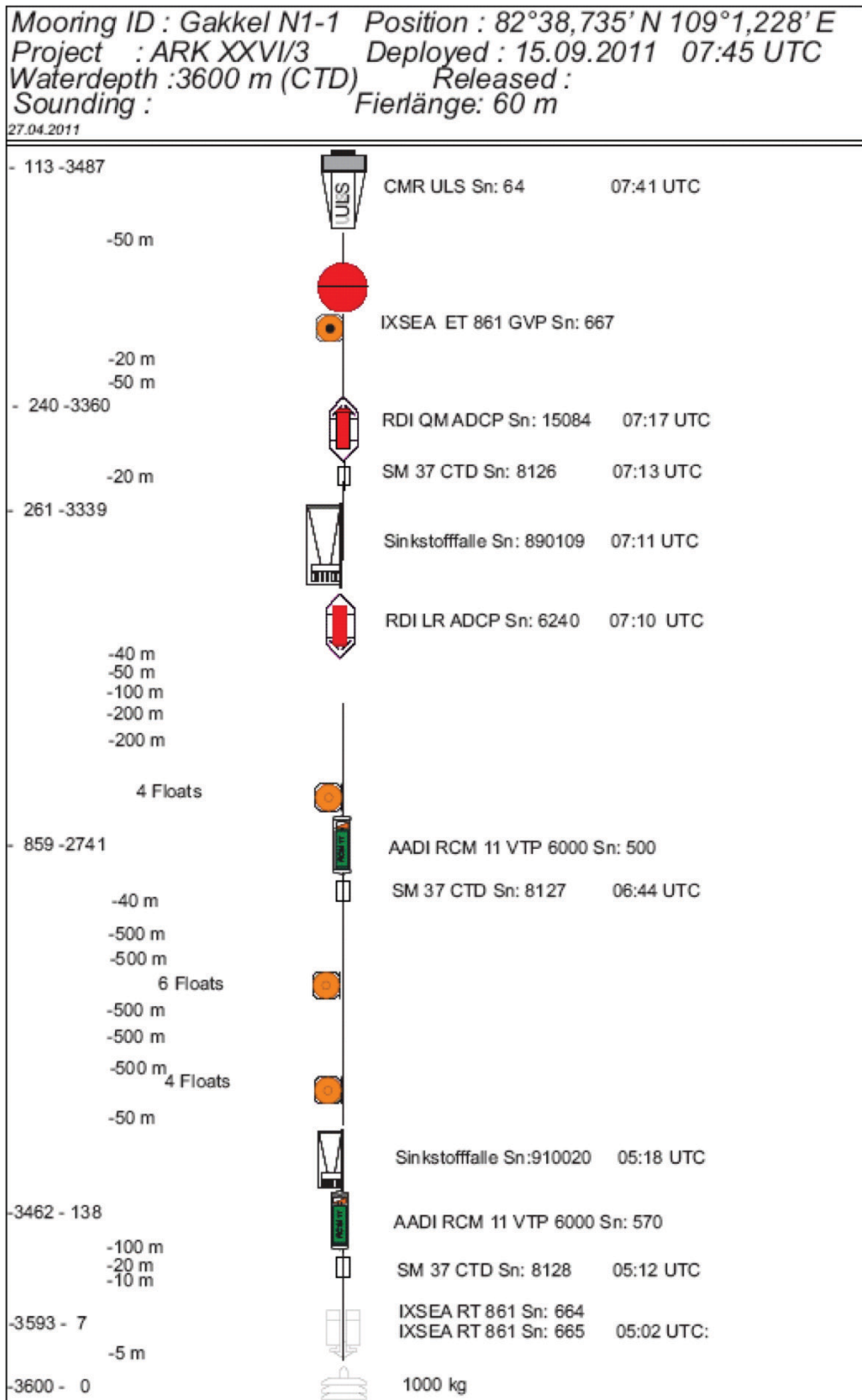


Fig. 4.21: Schematics of the mooring N1-1 deployed in the Nansen Basin (south-western white cross in Fig.4.3).

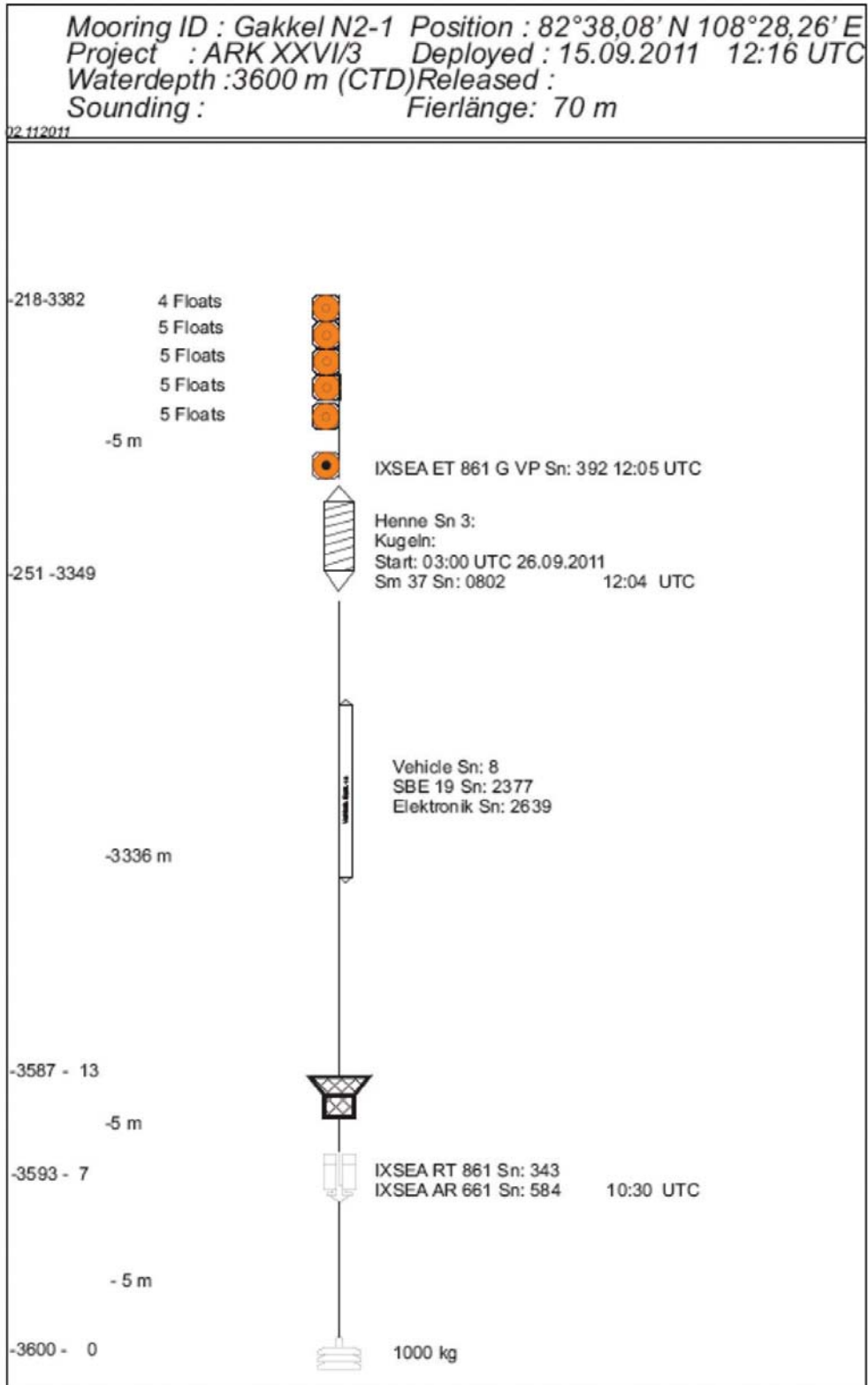


Fig. 4.22: Schematics of the mooring N2-1 deployed in the Nansen Basin (south-western white cross in Fig.4.3).

5. GEOCHEMISTRY

5.1 The carbonate system

Adam Ulfsbo and Ylva Ericson,
PI Leif Anderson not on board

University of Gothenburg,
Department of Chemistry, Sweden

Background and objectives

The overarching objective of this study is to further improve our understanding of the Arctic Ocean carbon system, with an emphasis on carbon fluxes and ocean acidification. More specifically we aim at increasing our understanding of the feedbacks of the biogeochemical components of the Arctic Ocean carbon system, which include the assessment of likely changes in the export of marine produced organic matter to the deep central Arctic Ocean when the sea ice coverage is absent during the productive summer season. A summer sea ice free Arctic Ocean will further result in more brine formation that contributes to deep water formation as a larger winter sea ice production is expected (sea ice production is larger in open water than ice covered), possibly in combination with a higher surface water salinity if mixing of the upper water layers increases. Both changes in export production and ventilation of the deep waters impact the sequestration of anthropogenic CO₂. Finally we also aim at assessing the "natural" ocean acidification, i.e. the pH reduction caused by biogeochemical processes in the ocean, in relation to that originating from uptake of anthropogenic CO₂.

Work at sea

The constituents of the marine inorganic carbonate system determined on board within hours of sampling were pH, Total Dissolved Inorganic Carbon (DIC), and Total Alkalinity (TA). Two 250 mL water samples were taken from the CTD-rosette at as many depths as possible from 55 stations, resulting in a total of 1,253 samples analyzed. The water sampling procedure was performed according to Dickson et al. (2007). Samples were put in water baths, allowing the samples to reach a temperature of 15 °C prior to analysis. pH was determined first, and then TA from the same bottle. DIC was determined from the second sample bottle. All samples were taken and analyzed by the onboard participants above. TA and pH were also determined (61 samples) from low resolution (0.5-30 m) manual CTD casts at ice stations 209-1, 218-1, 222, 227-1, 230-1, 235-1, 239-1, 245-1 and 250-1, sampled by the sea-ice biogeochemistry group (Dieckmann, AWI).

pH was determined spectrophotometrically using the sulphonephthalein dye, m-cresol purple, as indicator (Clayton and Byrne, 1993). The method is based on the absorption ratio of the indicator at wavelengths 434 and 578 nm using a 1-cm flow cell. The magnitude of the perturbation of seawater pH caused by the addition of indicator solution was calculated and corrected for using the method described in Chierici et al. (1999). TA was determined by open-cell potentiometric titration with 0.05 M HCl, according to Haraldsson et al. (1997) based on Gran evaluation. The sample is dispensed into a titration vessel from a thermostated pipette. DIC

5.1 The carbonate system

was determined using a coulometric method (Johnsson, 1993) with the MIDSOMMA system (Mintrop, 2005). The sample is dispensed from a thermostated pipette into a stripper, where the sample is acidified and all inorganic carbon species are converted into aqueous CO_2 . The evolving CO_2 is rapidly removed from the stripper by a carrier gas (N_2) via a condenser to the coulometer. Precision and accuracy for TA and DIC are controlled against certified reference material (CRM) supplied by Andrew Dickson (Scripps Institution of Oceanography, San Diego, USA). The precision of pH measurements is evaluated from replicates. The accuracy of spectrophotometric pH values is difficult to assess, since it relies ultimately on the physicochemical characteristics of the indicator solution, but is mainly set by the equilibrium constants of the indicator.

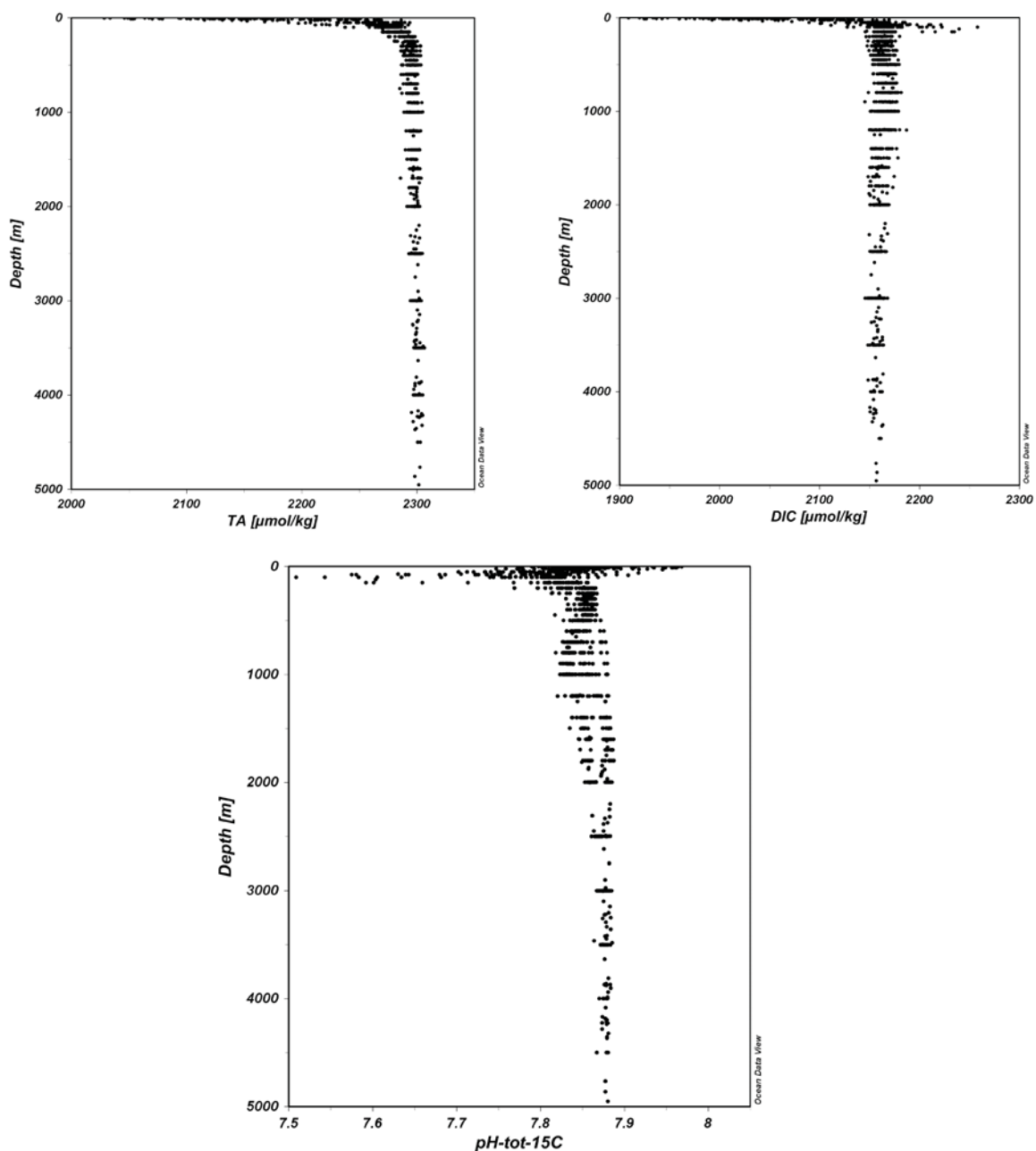


Fig. 5.1. Preliminary results of the carbonate system depicted as depth profiles of TA, DIC and $\text{pH}_{\text{tot}}^{15\text{C}}$.

Preliminary results/expected results

Primary and secondary quality control has to be done after a careful reevaluation of all measurements back at the University of Gothenburg. The data will also be checked against continuous surface pCO₂ measurements from the permanently installed system (Hoppema, AWI). Preliminary results of the carbonate system are shown as depth profiles of DIC, TA and pH_{tot}^{15C} in Fig. 5 1.

References

- Chierici, M., Fransson, A., Anderson, L.G., 1999. Influence of m-cresol purple indicator additions on the pH of seawater samples: correction factor evaluated from a chemical speciation model. *Mar. Chem.*, 65, 281-290.
- Clayton, T.D., Byrne, R.H., 1993. Spectrophotometric seawater pH measurements: total hydrogen ion concentration scale calibration of m-cresol purple and at-sea results, *Deep-Sea Res. I*, 40(10), 2115-2129.
- Dickson, A.G., Sabine, C.L. and Christian, J.R. (Eds.) 2007. Guide to best practices for ocean CO₂ measurements. PICES Special Publication 3, 191 pp.
- Haraldsson, C., Anderson, L.G., Hassellöv, M., Hulth, S., Olsson, K., 1997. Rapid, high-precision potentiometric titration of alkalinity in the ocean and sediment pore waters. *Deep Sea Res. I*, 44, 2031-2044.
- Johnson, K.M., Wills, K.D., Butler, D.B., Johnson, W.K., Wong, C.S., 1993. Coulometric total carbon dioxide analysis for marine studies: maximizing the performance of an automated gas extraction system and coulometric detector. *Mar. Chem.*, 44, 167-187.
- Mintrop, L., 2005. MIDSOMMA manual version 2.0, Marine analytics and data (MARIANDA), Kiel, Germany.

5.2 Radium and Thorium isotopes

Michiel Rutgers van der Loeff, Daniel Scholz
Alex Charkin

Alfred-Wegener Institut
POI-FEBRAS, Vladivostok

Objectives

The particle export from surface water can be determined with the short lived isotope ²³⁴Th (half-life 24 days). During ARK-XXII/2 in 2007 we have found that ²³⁴Th-based export rates of carbon were very low in the central Arctic (Cai et al., 2010), but there were indications of enhanced particle fluxes in the area of the Lomonosov Ridge. During the present expedition we wanted to repeat these measurements in coordination with the more extensive biological sampling of the PEBCAO program and as background for the data to be collected with the sediment traps deployed in the Gakkel Ridge area.

Four radium isotopes are supplied to the ocean by contact with the continent or (deep-sea)-sediments: ²²³Ra, (half-life 11.4 d); ²²⁴Ra (3.7 d), ²²⁶Ra (1620 y) and ²²⁸Ra (5.8 y). The distribution of these isotopes in seawater has been shown to be most helpful to evaluate shelf-basin exchange and water residence times. ²²⁸Ra is

released by sediments and accumulates to high activities over the Arctic shelves. When these waters are transported in the fresh surface water layer over the central Arctic Ocean towards Fram Strait, the signal decays with the half-life of 5.8 y. The isotope is therefore used to trace this transport of shelf-influenced waters in the Trans Polar Drift. During this transport, the granddaughter ^{228}Th , which is efficiently removed on the shelves, grows towards equilibrium. The distribution of the $^{228}\text{Th}/^{228}\text{Ra}$ ratio is therefore determined by a competition between ingrowth, which depends on time (^{228}Th half-life 1.9 yr) and removal, which depends on particle flux.

This shows why, apart from the interest for the carbon cycle, the distribution of scavenging rates is also important for the interpretation of the behaviour of other trace elements and isotopes like ^{228}Th . We will derive this distribution in first line from the distribution of the total $^{234}\text{Th}/^{238}\text{U}$ ratio in surface waters. But further information has been obtained from the distribution of suspended material from direct filtrations and from transmissometry. These scavenging rates will then be used to interpret the $^{228}\text{Th}/^{228}\text{Ra}$ data and determine to what extent these isotope data can be used as time marker for shelf waters.

The short-lived radium isotopes ^{224}Ra and ^{223}Ra are used extensively for the study of submarine groundwater discharge. Because we were not allowed to work in the Russian EEZ, it was unlikely that we would see any excess activities of these isotopes due to their release from the coast or shelf sediments. We have therefore primarily used them as proxies for their longer lived parents ^{228}Th and ^{227}Ac .

Work at sea

We have taken samples for ^{234}Th analysis in coordination with the sampling for plankton, POC, chlorophyll by the biologists. We have determined the ^{234}Th profiles in the upper 200 m of the water column on a total of 17 stations. The total ^{234}Th samples have been counted onboard using RISO beta counters mounted in the geochemistry container. Final ^{234}Th activities can only be given after the yields have been determined from the recovery of a ^{230}Th spike added to every sample. These yield measurements will be made after decay of the ^{234}Th (a minimum of 6 months) with mass spectrometry in the home laboratory. The activity of the parent nuclide, ^{238}U , is usually obtained from salinity. We have collected a series of samples to check the applicability of the U/salinity relationship established in other oceans through mass spectrometry. From the $^{234}\text{Th}/^{238}\text{U}$ ratio we will determine the scavenging rates in the surface water. This will give us an estimate of POC export, which we can compare with the results of the 2007 expedition and with fluxes we hope to measure with the sediment traps deployed in the Gakkel Ridge area. In order to convert thorium to POC fluxes, we will determine the $\text{POC}/^{234}\text{Th}$ ratio on particulate matter that we obtained by filtration of 8-L water samples collected at 200 m depth over precombusted QMA filters. The relationship between the $\text{POC}/^{234}\text{Th}$ ratio determined on bulk suspended matter and size-fractionated material was determined on the previous expedition by Pinghe Cai.

Because of the special interest during this expedition in processes in the water column immediately under the ice, we have, in addition to the profiles measured in CTD casts from the ship, also determined the ^{234}Th profiles in the upper 16 m of the water column under the ice. For this purpose, samples were collected during ice stations 209, 212, 218, 222, 227, 230, 235 by suction through a plastic tube into 4-L plastic containers. On later ice stations 245 and 250, low air temperatures

caused freezing of the water in the tubing, and samples were collected with the 2-L water samplers used by the sea-ice biogeochemistry group (Dieckmann).

For radium isotopes, large volume surface water samples were collected into 300-L tanks. Each sample is filtered through a 0.8μ supor filter and then passed at a flow rate of < 1 L/min using a peristaltic pump through MnO_2 -impregnated acrylic fiber to scavenge radium isotopes. Fibers are partially dried using compressed air, and short-lived ^{223}Ra and ^{224}Ra measured at sea using RaDeCC delayed coincidence alpha detectors. The longer-lived isotopes will be measured on the fibers by leaching, coprecipitation of Radium on BaSO_4 and gamma counting ^{228}Ra and ^{226}Ra in the shore-based lab. During the GEOTRACES Radium intercalibration it has been observed that ship's seawater intake systems may contain ^{228}Th , which can serve as a source for ^{224}Ra . After the first samples collected in the fish lab from the ship's seawater inlet had given high count rates, we checked this problem by comparing (stations 201-212) the activities obtained from samples collected much closer to the intake (basin in the front container storage room/ Ladeluke vorn) and with samples collected through a new 50-m PVC tube with a pump (Grundfoss Brunnenpumpe or GFPump) deployed overboard the ship, usually during CTD casts. Indeed the samples collected with the pump showed clearly the lowest activities and we decided to use that sampling exclusively (from station 217 onward). Surface water samples were collected at a total of 41 stations.

Preliminary results

The ^{224}Ra data measured immediately on board ship (Fig. 5.2) are thought to represent the total activity of the mother nuclide ^{228}Th . The activity of particulate ^{228}Th (collected on filters) and of its parent ^{228}Ra has to be measured later in the home laboratory. The geographical distribution of ^{224}Ra shows enhanced activities upon crossing the Trans Polar Drift in the vicinity of the Lomonosov Ridge.

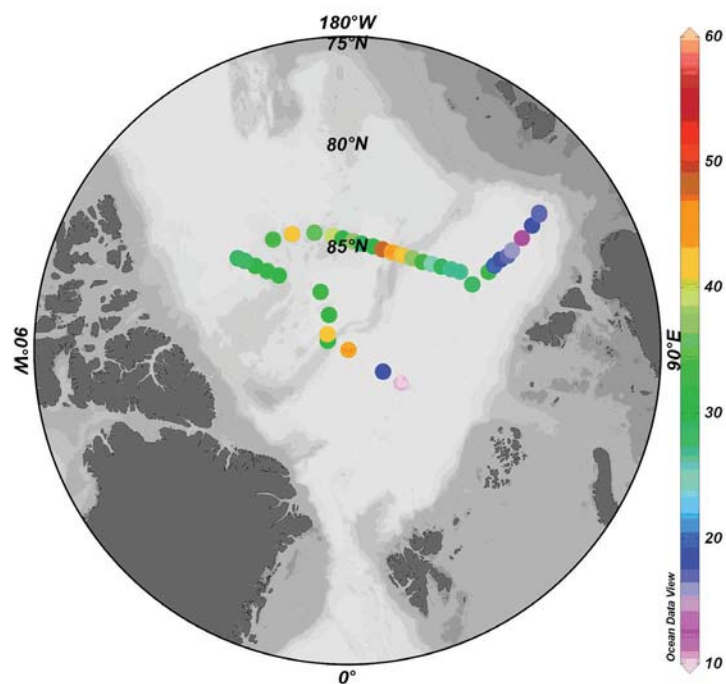


Fig. 5.2. Preliminary results of the distribution of ^{224}Ra (dpm/m^3) in surface waters during ARK-XXVI/3

References

Cai, P., Rutgers v.d. Loeff, M. M., Stimac, I., Nöthig, E.-M., Lepore, K., and Moran, S. B., 2010. Low export flux of particulate organic carbon in the central Arctic Ocean as revealed by ^{234}Th : ^{238}U disequilibrium. *Journal of Geophysical Research - Oceans* 115, C10037, doi:10.1029/2009JC005595.

5.3 Tracing terrestrial carbon across the Arctic shelf and slope

Alexander Charkin

POI-FEBRAS Vladivostok

Michiel Rutgers van der Loeff

Alfred-Wegener-Institut

Objectives

The Arctic Ocean receives >10% of the global river sediment discharge while only hosting 1% of the total ocean volume. Furthermore, the Eurasian part of the Arctic Shelf is the world's largest continental shelf sea system strongly influenced by high input of terrigenous material derived from surrounding land masses and supplied by large river systems. The productivity is relatively low in the Arctic Ocean in comparison with other world regions, because of the permanent ice cover. Only along ice edges and in some areas that are ice free during summer months, sometimes higher productivities occur. Therefore, the sediments in the Arctic Ocean mainly show a terrigenous composition, and biogenic particles only occur in minor amounts. Our study focuses on the investigations of the major, trace, and rare earth elements (REE) geochemistry, organic carbon (OC), isotopic ($\delta^{13}\text{C}$) composition and carbon/nitrogen (C/N) ratios of the sedimentary material for the identification of the terrestrial signal across the Arctic Shelf and slope.

Work at sea

Water samples for suspended particular matter (SPM) and particulate organic carbon (POC) filtration have been collected from the rosette system. The SPM for geochemistry of rare earth elements was obtained by filtration through membrane filters with pore diameter of 0.47 μm . The POC for organic carbon concentration, isotopic ($\delta^{13}\text{C}$) composition and carbon/nitrogen (C/N) ratios was obtained by filtration through borosilicate glass fiber filters (GF/F; Whatman Inc. with approximate pore diameters of 0.7 μm). The filtered water volume for SPM and POC was up to 4 l, depending on sediment load. Additionally, 20 surface sediment samples (upper 2 cm) have been collected from cores taken with the Multicorer.

Expected results

In total, we obtained 220 samples of SPM, POC and 20 samples of surface sediments for the analysis of the major, trace, and rare earth elements (REE) geochemistry, organic carbon (OC) content, isotopic ($\delta^{13}\text{C}$) composition. Elementary (C,N) and isotopic ($\delta^{13}\text{C}$) composition of SPM and bottom sediments will be determined after the cruise by Carlo Erba elemental analyzers and a Finnigan MAT Delta Plus mass spectrometer, respectively, at the International Arctic Research Center, University of Alaska, Fairbanks (USA) or with similar instruments at Stockholm University (Sweden). REE elements will be analyzed in the Institute of chemistry FEB RAS, Vladivostok (Russia).

5.4 ^7Be as tracer for determining atmospheric deposition of trace elements

Ben Galfond

Rosenstiel School of Marine and Atmospheric
Sciences (RSMAS) Miami, USA

Not on board: David Kadko, William Landing

Objectives

The atmospheric input of numerous chemical species into the global ocean equals or exceeds that from river sources and thus constitutes an important budgetary component for these elements. The atmospheric input of trace elements plays a key role in ocean biogeochemical processes as well, unfortunately the assessment of this input is difficult as measurements of deposition rates to the ocean -particularly the Arctic- are rare and susceptible to problems of temporal and spatial variability. Given the dearth of direct measurements, the ocean community has relied on atmospheric transport and deposition models that are unconstrained as to the amounts of rainfall delivered to the ocean and the parameterization of aerosol removal processes. If such parameters could be accurately assessed, then the chemical concentration of aerosols could be transformed to actual estimates of flux.

Indirect methods, such as the use of natural radionuclides delivered to the ocean from the atmosphere, are often used to estimate atmospheric inputs. During this expedition we have used measurements of ^7Be in the surface waters, snow/ice cover and in the lower atmosphere, coupled with trace element measurements in aerosols, to provide estimates of the atmospheric input of relevant trace elements into the Arctic Ocean. The ability to readily derive ^7Be flux from the ocean/ice inventory provides the means to link the chemical concentration data of precipitation and aerosols to flux. We have also addressed the partitioning of ^7Be and trace elements between the ice/snow and the open water. This method could ultimately be applied to seasonal study in the Arctic as the partitioning would be expected to vary throughout the year. This in turn would give insight into how trace element deposition will change as sea ice conditions in the Arctic evolve in the future.

^7Be is a cosmic ray produced radioisotope that becomes associated with particles in the troposphere and subsequently deposited to the surface ocean. Because of its relatively short half-life (53.3 days) it is reasonable to equate the inventory of ^7Be decay in the upper ocean and snow, to the flux of ^7Be from the atmosphere. This provides a key linkage between the atmospheric concentration of chemical species and their deposition to the ocean. Such species include many of interest to the GEOTRACES program such as Hg, Al, Mn, Fe, Cu, Zn, and Cd.

Work at sea

At open water stations, mixed layer seawater from the ship's internal system was collected in 600 L tanks, which was then filtered through iron impregnated acrylic fibers, which bind the ^7Be , allowing for later measurements on land. For ice stations, the mixed layer samples were instead filtered *in-situ* on the ice floe. This presents us with a sample that is unperturbed by mixing from the ship. A mobile CTD cast performed by the group of Dieckmann allowed us to target the center of the mixed layer at every station. Samples of snow, ice cores, and meltpond water

were also collected and then precipitated with FeCl₃ for transport back to land. A pump was used to fill 1000 L tanks on the deck of the ship from a depth of 40 m, allowing us to assess the complete water column ⁷Be inventory. Aerosols were collected on paper filters for analysis of ⁷Be and trace metal content. Quartz fiber filters allow for the study of both ⁷Be and mercury as well.

5.5 Net community productivity using dissolved O₂/Ar/²²²Rn

Nicolas Cassar

Michiel Rutgers van der Loeff, Daniel Scholz

Duke University

Alfred-Wegener-Institut

Objectives

The objective of this project is to estimate net community productivity in the Arctic Ocean using dissolved O₂/Ar measurements, and constrain the biogeochemical controls on carbon fluxes. Oxygen in the mixed layer is influenced by biology, and by physical processes such as bubble injection, temperature and pressure changes. Because argon (Ar) has similar solubility properties as oxygen, the oxygen derived from physical processes can be estimated from the argon concentration relative to its saturation ([Ar]^{sat}). The oxygen derived from biology is equal to the total oxygen minus the oxygen derived from physical processes.

²²²Rn was used as an independent measure of air-sea exchange. ²²²Rn is produced in the water column from ²²⁶Ra dissolved in seawater. Exchange with the atmosphere creates a depletion in surface waters that can be used as quantification of air-sea exchange. This will give us an additional tool to convert the oxygen over- or undersaturation derived from O₂/Ar ratios into oxygen fluxes and thus into net community productivity (NCP).

5.5.1 Net community production using O₂/Ar ratios in surface waters.

Nicolas Cassar

Duke University

Work at sea

Biological oxygen supersaturation was measured continuously by Equilibrator Inlet Mass Spectrometry (EIMS, Fig. 5.3), a method previously described (Cassar et al., 2009). Briefly, seawater from the ship's underway system was pumped through a gas equilibrator, the headspace of which was connected to a quadrupole mass spectrometer for continuous elemental O₂/Ar ratio measurements. The ion current ratio was calibrated by periodically sampling ambient air. From the O₂/Ar supersaturation, a gas exchange rate, and the oxygen concentration at saturation, the net biological oxygen flux across the ocean surface will be estimated.

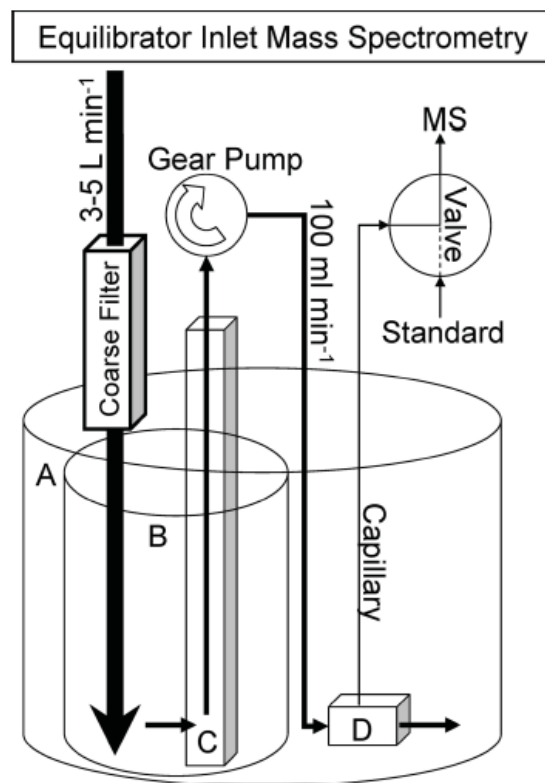


Fig. 5.3. Setup of the Equilibrator Inlet Mass Spectrometry

The large seawater reservoir (A) sits in a sink. After going through an inline coarse filter (500 μm pore size), seawater flows into the inner reservoir (B) at a rate of 3-5 L min^{-1} (large arrow). Most of the water running into B overflows into A, which is used as a water bath thermostatted to the temperature of ambient seawater. A small fraction (100 mL min^{-1}) of the high flow rate is pulled with a gear pump through a filter sleeve (C), with 100 and 5 μm pore size on the outside and inside, respectively. From the gear pump, the seawater flows through the equilibrator (D). The equilibrator sits in reservoir A to keep its temperature identical to that of the incoming seawater. A capillary, attached to the headspace of the equilibrator, leads to a multiport Valco valve. This valve alternates between admitting gas from the equilibrator and ambient air to the quadrupole mass spectrometer. An optode (not shown) in container B measures total oxygen saturation. Also not shown is a water flow meter located downstream of the equilibrator and thermocouples monitoring temperatures throughout the system (from Cassar et al. 2009)

A transmissometer was also installed on the ship's underway seawater system in order to estimate semi-quantitatively the POC concentration (Gardner et al. 1993). The transmission signal will be calibrated with POC measurements performed every few hours by the group of A. Boetius.

Preliminary results

Results will only be available after calibration of the ion current ratio 32/40 (O_2/Ar) signal and transmissometer data. Our preliminary observations suggest large biological activity in the marginal sea ice zone and potentially in regions above ridges.

5.5.2 Gas exchange rate using ^{222}Rn depletion in surface waters

Michiel Rutgers van der Loeff , Daniel Scholz

Alfred-Wegener-Institut

Objectives

In order to derive gas exchange rates from the measurements of oxygen saturation, we need the piston velocity. In open water this is usually taken from empirical relationships between windstress and piston velocity. Few data exist for ice-covered seas. Originally it has been widely assumed that ice cover would completely prevent gas exchange, but Fanning and Torres (1991), using the depletion of ^{222}Rn in surface waters as tracer, reported significant gas exchange in the ice covered Barents Sea, comparable to 70% of the open ocean value. Much lower exchange rates were found recently by Loose and Schlosser (2010). It was our aim to use the ^{222}Rn technique to derive gas exchange rates in the range from fully ice-covered to open water conditions.

Work at sea

We have determined the ^{222}Rn activity profile in the upper 50 m of the water column at 18 stations using the method of Mathieu et al. (1988). At each sampling depth a 30-L sample was collected with the Multiple Water Sampler and 27 liter was allowed to flow into evacuated PVC containers. After stripping the samples for Radon, the samples were passed over a MnO_2 -coated fibre to collect the Radium parent. As standard sampling depths we used 2, 5, 10, 20, 30, 50 m. Due to the strong stratification with a stable halocline usually at 20-30 m depth, we did not expect any deeper mixing on the time scale covered by ^{222}Rn (3.8 days half life). Any gas exchange with the atmosphere should be seen in a depletion of ^{222}Rn in the surface water relative to its parent ^{226}Ra .

In an attempt to see possible gas exchange on a smaller scale in the water just below the ice, we have collected 5-L water samples from just below the ice. A plastic tube was lowered through a hole drilled in the ice and samples were collected by connecting the tube (after rinsing with a hand-operated vacuum pump) to 5.8-L evacuated glass jars. With the same Radon stripping technique Radon was determined in these samples, but because of the lower volume the relative error in the data is 5 times larger.

Preliminary results

Exact data on ^{222}Rn depletion can only be given after the determination of the activity of the parent ^{226}Ra which has to follow in the home laboratory. We know that ^{226}Ra is correlated with salinity and silicate content, and we also know that ^{226}Ra is higher in water of Pacific than of Atlantic origin. Indeed, the ^{222}Rn activities in the water below the surface mixed layer tended to be highest in the stations in the middle of the expedition (approximately stations 218-239) where we know from nutrient data (biogeochemistry group) that the water was largely of Pacific origin. But as we do not expect large gradients in ^{226}Ra over the upper 50 m, the ^{222}Rn profiles already give an indication of the existence of a ^{222}Rn depletion in surface waters.

Only the last four stations (273, 276, 280, 285) were in fully open water. Here we observed a clear depletion of ^{222}Rn in the upper three horizons (2, 5, and 10m, Fig. 5.4). This is in good agreement with the many studies where ^{222}Rn has been used

to quantify gas exchange rates. However, in the stations where we had full ice cover (212-245) we did not observe a significant difference between the upper 10 m and the deeper samples, which brings us to the preliminary conclusion that the gas exchange rate is here severely limited, at any rate stronger than suggested by the results of Fanning and Torres.

The sampling directly under the ice was successful only on the ice stations 212, 218, 222, 227, 230 and 235. During later ice stations the low air temperatures caused immediate freezing of the water in the tubings and prevented proper sampling. The results of the under ice sampling with 5-L jars have inherently larger errors than the results obtained with 30-L samples from the ship (Fig. 5.4). The lack of a significant difference between the two sampling strategies implies that we have no indication of even a thin layer under the ice with enhanced gas exchange with the atmosphere.

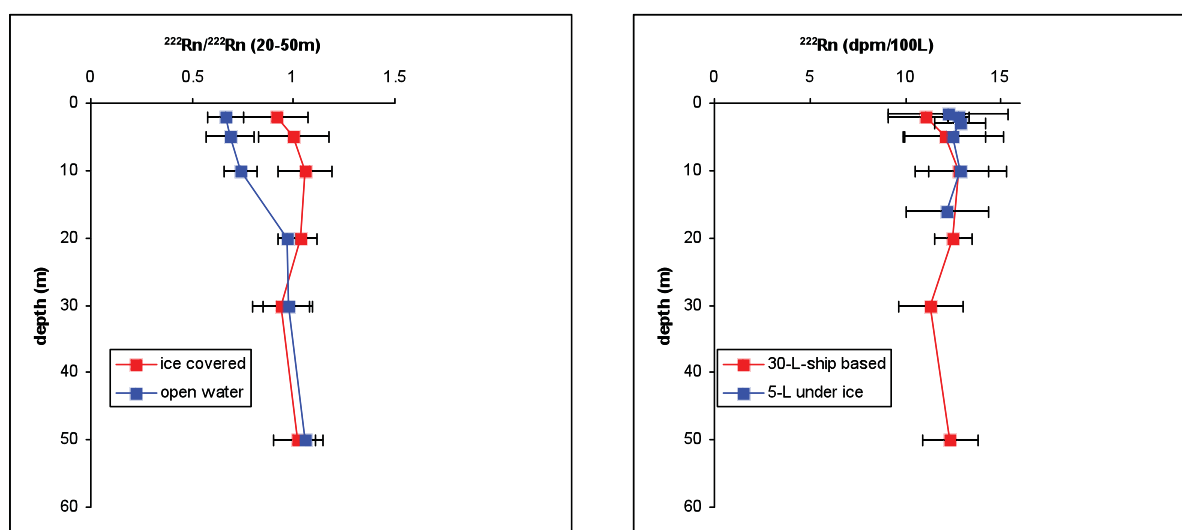


Fig. 5.4. Left: Average profiles of ^{222}Rn activity (with standard error) in the upper 50 m, distinguishing stations with full ice cover (red, $n=9$) and with fully open water (blue, $n=4$), normalized to the respective average activities in the 20-50 m layer. Right: average profiles of ^{222}Rn activity (with standard error) at ice stations as determined in 27-L samples collected from the ship (red, $n=9$) and in 5-L samples collected through a hole in the ice (blue, $n=6$).

References

- Cassar, N., Barnett, B.A., Bender, M.L., Kaiser, J., Hamme, R.C., Tilbrook, B., 2009. Continuous High-Frequency Dissolved O_2/Ar Measurements by Equilibrator Inlet Mass Spectrometry. *Anal. Chem.* 81, 1855-1864.
- Fanning, K. A. and Torres, L. M., 1991. ^{222}Rn and ^{226}Ra : indicators of sea-ice effects on air-sea gas exchange. In: E., S., E., H. C. C., and A., O. N. (Eds.), Pp. 51-58 in *Proceedings of the Pro Mare Symposium on Polar Marine Ecology*, Trondheim. 12-16 May 1990. *Polar Research* 10(1).

5.6 Mercury cycling in the Arctic

Gardner, W. D., Walsh, I. D., Richardson, M. J. 1993. Biophysical forcing of particle production and distribution during a spring bloom in the North Atlantic. *Deep-Sea Research II*. 40, 171-195.

Loose, B. and Schlosser, P., 2010. Sea ice and its effect on CO₂ flux between the atmosphere and the Southern Ocean interior. *Journal of Geophysical Research* 116, C11019, doi:10.1029/2010JC006509.

Mathieu, G. G., Biscaye, P. E., Lupton, R. A., and Hammond, D. E., 1988. System for measurement of ²²²Rn at low levels in natural waters. *Health Physics* 55, 989-992.

5.6 Mercury cycling in the Arctic

Ben Galfond

RSMAS, Miami

Michiel Rutgers van der Loeff

Alfred-Wegener-Institut

Samples taken for: Lars-Eric Heimbürger (Geosciences Environment Toulouse at Midi-Pyrenees Observatory OMP, Toulouse)

Objectives

Major objective of this program was exploring the role of the Arctic Ocean in the global mercury cycle. Key questions are:

1. What controls methyl mercury (MeHg) trends and variability in the Arctic Ocean?
2. Is the Arctic a sink for atmospheric Hg contamination?
3. What is the environmental response of the MeHg cycle to climate change and increasing anthropogenic emissions?
4. What are the causes for the alarming rise of Hg levels in Arctic biota?

Work at sea

As the PI was not able to participate in the expedition, this project was severely limited. Samples for the analysis of MeHg were collected from the CTD/Rosette system at stations 218, 245, 273, 280 by Ben Galfond.

Expected results

Alarming rise in Hg levels of Arctic marine biota has been attributed to increased anthropogenic Hg emissions. However, the Hg species that accumulates along the trophic chain is MeHg. MeHg is produced in the oceanic water column during the remineralization of organic matter. This process seems to be independent from atmospheric Hg deposition. The basis of the food web structure determines the amount of MeHg that is produced in situ. We measured for the first time MeHg in the central Arctic Ocean. This is critical to predict the impact of ongoing global warming on the Arctic Hg cycles. Total and MeHg have been determined on 4 stations.

5.7 Distribution of ^{236}U and of Cs isotopes

Michiel Rutgers van der Loeff

Alfred-Wegener-Institut

Objectives

^{236}U is an anthropogenic radionuclide introduced in the environment by nuclear test explosions and by reprocessing of nuclear wastes. The invasion of this transient tracer into the World Ocean has recently become an issue of much interest. After the nuclear accident in the power plants of Fukushima, March 2011, it is important to know how the radioactivity released spreads over the globe. A nuclide that is readily detected is ^{134}Cs (2 y half-life).

Work at sea

We have collected samples for analysis of ^{236}U by two teams. 1-L surface samples were collected at 15 stations for the group of Gideon Henderson, University of Oxford to be analysed by mass spectrometry. Full depth profiles of 15-20L samples were collected in the deep basins (stations 204 and 218 in the Eurasian Basin, stations 226 and 245 in the Makarov Basin, station 235 in the Canada Basin). These samples will be analysed by Marcus Christl (ETH, Zürich) with Accelerator Mass Spectrometry. For the analysis of Cs isotopes we have collected 21 100-L samples (14 from the ship's seawater inlet, 7 from meltponds on ice stations). These samples will be analysed for ^{134}Cs and ^{137}Cs by gamma spectrometry in the home laboratory.

Work at sea

The distribution of ^{236}U will be used to investigate what this novel tracer can tell us about the transport of Atlantic water and to quantify ventilation rates of deep waters in the Arctic. The distribution of ^{134}Cs will allow us to judge whether significant amounts of nuclides released by the Fukushima accident had reached the Arctic half a year after the event.

6. BIOGEOCHEMISTRY

Gerhard Dieckmann, Ellen Damm, Elisabeth Alfred-Wegener-Institut
Helmke, Kai-Uwe Ludwigowski, Claudia
Bureau, Laura Wischnewski, Eva
Kirschenmann

Objectives

The aim of the biogeochemistry group was essentially to characterise the biogeochemical properties and processes in and below the sea ice.

Sea ice is a structuring component of the Arctic Oceans and plays a pivotal role in the biogeochemical cycles of Arctic marine ecosystems. The sea-ice cover greatly affects energy and material fluxes between the ocean and the atmosphere, and provides a habitat for diverse microbial assemblages, which in terms of biomass are generally dominated by algae.

The biogeochemistry of Arctic sea ice has been poorly documented to date. Our aim was to obtain information on biogeochemical processes in sea ice during its seasonal transition. Our specific objectives were: i) to make an extensive characterization of the biogeochemical environment experienced by sea ice communities, ii) to investigate microbiological processes in relation with the physical-chemical environment, iii) to investigate the methane cycle in sea ice and sea ice/water interface, iv) to investigate the occurrence and abundance of cryogenic carbonate minerals (CaCO_3) in sea ice as part of its internal carbon cycle, v) to investigate the fate of land derived organic matter in sea ice, and vi) to study the hydrography at the sea ice/water interface.

Work at sea

Extensive sampling took place during 15 ice stations. Samples were taken from: i) sectioned ice cores in collaboration with the sea ice physics group for bulk ice measurements, ii) sackholes drilled in sea ice, and iii) depth profiles of seawater taken with a CTD from the ice to avoid influences from the ship. Where possible, water samples were taken directly under the ice at high resolution (e.g. 0.1 m, 0.5 m, 1 m, 2 m). Further samples were generated by a number of experiments designed to investigate the contribution of the major sea ice biogeochemical parameter, i.e. methane.

The collected samples provided data of salinity, temperature, pH and total alkalinity, chlorophyll, and coloured dissolved organic matter (C-DOM), major dissolved inorganic nutrients, nitrate plus nitrite ($[\text{NO}_x]$), phosphate ($[\text{P}]$), and silicate ($[\text{Si}]$), dissolved organic carbon (DOC). The determination of other parameters will be conducted in the home laboratories. The sectioned cores were returned to the laboratory where they were allowed to melt at $+4^\circ\text{C}$. Calcium carbonate was analysed from all cores.

Sea-ice brine was collected from sackholes and the lower-most centimetres of the sea-ice floe were sampled by means of ice coring. These samples were used for the determination of the same parameters as the ice cores. Kemmerer water samplers were deployed through the core holes for water samples for analyses corresponding to the ice core and brine analyses.

A total of 180 samples were taken for the determination of dissolved organic matter (DOM) at representative stations. Bulk determinations of dissolved organic carbon (DOC) and nitrogen (DON) will be carried out after the cruise in the home lab.

DOM samples were taken for bulk determinations (DOC/DON) and extracted from seawater using PPL sorbent (enrichment of DOM by solid phase extraction). DOM sampling was decided after consulting the fluorescence profiles on the CTD. Different water masses were sampled (e.g. fluorescence max. and 10 m above sea bottom) and chemically characterized after the enrichment using ultrahigh resolution mass spectrometry (FT-ICR-MS) in the home lab. Additionally all samples were extracted on board using solid phase extraction with PPL sorbent. This will facilitate the analysis of detailed chemical DOM characteristics by ultrahigh resolution mass spectrometry also later at the home lab.

Sea-ice brine, Kemmerer bottle samples and water samples taken with the rosette sampler at different depths were analysed for nitrate, nitrite, ammonium, phosphate and silicate content immediately on board with an Autoanalyzer-System according to standard methods.

Methane and DMS was immediately measured on board ship, using gas chromatographs equipped with a flame ionization detector (FID) and a pulsed flame photometric detector (PFPD), respectively. Furthermore, DMSP particular and dissolved was analysed in seawater, ice and sediments. Gas samples were stored for analyses of the $\delta^{13}\text{C}_{\text{CH}_4}$ values in the home laboratory. In addition to the sea ice sampling, different water masses were sampled by CTD rosette from the ship at discrete depths throughout the water column at 60 stations. Samples were treated the same as the sea ice samples.

The bacterial communities of sea ice, meltponds and under ice water (0.5 m) were investigated at all 15 sea-ice stations by determining bacterial biomass, total numbers, bacterial diversity and bacterial community structure as well as secondary production.

Bacterial secondary production was determined on board under *in-situ* like temperature conditions. Although the results between the different stations varied considerably at least clear differences between sea ice and meltpond communities of the Eurasian and Pacific part of the Arctic Ocean became obvious. Cultural work was done with selected samples only. These cultures will be the basis for the isolation of representative sea-ice and melt-pond strains and will help to understand survival and reproduction capabilities of the different types and will give new ideas concerning adaptation strategies.

Final working steps will be done in the home laboratory. After completion of the whole set of analyses, like filtration, preservation, washing and freezing, we will be able to compare the new data set from predominantly first-year ice with material from 1997, 1999, and 2001 from predominantly multiyear sea ice and Antarctic sea-ice communities.

Preliminary results

Fig. 6.1 shows an example of a typical profile of salinity and temperature obtained with the SEACAT CTD deployed through an ice core hole at station 218. Shown are the down and up casts. The dramatic temperature rise and low salinities in the top meter of the water column at the sea ice water interface is clearly indicative of melting, whereas the top 20 meters of the water column below the ice appears to be well-mixed. This is followed by a clear rise in temperature and increase in salinity below a depth of 20 to 25 meters, which is again followed by a drop in temperature and decrease in salinity.

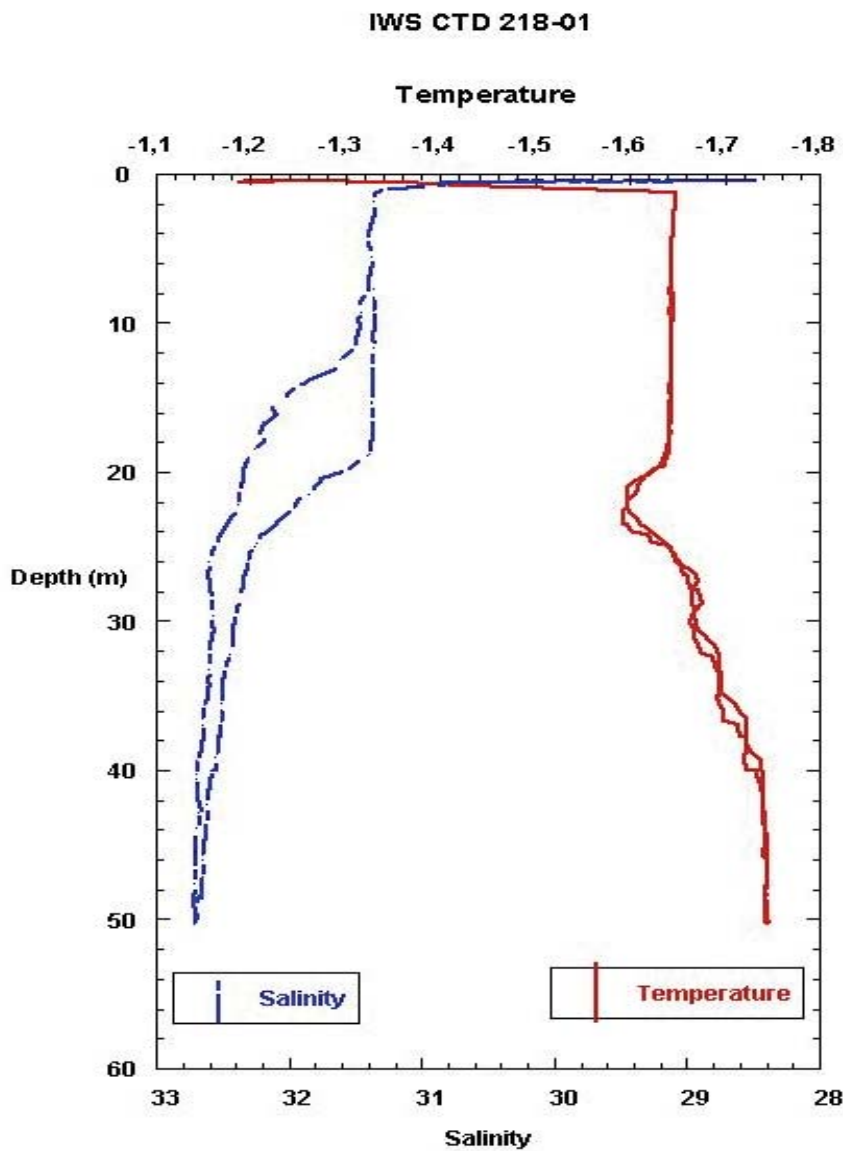


Fig. 6.1: A scrutiny of the data as well as comparison with the ship's CTD data is essential before the hydrographic features under the sea ice can be clearly interpreted.

7. MARINE BIOLOGY

7.1 Biology of sea-ice and related ecosystems

Ilka Peeken	AWI/MARUM
Christophe Boissard	LSCE/CNRS
Mar Fernandez Mendez	AWI/MPI
Kristin Hänselmann	AWI/University Hamburg

Objectives

The decrease in summer sea-ice extent and in the concentration of multiyear ice (MYI) is expected to have major implications for the sea-ice biota by affecting its biomass, primary productivity and biodiversity. Due to the high spatial heterogeneity of sea-ice biota, current estimates of total biomass still need to be improved by using remotely operated vehicles equipped with biomass sensors.

The loss of sea ice might be favourable for the phytoplankton primary production by increasing the length of the growing season. However, nutrient availability is considered to be the limiting factor controlling primary production in the Arctic Ocean. Nutrient depletion together with warming has been shown to lead to an increase in especially small phytoplankton, resulting in relatively poor food quality at higher trophic levels. Additionally, the replacement of MYI by first year ice (FYI) will further increase the occurrence of melt ponds, an ecosystem that has been largely overlooked in previous investigations.

Phytoplankton and sea-ice algae have an influence on the production of organic compounds some of which can have a significant influence on the photochemistry of the atmosphere, particularly unsaturated hydrocarbons (such as isoprene:2-methyl-1,3 butadiene, or light alkenes) and carbon monoxide (CO) which have a strong impact on the OH radical and ozone budget as well as on the formation of organic aerosols playing an important role on cloud-condensation nuclei (CCN) number and thus on cloud lifetime and properties.

Our questions and objectives for this cruise were:

- What are the relative contributions to primary productivity (PP) of the different phototrophic communities in the central Arctic Ocean?
- Will higher light intensities due to thinner ice boost PP in the ice in summer or will it be limited by nutrient supply?
- What are the contributions of pico- and nanoplankton in the various habitats?
- How are biodiversity and carbon pool changing in the different sea ice types and melt ponds?
- Establish optical measurements for biomass estimation in sea ice for the central Arctic (collaboration with sea ice physicist).

7.1 Biology of sea-ice and related ecosystems

- Investigate the spatial-temporal variability of reactive gases in seawater and sea-ice in relation to the distribution of algae species and its effect on the aerosol production.

Work at sea

General sampling and biological variables

At 11 ice stations, biological measurements were carried out (see Fig. 3.15) starting with station 203 (1st) and ending with station 250 (11th). The work consisted of sampling of melt ponds (minimum 3 replicates) and sea-ice cores. Water from the upper 30 m below the ice was taken in collaboration with G. Dieckmann (AWI, CTD profile measurements) and E. Damm (AWI, group in charge of methane and DMS analyses). Sampling and measurement strategy of sack holes was made with the help of N. Cassar (Duke University).

Biological ice cores were sectioned into 10 cm slices, which were diluted with 0.2 µm filtered sea water (200 ml for each cm of ice) and thereafter allowed to melt during the next 24-48 hours at a temperature of 4°C under low-light conditions. From these samples and the melt-pond water, various subsamples were taken for measurements of primary productivity and species composition (microscopy, flow cytometry, DNA and pigment determinations). To investigate the carbon cycle, samples for POC (Particulate Organic Carbon), DOC (Dissolved Organic Carbon) and TEP (Transparent Exopolymers) were taken. Additional subsamples of Biogenic Particulate Silica, PABS (Particle Absorbtion) and CDOM (Chromophoric Dissolved Organic Matter) were taken. At 6 stations, additional size-fractionated samples (0-3, 3-10 and larger 10 µm) were taken from the melt ponds and the lowest section of the ice cores. From under-ice water and sack holes only samples for pigments and flow cytometry were taken at all depth, while occasionally additional PP measurements directly under the ice were done.

Towards the end of the cruise the spatial variability for the production of trace gases and ice algae in sack holes was investigated by two helicopter flights (Tab. 7.1) stopping randomly at 5 suitable floats each and samples for trace gases, nutrients, oxygen, pigments and flow cytometer were taken.

Tab 7.1: Position and dates of the helicopter flights with sack-hole sampling.

Date	12.09.2011		Date	14.09.2011	
(Float)	Lat.	Long.	(Float)	Lat.	Long.
#1	83°55.74'N	132°07.50'E	#1	83°08.80N	116°45.31E
#2	83°57.68'N	132°01.72'E	#2	83°09.67N	116°34.12E
#3	84°00.29'N	132°11.60'E	#3	83°10.16N	116°31.56E
#4	84°01.91'N	131°46.48'E	#4	83°10.7N	116°31.30E
#5	83°58.99'N	131°37.80'E	#5	83°11.5N	116°29.70E

For the optical cores, the ice cores were divided in surface (upper 20 cm), bottom (lower 20 cm) and the middle part. To avoid the dilution of the optical signal, these

cores were allowed to melt at 4°C (within 48-72 hours) and thereafter samples for pigments, PABS and CDOM were taken. These data will be used to calibrate the hyperspectral measurements obtained by the optical sensors (see "3. Sea ice physics"). For comparison of the different ice-melting techniques between the optical and the biological cores (with and without adding seawater) additional flow cytometer samples for the pico- and nano-algae were analysed.

Except for PP and flow cytometer samples, all other variables were stored for further analysis at the AWI.

Flow-cytometer measurements

Flow-cytometer measurements have been carried out with an Accuri C6 flow cytometer. The instrument is equipped with a blue (488 nm) and a red (620 nm) laser. To check the general performance of the instrument and to calibrate the Forward Scatter Signal (FSC) an Invitrogen size calibration kit F-13838 was used. To each sample Polychromatic latex beads (1 µm, Polyscience) was added to monitor the optical system and to check for clogging of samples. The various phytoplankton types were identified by applying the autofluorescence of the red (FL3) versus the orange (FL2) channel according to Marie et al. (2005). Each sample was analysed for 3 minutes at a custom flow rate of 100 µl min⁻¹, using a core size of 40 µm. In total three size groups were identified: pico-plankton (0-3 µm), small nanoplankton (3-10 µm) and large nanoplankton (10-25 µm). To get a rough estimate of the biomass of each group, the FL3 (Chl a) fluorescence signal from each group was multiplied with the cell number and divided by 10⁸ to retrieve the presented arbitrary biomass values (Fig. 7.1 and 7.2).

Primary production measurements

A total of 150 samples were analysed covering diverse habitats: sea ice, melt ponds, water under the ice and surface water (both, from ice-covered and non-ice covered regions). All samples were spiked with ¹⁴C bicarbonate (1 µCi ml⁻¹), distributed in four plastic bottles (three light and one dark; 20 ml each with 35 ml headspace) and incubated in the laboratory for 24 hours under stable temperature and light conditions: -1.9°C and 10 µmol photons m⁻² s⁻¹. After the incubation, samples were filtered through a 0.2 µm pore size nitrocellulose acetate filter and fumed overnight with 6 M HCl. The amount of ¹⁴C assimilated as POC (radioactively labelled Particulate Organic Carbon) by the cells was determined by liquid scintillation, adding Filter Count scintillation cocktail to the filters. Rates of Net Primary productivity were then calculated as follows:

Primary Production rate (µgC L⁻¹ d⁻¹) =

$$((\text{CPM sample} - \text{CPM dark}) \times \text{DIC} \times 1,05) / (\text{CPM added} / (100 \mu\text{l} * 10^{-6}) \times \text{Vol} \times \text{Time})$$

where CPM refers to the Counts per Minute given by the scintillation counter and DIC is the natural dissolved inorganic carbon concentration of the sample. Therefore for each sample analysed, a 2 ml subsample was fixed with HgCl₂ in order to determine DIC concentration by flow injection back on land.

Trace gases and aerosols

Light hydrocarbons and CO concentrations were measured from different types of samples. While the ship was moving, continuous analysis of *in-situ* surface sea water was measured. During the ice stations, a total of 18 vertical profiles under the ice (surface level down to 30 m depth) were performed using a Kemmerer bottle. 20 additional samples were taken from the sack holes and melt ponds. Towards the end of the cruise trace gases were measured in water from melted ice-cores taken from the sack holes.

For analysis the water was introduced in an equilibration chamber where dissolved gases were equilibrated with clean synthetic air, and analysed by a gas chromatograph (GC). Two instruments were used: a GC equipped with a PID (photo-ionization detector) for unsaturated hydrocarbon quantification and a GC equipped with a mercuric oxide detector for CO monitoring. Measurement frequency was approximately 30 minutes for dissolved hydrocarbons and 5 minutes for dissolved CO. Gases present in the ice were extracted in a different way by following the procedure of Xie and Gosselin (2005).

Aerosols were continuously collected using an Aethalometer for black carbon assessment and an automated PARTISOL for organic aerosols in the CCN mode (Aerodynamic Diameter, A.D. < 0.2 μm , 6 h time resolution).

Preliminary Results

Flow-cytometer measurements

Preliminary results of the flow-cytometer measurements of the melt pond water (Fig. 7.1) indicated a high spatial variability of the algae biomass < 25 μm even within one station. Although the melt ponds were not always connected with the underlying water, the latter seems to influence the standing stocks of the melt ponds as can be seen by the highest observed biomass in the Atlantic sector of the investigation area. Small and large nano-plankton dominated the algae in this habitat. However, a clear preference for certain size groups depending on the water mass was not observed.

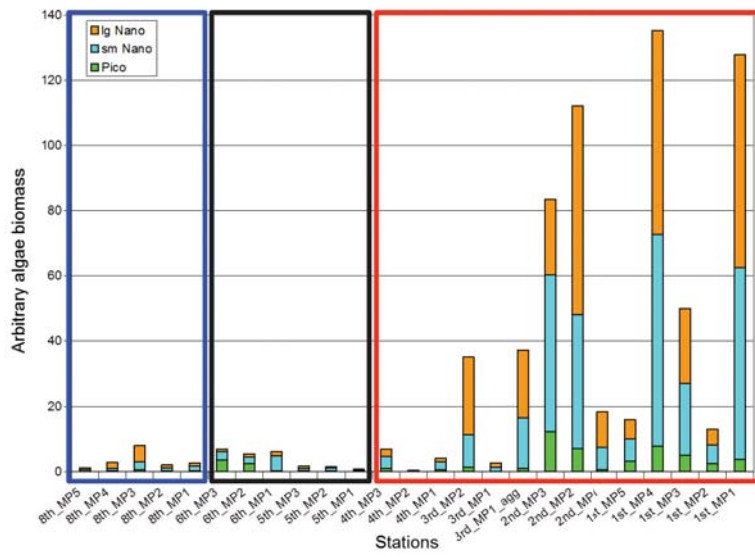


Fig. 7.1: Arbitrary biomass of plankton < 25 μm for pico-plankton, small nano-plankton (sm) and large (lg) nano-plankton from several melt ponds (MP) at various ice stations (indicated by number). Coloured rectangles around the stations indicate the three different water masses based on nutrient data; red Atlantic, blue Pacific and black mixed water masses.

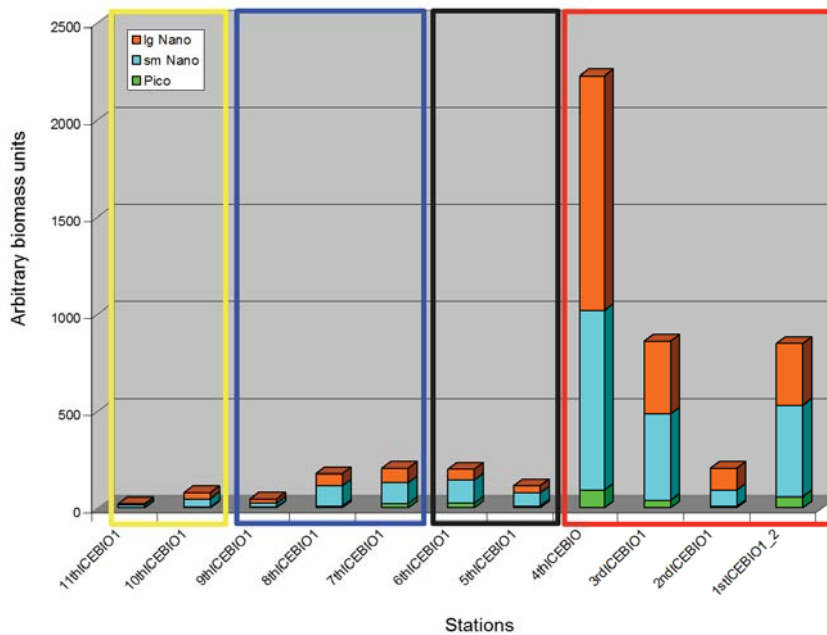


Fig. 7.2: As Fig.7.1 for integrated biological ice cores (ICEBIO). A yellow rectangle indicates an additional mixed water mass during the last two ice stations.

Integrated concentrations of the arbitrary biomass from ice cores showed a similar pattern as observed for the melt ponds with highest standing stocks in the Atlantic sector of the investigation area (Fig. 7.2). However, no clear size preferences of an algae group could be attributed to a given water mass. Towards the end of the cruise, standing stocks of ice algae were very low and an effect of the progressing season cannot be excluded.

Preliminary results from the CTD profiles, sack holes and under-ice water samples also indicated a general higher standing stock in the Atlantic water masses during this cruise. In contrast, Pacific water masses, characterized by low nitrate concentration supported only low algae biomass highlighting the importance of nutrients for the development of the Arctic ecosystem.

Primary production

Preliminary results of net primary productivity rates (NPP) in ice-covered surface waters were low ($<10 \mu\text{g C L}^{-1} \text{d}^{-1}$) compared to open coastal waters close to the Laptev Sea ($<25 \mu\text{g C L}^{-1} \text{d}^{-1}$). (Note that all rates shown have not been Chl a normalized yet and have been calculated assuming a constant DIC of $2400 \mu\text{g C L}^{-1}$) Preliminary rates were very variable and relatively low in general ranging from 0.1 to $25 \mu\text{g C L}^{-1} \text{d}^{-1}$ (Fig. 7.3). Samples from Pacific-derived, nutrient depleted waters, which showed very low N:P ratios (below 2), tended to have lower NPP values than those from Atlantic influenced waters, although nutrient contents were also very low there.

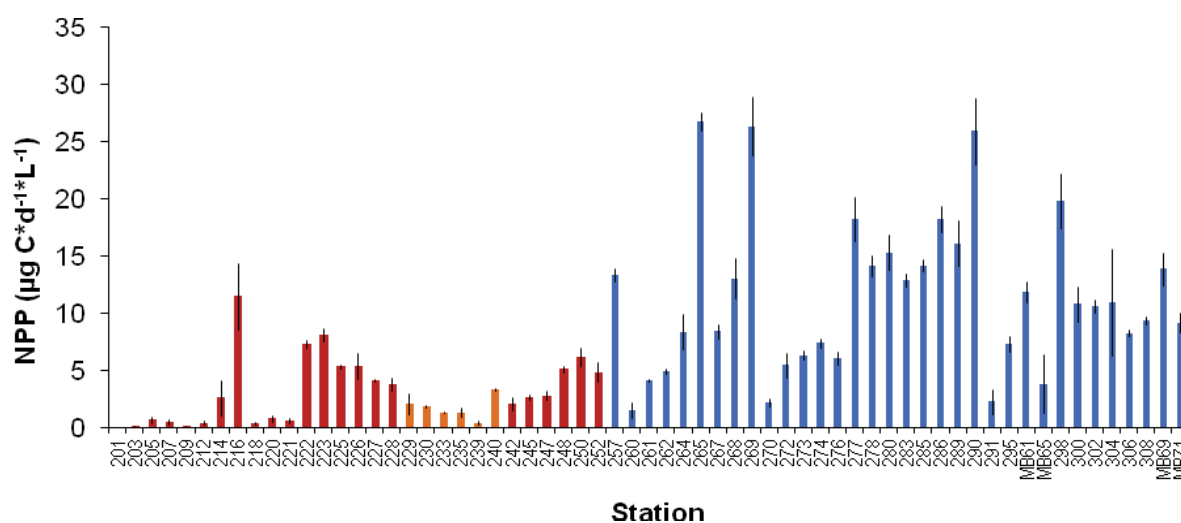


Fig. 7.3: Surface water net primary productivity rates in the central Arctic at 4°C and $10 \mu\text{mol photons m}^{-2} \text{s}^{-1}$. Red corresponds to Atlantic influenced water masses, orange to Pacific influenced water masses and blue to coastal waters close to the Laptev Sea. Stations also represent a temporal sequence starting in early August and finishing in late September.

In order to investigate the nutrient limitation of phytoplankton communities in these different water masses, three nutrient limitation bioassays were performed by splitting the samples in eight different bottles to which different nutrient combinations were added (nitrate, phosphate and silicate). None of the nutrients triggered a clear increase in the carbon-uptake rate compared to the control, with no addition of nutrients. As an example the results for the experiment performed with station 233, in Pacific influenced waters is shown in Fig. 7.4.

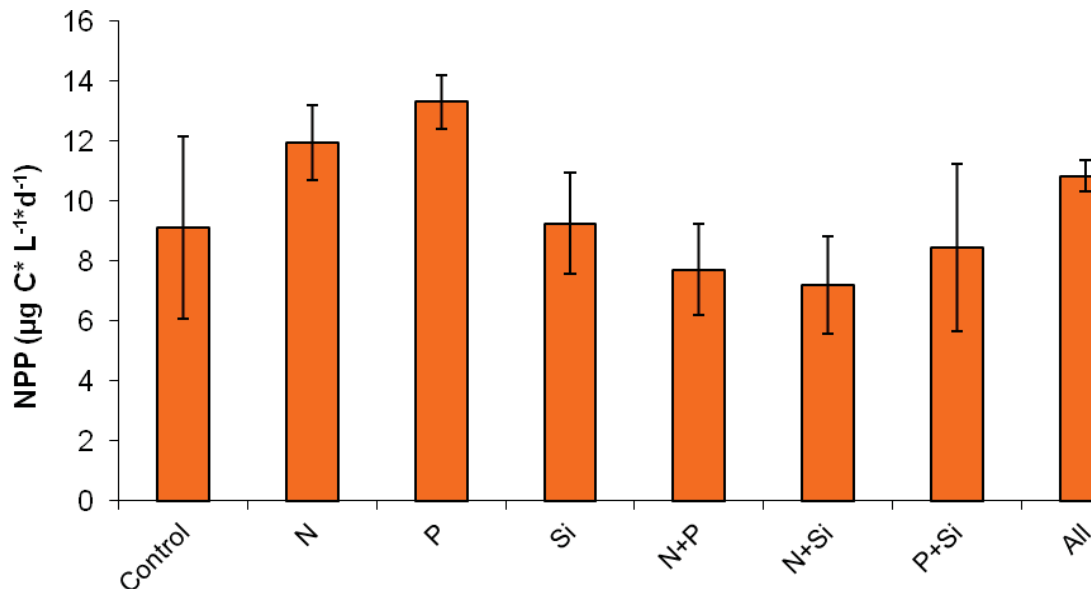


Fig. 7.4: Nutrient bioassay from Station 233 (Pacific influenced waters). Mean net-primary productivity rates of the different treatments after 3 days of acclimation and 5 days incubation under stable conditions: 4°C and 10 µmol photons m⁻² s⁻¹. The control had no addition of nutrients and the "All" treatment had all three nutrients added. Error bars indicate standard deviation from three replicates.

Sea-ice and melt-pond carbon-fixation rates have to be re-calculated with the real DIC values once measured. Despite the fact that the rates will probably decrease when the real DIC value is taken (expected to be much lower than in sea water because salinity is also lower in these habitats and salinity and DIC concentration are positively correlated), melt ponds and sea ice seem to highly contribute to primary productivity in the Arctic during late summer (Fig. 7.5). In the ice cores, NPP was differently distributed along the cores. For example: at the last three ice stations the highest rates were found in the bottom 20 cm of the ice, while at stations 203, 212, 218 and 222 the highest activity was detected in the surface 20 cm of the ice.

Melt ponds, covering up to 60% of the ice surface, also showed a great variability in terms of primary productivity both in and between stations. Several melt pond samples were analysed under the microscope, revealing complex communities

7.1 Biology of sea-ice and related ecosystems

formed by several diatom species (many of them dead or in resting spore state), dinoflagellates, turbellaria, rotifers, ciliates, foraminifera. Grazing could be observed to be a very active process but was not quantified.

In summary, high spatial variability of PP, both in sea-ice cores and melt ponds, was the main characteristic of the Arctic summer ice sampled during this cruise. Together with the large small-scale variability makes up scaling of carbon fixation rates to the entire Arctic a challenging task.

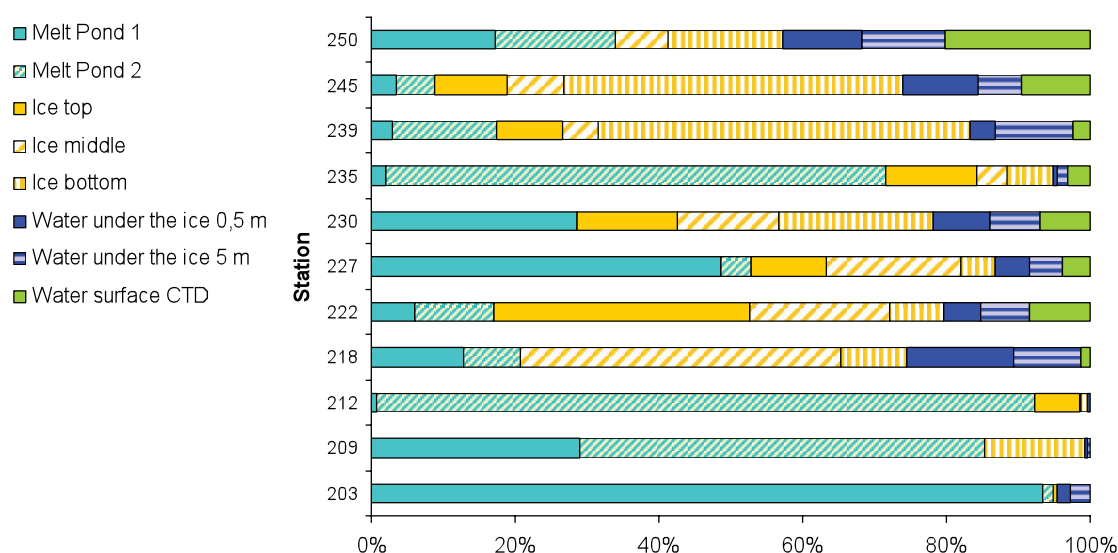


Figure 7.5: Relative contributions to primary productivity of the different habitats: melt ponds, sea ice, water under the ice and surface water in each ice station. Calculated using non-biomass normalized rates and constant sea-water DIC concentrations for all habitats.

Trace gases

Data processing is still on the way; the full interpretation will be made using the biological measurements and the physical parameters measured during the samplings.

A preliminary vertical profile (Fig. 7.6) for the different variables (total light hydrocarbons, isoprene, propene (C_3H_6) and CO) depict that concentrations observed for each compound in sack holes were much higher than the concentrations in the water column. In addition, CO concentrations were by an order of magnitude higher than the hydrocarbon concentrations. For all gases a strong vertical gradient in the very shallow water layers (1-2 m) was observed. These general findings were systematically found on all other investigated profiles.

Aerosols filters will be analysed in the home laboratory.

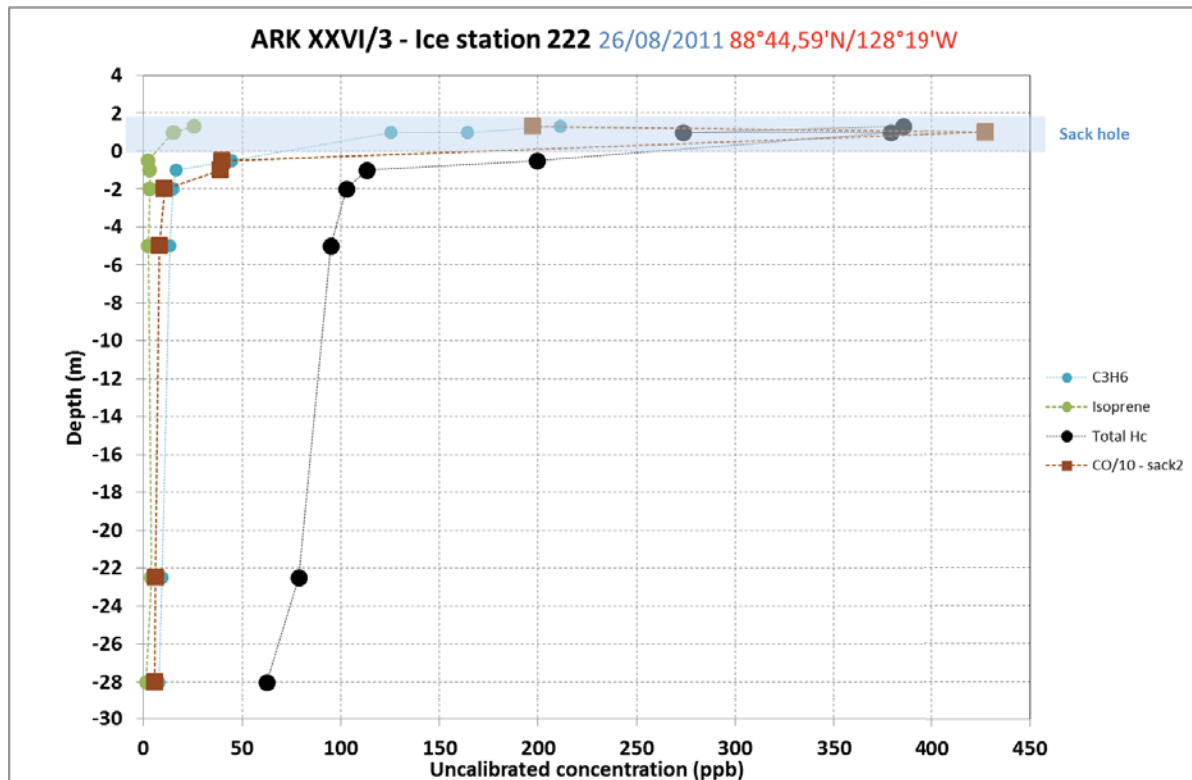


Fig. 7.6: Vertical profiles of propene (C_3H_6), isoprene, of total light hydrocarbons (Hc) and carbon monoxide (CO) from Station 222 under the ice in comparison to the sack holes sampled on the ice. (Note that all concentrations are not finally calibrated yet and that the CO concentrations from the sack holes were divided by 10 for better readability).

References

- Marie, D., Simon, N. & Vaultot, D. (2005) Phytoplankton cell counting by flow cytometry, in: Algal Culturing Techniques, edited by: Andersen, R. A., Elsevier Academic Press
- Xie, H. & Gosselin, M. (2005) Photoproduction of carbon monoxide in first-year sea ice in Franklin Bay, southeastern Beaufort Sea, *Geophys. Res., Lett.*, 32, doi:10.1025

7.2 Plankton Ecology and Biogeochemistry in a Changing Arctic Ocean (PEBCAO)

Antje Boetius, Alexandra Cherkasheva, Alfred-Wegener-Institut
 Estelle Kiliyas, Ilka Peeken, Olivia Serdeczny
 Not on board: Eva - Maria Nöthig

Objectives

The project PEBCAO (Plankton Ecology and Biogeochemistry in a Changing Arctic Ocean) is focused on studying plankton and microbial processes relevant for biogeochemical cycles in the Arctic Ocean. In order to understand and track

consequences of climate change for the pelagic ecosystem, both long-term field observations and experimental work with Arctic plankton species and communities are needed to gain knowledge about their feedback potential in the future Arctic Ocean.

Biogeochemistry, phytoplankton & vertical particle flux

Recent investigations indicate that rising temperatures and freshening of polar surface waters promote a shift in the phytoplankton community towards a dominance of smaller cells. A change in size of the primary producers could have significant consequences for the entire food web and for the cycling and sequestering of organic matter. An increase in ice-free areas as well as CO₂- and temperature-related changes will also affect plankton and the carbonate chemistry of the ocean; even small changes in the biological pump could significantly affect atmospheric CO₂ concentration. In such a scenario, picoplankton can comprise a large pool of biomass and can attain high abundances. Therefore, we particularly need to understand how environmental parameters influence the diversity, occurrence and distribution of the picoplankton.

In this context, results collected during this cruise will be compared with results obtained during former cruises to answer questions like: Is there a shift of the phytoplankton community towards smaller cells? Are there any intrusions of Atlantic species into the Arctic Ocean? How does the phytoplankton community differ between different water masses? Do observed changes in the pelagic realm influence the vertical particle flux of organic matter?

Primary production & phytooptics

At high latitudes ocean color satellite data have a sparse coverage due to the presence of sea ice, clouds and low sun elevation angles. This is the main cause that satellite ocean colour algorithms which achieve large-scale information on primary production perform poorly in these regions. Therefore, our main aim for TransArc was to collect in-situ data that allow us to adopt satellite global primary production algorithms (as far as the satellite reaches northern latitudes) for the Arctic Ocean. Furthermore, in-situ optical measurements and the photosynthetic characteristic of phytoplankton in the central part of the Arctic Ocean were sampled because so far only a few data of phytoplankton characteristics on larger temporal and spatial scales than obtained from discrete water samples exist.

Work at sea

Samples have been collected along two transects; some additional stations were sampled in the outer Laptev Sea. In addition, surface water was sampled along the ship's route (see Fig. 7.7).

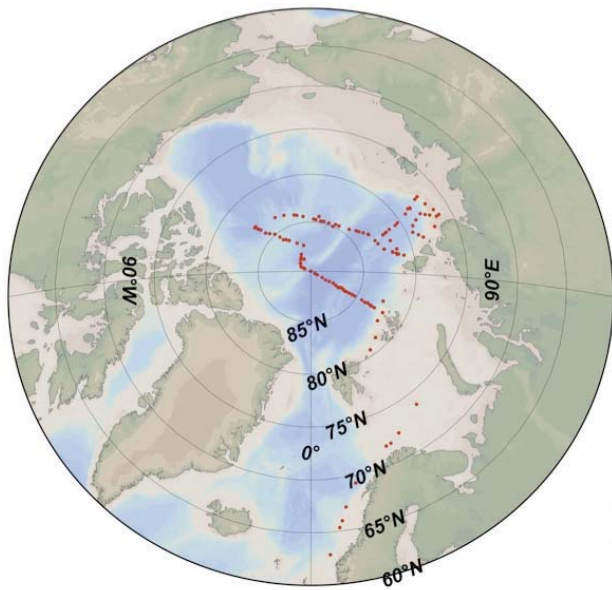


Fig. 7.7: Stations sampled by the PEBCAO group

Biogeochemistry, phytoplankton & vertical particle flux

Samples for phytoplankton ecology investigations were taken from the CTD-rosette at 87 stations at 5 to 8 depths according to the water mass structure (at 66 stations the upper 70 m were sampled, at 21 stations the upper 200 m were sampled). On 10 of the stations, under-ice plankton was sampled at 0.5, 1 and 5 m, respectively. Ocean surface water was sampled every 20-60 miles from the ship's flow through membrane pump at 97 spots. At all 87 stations and at the 97 spots, samples have been taken for analysing biogeochemical and biooptical parameters such as chlorophyll a, pigments (HPLC), absorption of particulates, CDOM and phytoplankton and CDOM fluorescence. Samples to determine seston, particulate organic carbon (POC), particulate organic nitrogen (PON), and particulate biogenic silica (PbSi), phytoplankton and protozooplankton were taken at selected stations. The water was filtered through pre-combusted Whatman GF/C glass-fiber filters, polycarbonate and, cellulose acetate filters and stored deep-frozen at -20°C or -80°C for later analyses in the home laboratory. The abundances of autotrophic pico- and nanoplankton, and small microplankton were determined with the flow cytometer directly on board. Microscope identification and enumeration of larger nanoplankton and microplankton will be carried out later in the home laboratory at AWI. Samples are preserved and stored at a cool and dark place.

Due to the small size and thus complicated phenotypic characterization the smallest phytoplankton fraction, picoplankton ($0.2\text{-}2.0\ \mu\text{m}$), is difficult to detect and assess. However, a proper identification down to the species level can be achieved by the application of molecular methods. Thus, in order to investigate the genetic diversity of picoeukaryotes special filter samples for DNA analyses were taken during the cruise. Additionally some water samples were taken into culture for later microscopy analyses. Surface water samples were taken twice a day from the membrane pump and 3 depth were sampled from 58 CTD casts. According to the fluorescence probe profile, one sample was taken from the surface layer, one from the chlorophyll maximum and one from a depth of approximately 50 m. For the DNA analyses a size fractionation was performed. Two liters of the water sample

were first filtered through a membrane filter (Millipore) with a pore size of 10 μm . Afterwards the flow trough was filtered through a second membrane filter with a pore size of 3 μm and finally the flow trough of the previous filtration was filtered through a membrane filter with a pore size of 0.4 μm . All in all, three different phytoplankton size fractions were achieved from every water sample taken, above 10 μm , between 3 and 10 μm and between 0.4 μm and 3 μm . After filtration the samples were stored immediately at -80°C .

Vertical particle flux of particulate matter under the almost permanent ice cover will be investigated by means of sediment traps which were deployed in two moorings near the Gakkel Ridge (two in the Nansen Basin and two in Amundsen Basin; both deployed at ~ 200 m & ~ 150 m above the sea floor) for one year (see oceanography, chapter 4). The traps were equipped with 20 sampling jars each and pre-programmed individually. They will be recovered in summer 2012 during the *Polarstern* expedition "IceArc" (ARK-XXVII/3).

Primary production & phytooptics

In-situ radiance and irradiance measurements at high spectral resolution down to 110 m have been carried out using a TriOS RAMSES radiometer. Every measurement includes spectra of downwelling irradiance (sensor 5038), upwelling irradiance (sensor 81EA) and upwelling radiance (sensors 82D6 and 81E6). These data will later be used to validate radiative transfer modeling through the water column.

The photosynthetic characteristic of phytoplankton has been investigated by measurements of the variable fluorescence in the upper 110 m. A FastTracka Fast Repetition Rate Fluorimeter (FRRF) exposes phytoplankton to a series of flashes of blue light at 200 kHz repetition rate and then records the fluorescence signal. From this signal the efficiency of the photochemical conversion during photosynthesis of the observed algal population was calculated. The data will be later processed with e.g. "Submersible FRRF Data Reduction – FRS1" software. These estimates will be used to validate one of the key parameters in satellite primary production modeling – the photosynthetic yield.

Preliminary/expected results

All samples have to be finally analyzed in the home laboratory at AWI. Results obtained with the flow cytometer showed distinct differences between Atlantic and Pacific influenced water masses with much higher cell concentrations in the 'Atlantic part' of the Arctic Ocean with highest counts at the beginning of the cruise in early August. To investigate the community structure and the diversity of picoeukaryotes, ribosomal fingerprinting technology (ARISA) as well as pyrosequencing will be applied. We speculate to find less biomass and a trend towards smaller cells in comparison with results obtained during former cruises.

Combined with the data collected for chlorophyll a and phytoplankton specific absorption the optical measurements will serve as ground truth data for the adaptation of the global satellite primary production algorithm to the Arctic Ocean.

7.3 Zooplankton investigations

Hans-Jürgen Hirche¹, Russell R.
Hopcroft², Ksenia N. Kosobokova³,
Elizaveta A. Ershova²

¹Alfred-Wegener-Institut
²UAF
³SIO

Objectives

What drives the productivity of the Arctic Ocean has remained a central question in polar research for more than a century. Given the extreme seasonality of this habitat, how do organisms persist over the prolonged periods of low primary productivity? Investigations in the Greenland Sea and Eurasian Basin in the early 1990s demonstrated that the composition and distribution of pelagic fauna in the Arctic Ocean is strongly affected at regional and even basin scales by the inflow of Atlantic water (Hirche & Mumm, 1992; Mumm, 1993; Kosobokova & Hirche, 2000) that enters via Fram Strait and from the Barents Sea shelf into the Eurasian Basin (Hirche & Mumm, 1992; Kosobokova & Hirche, 2000). The environmental niche - preferences and tolerances - of these advected species then determines their success at inhabiting the Arctic basins. While many expatriated species die off shortly after entering the Arctic Ocean, others survive due to their starvation potential, or even continue their development for some time, such that the distribution of those unsuccessful is dependent on a combination of transport velocity and survival time.

Given their connection to adjoining waters, as well as local productivity, the Arctic's biological communities are sensitive to changes in circulation as well as sea ice cover. During the 1990s, various observations indicated that the properties and circulation of Atlantic-derived water in the Arctic Ocean had changed considerably. In the Eurasian Basin, the Atlantic layer became warmer and saltier (Schauer et al., 2004) and the boundary between the Atlantic and Pacific waters moved further into the Canada Basin (McLaughlin et al., 2002). A simple increased advection of Atlantic populations might only increase the sedimentation of advected biogenic material, however, coincident warming could also favor the survival of the Atlantic communities, provided there is adequate food to sustain them. Given sufficient warming, expatriated fauna might begin to replace the resident Arctic fauna which is characterized by slow growth and low biomass (Hirche & Mumm, 1992; Kosobokova & Hirche, 2000, 2009; Hirche & Kosobokova, 2007). The situation is further complicated by the pronounced decline of summer sea ice cover observed over the past decade.

In order to understand the processes and factors regulating the survival of both the advected Atlantic zooplankton and the resident fauna within the Arctic Ocean, the work of the zooplankton team focused on the following tasks:

Patterns

Relate the composition, abundance, biomass and spatial distribution of zooplankton communities across the basins and ridges to water circulation patterns and primary productivity. Determine the present environmental status of the Arctic Ocean, compare it to earlier cruises, and improve projections of future status or change.

Rates

Relate the reproductive state of dominant copepod species to environmental factors, including the continued analyses of biochemical composition (i.e. lipid

7.3 Zooplankton investigations

storage) and stable isotopes to understand the life strategies and trophodynamic relationships of species.

Genetics

Build the DNA sequence library needed for emerging molecular approaches to community structure. Determine if regional or basin-scale population structure exists within the Arctic using molecular markers.

Outreach

Share the diversity of the Arctic planktonic life through images and public resources.

Work at sea and preliminary results

Sampling

For the investigation of species composition and distribution, zooplankton were collected by a multiple closing net (Model MAXI, 0.5 m² mouth opening, Hydrobios, Kiel). The Mutinet was equipped with 150 µm mesh nets and provided stratified sampling of the entire water column from the surface to the bottom at a total of 29 stations, with two sequential casts occurring at one deeper station (Fig. 7.8 and Tab. 7.2). Sampling was carried out on two large transects covering all basins and crossing all ridges of the Arctic Ocean. From five to seven layers were sampled in the shelf and continental slope regions, and from nine to fifteen layers at stations off the shelf. The majority of stations were taken in the deep region (21 stations total, eleven of them deeper than 3000 m, plus four deeper than 4000 m), while five were taken in the slope region, and only three in the shelf region (depths <400 m) (Tab. 7.2). The samples were preserved in 4 % borax-buffered formaldehyde for later processing.

Live animals for experiments, and for biochemical and physiological measurements, were collected in the upper 300 m with a bongo net (300 µm and 500 µm mesh), or from a 60 cm diameter (300 µm mesh) net attached to the outside of the Mutinet.

Genetics

It is proposed that in the future, the diversity within zooplankton samples will be determined via high throughput molecular sequencing. Such technologies will require a complete “library” of the target sequences to ultimately determine the species they represent. During the cruise, a total of 139 planktonic metazoan species were identified within our non-quantitative live samples. Representatives of each were removed, placed in 95% ethanol, and stored at -80°C for later determination of their COI sequences plus some additional mitochondrial or nuclear target regions. This yield represents the majority of the zooplankton species known from the Arctic basins, with only the rarest species still remaining unsampled. For the three most dominant copepod species – *Calanus hyperboreus*, *C. glacialis*, and *Metridia longa* – samples are prepared to explore population genetics at high spatial resolution. The relative availability of most other species will restrict our analysis to a simple comparison of the Eurasian to the Amerasian basin populations.

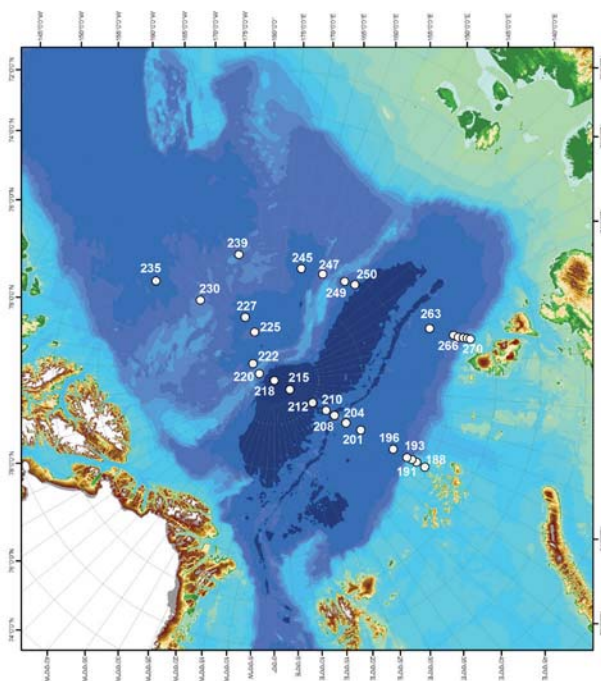


Fig. 7.8: Station map of zooplankton sampling

Tab. 7.2: Zooplankton sampling stations

ARK 26/3	5.8.-7.10.2011					Egg production expts		
	Station	Date	Lat (N)	Lon	MN/#samples	Bongo	<i>C.glacialis</i>	<i>Metridia longa</i>
	188	9.8.	82°10'	60°E	220/5	200	x	x
	190	9.8.	82°36'	59°55' E	270/5	200	x	
	191	10.8.	82°50'	60°E	960/7	300	x	x
	193	10/11.8.	83°45'	59°58' E	3000/9	300		x
	196	12.8.	83°52'	60°30' E	3570/9	1500	x	
	201	13/14.8.	85°31'	59°53' E	3900/9	500	x	x
	204	15.8.	86°14'	59°23' E	3200/9	300	x	x
	208	17.8.	86°51'	60°11' E	2850	300	x	x
	210	18.8.	87°17'	59°57' E	4180	300	x	x
	212a	19.8.	87°17'	59°38' E	760	300	x	x
	212b	20.8.	88°01'	59°03' E	4320			
	215	21.8.	89°11'	61°04' E	4325	300	x	x
	218	23.8.	89°53'	54°07' E	4250	300	x	x
	220	24.8.	89°16'	117°03' W	2050	300	x	x
	222	26.8.	88°45'	128°19' W	3900	300	x	x
	225	28.8.	87°39'	157°37' W	2350	300	x	x
	227	29.8.	86°52'	155°06' W	3815	300	x	x
	230	1.9.	85°04'	137°11' W	1800	300	x	x
	235	3.9.	83°01'	129°59' W	3450	300	x	x

7.3 Zooplankton investigations

ARK 26/3	5.8.-7.10.2011					Egg production expts		
	Station	Date	Lat (N)	Lon	MN/#samples	Bongo	<i>C.glacialis</i>	<i>Metridia longa</i>
	239	6.9.	84°05′	164°13′W	1960	300	x	x
	245	9.9.	84°48′	166°31′W	3350	300	x	x
	247	10.9.	84°44′	155°36′W	2180		x	x
	249	11.9.	84°31′	144°37′E	1980		x	x
	250	11.9.	84°22′	139°50′E	3650		x	
	263	15.9.	82°36′	108°24′E	3525		x	x
	266	16.9.	81°39′	104°01′E	2980		x	x
	267	17.9.	81°29′	103°10′E	2530		x	x
	268	17.9.	81°16′	102°39′E	2170		x	x
	269	17.9.	81°07′	102°15′E	1385		x	x
	270	18.9.	80°58′	101°51′E	370		x	x

Image library

During this cruise, we have continued to build on efforts begun under the ArcOD project of Census of Marine Life program to create an image library for metazoan Arctic zooplankton. About 1800 digital images have been taken during the cruise, encompassing most of species encountered. These images will begin to appear on the Arctic Ocean Diversity website (<http://www.arcodiv.org>), as well as the Encyclopedia of Life (<http://www.eol.org>), post-cruise.

Distribution and condition of three dominant copepods in relation to hydrography

Substantial numbers of the copepods *Calanus hyperboreus* and *Metridia longa* are probably advected into the Arctic Basin within the Atlantic Inflow from the Greenland Sea, while many *C. glacialis* originate from adjoining marginal seas, like the Barents or Kara seas. In order to understand and predict their fate in the Arctic Ocean, we documented their body's dry weight, lipid content, and reproductive state.

Dry mass

Dry mass is a general parameter integrating all body compounds. It will be determined from females and copepodite stage V of specimens sorted alive and then deep frozen at -25°C).

Lipids

Lipids are accumulated during the productive Arctic summers. They are used as energy reserves to sustain animals during the winter, and for gonad maturation and egg production during the following season. Measuring the volume of the lipids accumulated provides an index of how successful the species has been in a given year, and how this varies regionally. During the cruise, we have imaged copepodite stages V and VI of *C. hyperboreus* and *C. glacialis* at each station. From sets of 50 animals per stage per species (ca. 5800 animals in total) we will determine body size and lipid volumes by semi-automated image analysis. These estimates will be compared to – and calibrated with – the measured mean-dry mass of the animals imaged.

Egg production

Egg production is a direct measure of reproductive activity of a population. Egg production experiments were set up for *C. glacialis* and *M. longa* at all stations. No experiments were conducted with *C. hyperboreus*, as this species spawns only in winter (Hirche and Niehoff, 1996). Typically, 48 single females of *C. glacialis* were incubated for at least 48 hours in 15 ml cell wells. *C. glacialis* laid eggs in only 5 of the 29 experiments, and only in the Eurasian Basins during first half of August at locations observed to have higher chlorophyll concentrations.

Eggs production experiments

Eggs production experiments with *Metridia longa* were conducted at 25 stations (Tab. 7.2). On each station, 48 females were sorted from the bongo net samples and then set individually into 70 ml towers filled with filtered sea-water. The towers contained a 300 µm mesh positioned 0.5 cm above the cell bottom, which allowed the eggs to fall through thereby avoiding egg disturbance or cannibalism (Hopcroft et al., 2005). Females were kept at 0°C for 48-96 hours, during which eggs were produced from 20 of 25 stations. Eggs were counted upon termination of the experiment; eggs-laying females were individually preserved in formalin for later measurements. From several stations (St. 188, 191, 193, 204), egg-laying females were kept an additional 3 weeks to monitor egg production under starvation conditions, during which time egg production slowly/rapidly declined. At these same stations, eggs were kept to monitor hatching success rate and hatching time. Generally, eggs took 5-7 days to hatch; most of the eggs that did not disintegrate in the first 1-2 days ("good" eggs) and hatched successfully into nauplii. The percentage of "good" eggs varied from station to station; from female to female; and even in different clutches of the same female. An additional 50 *M. longa* females were incubated from the beginning of the cruise in filtered sea-water to study longer-term mortality rate due to starvation: nearly all survived the entire 5 weeks.

Egg production and starvation of mesopelagic species

Egg production experiments were also carried out on *Spinocalanus horridus* from stations 225 and 229, *Scaphocalanus acrocephalus* from St. 212 and *Heterorhabdus norvegicus* from stations 250 and 267. Females were set individually in 15 ml cell wells in filtered sea-water and monitored daily for produced eggs. Eggs were produced by 3 *Spinocalanus horridus* females, by 2 *Scaphocalanus acrocephalus* and by a single *Heterorhabdus norvegicus*.

Patterns

The pattern of zooplankton abundance and biomass are typically determined post-cruise, however, the four dominant calanoid copepod species (*Calanus hyperboreus*, *C. glacialis*, *C. finmarchicus* and *Metridia longa*) were enumerated in the preserved Multinet collections from about half the stations during the cruise. All copepodite stages of the four species were counted in the entire sample. Prosome length was used to distinguish the young stages (CI-CIII) of three *Calanus* species as well as adults and CVs of the closely related *C. glacialis* and *C. finmarchicus*, according to Hirche & Kosobokova (2011). The highest abundances were found along the slopes and over the ridges, with all copepodite stages observed in *C. hyperboreus*, *C. glacialis*, and *Metridia longa*, but only late copepodites observed

7.3 Zooplankton investigations

for *C. finmarchicus*. The population stage composition helps to better understand the reproductive status of these populations and their life histories. It indicates that *C. finmarchicus* does not reproduce within the Arctic Ocean. Biomass will be calculated from published (Richter, 1994) and unpublished taxon-specific length-dry weight (DW) relationships, and individual dry weights (Kosobokova et al., 1998). These data, and that added post-cruise, on zooplankton in the four major basins of the Arctic Ocean will be related to hydrography, bottom topography and the distribution of primary production to better elucidate their distributional patterns.

References

- Hirche, H.J. & Mumm, N. (1992). Distribution of dominant copepods in the Nansen Basin, Arctic Ocean, in summer. *Deep-Sea Res.* 39 Suppl. 2: S485-S505.
- Hirche, H.J. & Niehoff, B. (1996). Reproduction of the Arctic copepod *Calanus hyperboreus* in the Greenland Sea - field and laboratory observations. *Polar Biol.* 16: 209-219.
- Hirche, H.J. & Kosobokova, K.N. (2007). Distribution of *Calanus finmarchicus* in the northern North Atlantic and Arctic Ocean - expatriation and potential colonization. *DPR II*, 54: 2729-2747.
- Hirche, H.J. & Kosobokova, K.N. (2011). Winter studies on zooplankton in Arctic seas: the Storfjord (Svalbard) and adjacent ice-covered Barents Sea. *Marine Biology* 158:2359-2376
- Hopcroft, R.R., Pinchuk, A.I., Byrd, A. & Clarke, C. (2005). The paradox of *Metridia* spp. egg production rates: A new technique and measurements from the coastal Gulf of Alaska. *Mar. Ecol. Prog. Ser.* 286: 193-201.
- Kosobokova, K.N. (1998). New data on the life cycle of *Calanus glacialis* in the White Sea based on seasonal observations of its genital system development. *Oceanology* 28 (3):347-355
- Kosobokova, K.N. & Hirche, H.J. (2000). Zooplankton distribution across the Lomonosov Ridge, Arctic Ocean: species inventory, biomass and vertical structure. *Deep-Sea Res.* I 47: 2029-2060.
- Kosobokova, K.N. & Hirche, H.J. (2009). Biomass of zooplankton in the eastern Arctic Ocean - a base line study. *Prog. Oceanogr.* 82:265-280.
- McLaughlin, F., Carmack, E., MacDonald, R.W., Weaver, A.J. & Smith, J. (2002). The Canada Basin 1989–1995: Upstream events and farfield effects of the Barents Sea. *J. Geophys. Res.* 107, doi:10.1029/2001JC000904.
- Mumm, N. (1993). Composition and distribution of mesozooplankton in the Nansen Basin, Arctic Ocean, during summer. *Polar Biol.* 13: 451-461.
- Richter, C. (1994). Regional and seasonal variability in the vertical distribution of mesozooplankton in the Greenland Sea. *Berichte zur Polarforschung*, 154: 1-87
- Schauer, U., Fahrbach, E., Osterhus, S. & Rohardt, G. (2004). Arctic warming through the Fram Strait: Oceanic heat transport from 3 years of measurements. *J. Geophys. Res.* 109(C06026), 10.1029/2003JC001823.

8. MARINE GEOLOGY

Tina Kollaske¹, Jens Matthiessen¹,
Ann-Katrin Meinhardt², Norbert
Lensch¹, Patricia Slabon¹, Mirko
Sühs¹, Hao Zao¹

¹) Alfred-Wegener-Institut
²) Institute for Chemistry
and Biology of the Marine
Environment, Oldenburg

Introduction and objectives

The overall goals of the marine-geological research programme are (1) high-resolution studies of changes in paleoclimate, paleoceanic circulation, paleoproductivity, and sea ice distribution in the Central Arctic Ocean and at the adjacent continental margins during the Quaternary, and (2) the long-term history of the Mesozoic and Cenozoic Arctic Ocean and its environmental evolution from a (sub-)tropical to an ice-covered polar ocean. In areas such as the Alpha-Mendeleev Ridge, pre-Quaternary sediments are cropping out close to the seabed, which could even be cored with coring gears aboard *Polarstern* and which would allow to study the Mesozoic/Tertiary history of the (preglacial) Arctic Ocean. Especially, data for the reconstruction of the long-term paleoclimatic history of the Arctic Ocean are sparse.

A large set of sediment cores from the eastern Arctic Ocean has been studied in the past 20 years resulting in relatively well-constrained spatial reconstructions of paleoceanographic variability in the Eurasia Basin and of the marine part of ice sheets in Eurasia in the Middle to Late Pleistocene. Reconstructions for the western Arctic are still based on comparably few records, and in particular the central regions such as the Alpha Ridge have been mainly sampled from drifting ice islands in the 1960s and 1970s due to the inaccessibility for surface ships. Since *Polarstern* has collected sediment cores for the first time at the western Alpha and northern Mendeleev Ridges during ARK-XIV/1a in 1998, sea-ice cover in the Arctic Ocean has deteriorated considerably. It reached a historical low in extent in 2007, and *Polarstern* could sample again the western Alpha Ridge during ARK-XXII/3. Therefore, it was attempted during ARK-XXVI/3 to break through to the eastern Alpha Ridge where, besides Pleistocene sediments, isolated occurrences of Mesozoic and Paleogene sediments have been cored by chance from drifting ice islands. Recoring at these sites had a high priority because knowledge of the Pre-Pleistocene history of the Amerasia Basin is just based on data from these four locations. However, two attempts during this expedition failed due to the presence of multi-year sea ice despite a generally low extent of sea ice in 2011. Thus, the central Alpha Ridge may still be reached by *Polarstern* only if supported by a second icebreaker.

The new results will be related to those obtained from previous expeditions to the Central Arctic Ocean and the Eurasian continental margin. It was the aim of this expedition to fill gaps in the network of sediment cores collected during expeditions ARK-XIV/1a, ARK-XXII/3 and ARK-XXIII/3 at the western Alpha and Mendeleev Ridges that is required to study regional changes in paleoclimate,

paleoceanic circulation, paleoproductivity, sea-ice distribution and ice sheet dynamics on the surrounding continents in the Pleistocene in a relatively high resolution. Furthermore, the mapping of key lithological layers may allow the correlation paleoenvironmental events across the Arctic Ocean.

In this framework, the geological programme included specific projects, e.g. mapping sea floor structures along the ship's track by swath bathymetry and sediment echosounder, re-sampling stations visited during ARK-VIII/3 and ARK-IX/4 in 1991 and 1993, respectively, to possibly identify the impact of recent climate change on benthic foraminifer faunas, and collecting surface sediments for calibration of paleoceanographic proxies such as biomarkers, benthic foraminifer faunas, and stable oxygen and carbon isotope composition of planktic and benthic foraminifers. Finally, inorganic geochemistry studies, initiated during ARK-XXIII/3 in 2008 to unravel the origin of manganese-rich layers in the Arctic Ocean, were continued to supplement the records from the East Siberia continental margin with data sets from the various basins visited during the expedition. In the following, we will describe the methods related to work during the expedition.

The geological station work was conducted along the oceanographic transects outside the Russian EEZ. Sites on submarine highs were selected for coring by using information on sea floor and sub-bottom structure from swath bathymetry and sediment echosounding (Hydrosweep and Parasound) to obtain hemipelagic sedimentary records not overprinted by sediment redeposition. Surface and sub-surface sediments were taken by gravity corer, giant box corer, and multicorer.

8.1 Multi-beam bathymetry

Patricia Slabon

Alfred-Wegener-Institut

Objectives

The main task of the bathymetric work was to conduct multibeam (MB) surveys in support of the geological and oceanographical programs using the new Hydrosweep DS-3 system (Atlas Hydrographic), and monitor the data acquisition to ensure high resolution spatial depth information throughout the expedition. Due to the reduced number of MB-staff, no data processing was carried out. The recorded MB-data is a valuable contribution to datasets of IBCAO (International Bathymetric Chart of the Arctic Ocean) and GEBCO (General Bathymetric Chart of the Ocean).

Another interest was to create a progress report about the new operation software of Hydrosweep DS-3 and the acquisition system HYPACK, which were installed in October 2010. Several open questions remained after the acceptance test and sea trials, which were reviewed during this cruise in detail. All problems concerning data collection and visualization were reported to the corresponding companies. Jointly with the system manufacturer and HYPACK it was tried to solve these problems.

Work at sea

The multibeam survey was started on August 6, 2011 at 9:00am UTC for testing purposes. After solving several technical problems, data acquisition was started in the main research area on August 13 at 8:47am UTC within the Norwegian EEZ

and was continued until September 22 at 7.30pm UTC, before entering the Russian EEZ. No data acquisition was carried out within the Russian EEZ.

At the beginning of the cruise, Hydrosweep (Hydromap Control) caused several system errors that generally were solved by total system shut down and restart. The HYPACK software caused also problems that forced repeatedly a restart of the system. Apart from all technical problems, HYPACK and Hydrosweep operated relatively stable. Runtime errors, occurring randomly, did not require any repair or a complete reboot of the system.

When leaving the Russian EEZ on September 29 at 3:29pm UTC into international waters and entering the Norwegian EEZ, data acquisition was continued until October 3, 2011 at 9:31am UTC. During the transit to Bremerhaven, heavy sea off the Norwegian coast caused systematic errors and thus poor depth measurements, obviously due to unsatisfactory measurements of ships attitude. These effects were mainly observed in shallow water regions.

In the deep-sea, Hydrosweep was operated in Equal Footprint Beam Spacing mode using a defined number of 345 beams per ping. The used frequency is 15.5 kHz. The aperture angle of the sonar fan can be selected between several predefined seafloor coverages. During this cruise an opening angle of 100% starboard/100% portside, depending on the water depth was used. A larger angle of 200%/200% created low resolution and poor data quality. Only in shallow waters between 100 m and 350 m the wider swath of 200%/200% was chosen. In waters less than 100 m, resulting depths show systematic errors in particular in the outer beams. In areas with water depths of less than 100 m an angle of 150%/150% was used.

Data acquisition was conducted using HYPACK software. The recorded data is stored in files of 30 minutes time interval in the internal HYPACK raw formats *.HSX and *.RAW (e.g.: ARK26-3_2011__2291239_0.HSX). In areas exceeding 84°N the universal polar stereographic projection (UPS) was used for visualization, otherwise the UTM projection. As data processing was not carried out, only selected files were checked for correct values of heading and course over ground (CoG) by comparing the MB-data to the D-SHIP Navigation files. Furthermore some files were visualized and checked using CARIS HIPS. For the generation of working maps onboard, few data were exported as ASCII files (longitude, latitude, depth).

During Hydrosweep operation, the actual swath is displayed on the screen. This information is used to find suitable locations especially for the marine geological work in real time. Due to technical problems regarding the import of the SVP (Sound Velocity Profile) into Hydromap Control, correct multibeam depths were not available.

Echo sounders derive the water depth from the travel time of the acoustic signal running from the transducer to the sea floor and back to the receiver. The exact sound velocity in the water column, which depends on pressure, temperature and salinity, is needed. The depth precision can vary strongly due to regional and local variations of the physical parameters in the water column that affect the sound velocity. A well-established technique to derive the water sound velocity is to perform CTD (Conductivity, Temperature and Depth) casts.

The *.cnv files, derived from the CTD values, containing the water depth and the matching sound velocity were processed in the sound velocity profile viewer and stored as *.vel-file for HYPACK/HYSWEEP and without extension for the ATLAS

8.1 Multi-beam bathymetry

SENSOR MANAGER. The ATLAS SENSOR MANAGER reads sound velocity profiles containing up to 128 points and imports the profile into Hydromap Control. 27 CTD-Profiles were processed and used for the water sound velocity correction.

During transits no sound velocity profiles were available. Hence the recorded measurements must be processed using external sound velocity data as available for example from ODV (ocean data view), before using them for mapping purposes.

Preliminary results

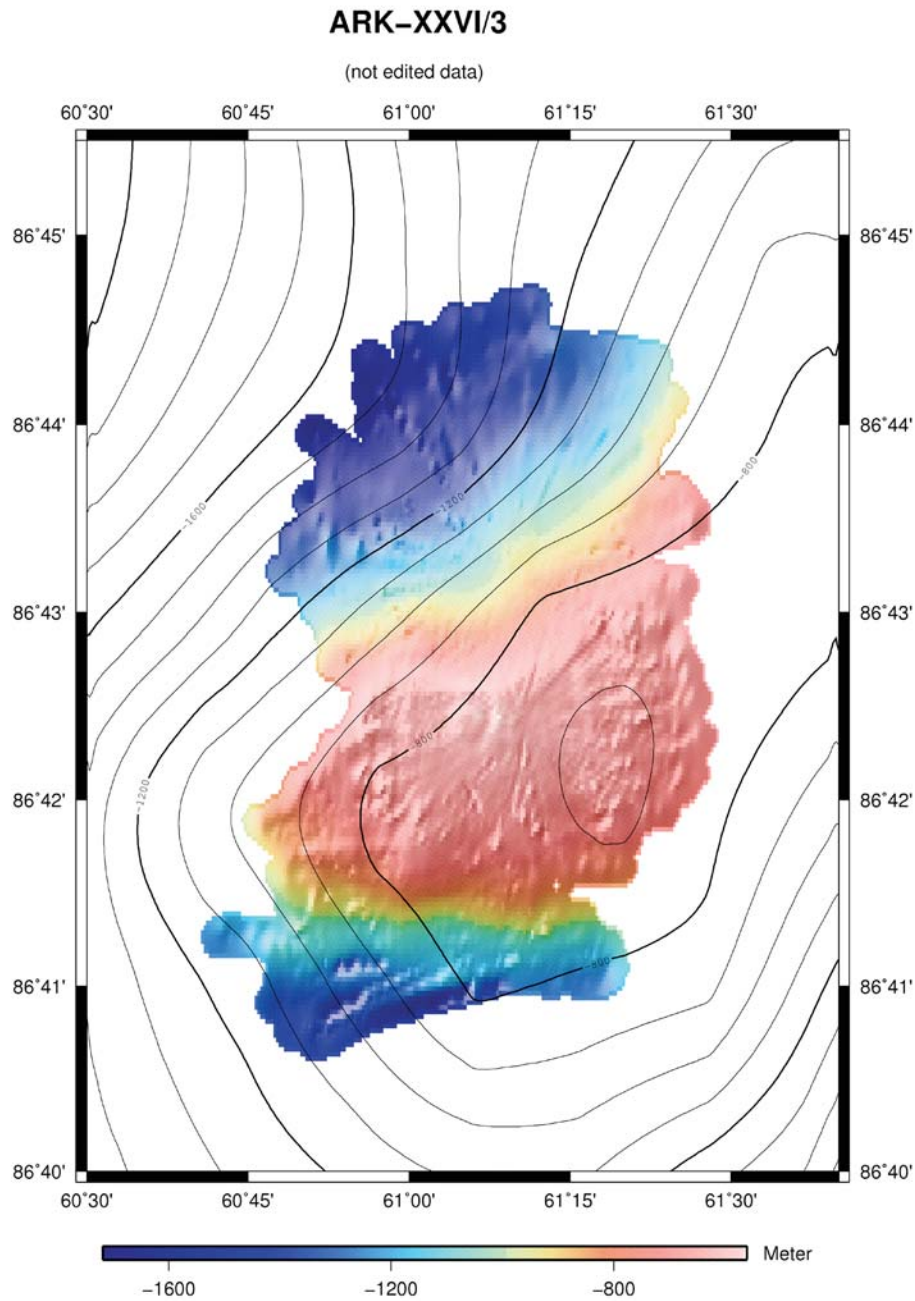
During the expedition a nearly continuous recording of data was achieved, except for few gaps caused by unexpected system errors and shutdowns. During 36 days of work in the main search area, a profile length of about 3480 nm (6450 km) was surveyed, generating 7.2 m. pings and 102 bn. beams (before editing). The amount of raw data storage volume is 18.5 GB created by 3778 separate files divided into *.HSX- and *.RAW-files. The observed depths vary between less than 100 meters in the coastal regions of Norway and Greenland and up to 5300 meters in a central valley of the Gakkel Ridge.

Despite the almost permanent ice coverage and the mentioned problems the system worked over periods reliable and provided high quality data. Some disturbances in the data could not be avoided during ice breaking.

The GEBCO_08 - Grid (General Bathymetric Chart of the Oceans) gives an overview on the morphology of the region. These data can be used for general planning. The recorded data differ at several places, due to the low resolution (2 km x 2 km) of the global GEBCO dataset, which is partly based on derived satellite gravity data and sparse bathymetric echo sounder data collected by submarines and icebreakers.

The difference between the GEBCO_08 model and the multibeam data are shown in Fig. 8.1.

Seamount – Gakkel Ridge



Alfred Wegener Institute for Polar and Marine Research, Bremerhaven (2011)

Fig. 8.1: Example of differences between bathymetry at the Karasik Seamount from IBCAO (contour lines) and unedited multibeam bathymetry of this cruise (color coded and shaded).

8.2 Marine sediment echosounding using Parasound

Jens Matthiessen, Tina Kollaske

Alfred-Wegener-Institut

Objectives

The structure of bottom and sub-bottom sediments was characterized by its acoustic behaviour as recorded in reflection patterns of the hull-mounted Parasound system. It was used routinely during the expedition to select coring stations based on acoustic pattern and backscatter, and to record the acoustic facies along the ship's track.

Work at sea

The Parasound system generates two primary frequencies that may be chosen between 18 and 23.5 kHz and are transmitted in a narrow beam of 4° at high power. Two secondary harmonic frequencies are generated by the so-called "Parametric Effect", caused by the non-linear acoustic behaviour of water, one of these is the difference (e.g. 4 kHz) and the other one the sum (e.g. 40 kHz) of the two primary frequencies, respectively. Sub-bottom penetration may be up to 200 m (depending on sediment conditions) with a vertical resolution of ca. 30 cm. Since the sediment-penetrating pulse is generated within the narrow beam of the primary frequencies, lateral resolution is very high compared to conventional 4 kHz-systems.

The Deep Sea Sediment Echo Sounder Parasound (Atlas Hydrographic, Bremen, Germany) was upgraded from DS II to DS III-P70 in 2007 and was thoroughly tested during three sea-trials (for a summary see Niessen & Matthiessen in Jokat, 2009). Details of this system have been described by Niessen et al. (in Klages & Thiede, 2011, in Schiel, 2009, and in Macke, 2009). Information about system set up, the hardware and software may be found in Niessen & Matthiessen (in Jokat, 2009) and the operator manuals of Atlas Hydromap Control and Atlas Parastore. The selected modes of operation, sounding options and ranges used during the cruise are summarized in Tab. 8.1. The Hydrosweep depths had to be used as system depth source during the latter part of the expedition because the DWS (Deep Water System; Simrad Echosounder) system completely failed.

During ARK-XXIII/3 in 2008 the new system was tested under relatively light ice conditions while here it was operated in areas with a multi-year sea-ice cover.

Tab. 8.1: Settings of ATLAS HYDROMAP CONTROL for operating Parasound during cruise ARK-XXVI/3 (P-SBP Parametric Sub-Bottom Profiling; SBES Single-Beam Echo-Sounder).

Used Settings	Selected Options	Selected Ranges
Mode of Operation	P-SBP/SBES	PHF, SLF
Frequency	PHF	18.75kHz
	SLF	4.166kHz

Used Settings	Selected Options	Selected Ranges
Pulselength	No. Of Periods Length	2 0.5ms
Transmission Source Level	Transmission Power Transmission Voltage	100% 159 V
Beam Steering	none	
Mode of Transmission	Single Pulse Quasi-Equidistant	interval 400-1200ms
Pulse Type	Continuous Wave	
Pulse Shape	Rectangular	
Receiver Band Width	Output Sample Rate (OSR) Band Width (% of OSR)	6.1kHz 66%
Reception Shading	none	
System Depth Source	Fix Min/Max Dept Limit	Maunal Other (DWS or HS) Atlas Parastore
Water Velocity	C-Mean C-Keel	Manual 1500m/s System C-keel
Data Recording	PHF SLF SGY	Full Profile Full Profile Full Profile

Digital data acquisition and storage were switched on in the Barents Sea on August, 6 at 17:02 UTC, and was switched off after a day of testing when *Polarstern* entered the Russian EEZ on August 7 at 17:54 UTC. After the ship has left the Russian EEZ on August 9 in the Nansen Basin the system was started again at 09:23 UTC. The system has been switched off again from September 14 at 11:16 UTC to September 19 at 06:57 UTC when station work was conducted off Zevernaya Zemlya. Data acquisition was finally stopped and the system switched off at the Laptev Sea continental slope on September 22 at 19:30 UTC when the ship entered the Russian EEZ to conduct the last oceanographic transects before leaving the working area through Vilkitsky Strait.

Acquisition included PHF (Primary High Frequency) and SLF (Secondary Low Frequency) data during the entire cruise. Both PHF and SLF traces were visualized as online profiles on screen. SLF profiles (100 m or 200 m depth windows) and online status (120 s intervals) were printed on A4 pages.

For the entire period and simultaneously with sounding six different types of data files were stored on hard disc:

8.2 Marine sediment echosounding using Parasound

- PHF data in ASD (Atlas Sounding Data) format
- PHF data in PS3 format
- SLF data in ASD format
- SLF data in PS3 (Export format of Parasound data) format
- SLF data in SGY format
- Navigation data and general Parasound settings (60s intervals) in ASCII format
- Auxiliary data about ATLAS PARASTORE 3 settings in ASCII format.

All ASD data are automatically packed into "cabinet files" by Atlas software. The files are named according to date and time of recording (containing about ten minutes of acquired data per file). The data have been sorted daily into folders according to data type and recording dates (0 to 24 hours UTC), copied to the storage PC via LAN and checked for completeness and readability (ATLAS PARASTORE-3 in replay mode, selectively only). Once checked, the data folders were copied to the *Polarstern* mass storage and to an external hard disc for daily back-ups and final transfer into the AWI database after the end of cruise. In total 39,092 folders of data with a total volume of 181 GB were transferred.

During the entire period of acquisition the system was operator controlled (watch keeping). Book keeping was carried out including basic Parasound system settings, some navigation information, various kinds of remarks as well as a low-resolution hand-drawn bathymetry plot with preliminary data interpretation of SLF online profiles, which provides an overview about echo types and specific findings during the cruise.

Time windows with data of specific interest (e.g. geological situations at or near stations, special observations, key examples for different types of facies or stratigraphy) were selected and replayed during the cruise using optimal settings of ATLAS PARASTORE-3. The examples shown in figures Fig. 8.2 to 8.5 were processed with the SENT program.

In contrast to ARK-XXVI/3, the system operated in a stable mode throughout this expedition. A single system crash was caused by the operator at the beginning of the expedition in the Barents Sea. Sea ice affected the quality of the data to a variable degree causing noisy records with some traces missing. More extensive data loss and a poor data quality mainly resulted from heavy ice conditions or slopes at submarine highs too steep to return a signal from the seafloor. In a few cases when both Parasound and Hydrosweep recorded wrong water depths data were lost as well. Usually, the PHF signal allowed identifying the sea floor, even on steep slopes or during heavy ice conditions.

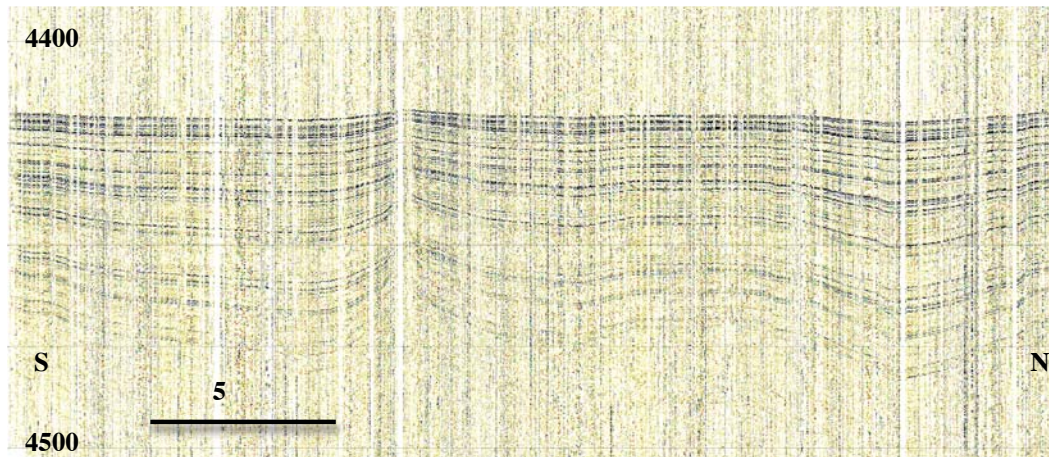


Fig. 8.2: Parasound example from the Amundsen Basin.

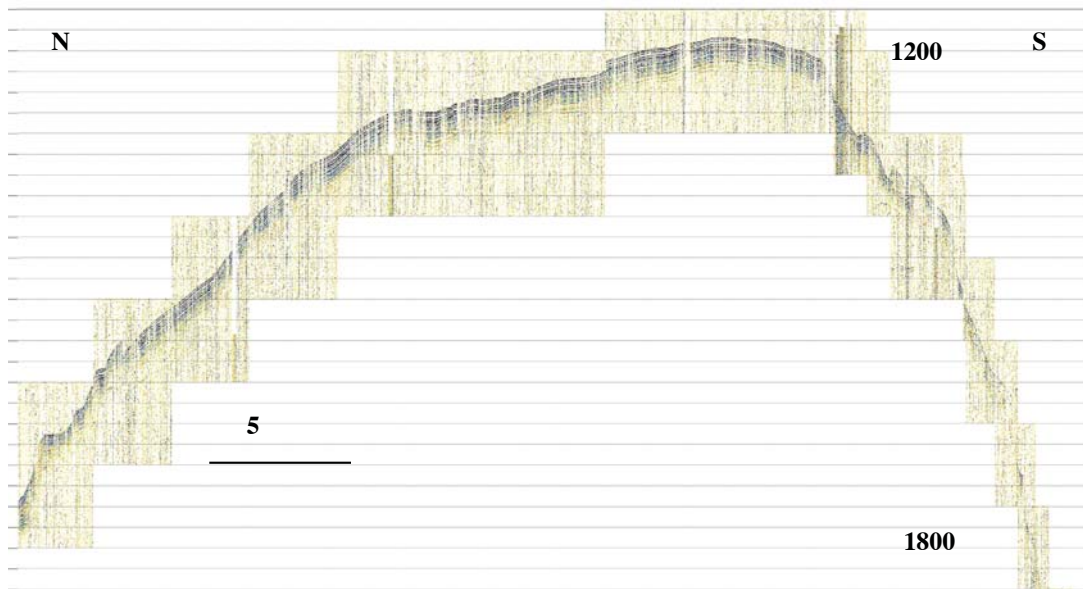


Fig. 8.3: Parasound example from the Lomonosov Ridge

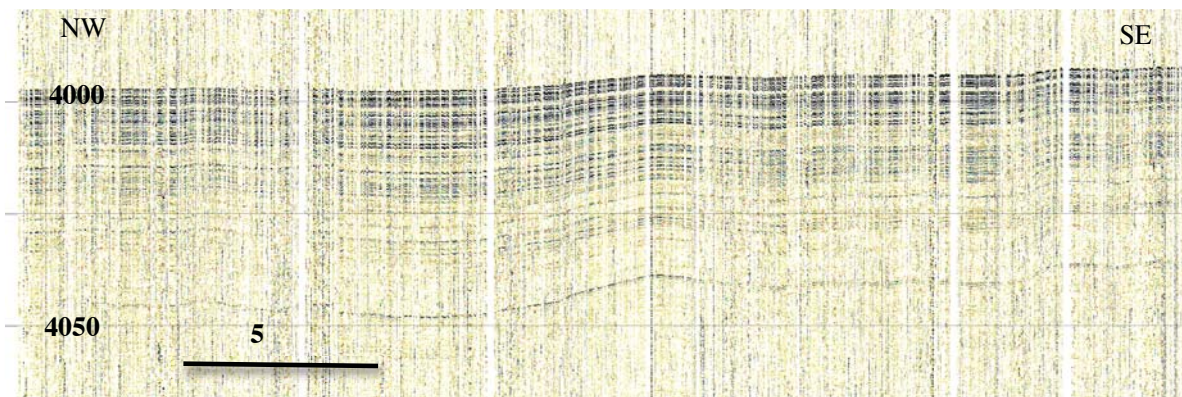


Fig.8.4: Parasound example from the Makarov Basin

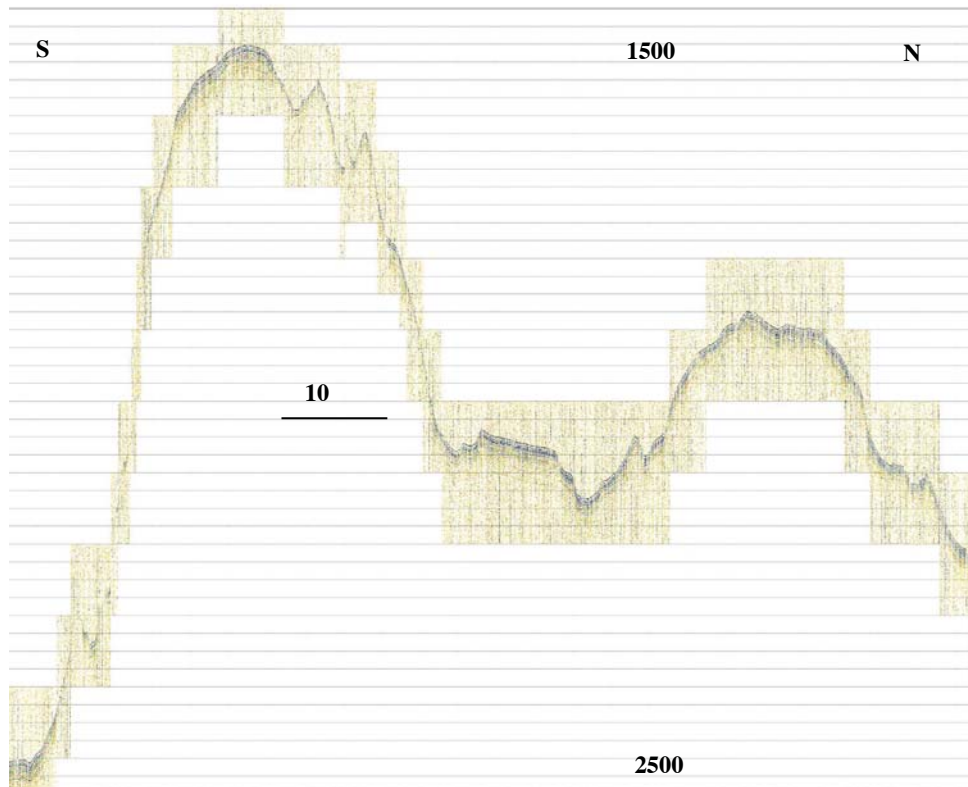


Fig. 8.5: Parasound example from the northern Mendeleev Ridge

Preliminary results

Eurasian Basin

The Parasound records from the Nansen and Amundsen Basins along the 60°E transect are comparable to those obtained during previous *Polarstern* expeditions ARK-VIII/3 (Bergmann, 1996), ARK-XIV/1a (Jokat, 1999), ARK-XVII/2 (Hatzky, 2008) and ARK-XXII/3 (Schauer, 2008). The sediments are acoustically stratified and show a rather regular pattern of sub-parallel reflectors (Fig. 8.2). Penetration into the relatively flat-lying sea floor was up to 60 m. Few data could be obtained from the Gakkel Ridge because slopes were too steep. However, some records show evidence for mass flow deposits. Penetration generally decreased towards the Lomonosov Ridge, where some v-shaped relatively narrow, shallow incisions (less than 10 m) have been recorded in the basin. Further to the east (135 – 120°E off the Laptev Sea) echo character changed from acoustically stratified sub-parallel sediments with up to 50 m thickness at the slope of Lomonosov Ridge to a rather wavy irregular sediment pattern in the deep Amundsen Basin with decreased penetration (less than 30 m), considerable changes in thickness of individual units over short distances, laterally restricted lens-shaped acoustically transparent sediment bodies and v-shaped relatively narrow up to 30 m deep incisions. At the Laptev Sea continental slope comparable acoustic reflections have been observed, but these changed more frequently over short distances than further to the north.

The variable acoustic character of the sediments reflects strongly variable depositional conditions. Sediments may be of pelagic origin along the 60° E transect in the basins distal to submarine slopes but coring during ARK-VIII/3 revealed

the presence of thick turbidites in these basins (Fütterer, 1992). Kristoffersen et al. (2004) have mapped a submarine fan and a deep-sea channel system in the Amundsen Basin extending from the Lincoln Sea off northern Greenland to the deep sea plain at the North Pole. The small incisions recorded at the North Pole may represent distributary channels of the distal channel system. Thus, thick turbidites might have originated at the northern Greenland continental slope. Proximal to the Laptev Sea, comparable conditions might have prevailed with a substantial supply of sediments from the Laptev shelf being transported downslope into the deep sea. The acoustic facies at the slope may be additionally influenced by the slowly spreading Gakkel Ridge because the cruise track followed more or less the axis of the rift.

Lomonosov Ridge

The Lomonosov Ridge has been crossed twice at ca. 89°N, 115°W and 84°N, 150°E, respectively. The records are comparable to those obtained during ARK-VIII/3 (Bergmann, 1996), ARK-XIV/1a (Jokat, 1999) and ARK-XXII/3 (Schauer, 2008). Acoustically stratified sediments drape the ridge down to 40m depth indicating pelagic sedimentation and absence of glacial erosion (Fig. 8.3). The uppermost about 5 m show stronger reflection amplitudes. Internal reflectors are hardly visible at the slopes (see Fig. 8.3) and usually only the seafloor is reflected in the PHF signal if slopes were not too steep.

Makarov Basin

The bathymetry of the Makarov Basin is quite variable because of numerous submarine highs that have been crossed along the ship's track. The basin has been crossed twice at ca. 89-86°N, 115-150°W and 85-84°N, 180-150°E. Although data quality is particularly poor along the western transect due to heavy ice conditions acoustically stratified up to 40-50 m thick sediments have been recognized both in the deeper part of the basin and on submarine highs suggesting pelagic depositional conditions (Fig. 8.4). The uppermost 3 to 4 m depict stronger reflection amplitudes. Thus, the acoustic facies is comparable to those recorded during ARK-XIV/1a (Jokat, 1999) and ARK-XXII/3 (Schauer, 2008).

Alpha Ridge

At the junction of the Alpha and Mendeleev Ridge at ca. 140°W acoustically stratified sediments are replaced by undulating sea floor reflections and common side echos. Comparable reflections have been observed parallel tracks studied during ARK-XXII/2 (Schauer, 2008) whereas on tracks further to the west acoustically stratified sediments have been observed during ARK-XIV/1b (Jokat, 1999). The undulating seafloor reflections and side echos might be related to a possible extraterrestrial impact suggested by Kristoffersen et al. (2008) to explain extensive seabed disturbance in the Alpha Ridge region.

Northern Mendeleev Ridge

The acoustic facies on the northern Mendeleev Ridge is somewhat variable due to a variable topography consisting mainly of acoustically stratified sediments with a penetration of up to 40 m (Fig. 8.5) and subordinate undulating sediments with almost absence of sub-parallel reflections. The uppermost 2 to 3 m are characterized by stronger reflection amplitudes.

8.3 Sediment cores

Antje Boetius¹, Alex Charkin²,
Elisabeth Helmke¹, Tina Kollaske¹,
Jens Matthiessen¹, Ann-Katrin
Meinhardt³, Norbert Lensch¹,
Patricia Slabon¹, Mirko Sühs¹, Hao
Zao¹

¹Alfred-Wegener-Institut
²POI-FEBRAS, Vladivostok
³Institute for Chemistry
and Biology of the Marine
Environment, Oldenburg

Work at sea

Near-surface sediments and longer sedimentary sequences were sampled at 22 stations (Fig. 8.6). Near-surface sediments were collected with a giant box corer (GKG, 50 cm x 50 cm x 60 cm) at 6 stations and a multicorer (MUC) with 8 tubes (diameter 10cm) at 19 stations. The MUC was preferred to the GKG because bottom water and an absolutely undisturbed sediment-water interphase was required for sampling the uppermost sediment layers at cm intervals for foraminiferal (chapter 8.3.1), for an extensive pore water sampling program (chapter 8.3.3), and for benthic biological (chapter 8.3.2), biogeochemical (chapter 6), and geochemical studies (chapter 5.3).

After recovery of the MUC the individual tubes were sampled for various purposes (Tab. 8.2). Single tubes were cut into 1 cm slices for inorganic geochemistry and for archiving. One tube was used on some stations for pore water sampling. The uppermost 6 cm of two to three tubes were sampled for foraminiferal analysis while a second set of two tubes was subsampled for various biological studies. Surface sediments were sampled for geochemical, organic geochemical analysis as well as microbiological studies.

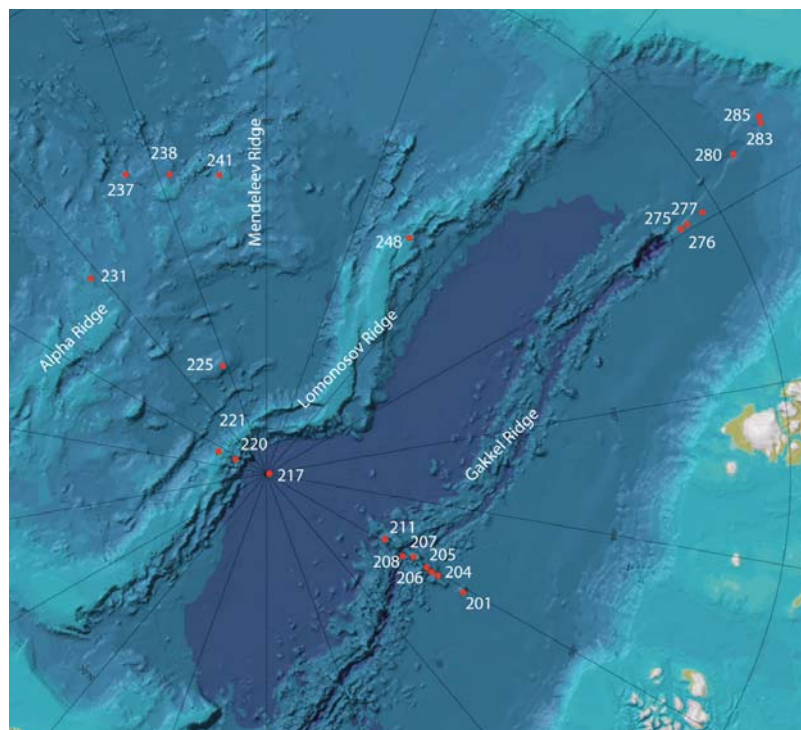


Fig. 8.6 Geographic location of bottom sampling stations. Numbers refer to station numbers of ARK-XXVI/3 (PS78).

Tab. 8.2: List of samples taken from MUC and GKG.

Station	Gear	ARKVIII/3 1991	Pore Water	Inorganic Geochemistry	Benthic Foraminifers	Benthos 0-10	Microbiology	Organic Geochemistry	Geochemistry	Archive	X-radiography
PS78/201-7	MUC		X	X	X	X	X	X	X	X	
PS78/204-4	MUC	PS2163		X	X	X	X	X	X	X	
PS78/205-5	MUC	PS2164		X	X	X	X	X	X	X	
PS78/206-2	MUC	PS2165	X	X	X	X	X	X	X	X	
PS78/206-4	GKG	PS2165		X	X	X	X	X	X	X	X
PS78/207-4	GKG		sponge mat, sampling only for biology	X	X	X	X	X	X	X	
PS78/208-1	MUC	PS2166	X	X	X	X	X	X	X	X	
PS78/211-1	MUC	PS2170	X	X	X	X	X	X	X	X	
PS78/217-1	MUC	PS2190	X	X	X	X	X	X	X	X	
PS78/220-1	MUC		X	X	X	X	X	X	X	X	
PS78/221-3	MUC			X	X	X	X	X	X	X	
PS78/221-5	GKG			X	X	X	X	X	X	X	X
PS78/225-4	MUC		X	X	X	X	X	X	X	X	
PS78/231-1	MUC			X	X	X	X	X	X	X	
PS78/231-3	GKG			X	X	X	X	X	X	X	
PS78/237-1	MUC		X	X	X	X	X	X	X	X	
PS78/238-2	GKG			X	X	X	X	X	X	X	
PS78/241-3	GKG			X	X	X	X	X	X	X	
PS78/248-4/5	MUC		X	X	X	X	X	X	X	X	
PS78/275-1	MUC		X	X	X	X	X	X	X	X	
PS78/276-6	MUC			X	X	X	X	X	X	X	
PS78/277-2	MUC		X	X	X	X	X	X	X	X	
PS78/280-6	MUC		X	X	X	X	X	X	X	X	
PS78/283-2	MUC			X	X	X	X	X	X	X	
PS78/285-6	MUC		X	X	X	X	X	X	X	X	

The GKG was successfully used at 5 stations but at station 207 only sponge mats and rocks (basalts?) were recovered. Recovery ranged from 30 to 40 cm. After the surface was photographed and described two archive tubes (diameter 12 cm) were pushed into the sediment. Surface sediments were then sampled for sedimentological, organic geochemical and micropaleontological analysis. After opening the front side of the GKG the profile was photographed and then sampled continuously for x-radiography and archive purposes (2-3 boxes). MUC and GKG samples were frozen (-20 to -80° C) or stored at 4° C.

Long sediment cores were obtained at 8 stations with a gravity corer (SL) of 5 or 10 m length and 12 cm diameter with a penetration weight of 1.5 t. Prior to opening, some sediment cores were sampled for pore water in a cool room at 4°C (chapter 8.3.3.). After core sections have warmed to room temperature for at least 24 hours, the sediment cores were logged using the Multi-Sensor-Core-Logger (MSCL). Then, cores were opened, photographed and described, and sediment slices for X-ray photography and samples for determination of water content were taken. Colour spectrometry and point susceptibility measurements were conducted on split core halves. Selected x-ray photographs were analysed for sedimentary structures and content of coarse-ice rafted debris (IRD) larger than 2 mm. Discrete sampling was only done for inorganic geochemistry on a core PS78/248. All sediment cores were stored onboard in a cool container at 4°C and were transferred to the *Polarstern* core repository in Bremerhaven after the expedition.

Shipboard analyses performed on the sediment cores are described in the following chapters but standard methods such as photography, x-ray radiography, counts of gravel-sized particles) are not included. Descriptions of these methods may be found in Jokat (2009).

All shipboard data (sediment core descriptions, photographs, digitized negatives of x-ray radiographs, physical property data, colour spectrophotometry, counts of gravel-sized particles) will be stored in the Pangaea database.

8.3.1 Benthic foraminifera communities of the Amerasian and Eurasian Basins and the trace metal ratios recorded in calcareous tests of benthic foraminifera

Mirko Sühs

Alfred-Wegener-Institut

not on board: Jutta Wollenburg,

Objectives

The major goal was to supplement our existing data set on benthic foraminifer distribution in the Arctic Ocean. Furthermore, we started a new project to evaluate the environmental controls of trace metal ratios recorded in calcareous shells of benthic foraminifers.

Work at sea

For this purpose short sediment cores were collected at 24 stations in the Eurasian and Amerasian Basins from 1600 to 4100 m water depth (Fig.8.6; Tab. 8.2). Two to three multicorer tubes from each coring site were sliced in 1-cm steps from

the surface to 6 centimeters sub-bottom depth. The subsamples were transferred into plastic bottles and mixed with an equivalent volume of ethanol-Rose Bengal mixture (1g Rose Bengal/l ethanol). Rose Bengal is a protein stain and allows in subsequent faunal analyses to discriminate living (protoplasm bearing) from empty shells.

Expected results

In the next months we will analyse the biocoenoses and taphocoenoses, carry out trace metal analyses on shells of key foraminifers and correlate the results with the environmental conditions at the sites. Since the incorporation of trace metals is influenced by temperature, pH and the carbonate ion system, these environmental parameters are of particular importance. Since some stations have been already sampled 20 years ago, comparative trace metal and faunal investigations will identify effects of the most recent and prevailing environmental change in this highly sensitive area.

8.3.2 Benthic processes

Antje Boetius

Alfred-Wegener-Institut

Objectives

MUC subsamples were taken to analyze chlorophyll pigment concentrations as a proxy for marine detritus sedimentation, bacterial cell counts and total phospholipid concentration, as well as potential hydrolytic enzymatic activities and bacterial diversity.

Work at sea

At every site, 2 cores were taken (Tab. 8.2). One was sliced every cm for the first 10 cm and preserved by deep-freezing for different molecular methods such as the DNA community fingerprinting technique ARISA. The other one was sampled by cut-off syringes for cell counts, lipid analyses, and other biogeochemical parameters. For cell counts, 1mL sediment was added to 2% 9mL formalin-sea water solution, and preserved at 4°C.

Expected results

These samples will provide an overview on microbial benthic activities at water depths of 1,500-5,500 m, in areas, which were last sampled 10-20 years ago.

8.3.3 Inorganic geochemistry of Arctic Ocean sediments

Ann-Katrin Meinhardt

Institute for Chemistry and Biology of
the Marine Environment, Oldenburg

Objectives

The goal of the geochemical program was a detailed investigation of Arctic Ocean sediments and pore waters. The main focus will be to investigate the formation mechanism and geochemical expression of repetitively occurring brown coloured

sediment layers (“manganese cycles”). In Arctic Ocean sediments distinct dark brown intervals, which are rich in Mn and Fe compared to other hemipelagic sediments, alternate with light olive/yellowish brown intervals, which are comparably poor in these elements. There are different explanations for the formation mechanism of these colour cycles. Primary sources of Mn and Fe in the Arctic Ocean are the circum-Arctic rivers, which drain extensive peat bogs rich in both, Mn and Fe. The input of metals to the deeper ocean basins is controlled by climatic features, i.e., higher riverine input during warmer conditions and lower input during colder conditions, or changes in ventilation of the bottom waters. Another explanation for the cyclicity may be diagenetic overprinting after deposition. During organic matter degradation, microbially mediated dissolution of metal (oxyhydr)oxides may occur in the absence of free oxygen under suboxic to anoxic conditions. The reduced metal species are then liberated to the pore water. Upon diffusion to the oxic/suboxic boundary, the reduced metal species may again precipitate and form a new sedimentary Mn/Fe peak. Multiple dark brown Mn- and Fe-rich intervals may be formed in this way after deposition. Our work focuses at a combination of both, sediment and pore water analyses to obtain information about the importance of organic matter degradation in Arctic Ocean sediments and the diagenetic mobility of metals like Mn and Fe.

Work at sea

Sampling of pore water was performed at 18 stations (Tab. 8.3) shortly after sediment recovery. The sediment cores (MUC or SL) were transported into the 4 °C laboratory, where the pore waters were sampled by the rhizon technique. Pore water sampling of giant box corers was not performed due to problems during ARK-XXIII/3 (Jokat, 2009). A rhizon is a polymer filter with 0.1 µm pore size, which is attached to a PE/PVC tube with a luer lock. The MUC tubes were prepared with pre-drilled 3.8 mm holes in 1 cm resolution, which were taped during the coring process. In the cooling laboratory, the rhizons were stuck into the tube at variable resolution (~1 to 5 cm). A syringe was attached to every rhizon and vacuum was applied with the help of a spacer (Fig. 8.7). Pore waters of the SL were sampled in a similar way by drilling holes into the liner at ~20 cm resolution and inserting the rhizons (Fig. 8.8). Variable amounts of pore water were retrieved, mostly ~10 ml, depending on sediment features like porosity and sampling time. After sampling, the rhizons were removed, the cores were sealed and the pore water was filled in PP-tubes. Several fractions were obtained (1. untreated, for the determination of labile components and nutrients; 2. acidified, for the determination of metals after the cruise; 3. oxygenated [for reactive Mn, see below]) and stored at 4 °C. Rhizons were cleaned with 10% HCl and Milli-Q-Water for re-use.

Sediment samples of the MUC cores were taken at 1 cm resolution with a plastic spatula and stored in plastic bags. Sediment samples of a GC (PS78/248-6) were taken with plastic spatula at variable resolution, depending on discernible sediment properties, and stored in plastic bags.

For the determination of reactive Mn, a fraction of the pore water was left in the syringe and allowed to oxidise for ~48 hours. After this time the pore water was filled in PP-tubes with a syringe filter and was acidified with HNO₃.

Directly after dividing the pore water into the different fractions, analyses of ammonium and total alkalinity were performed. Both parameters were determined via photometric methods using a microtiter plate reader, which only consumes less than 0.5 ml per sample. The preserved pore water fractions will be analysed

onshore for several dissolved ions and metals (e.g. nitrate, phosphate, manganese, iron and other main and trace elements) via photometric methods, ICP-OES and ICP-MS. The sediment samples will be freeze-dried, ground and analysed for major and minor elements and bulk parameters using X-Ray Fluorescence, coulometry, combustion analyses, ICP-OES and ICP-MS.

Tab. 8.3: List of pore water samples, sediment samples and measured parameters on board

Station	Gear	Sediment	Alkalinity	Ammonium	Acidified split	Reactive Mn split
PS78/201-7	MUC	X	X	X	X	
PS78/206-2	MUC	X	X	X	X	
PS78/206-3	GC		X	X	X	X
PS78/208-1	MUC	X	X	X	X	
PS78/211-1	MUC	X	X	X	X	
PS78/217-1	MUC	X	X	X	X	
PS78/220-6	MUC	X	X	X	X	
PS78/220-7	GC		X	X	X	X
PS78/225-4	MUC	X	X	X	X	
PS78/231-2	MUC	X				
PS78/231-2	GC		X	X	X	X
PS78/237-1	MUC	X	X	X	X	
PS78/237-3	GC		X	X	X	X
PS78/248-4	MUC	X	X	X	X	
PS78/248-6	GC	X	X	X	X	X
PS78/275-1	MUC	X	X	X	X	
PS78/277-2	MUC	X	X	X	X	
PS78/280-6	MUC	X	X	X	X	
PS78/285-6	MUC	X	X	X	X	

8.3 Sediment cores

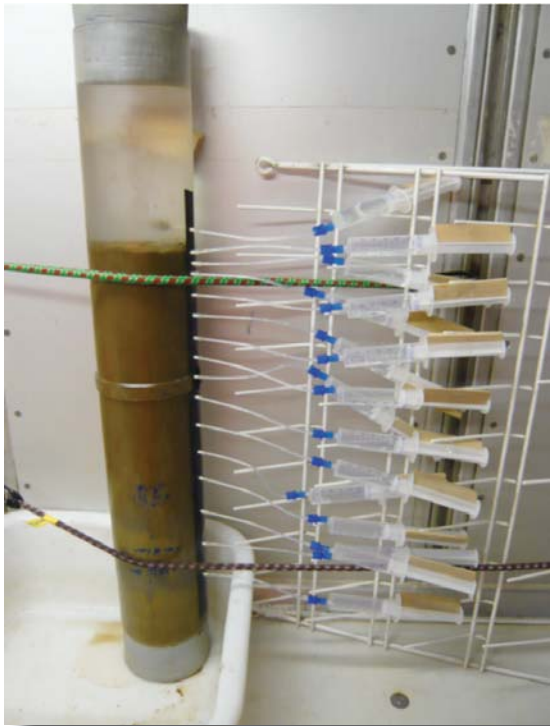


Fig. 8.7: Pore water sampling of a MUC



Fig. 8.8: Pore water sampling of GC segments

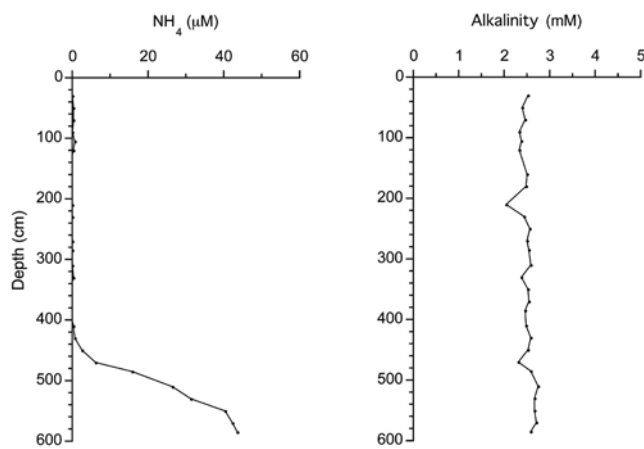


Fig. 8.9: Pore water profile of sediment core PS78/248-6 (SL)

Preliminary results

In most of the cores, pore water ammonium values are low, ranging close to the detection limit of the method and $\sim 10 \mu\text{M}$, and show no trends with depth. One exception is core PS78/248-6 (Fig. 8.9, Lomonosov Ridge) with increasing values from ~ 470 cm core depth up to $\sim 44 \mu\text{M}$ at 585 cm.

Both ammonium and inorganic carbon species (=alkalinity) are metabolites of microorganisms. Increasing ammonium values with depth are indicative for the increasing degradation of organic matter in the sediment. But compared to other marine settings, the observed values are rather low. Alkalinity values of all cores show little variability with depth and range mostly between 2 and 3 mM (Fig. 8.9)

In the reactive Mn experiment, the fraction that was allowed to oxidise showed no precipitation of solid, oxidised Mn. This visual observation needs to be tested by quantitative Mn measurements of both fractions.

These very first results illustrate the general low productivity in the Arctic Ocean. In one of the sediment cores (PS78/248-6) the increase of ammonium with depth indicates that diagenetic processes may occur deeper in the sediment. Further analyses of other parameters are necessary for a comprehensive study.

8.3.4 Non-destructive sediment core measurements

Non destructive measurements at cm intervals have been performed on whole cores and split core halves to provide initial information on the physical properties of the sediments and the variability of sedimentary colours.

In combination with sediment core descriptions and x-ray radiographs they allow a first interpretation of the paleoenvironment and enable to more precisely select discrete samples for detailed analysis. Furthermore, these parameters may be used to correlate distinct sedimentary unit over long distances.

8.3.5 Multi-sensor core logging

Jens Matthiessen, Tina Kollaske

Alfred-Wegener-Institut

Measurements in the ship laboratory included non-destructive, continuous determinations of wet bulk density (wbd), P-wave velocity (vp) and magnetic susceptibility (ms) at 10 mm intervals on all cores (GKG, SL) obtained during the cruise. The Multi Sensor Core Logger (MSCL14n, GEOTEK Ltd., UK) was used to measure core temperature, core diameter, P-wave travel time, gamma-ray attenuation and ms. The principle of logging cores is described in more detail in previous *Polarstern* cruise reports (e.g. Niessen et al. in Jokat, 2009). The orientation of the P-wave and gamma sensors was horizontal. Gravity cores were measured in coring liners including end caps. Details of measurements, calculations and technical specifications of the used MSCL may be found in Niessen et al. (Jokat, 2009). Prior to measuring a sediment core, a standard core consisting of different proportions of aluminium and water as described in Best & Gunn (1999) has been logged for calculation of WBD.

To obtain a higher resolution at cm intervals, ms was measured on split cores with

a Multi Sensor Core Logger XZ (MSCL-XZ, GEOTEK Ltd., UK) using a Bartington MS2E point sensor. Visual inspection of loop and point sensor data showed a good correlation (possible causes of offsets have been discussed by Niessen et al. in Jokat, 2009). All data will be stored as a function of core depth in the databank PANGAEA.

8.3.6 Spectral photometry

Jens Matthiessen

Alfred-Wegener-Institut

During expedition ARK-XXVI/3 a Multi Sensor Core Logger XZ (MSCL-XZ, GEOTEK Ltd., UK) and a attached Minolta colour spectrophotometer CM-2600d was used to measure reflectance spectra of gravity cores. Reflectance spectra were collected in 39 spectral bands between 360 and 740 nm in 10-nm spectral bands with 10 mm aperture. Measurement spacing was generally set to 1 cm. The split core surfaces of the archive halves were covered by a standard film to protect the spectrophotometer.

Output files are the greyscale reflectance, the chroma, hue and value of the Munsell Colour Chart, the CIE XYZ colour space (defined according to the RGB colours, CIE 1931), the CIE L*a*b* colour space (referred to as CIELAB space, Commission Internationale de l'Éclairage L*a*b* colour space 1976) and the percentage values of the spectra in 10 nm steps. Data output are Tab-delimited ASCII (.csv files) that were converted into Excel files (.xls) and edited for each sediment core separately in Excel sheets. Obvious outliers e.g. due to uneven core surfaces or holes as noted while measuring were deleted from the data set. After final editing all data will be deposited separately for each sediment core under the respective station and cast number in the data bank PANGAEA.

Preliminary results from sediment core analysis

Sediment surfaces

The relatively few sediment surfaces obtained with the GKG do not allow to distinguish regional trends in the distribution of sedimentary facies. Grain size composition of the generally brownish sediments is quite variable ranging from clays to sandy silty clays but most surfaces are relatively coarse-grained. This might be due to the selection of sites on elevated submarine structure where bottom currents might have winnowed the fine fraction. Gravel (up to 2 - 3 cm) is common on most surfaces. Among the biogenic components corroded shells and shell fragments are common, while larger calcareous foraminifers were rarely observed on surfaces.

A common feature is the occurrence of sponges and sponge spicules at some locations both in GKG and MUC. In particular at the Karasik Seamount (Gakkell Ridge), sponges and spicules form dense mats in the uppermost centrimeters at stations 205, 206, and 207. At station 207 on the top of the seamount sponge mats cover basaltic? rocks while at the other stations they overlain siliciclastic sediments. Additionally, at station 248 on the Lomonosov Ridge sponges were recovered with a multi corer.

Sediment cores

All sediment cores are characterized by some colour variation with brownish layers alternating with light brownish/olive layers. Except for SL 206 from Gakkel Ridge that has a pronounced lithological variability throughout the core the lithofacies is more variable in the upper part of the sediment cores with distinct alternations of coarse-grained layers, sometimes comprising gravel-sized ice-rafted debris (IRD), and fine-grained layers. The lower part is relatively fine-grained composed of silty clays to clayey silts with few thin intervals of coarser material. Based on this pronounced change in lithofacies, the lithology of the new sediment cores may be subdivided into two units (e.g. PS78/231-2; Fig. 8.10) as it has been done in cores collected during ARK-XXIII/3 across the southern Mendeleev Ridge (Stein et al., 2010b). Additionally, sediment cores at the Alpha Ridge may be correlated by distinct physical property events (Sellén et al., 2010).

Prominent sedimentary units may form key lithostratigraphic marker beds to correlate sediment cores over longer distances. The sediment cores GC 206, 220, 221, and 248 from the Gakkel and Lomonosov Ridges exhibit a characteristic dark grayish layer that may correspond to a unique lithostratigraphic horizon independently dated in a number of sediment cores to late MIS 4 (e.g. Sellén et al., 2008). In the Amerasian Basin, detrital carbonate-rich layers in Unit I of GC 231, 237, 238 and 241 allow a tentative correlation to well-known key lithostratigraphic marker beds (white and pink-white layers) recognized in numerous sediment cores located on the Alpha and Mendeleev Ridges (e.g. Clark et al., 1980; Minicucci & Clark, 1983; Mudie & Blasco, 1985; Stein et al., 2010a,b; Matthiessen et al., 2010; Fig. 8.10) but their chronostratigraphic position has not been resolved yet. In sediment cores from the Alpha Ridge the eye-catching pinkish component in these layers is apparently absent (Clark et al., 1980; Jokat, 1999; Schauer, 2008) making assignment to one of the markers beds difficult. Nevertheless, all these layers are confined to Unit I.

This unit can be further subdivided according to the standard lithostratigraphy established by Clark et al., (1980) for the Alpha and Mendeleev Ridges but individual units may vary in thickness and/or may be even absent. The coarse-grained lithological units of this lithostratigraphy (Fig.8.10, marked by letters in the IRD column) may be potentially useful for supra-regional correlation (compare with IRD records in Stein et al., 2010b).

Correlating the upper sedimentary units in GKG and MUC from the western Alpha Ridge to the southern Mendeleev Ridge clearly show an increase in thickness of units to the south (Fig. 8.11) as has been suggested already from computing average sedimentation rates (Stein et al., 2010a,b). The upper brown layers are clearly separated at the southern Mendeleev Ridge by a light brown/olive unit that thins out to the north. The uppermost white layer W3 decreases in thickness as well and is hardly visible at the western Alpha Ridge. This layer is also not visible in sediment core GC221 from the Lomonosov Ridge.

Due to its lithological uniformity Unit II may be primarily subdivided based on colour variations (Fig. 8.10) according to Stein et al. (2010b; sediment lightness, a^* and b^* values; units A, A1 etc.) and these distinct changes may be traced along the Mendeleev and Alpha Ridges over long distances.

8.3 Sediment cores

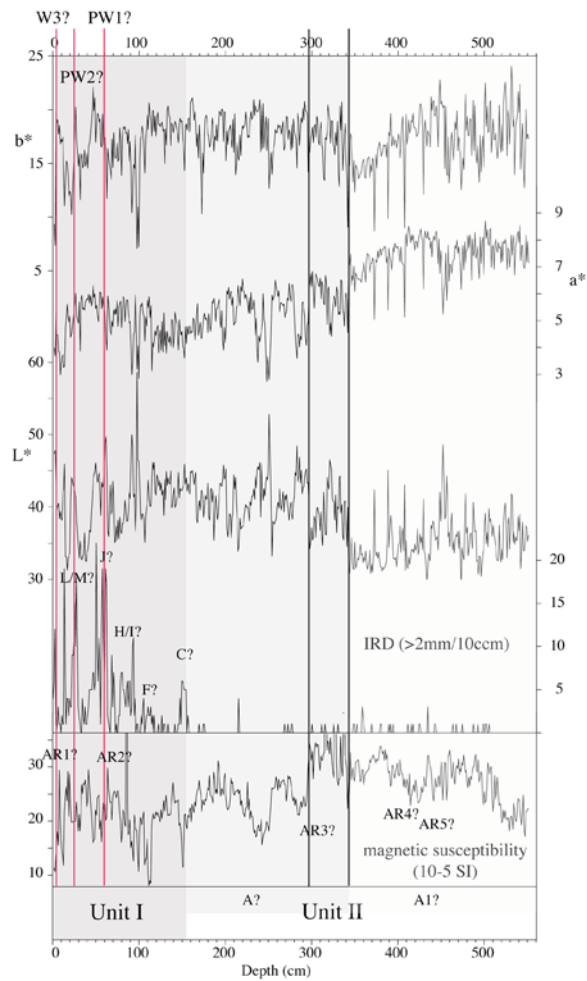


Fig. 8.10: Lithostratigraphic units, magnetic susceptibility, IRD content, L^* lightness, a^* red-green colour space, and b^* yellow blue colour space of sediment core PS78/231-2. Potential tie points in physical properties are marked in the magnetic susceptibility record (AR1-AR5, according to Séllen et al., 2010). Detrital carbonate-rich layers are marked with red lines. Black lines indicate distinct steps in colour data (see Stein et al. 2010b, Fig. 11).

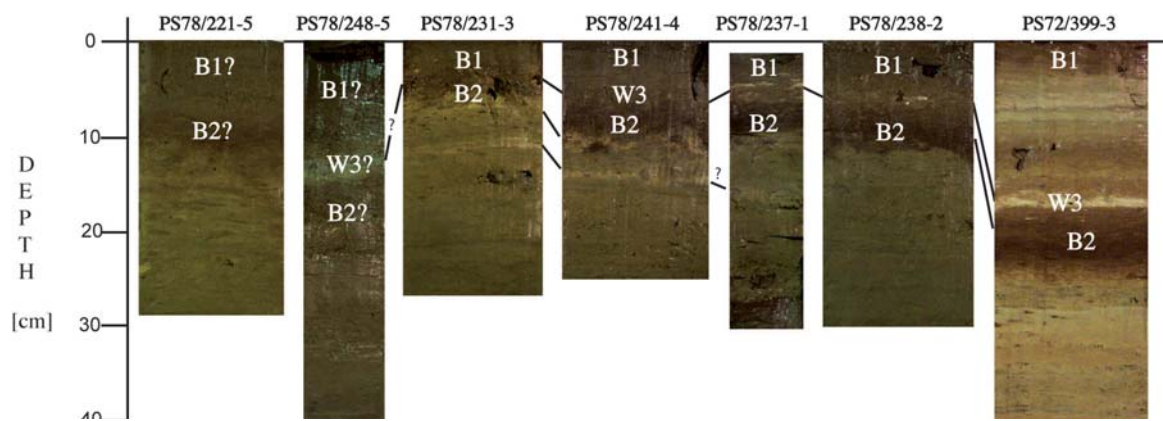


Fig. 8.11: Tentative correlation of lithological marker beds in near-surface sediments from Lomonosov Ridge (PS78/221-5, PS78/248-5), Alpha Ridge (PS78/231-3) and Mendeleev Ridge (PS78/241-4, PS78/237-1, PS78/238-2) based on identification of brown beds B1 and B2, and white bed W3 in box core PS72/399-3 by Stein et al. (2010b). For locations of cores see Fig. 8.6.

References

- ATLAS Hydrographic (2007): ATLAS HYDROMAP CONTROL Operator Manual. Doc.-Id.: ED1060 G 312, File: ED-1060-G-312_V5-0. Edition: 04.2007. ATLAS HYDROGRAPHIC, Bremen, Germany.
- ATLAS Hydrographic (2007): ATLAS PARASTORE-3 Operator Manual. Doc. Id.: ED 6006 G 212:/ Version: 4.0 / Edition: 05/2007. ATLAS HYDROGRAPHIC, Bremen, Germany.
- Bergmann, U. (1996): Interpretation digitaler Parasound Echolotaufzeichnungen im Östlichen Arktischen Ozean auf der Grundlage physikalischer Sedimenteigenschaften. Reports on Polar Research, Dissertation, Alfred Wegener Institute for Polar and Marine Research, Bremerhaven, 83, 164 pp.
- Best, A. I., Gunn, D.E. (1999) Calibration of marine sediment core loggers for quantitative acoustic impedance studies. *Marine Geology*, 160, 137-146.
- Clark, D.L., Whitman, R.R., Morgan, K.A. & Mackey, S.D. (1980): Stratigraphy and glacial-marine sediments of the Amerasian Basin, Central Arctic Ocean. *Geological Society of America, Special Papers*, 181: 57p.
- Fütterer, D.K. (1992, ed.): The expedition ARK-VIII/3 of RV „Polarstern“ 1991. Reports on Polar Research, 1992. 107: p. 267.
- Hatzky, J. (2008): Analyse von Bathymetrie und akustischer Rückstreuung verschiedener Fächersonar- und Sedimentecholot-Systeme zur Charakterisierung und Klassifizierung des Meeresbodens am Gakkel-Rücken, Arktischer Ozean. Dissertation, Alfred Wegener Institute for Polar and Marine Research, Bremerhaven, 231pp.
- Jakobsson, M., R. Macnab, L. Mayer, R. Anderson, M. Edwards, J. Hatzky, H. W. Schenke, and P. Johnson (2008), An improved bathymetric portrayal of the Arctic Ocean: Implications for ocean modeling and geological, geophysical and oceanographic analyses, *Geophysical Research Letters*, doi: 10.1029/2008gl033520.
- Jokat, W. (1999): Arctic '98: The Expedition ARKTIS-XIV/1a of Research Vessel Polarstern in 1998, Reports on Polar and Marine Research, Alfred Wegener Institute for Polar and Marine Research, Bremerhaven, 308, 159 pp.
- Jokat; W. (2009): The Expedition of the Research Vessel „Polarstern“ to the Arctic in 2008 (ARK-XXIII/3). Reports on Polar and Marine Research, Alfred Wegener Institute for Polar and Marine Research, Bremerhaven, 597, 221 pp.
- Klages M. & Thiede J. (2011).- The expeditions ARKTIS-XXII/1a-c of the research vessel „Polarstern“ in 2007/ Ed. by Michael Klages and Jörn Thiede with contributions of the participants. Reports on Polar and Marine Research, 627, 194pp.
- Kristoffersen, Y., Hall, J.K., Hunkins, K. Ar dai, J., Coakley, B.J., Hopper, J.R. & Healy 2005 seismic team (2008). Extensive local seabed disturbance, erosion and mass wasting on Alpha Ridge, Central Arctic Ocean: possible evidence for an extra-terrestrial impact? *Norwegian Journal of Geology* 88: 313-320.
- Kristoffersen, Y., M. Y. Sorokin, Jokat, W & Svendsen, O. (2004). A submarine fan in the Amundsen Basin, Arctic Ocean. *Marine Geology* 204: 317-324.
- Macke A. (2009): The Expedition of the Research Vessel Polarstern to the Antarctic in 2008 (ANT-XXIV/4), Reports on Polar and Marine Research, Alfred Wegener Institute for Polar and Marine Research, Bremerhaven, 591, 64 pp.
- Matthiessen, J., Niessen, F., Stein, R. and Naafs, B.D. (2010): Pleistocene glacialmarine sedimentary environments at the Eastern Mendeleev Ridge, Arctic Ocean. *Polarforschung* 79: 123-137.

8.3 Sediment cores

- Minicucci, D.A. & Clark, D.L. (1983): A late Cenozoic stratigraphy for glacial-marine sediments of the eastern Alpha Cordillera, Central Arctic Ocean.- In: B.F. Molnia (Ed.), *Glacial-marine sedimentation*, 331-365. New York, London: Plenum Press.
- Mudie, P.J. & Blasco, S.M. (1985): Lithostratigraphy of the Cesar cores.- In: H.R. Jackson, P.J. Mudie & S.M. Blasco (Eds.), *Initial geological report on CESAR - the Canadian expedition to study the Alpha Ridge, Arctic Ocean*, Geological Survey of Canada Paper, 59-99.
- Schauer, U. (2008): The Expedition ARKTIS-XXII/2 of the Research Vessel Polarstern in 2007, *Reports on Polar and Marine Research*, Alfred Wegener Institute for Polar and Marine Research, Bremerhaven, 579, 264 pp.
- Schiel, S. (2009:.) The Expedition of the Research Vessel Polarstern to the Antarctic in 2007 (ANT-XXIV/1), *Reports on Polar and Marine Research*, Alfred Wegener Institute for Polar and Marine Research, Bremerhaven, 592, 114 pp.
- Sellén, E., Jakobsson, M. & Backman, J. (2008): Sedimentary regimes in Arctic's Amerasian and Eurasian Basins: Clues to differences in sedimentation rates. *Global and Planetary Change*, 61: 275-284.
- Sellén, E., M. O'Regan & M. Jakobsson (2010): Spatial and temporal Arctic Ocean depositional regimes: a key to the evolution of ice drift and current patterns. *Quaternary Science Reviews*, 29: 3644-3664.
- Stein, R., Matthiessen, J., Niessen, F. (2010a): Re-coring of T3 Island key core FL-224 (Nautilus Basin, Arctic Ocean): sediment characteristics and stratigraphic framework. *Polarforschung*, 79: 81-96.
- Stein, R., Matthiessen, J., Niessen, F., Krylov, A., Nam, S., Bazhenova, E. (2010b): Towards a better (litho-) stratigraphy and reconstruction of Quaternary paleoenvironment in the Amerasian Basin (Arctic Ocean). *Polarforschung* 79: 97-121.

APPENDIX

A.1 Participating Institutions

A.2 Cruise Participants

A.3 Ship's Crew

A.4 Station list

A.1 BETEILIGTE INSTITUTE / PARTICIPATING INSTITUTES

	Adresse/Address
AWI	Alfred-Wegener-Institut für Polar- und Meeresforschung in der Helmholtz-Gemeinschaft Am Handelshafen 12 27570 Bremerhaven/Germany
DU	Duke University Durham Division of Earth and Ocean Sciences Old Chemistry Bldg. NC 27708, USA
DWD	Deutscher Wetterdienst Geschäftsbereich Wettervorhersage Seeschiffahrtsberatung Bernhard Nocht Str. 76 20359 Hamburg/Germany
FIMR	Finnish Institut of Marine Research Erik Palménin aukio 1, P. O. Box 2, 00561 Helsinki/ Finland
HeliService	HeliService International GmbH, Deutschland Am Luneort 15 27572 Bremerhaven/Germany
ICBM	Institute for Chemistry and Biology of the Marine Environment Microbiogeochemistry Carl von Ossietzky University Oldenburg P.O. Box 2503 26111 Oldenburg/Germany
LSCE	Laboratoire des Sciences du Climat et de l'Environnement , France Unité mixte CNRS-CEA-UVSQ Orme des Merisiers, Bât. 701 91191 Gif sur Yvette Cedex/France
OPTIMARE	OPTIMARE Sensorsysteme AG Am Luneort 15a, 27572 Bremerhaven/Germany

Adresse/Address

POI	FEBRAS Pacific Oceanological Institute - Far Eastern Branch of Russian Academy of Sciences/Russia POI FEBRAS, 43 Baltic street Vladivostok 690041/Russia
RSMAS	Rosenstiel School of Marine and Atmospheric Sciences , USA Division of Marine and Atmospheric Chemistry, RSMAS/MAC, University of Miami 4600 Rickenbacker Causeway Miami, FL 33149/USA
SIO	P.P. Shirshov Institute of Oceanology Russian Academy of Science 36 Nachimovsky prospect, Moscow, 117851/Russia
UAF	University of Alaska Fairbanks 120 O'Neill, P.O. Box 757220, Fairbanks, AK 99775-7220/USA
UGot	University of Gothenburg Department of Chemistry, SE-412 96 Gothenburg/Sweden

A.2 FAHRTTEILNEHMER / PARTICIPANTS

Name/ Name	Vorname/ First Name	Institut/ Institute	Beruf/Profession
Allhusen	Erika	AWI	Technician Biogeochemistry
Boetius	Antje	AWI	Biologist
Boissard	Christophe	LSCE	Biologist
Brauer	Jens	HeliService	Pilot
Bureau	Claudia	AWI	Biologist
Cassar	Nicolas	DU	Chemist
Charkin	Alexander	POI	Chemist
Cherkashe- va	Alexandra	AWI	Biologist
Damm	Ellen	AWI	Chemist
Dieckmann	Gerhard	AWI	Biologist
Ericson	Ylva	UGot	Chemist
Ershova	Elizabeth	UAF	Biologist
Fernandez	Mendez	Mar	(AWI/MPI) Biologist
Galfond	Ben	RSMAS	Chemist
Hänselmann	Kristin	(AWI)	Biologist
Heckmann	Hans	HeliService	Pilot
Helmke	Elisabeth	AWI	Biologist
Hendricks	Stefan	AWI	Scientist, sea ice physics
Hirche	Hans-Jürgen	AWI	Biologist
Hopcroft	Russ	UAF	Biologist
Hoppmann	Mario	AWI	Physicist
Hunkeler	Priska	AWI	Student, sea ice physics
Katlein	Christian	AWI	Student, sea ice physics
Kilias	Estelle	AWI	Biologist
Kirschen- mann	Eva	AWI	Student, Biogeochemistry
Kollaske	Tina	AWI	Student, geology
Kosobokova	Ksenia	SIO	Biologist
Lensch	Norbert	AWI	Technician Geology
Lud- wichowski	Kai-Uwe	AWI	Chemist
Matthiessen	Jens	AWI	Scientist, geology
Meinhardt	Ann-Katrin	ICBM	Student, geology
Möllendorf	Carsten	HeliService	Mechanic
Nicolaus	Marcel	AWI	Scientist, sea ice physics
Peeken	Ilka	AWI	Biologist
Pisarev	Sergey	SIO	Oceanographer

Name/ Name	Vorname/ First Name	Institut/ Institute	Beruf/Profession
Rabe	Benjamin	AWI	Oceanographer
Ricker	Robert	AWI	Student, sea ice physics
Rentsch	Harald	DWD	Meteorologist
Rudels	Bert	FIMR	Oceanographer
Rutgers vd Loeff	Michiel	AWI	Chemist
Schauer	Ursula	AWI	Chief scientist
Scholz	Daniel	AWI	Student, chemistry
Serdeczny	Olivia	AWI	Technician. biology
Slabon	Patricia	AWI	Student, bathymetry
Sonnabend	Hartmut	DWD	Meteorol. Technician
Sühs	Mirko	AWI	Student, geology
Sumata	Hiroshi	AWI	Oceanographer
Ulfsbo	Adam	UGot	Chemist
Vaupel	Lars	HeliService	Pilot
Waddington	Ian	UAF	Technician oceanography
Wischnewski	Laura	AWI	Biologist
Wisotzki	Andreas	AWI	Technician oceanography
Zenk	Oliver	Optimare/AWI	Technician oceanography
Zou	Hao	AWI	Geologist

A.3 SHIP'S CREW

Name	Rank
Schwarze, Stefan	Master
Grundmann, Uwe	1st Offc.
Krohn, Günter	Ch. Eng.
Gumtow, Philipp	2nd Offc.
Lauber, Felix	2nd Offc.
Rackete, Carola	3rd Offc.
Rudde-Teufel, Claus	Doctor
Hecht, Andreas	R.Offc.
Minzlaff, Hans-Ulrich	2nd Eng.
Sümnicht, Stefan	2nd Eng.
Holst, Wolfgang	3rd Eng.
Scholz, Manfred	ElecEng.
Dimmler, Werner	ELO
Himmel, Frank	ELO
Muhle, Helmut	ELO
Nasis, Ilias	ELO
Loidl, Reiner	Boatsw.
Reise, Lutz	Carpenter
Bäcker, Andreas	A.B.
Brickmann, Peter	A.B.
Guse, Hartmut	A.B.
Hagemann, Manfred	A.B.
Scheel, Sebastian	A.B.
Schmidt, Uwe	A.B.
Wende, Uwe	A.B.
Winkler, Michael	A.B.
Preußner, Jörg	Storek.
Elsner, Klaus	Mot-man
Pinske, Lutz	Mot-man
Schütt, Norbert	Mot-man
Teichert, Uwe	Mot-man
Voy, Bernd	Mot-man
Müller-Homburg, R.-D	Cook
Martens, Michael	Cooksmate
Silinski, Frank	Cooksmate
Czyborra, Bärbel	1.Stwdess
Wöckener, Martina	Stwdss/Kr

Name	Rank
Kraft, Henry	2.Steward
Möller, Wolfgang	2.Steward
Silinski, Carmen	2.Stwdess
Streit, Christina	2.Stwdess
Sun, Yong Sheng	2. Steward
Yu, Kwolk Yuen	Laundrym.

A.4 STATIONSLISTE /STATION LIST PS78

Station	Date	Time	Gear	Action	Position Lat	Position Lon	Water Depth [m]
PS78/187-1	07.08.11	11:57	CTD/RO	in the water	77° 6.41' N	28° 48.38' E	211,2
PS78/187-1	07.08.11	12:07	CTD/RO	on ground/ max depth	77° 6.42' N	28° 47.83' E	210,9
PS78/187-1	07.08.11	12:08	CTD/RO	hoisting	77° 6.42' N	28° 47.78' E	210,9
PS78/187-1	07.08.11	12:20	CTD/RO	on deck	77° 6.42' N	28° 47.25' E	210
PS78/187-2	07.08.11	12:26	MN	in the water	77° 6.42' N	28° 46.97' E	209,6
PS78/187-2	07.08.11	12:35	MN	on ground/ max depth	77° 6.43' N	28° 46.58' E	208,9
PS78/187-2	07.08.11	12:36	MN	hoisting	77° 6.43' N	28° 46.54' E	208,9
PS78/187-2	07.08.11	12:46	MN	on deck	77° 6.42' N	28° 46.17' E	209,2
PS78/187-3	07.08.11	13:06	BONGO	in the water	77° 6.42' N	28° 45.36' E	208,7
PS78/187-3	07.08.11	13:10	BONGO	on ground/ max depth	77° 6.43' N	28° 45.17' E	209,1
PS78/187-3	07.08.11	13:10	BONGO	hoisting	77° 6.43' N	28° 45.17' E	209,1
PS78/187-3	07.08.11	13:16	BONGO	on deck	77° 6.44' N	28° 44.95' E	209,3
PS78/188-1	09.08.11	12:37	CAL	in the water	82° 10.10' N	60° 1.00' E	235
PS78/188-1	09.08.11	12:37	CAL	profile start	82° 10.10' N	60° 1.00' E	235
PS78/188-1	09.08.11	12:41	CAL	on ground/ max depth	82° 10.09' N	60° 1.06' E	236,5
PS78/188-1	09.08.11	12:41	CAL	hoisting	82° 10.09' N	60° 1.06' E	236,5
PS78/188-1	09.08.11	12:48	CAL	profile end	82° 10.11' N	60° 1.09' E	235,7
PS78/188-1	09.08.11	12:48	CAL	on deck	82° 10.11' N	60° 1.09' E	235,7
PS78/188-2	09.08.11	12:54	CTD/RO	in the water	82° 10.12' N	60° 1.09' E	237
PS78/188-3	09.08.11	13:04	RAMSES	in the water	82° 10.12' N	60° 1.04' E	234
PS78/188-2	09.08.11	13:06	CTD/RO	on ground/ max depth	82° 10.12' N	60° 1.05' E	235,7
PS78/188-2	09.08.11	13:08	CTD/RO	hoisting	82° 10.12' N	60° 1.06' E	237
PS78/188-3	09.08.11	13:13	RAMSES	on ground/ max depth	82° 10.13' N	60° 1.05' E	236,2
PS78/188-3	09.08.11	13:13	RAMSES	hoisting	82° 10.13' N	60° 1.05' E	236,2
PS78/188-2	09.08.11	13:19	CTD/RO	on deck	82° 10.14' N	60° 1.11' E	235,5
PS78/188-3	09.08.11	13:21	RAMSES	on deck	82° 10.15' N	60° 1.13' E	227,2
PS78/188-4	09.08.11	13:25	BONGO	in the water	82° 10.17' N	60° 1.10' E	251,5
PS78/188-4	09.08.11	13:36	BONGO	on ground/ max depth	82° 10.22' N	60° 0.81' E	233,7
PS78/188-4	09.08.11	13:36	BONGO	hoisting	82° 10.22' N	60° 0.81' E	233,7
PS78/188-4	09.08.11	13:44	BONGO	on deck	82° 10.23' N	60° 0.76' E	235,5
PS78/188-5	09.08.11	13:52	MN	in the water	82° 10.27' N	60° 0.88' E	232,7
PS78/188-5	09.08.11	14:02	MN	on ground/ max depth	82° 10.27' N	60° 0.73' E	237
PS78/188-5	09.08.11	14:02	MN	hoisting	82° 10.27' N	60° 0.73' E	237
PS78/188-5	09.08.11	14:10	MN	at surface	82° 10.28' N	60° 0.63' E	230

A.4 Stationsliste / station list PS 78

Station	Date	Time	Gear	Action	Position Lat	Position Lon	Water Depth [m]
PS78/188-5	09.08.11	14:23	MN	on deck	82° 10.38' N	60° 0.49' E	232,5
PS78/189-1	09.08.11	16:14	CTD/RO	in the water	82° 20.83' N	59° 59.72' E	331,2
PS78/189-1	09.08.11	16:27	CTD/RO	on ground/ max depth	82° 20.80' N	59° 59.68' E	329,5
PS78/189-1	09.08.11	16:27	CTD/RO	hoisting	82° 20.80' N	59° 59.68' E	329,5
PS78/189-1	09.08.11	16:33	CTD/RO	at surface	82° 20.80' N	59° 59.50' E	332,5
PS78/189-1	09.08.11	16:35	CTD/RO	on deck	82° 20.80' N	59° 59.52' E	332,5
PS78/190-1	09.08.11	19:06	CTD/RO	in the water	82° 36.07' N	59° 56.91' E	295
PS78/190-1	09.08.11	19:20	CTD/RO	on ground/ max depth	82° 36.08' N	59° 56.14' E	292,7
PS78/190-1	09.08.11	19:22	CTD/RO	hoisting	82° 36.08' N	59° 56.03' E	291,5
PS78/190-1	09.08.11	19:32	CTD/RO	on deck	82° 36.08' N	59° 55.49' E	291,2
PS78/190-2	09.08.11	19:37	BONGO	in the water	82° 36.08' N	59° 55.22' E	294
PS78/190-2	09.08.11	19:45	BONGO	on ground/ max depth	82° 36.09' N	59° 54.78' E	289,2
PS78/190-2	09.08.11	19:45	BONGO	hoisting	82° 36.09' N	59° 54.78' E	289,2
PS78/190-2	09.08.11	19:55	BONGO	on deck	82° 36.10' N	59° 54.22' E	290,7
PS78/190-3	09.08.11	20:07	MN	in the water	82° 36.12' N	59° 53.54' E	291,5
PS78/190-3	09.08.11	20:17	MN	on ground/ max depth	82° 36.14' N	59° 52.97' E	295,2
PS78/190-3	09.08.11	20:17	MN	hoisting	82° 36.14' N	59° 52.97' E	295,2
PS78/190-3	09.08.11	20:33	MN	on deck	82° 36.16' N	59° 52.07' E	296,2
PS78/191-1	09.08.11	23:01	CTD/RO	in the water	82° 50.20' N	60° 1.10' E	1010,7
PS78/191-1	09.08.11	23:29	CTD/RO	on ground/ max depth	82° 50.18' N	60° 0.28' E	1003,7
PS78/191-1	09.08.11	23:30	CTD/RO	hoisting	82° 50.18' N	60° 0.27' E	1003,5
PS78/191-1	09.08.11	23:53	CTD/RO	on deck	82° 50.14' N	59° 59.85' E	998,2
PS78/191-2	10.08.11	00:01	BONGO	in the water	82° 50.14' N	59° 59.85' E	999
PS78/191-2	10.08.11	00:13	BONGO	on ground/ max depth	82° 50.10' N	59° 59.67' E	995
PS78/191-2	10.08.11	00:14	BONGO	hoisting	82° 50.09' N	59° 59.67' E	1002,5
PS78/191-2	10.08.11	00:28	BONGO	on deck	82° 50.07' N	59° 59.40' E	992
PS78/191-3	10.08.11	00:39	MN	in the water	82° 50.02' N	59° 59.36' E	990
PS78/191-3	10.08.11	01:09	MN	on ground/ max depth	82° 49.93' N	59° 58.46' E	980,7
PS78/191-3	10.08.11	01:09	MN	hoisting	82° 49.93' N	59° 58.46' E	980,7
PS78/191-3	10.08.11	01:51	MN	on deck	82° 49.70' N	59° 57.57' E	965,5
PS78/192-1	10.08.11	05:11	CTD	in the water	83° 2.85' N	59° 56.79' E	2805,2
PS78/192-1	10.08.11	05:24	CTD	action	83° 2.81' N	59° 56.53' E	2786,5
PS78/192-1	10.08.11	06:06	CTD	on ground/ max depth	83° 2.86' N	59° 54.81' E	2674,4
PS78/192-1	10.08.11	06:07	CTD	hoisting	83° 2.86' N	59° 54.74' E	2666,7
PS78/192-1	10.08.11	07:10	CTD	on deck	83° 2.99' N	59° 51.67' E	2753,7
PS78/193-1	10.08.11	09:21	MOR	information	83° 4.05' N	59° 49.26' E	2760,9

A.4 Stationsliste / station list PS 78

Station	Date	Time	Gear	Action	Position Lat	Position Lon	Water Depth [m]
PS78/193-1	10.08.11	10:08	MOR	information	83° 4.34' N	59° 45.88' E	0
PS78/193-1	10.08.11	11:29	MOR	information	83° 4.22' N	59° 48.72' E	0
PS78/193-1	10.08.11	15:59	MOR	information	83° 5.02' N	59° 50.08' E	2854,2
PS78/193-1	10.08.11	16:10	MOR	action	83° 5.05' N	59° 50.85' E	2870,7
PS78/193-1	10.08.11	16:41	MOR	at surface	83° 5.02' N	59° 51.14' E	2875,2
PS78/193-1	10.08.11	17:12	MOR	on deck	83° 5.02' N	59° 49.02' E	2835,2
PS78/193-1	10.08.11	17:16	MOR	on deck	83° 5.02' N	59° 49.08' E	2835,5
PS78/193-1	10.08.11	17:19	MOR	on deck	83° 5.03' N	59° 49.25' E	2839,2
PS78/193-1	10.08.11	17:33	MOR	on deck	83° 5.08' N	59° 49.52' E	2842,7
PS78/193-1	10.08.11	17:56	MOR	on deck	83° 5.21' N	59° 49.81' E	2853
PS78/193-1	10.08.11	18:46	MOR	on deck	83° 5.53' N	59° 50.75' E	2904
PS78/193-2	10.08.11	19:04	CTD/RO	in the water	83° 6.38' N	59° 52.63' E	2977,2
PS78/193-2	10.08.11	20:09	CTD/RO	on ground/ max depth	83° 6.87' N	59° 54.68' E	3022,2
PS78/193-2	10.08.11	20:09	CTD/RO	hoisting	83° 6.87' N	59° 54.68' E	3022,2
PS78/193-2	10.08.11	21:11	CTD/RO	on deck	83° 7.35' N	59° 57.89' E	3041,5
PS78/193-3	10.08.11	21:15	BONGO	in the water	83° 7.45' N	59° 58.16' E	3044,5
PS78/193-3	10.08.11	21:28	BONGO	on ground/ max depth	83° 7.43' N	59° 58.93' E	3046,5
PS78/193-3	10.08.11	21:28	BONGO	hoisting	83° 7.43' N	59° 58.93' E	3046,5
PS78/193-3	10.08.11	21:41	BONGO	on deck	83° 7.44' N	59° 59.39' E	3053,5
PS78/193-4	10.08.11	21:48	MN	in the water	83° 7.60' N	59° 59.53' E	3052,2
PS78/193-4	10.08.11	23:23	MN	on ground/ max depth	83° 8.18' N	60° 5.07' E	3068,2
PS78/193-4	10.08.11	23:23	MN	hoisting	83° 8.18' N	60° 5.07' E	3068,2
PS78/193-4	11.08.11	01:04	MN	on deck	83° 8.82' N	60° 10.79' E	3088,2
PS78/194-1	11.08.11	02:30	CTD	in the water	83° 17.10' N	59° 52.58' E	3275,7
PS78/194-1	11.08.11	03:38	CTD	on ground/ max depth	83° 17.14' N	59° 53.34' E	3278,7
PS78/194-1	11.08.11	03:40	CTD	hoisting	83° 17.15' N	59° 53.34' E	3279
PS78/194-1	11.08.11	04:36	CTD	at surface	83° 17.37' N	59° 52.72' E	3285,7
PS78/194-1	11.08.11	04:37	CTD	on deck	83° 17.37' N	59° 52.70' E	3285,7
PS78/195-1	11.08.11	06:51	CTD/RO	in the water	83° 30.79' N	60° 2.49' E	3461,5
PS78/195-1	11.08.11	08:01	CTD/RO	on ground/ max depth	83° 31.41' N	60° 5.05' E	3463,2
PS78/195-1	11.08.11	08:02	CTD/RO	hoisting	83° 31.41' N	60° 5.11' E	3463,2
PS78/195-2	11.08.11	08:19	RAMSES	in the water	83° 31.55' N	60° 5.80' E	3463,2
PS78/195-2	11.08.11	08:39	RAMSES	on ground/ max depth	83° 31.72' N	60° 6.69' E	3462
PS78/195-2	11.08.11	08:40	RAMSES	hoisting	83° 31.73' N	60° 6.73' E	3462
PS78/195-2	11.08.11	08:46	RAMSES	on deck	83° 31.78' N	60° 6.98' E	3463
PS78/195-1	11.08.11	09:02	CTD/RO	on deck	83° 31.90' N	60° 7.81' E	3467
PS78/196-1	11.08.11	14:35	ICE	action	83° 49.80' N	60° 38.25' E	3590,5

A.4 Stationsliste / station list PS 78

Station	Date	Time	Gear	Action	Position Lat	Position Lon	Water Depth [m]
PS78/196-2	11.08.11	14:35	CTD	in the water	83° 49.80' N	60° 38.25' E	3590,5
PS78/196-3	11.08.11	14:52	GF PUMPE	profile start	83° 49.82' N	60° 38.00' E	3590,5
PS78/196-3	11.08.11	15:00	GF PUMPE	on ground/ max depth	83° 49.83' N	60° 37.82' E	3590,7
PS78/196-3	11.08.11	15:07	GF PUMPE	hoisting	83° 49.84' N	60° 37.65' E	3591
PS78/196-3	11.08.11	15:11	GF PUMPE	profile end	83° 49.84' N	60° 37.54' E	3591,5
PS78/196-2	11.08.11	15:46	CTD	on ground/ max depth	83° 49.91' N	60° 36.41' E	3590
PS78/196-2	11.08.11	15:47	CTD	hoisting	83° 49.92' N	60° 36.37' E	3589,5
PS78/196-2	11.08.11	16:45	CTD	at surface	83° 50.13' N	60° 33.76' E	3595,5
PS78/196-2	11.08.11	16:46	CTD	on deck	83° 50.13' N	60° 33.71' E	3594,7
PS78/196-4	11.08.11	16:56	BONGO	in the water	83° 50.18' N	60° 33.24' E	3594,5
PS78/196-4	11.08.11	17:53	BONGO	on ground/ max depth	83° 50.55' N	60° 30.52' E	3598,2
PS78/196-1	11.08.11	18:00	ICE	on ground/ max depth	83° 50.60' N	60° 30.20' E	3597,2
PS78/196-1	11.08.11	18:00	ICE	action	83° 50.60' N	60° 30.20' E	3597,2
PS78/196-4	11.08.11	18:40	BONGO	on deck	83° 50.92' N	60° 28.85' E	3600,7
PS78/196-5	11.08.11	18:51	MN	in the water	83° 51.04' N	60° 28.26' E	3602,2
PS78/196-5	11.08.11	20:40	MN	on ground/ max depth	83° 52.20' N	60° 27.97' E	3610,7
PS78/196-5	11.08.11	20:40	MN	hoisting	83° 52.20' N	60° 27.97' E	3610,7
PS78/196-5	11.08.11	22:31	MN	on deck	83° 53.24' N	60° 31.75' E	3615,7
PS78/197-1	12.08.11	05:04	CTD	in the water	84° 5.29' N	59° 58.04' E	3723,5
PS78/197-1	12.08.11	06:18	CTD	on ground/ max depth	84° 5.64' N	59° 54.24' E	3722,7
PS78/197-1	12.08.11	06:18	CTD	hoisting	84° 5.64' N	59° 54.24' E	3722,7
PS78/197-1	12.08.11	07:25	CTD	on deck	84° 6.18' N	59° 51.70' E	3720,5
PS78/198-1	12.08.11	11:32	ROV	in the water	84° 26.69' N	60° 5.24' E	3808,2
PS78/198-1	12.08.11	11:33	ROV	on ground/ max depth	84° 26.69' N	60° 5.31' E	3808,5
PS78/198-1	12.08.11	11:33	ROV	profile start	84° 26.69' N	60° 5.31' E	3808,5
PS78/198-1	12.08.11	12:44	ROV	profile end	84° 26.96' N	60° 9.74' E	3809
PS78/198-1	12.08.11	12:44	ROV	on deck	84° 26.96' N	60° 9.74' E	3809
PS78/198-2	12.08.11	13:07	CTD/RO	in the water	84° 26.99' N	60° 11.17' E	3798,7
PS78/198-2	12.08.11	14:25	CTD/RO	on ground/ max depth	84° 26.92' N	60° 14.89' E	3807
PS78/198-2	12.08.11	14:26	CTD/RO	hoisting	84° 26.92' N	60° 14.92' E	3807
PS78/198-3	12.08.11	14:45	RAMSES	in the water	84° 26.87' N	60° 15.42' E	3806,2
PS78/198-3	12.08.11	14:50	RAMSES	on ground/ max depth	84° 26.85' N	60° 15.51' E	3806,5
PS78/198-3	12.08.11	15:20	RAMSES	on deck	84° 26.75' N	60° 15.82' E	3805,2
PS78/198-2	12.08.11	15:32	CTD/RO	at surface	84° 26.71' N	60° 15.80' E	3805,5
PS78/198-2	12.08.11	15:33	CTD/RO	on deck	84° 26.71' N	60° 15.79' E	3805,2
PS78/198-4	12.08.11	15:46	MUWS	in the water	84° 26.67' N	60° 15.67' E	3805,2

A.4 Stationsliste / station list PS 78

Station	Date	Time	Gear	Action	Position Lat	Position Lon	Water Depth [m]
PS78/198-4	12.08.11	15:46	MUWS	profile start	84° 26.67' N	60° 15.67' E	3805,2
PS78/198-4	12.08.11	15:49	MUWS	on ground/ max depth	84° 26.66' N	60° 15.63' E	3805,2
PS78/198-4	12.08.11	15:51	MUWS	hoisting	84° 26.65' N	60° 15.60' E	3805
PS78/198-4	12.08.11	15:51	MUWS	profile end	84° 26.65' N	60° 15.60' E	3805
PS78/198-4	12.08.11	15:55	MUWS	in the water	84° 26.64' N	60° 15.54' E	3805
PS78/198-4	12.08.11	15:55	MUWS	action	84° 26.64' N	60° 15.54' E	3805
PS78/198-4	12.08.11	15:56	MUWS	on deck	84° 26.63' N	60° 15.52' E	3805
PS78/199-1	12.08.11	21:40	CTD/RO	in the water	84° 48.52' N	59° 45.83' E	3897,5
PS78/199-1	12.08.11	23:03	CTD/RO	on ground/ max depth	84° 49.17' N	59° 46.86' E	3897,2
PS78/199-1	12.08.11	23:04	CTD/RO	hoisting	84° 49.18' N	59° 46.90' E	3897,2
PS78/199-1	13.08.11	00:12	CTD/RO	on deck	84° 49.55' N	59° 49.54' E	3893
PS78/200-1	13.08.11	05:10	CTD	in the water	85° 8.34' N	59° 57.21' E	3918,7
PS78/200-1	13.08.11	06:27	CTD	on ground/ max depth	85° 8.49' N	59° 49.67' E	3918,7
PS78/200-1	13.08.11	06:27	CTD	hoisting	85° 8.49' N	59° 49.67' E	3918,7
PS78/200-1	13.08.11	07:34	CTD	on deck	85° 8.84' N	59° 42.41' E	3920,7
PS78/201-1	13.08.11	11:57	CTD/RO	in the water	85° 30.51' N	59° 52.88' E	3938,2
PS78/201-2	13.08.11	12:00	RAMSES	in the water	85° 30.52' N	59° 52.94' E	3938,2
PS78/201-1	13.08.11	12:07	CTD/RO	on ground/ max depth	85° 30.54' N	59° 53.09' E	3938,2
PS78/201-1	13.08.11	12:09	CTD/RO	hoisting	85° 30.55' N	59° 53.10' E	3938,2
PS78/201-2	13.08.11	12:22	RAMSES	on ground/ max depth	85° 30.62' N	59° 53.22' E	3938,2
PS78/201-2	13.08.11	12:22	RAMSES	hoisting	85° 30.62' N	59° 53.22' E	3938,2
PS78/201-1	13.08.11	12:24	CTD/RO	on deck	85° 30.63' N	59° 53.24' E	3938,2
PS78/201-2	13.08.11	12:28	RAMSES	on deck	85° 30.65' N	59° 53.27' E	3938,5
PS78/201-3	13.08.11	12:32	BONGO	in the water	85° 30.67' N	59° 53.30' E	3938,5
PS78/201-3	13.08.11	12:52	BONGO	on ground/ max depth	85° 30.77' N	59° 53.48' E	3938,5
PS78/201-3	13.08.11	12:52	BONGO	hoisting	85° 30.77' N	59° 53.48' E	3938,5
PS78/201-3	13.08.11	13:08	BONGO	on deck	85° 30.83' N	59° 53.61' E	3790,3
PS78/201-4	13.08.11	13:35	CTD/RO	in the water	85° 30.91' N	59° 53.77' E	3793,7
PS78/201-4	13.08.11	14:53	CTD/RO	on ground/ max depth	85° 30.99' N	59° 53.58' E	3782,2
PS78/201-4	13.08.11	14:55	CTD/RO	hoisting	85° 30.98' N	59° 53.56' E	3794,5
PS78/201-4	13.08.11	16:07	CTD/RO	at surface	85° 30.92' N	59° 51.91' E	3785,8
PS78/201-4	13.08.11	16:08	CTD/RO	on deck	85° 30.92' N	59° 51.87' E	3792,8
PS78/201-5	13.08.11	18:35	MUWS	in the water	85° 31.15' N	59° 42.08' E	3794,8
PS78/201-5	13.08.11	18:40	MUWS	on ground/ max depth	85° 31.15' N	59° 41.65' E	3795
PS78/201-5	13.08.11	18:40	MUWS	hoisting	85° 31.15' N	59° 41.65' E	3795
PS78/201-5	13.08.11	18:48	MUWS	profile start	85° 31.17' N	59° 40.95' E	3784

A.4 Stationsliste / station list PS 78

Station	Date	Time	Gear	Action	Position Lat	Position Lon	Water Depth [m]
PS78/201-5	13.08.11	18:48	MUWS	profile end	85° 31.17' N	59° 40.95' E	3784
PS78/201-5	13.08.11	18:48	MUWS	on deck	85° 31.17' N	59° 40.95' E	3784
PS78/201-6	13.08.11	19:05	MN	in the water	85° 31.20' N	59° 39.46' E	3794,8
PS78/201-6	13.08.11	21:14	MN	on ground/ max depth	85° 31.68' N	59° 29.88' E	3796,8
PS78/201-6	13.08.11	21:15	MN	hoisting	85° 31.68' N	59° 29.82' E	3796,8
PS78/201-6	13.08.11	23:18	MN	on deck	85° 32.24' N	59° 25.40' E	3796,6
PS78/201-7	13.08.11	23:30	MUC	in the water	85° 32.32' N	59° 25.39' E	3793
PS78/201-7	14.08.11	00:22	MUC	on ground/ max depth	85° 32.49' N	59° 25.01' E	3797
PS78/201-7	14.08.11	00:24	MUC	hoisting	85° 32.49' N	59° 25.01' E	3797,6
PS78/201-7	14.08.11	01:11	MUC	on deck	85° 32.57' N	59° 24.97' E	3796,3
PS78/202-1	14.08.11	05:09	CTD	in the water	85° 48.10' N	59° 59.53' E	3788
PS78/202-1	14.08.11	06:27	CTD	on ground/ max depth	85° 48.19' N	59° 55.91' E	3788,1
PS78/202-1	14.08.11	06:27	CTD	hoisting	85° 48.19' N	59° 55.91' E	3788,1
PS78/202-1	14.08.11	07:45	CTD	on deck	85° 48.35' N	59° 51.95' E	3787,6
PS78/203-1	14.08.11	12:00	ICE	action	85° 58.56' N	59° 25.16' E	3776,6
PS78/203-2	14.08.11	12:33	CTD/RO	in the water	85° 58.58' N	59° 25.11' E	3778,4
PS78/203-2	14.08.11	12:40	CTD/RO	on ground/ max depth	85° 58.58' N	59° 25.13' E	3778,5
PS78/203-2	14.08.11	12:40	CTD/RO	hoisting	85° 58.58' N	59° 25.13' E	3778,5
PS78/203-2	14.08.11	12:51	CTD/RO	on deck	85° 58.58' N	59° 25.16' E	3777,1
PS78/203-3	14.08.11	12:56	GF PUMPE	in the water	85° 58.58' N	59° 25.17' E	3780,2
PS78/203-3	14.08.11	13:03	GF PUMPE	on ground/ max depth	85° 58.58' N	59° 25.18' E	3777,2
PS78/203-3	14.08.11	13:03	GF PUMPE	profile start	85° 58.58' N	59° 25.18' E	3777,2
PS78/203-3	14.08.11	14:21	GF PUMPE	profile end	85° 58.54' N	59° 25.43' E	3777,8
PS78/203-3	14.08.11	14:22	GF PUMPE	on deck	85° 58.54' N	59° 25.44' E	3778,2
PS78/203-4	14.08.11	14:25	CTD	in the water	85° 58.54' N	59° 25.44' E	3777,7
PS78/203-5	14.08.11	14:37	RAMSES	in the water	85° 58.53' N	59° 25.46' E	3778,3
PS78/203-5	14.08.11	14:41	RAMSES	on ground/ max depth	85° 58.52' N	59° 25.47' E	3777,5
PS78/203-5	14.08.11	14:52	RAMSES	hoisting	85° 58.51' N	59° 25.47' E	3777,9
PS78/203-5	14.08.11	14:57	RAMSES	at surface	85° 58.50' N	59° 25.47' E	3777,7
PS78/203-5	14.08.11	14:59	RAMSES	on deck	85° 58.50' N	59° 25.47' E	3777,2
PS78/203-4	14.08.11	15:45	CTD	on ground/ max depth	85° 58.44' N	59° 25.41' E	3777,8
PS78/203-4	14.08.11	15:46	CTD	hoisting	85° 58.44' N	59° 25.40' E	3778,5
PS78/203-4	14.08.11	17:04	CTD	at surface	85° 58.30' N	59° 24.68' E	3778,6
PS78/203-4	14.08.11	17:06	CTD	on deck	85° 58.30' N	59° 24.65' E	3778,6
PS78/203-6	14.08.11	17:15	TEST	in the water	85° 58.28' N	59° 24.52' E	3780
PS78/203-6	14.08.11	18:19	TEST	on ground/ max depth	85° 58.20' N	59° 23.42' E	3778,5

A.4 Stationsliste / station list PS 78

Station	Date	Time	Gear	Action	Position Lat	Position Lon	Water Depth [m]
PS78/203-6	14.08.11	18:25	TEST	hoisting	85° 58.20' N	59° 23.30' E	3778,5
PS78/203-6	14.08.11	19:44	TEST	on deck	85° 58.21' N	59° 21.75' E	3777,9
PS78/203-1	14.08.11	20:40	ICE	on ground/ max depth	85° 58.26' N	59° 20.91' E	3777,9
PS78/203-1	14.08.11	20:40	ICE	on deck	85° 58.26' N	59° 20.91' E	3777,9
PS78/203-7	14.08.11	22:07	XCTD	in the water	86° 3.44' N	59° 30.84' E	3769
PS78/203-7	14.08.11	22:07	XCTD	on ground/ max depth	86° 3.44' N	59° 30.84' E	3769
PS78/203-8	14.08.11	23:04	XCTD	in the water	86° 6.92' N	59° 43.12' E	3770,2
PS78/203-8	14.08.11	23:04	XCTD	on ground/ max depth	86° 6.92' N	59° 43.12' E	3770,2
PS78/203-9	14.08.11	23:55	XCTD	in the water	86° 9.74' N	59° 34.88' E	3770,1
PS78/203-9	14.08.11	23:55	XCTD	on ground/ max depth	86° 9.74' N	59° 34.88' E	3770,1
PS78/204-1	15.08.11	01:54	CTD/RO	in the water	86° 14.39' N	59° 17.62' E	3091,6
PS78/204-1	15.08.11	02:59	CTD/RO	on ground/ max depth	86° 14.32' N	59° 19.55' E	3155,1
PS78/204-1	15.08.11	03:00	CTD/RO	hoisting	86° 14.32' N	59° 19.58' E	3146,7
PS78/204-1	15.08.11	03:54	CTD/RO	at surface	86° 14.26' N	59° 20.74' E	3194,3
PS78/204-1	15.08.11	03:55	CTD/RO	on deck	86° 14.26' N	59° 20.71' E	3189,4
PS78/204-2	15.08.11	04:06	MN	in the water	86° 14.25' N	59° 20.75' E	3193
PS78/204-2	15.08.11	05:49	MN	on ground/ max depth	86° 14.18' N	59° 22.68' E	3255,2
PS78/204-2	15.08.11	05:49	MN	hoisting	86° 14.18' N	59° 22.68' E	3255,2
PS78/204-2	15.08.11	07:31	MN	on deck	86° 14.11' N	59° 23.34' E	3295,4
PS78/204-3	15.08.11	07:44	BONGO	in the water	86° 14.10' N	59° 23.43' E	3298,5
PS78/204-3	15.08.11	07:59	BONGO	on ground/ max depth	86° 14.10' N	59° 23.59' E	3306,1
PS78/204-3	15.08.11	07:59	BONGO	hoisting	86° 14.10' N	59° 23.59' E	3306,1
PS78/204-3	15.08.11	08:09	BONGO	on deck	86° 14.10' N	59° 23.70' E	3305,8
PS78/204-4	15.08.11	09:11	MUC	in the water	86° 14.64' N	59° 8.56' E	2892,4
PS78/204-4	15.08.11	09:53	MUC	on ground/ max depth	86° 14.61' N	59° 8.89' E	2906,9
PS78/204-4	15.08.11	09:54	MUC	hoisting	86° 14.61' N	59° 8.89' E	2791,1
PS78/204-4	15.08.11	10:30	MUC	on deck	86° 14.62' N	59° 9.74' E	2917,8
PS78/204-5	15.08.11	12:26	XCTD	in the water	86° 18.26' N	59° 16.64' E	2291
PS78/204-5	15.08.11	12:26	XCTD	on ground/ max depth	86° 18.26' N	59° 16.64' E	2291
PS78/205-1	15.08.11	13:57	CTD	in the water	86° 19.98' N	59° 14.74' E	1951,4
PS78/205-1	15.08.11	14:07	CTD	on ground/ max depth	86° 19.95' N	59° 15.14' E	1969,6
PS78/205-1	15.08.11	14:09	CTD	hoisting	86° 19.94' N	59° 15.22' E	1973,9
PS78/205-1	15.08.11	14:19	CTD	at surface	86° 19.90' N	59° 15.61' E	1992,5
PS78/205-1	15.08.11	14:23	CTD	on deck	86° 19.89' N	59° 15.77' E	2002,2
PS78/205-2	15.08.11	14:25	RAMSES	in the water	86° 19.88' N	59° 15.86' E	2003,4

A.4 Stationsliste / station list PS 78

Station	Date	Time	Gear	Action	Position Lat	Position Lon	Water Depth [m]
PS78/205-2	15.08.11	14:45	RAMSES	on ground/ max depth	86° 19.80' N	59° 16.70' E	2076,3
PS78/205-2	15.08.11	14:45	RAMSES	hoisting	86° 19.80' N	59° 16.70' E	2076,3
PS78/205-2	15.08.11	14:50	RAMSES	at surface	86° 19.78' N	59° 16.97' E	2059,6
PS78/205-2	15.08.11	14:52	RAMSES	on deck	86° 19.78' N	59° 17.07' E	2076
PS78/205-3	15.08.11	14:59	MUWS	in the water	86° 19.73' N	59° 17.29' E	2102,3
PS78/205-3	15.08.11	15:01	MUWS	profile start	86° 19.72' N	59° 17.37' E	2112,3
PS78/205-3	15.08.11	15:01	MUWS	on ground/ max depth	86° 19.72' N	59° 17.37' E	2112,3
PS78/205-3	15.08.11	15:02	MUWS	hoisting	86° 19.72' N	59° 17.41' E	2114
PS78/205-3	15.08.11	15:02	MUWS	profile end	86° 19.72' N	59° 17.41' E	2114
PS78/205-3	15.08.11	15:06	MUWS	at surface	86° 19.70' N	59° 17.56' E	2130,4
PS78/205-3	15.08.11	15:11	MUWS	on deck	86° 19.67' N	59° 17.76' E	2150,2
PS78/205-4	15.08.11	15:15	CTD	in the water	86° 19.65' N	59° 17.93' E	2165,8
PS78/205-4	15.08.11	16:04	CTD	on ground/ max depth	86° 19.41' N	59° 19.80' E	2305,3
PS78/205-4	15.08.11	16:05	CTD	hoisting	86° 19.40' N	59° 19.83' E	2305,1
PS78/205-4	15.08.11	16:51	CTD	at surface	86° 19.16' N	59° 21.06' E	2328,2
PS78/205-4	15.08.11	16:52	CTD	on deck	86° 19.16' N	59° 21.08' E	2326,3
PS78/205-5	15.08.11	17:50	MUC	in the water	86° 20.19' N	59° 10.60' E	1947,7
PS78/205-5	15.08.11	18:16	MUC	on ground/ max depth	86° 20.07' N	59° 10.60' E	1924,9
PS78/205-5	15.08.11	18:17	MUC	hoisting	86° 20.06' N	59° 10.61' E	1922,9
PS78/205-5	15.08.11	18:42	MUC	on deck	86° 19.95' N	59° 10.32' E	1981,8
PS78/205-6	15.08.11	19:35	XCTD	in the water	86° 22.48' N	59° 26.60' E	2156,9
PS78/205-6	15.08.11	19:37	XCTD	on ground/ max depth	86° 22.62' N	59° 27.13' E	2531,3
PS78/205-6	15.08.11	19:37	XCTD	on deck	86° 22.62' N	59° 27.13' E	2531,3
PS78/205-7	15.08.11	19:39	XBT	in the water	86° 22.73' N	59° 28.74' E	2115,1
PS78/205-7	15.08.11	21:24	XBT	on ground/ max depth	86° 26.52' N	60° 4.89' E	1750,6
PS78/206-1	15.08.11	21:24	CTD/RO	in the water	86° 26.52' N	60° 4.89' E	1750,6
PS78/205-7	15.08.11	21:24	XBT	on deck	86° 26.52' N	60° 4.89' E	1750,6
PS78/206-1	15.08.11	22:00	CTD/RO	on ground/ max depth	86° 26.47' N	60° 6.05' E	1755,7
PS78/206-1	15.08.11	22:01	CTD/RO	hoisting	86° 26.47' N	60° 6.08' E	1755,2
PS78/206-1	15.08.11	22:32	CTD/RO	on deck	86° 26.44' N	60° 7.13' E	1762,6
PS78/206-2	16.08.11	00:06	MUC	in the water	86° 26.42' N	60° 4.89' E	1763,7
PS78/206-2	16.08.11	00:28	MUC	on ground/ max depth	86° 26.43' N	60° 5.75' E	1769,6
PS78/206-2	16.08.11	00:30	MUC	hoisting	86° 26.43' N	60° 5.88' E	1758,7
PS78/206-2	16.08.11	00:54	MUC	on deck	86° 26.44' N	60° 7.04' E	1761,7
PS78/206-3	16.08.11	01:34	GC	in the water	86° 26.56' N	60° 7.51' E	1774,5
PS78/206-3	16.08.11	02:00	GC	on ground/ max depth	86° 26.55' N	60° 9.27' E	1791,2

A.4 Stationsliste / station list PS 78

Station	Date	Time	Gear	Action	Position Lat	Position Lon	Water Depth [m]
PS78/206-3	16.08.11	02:02	GC	hoisting	86° 26.54' N	60° 9.44' E	1786,1
PS78/206-3	16.08.11	02:36	GC	on deck	86° 26.58' N	60° 11.09' E	1816,3
PS78/206-4	16.08.11	03:29	BC	in the water	86° 26.46' N	60° 11.66' E	1766,4
PS78/206-4	16.08.11	03:57	BC	on ground/ max depth	86° 26.49' N	60° 13.49' E	1818,6
PS78/206-4	16.08.11	03:58	BC	hoisting	86° 26.49' N	60° 13.54' E	1824,3
PS78/206-4	16.08.11	04:20	BC	at surface	86° 26.50' N	60° 14.99' E	1854,5
PS78/206-4	16.08.11	04:22	BC	on deck	86° 26.51' N	60° 15.13' E	1864,6
PS78/206-5	16.08.11	06:33	XCTD	in the water	86° 32.26' N	60° 41.51' E	2077,8
PS78/206-5	16.08.11	06:33	XCTD	on ground/ max depth	86° 32.26' N	60° 41.51' E	2077,8
PS78/207-1	16.08.11	10:47	ROV	in the water	86° 42.41' N	61° 9.60' E	577,8
PS78/207-1	16.08.11	10:47	ROV	on ground/ max depth	86° 42.41' N	61° 9.60' E	577,8
PS78/207-1	16.08.11	10:47	ROV	profile start	86° 42.41' N	61° 9.60' E	577,8
PS78/207-1	16.08.11	10:52	ROV	on deck	86° 42.42' N	61° 9.90' E	578,9
PS78/207-1	16.08.11	10:56	ROV	in the water	86° 42.43' N	61° 10.12' E	581,5
PS78/207-1	16.08.11	11:27	ROV	on deck	86° 42.48' N	61° 11.92' E	605,7
PS78/207-1	16.08.11	11:30	ROV	in the water	86° 42.48' N	61° 12.09' E	606,6
PS78/207-1	16.08.11	11:33	ROV	on deck	86° 42.49' N	61° 12.27' E	607,7
PS78/207-1	16.08.11	11:33	ROV	profile end	86° 42.49' N	61° 12.27' E	607,7
PS78/207-2	16.08.11	11:45	CTD/RO	in the water	86° 42.50' N	61° 12.95' E	613,5
PS78/207-2	16.08.11	12:04	CTD/RO	on ground/ max depth	86° 42.52' N	61° 14.05' E	619,1
PS78/207-2	16.08.11	12:07	CTD/RO	hoisting	86° 42.53' N	61° 14.23' E	619,5
PS78/207-2	16.08.11	12:32	CTD/RO	on deck	86° 42.55' N	61° 15.68' E	613
PS78/207-3	16.08.11	12:37	RAMSES	in the water	86° 42.56' N	61° 15.90' E	610,4
PS78/207-3	16.08.11	12:56	RAMSES	on ground/ max depth	86° 42.58' N	61° 17.09' E	614
PS78/207-3	16.08.11	12:57	RAMSES	hoisting	86° 42.58' N	61° 17.16' E	614,5
PS78/207-3	16.08.11	13:03	RAMSES	on deck	86° 42.59' N	61° 17.55' E	619,7
PS78/207-4	16.08.11	13:22	BC	in the water	86° 42.61' N	61° 18.79' E	631
PS78/207-4	16.08.11	13:33	BC	on ground/ max depth	86° 42.62' N	61° 19.55' E	636,1
PS78/207-4	16.08.11	13:34	BC	hoisting	86° 42.63' N	61° 19.62' E	636,4
PS78/207-4	16.08.11	13:48	BC	on deck	86° 42.66' N	61° 20.67' E	638,8
PS78/207-5	16.08.11	16:10	XCTD	in the water	86° 49.83' N	60° 4.77' E	2689,5
PS78/207-5	16.08.11	16:14	XCTD	information	86° 50.10' N	60° 8.13' E	2695,6
PS78/207-5	16.08.11	16:19	XCTD	in the water	86° 50.30' N	60° 8.24' E	2903,6
PS78/207-5	16.08.11	16:20	XCTD	on ground/ max depth	86° 50.36' N	60° 8.22' E	2919,2
PS78/207-5	16.08.11	16:21	XCTD	on deck	86° 50.43' N	60° 8.23' E	2969,9
PS78/208-1	16.08.11	21:11	MUC	in the water	86° 51.10' N	59° 50.77' E	3453,8

A.4 Stationsliste / station list PS 78

Station	Date	Time	Gear	Action	Position Lat	Position Lon	Water Depth [m]
PS78/208-1	16.08.11	22:00	MUC	on ground/ max depth	86° 51.14' N	59° 54.60' E	3398,1
PS78/208-1	16.08.11	22:02	MUC	hoisting	86° 51.15' N	59° 54.75' E	3370
PS78/208-1	16.08.11	22:42	MUC	on deck	86° 51.16' N	59° 57.89' E	3319,1
PS78/208-2	16.08.11	22:48	CTD/RO	in the water	86° 51.16' N	59° 58.27' E	3302,8
PS78/208-2	16.08.11	23:57	CTD/RO	on ground/ max depth	86° 51.13' N	60° 3.12' E	3161,6
PS78/208-2	16.08.11	23:58	CTD/RO	hoisting	86° 51.13' N	60° 3.19' E	3155,7
PS78/208-2	17.08.11	01:06	CTD/RO	on deck	86° 51.05' N	60° 7.34' E	3040,1
PS78/208-3	17.08.11	01:44	BONGO	action	86° 50.99' N	60° 9.23' E	3046,2
PS78/208-3	17.08.11	01:55	BONGO	on ground/ max depth	86° 50.98' N	60° 9.73' E	2964,3
PS78/208-3	17.08.11	01:56	BONGO	hoisting	86° 50.97' N	60° 9.78' E	2966,6
PS78/208-3	17.08.11	02:06	BONGO	at surface	86° 50.96' N	60° 10.23' E	2945,6
PS78/208-3	17.08.11	02:08	BONGO	on deck	86° 50.95' N	60° 10.31' E	2948,5
PS78/208-4	17.08.11	02:18	MN	in the water	86° 50.94' N	60° 10.75' E	2934
PS78/208-4	17.08.11	03:53	MN	on ground/ max depth	86° 50.79' N	60° 14.00' E	2867,4
PS78/208-4	17.08.11	03:53	MN	hoisting	86° 50.79' N	60° 14.00' E	2867,4
PS78/208-4	17.08.11	05:27	MN	at surface	86° 50.66' N	60° 16.49' E	2858,6
PS78/208-4	17.08.11	05:33	MN	on deck	86° 50.65' N	60° 16.64' E	2867,1
PS78/208-5	17.08.11	10:08	XCTD	in the water	86° 56.26' N	58° 55.04' E	4280,4
PS78/208-5	17.08.11	10:09	XCTD	on ground/ max depth	86° 56.33' N	58° 55.14' E	4467,4
PS78/208-6	17.08.11	10:20	XCTD	in the water	86° 56.56' N	58° 54.10' E	958,8
PS78/208-6	17.08.11	10:20	XCTD	on ground/ max depth	86° 56.56' N	58° 54.10' E	958,8
PS78/209-1	17.08.11	12:55	ICE	in the water	86° 59.24' N	58° 29.37' E	4719,7
PS78/209-2	17.08.11	12:57	CTD/RO	in the water	86° 59.24' N	58° 29.50' E	4713
PS78/209-2	17.08.11	13:08	CTD/RO	on ground/ max depth	86° 59.22' N	58° 30.18' E	4706,9
PS78/209-2	17.08.11	13:09	CTD/RO	hoisting	86° 59.22' N	58° 30.23' E	4723,1
PS78/209-2	17.08.11	13:26	CTD/RO	on deck	86° 59.19' N	58° 31.24' E	4699,9
PS78/209-3	17.08.11	13:32	RAMSES	in the water	86° 59.18' N	58° 31.60' E	4708,1
PS78/209-3	17.08.11	13:50	RAMSES	on ground/ max depth	86° 59.14' N	58° 32.64' E	4711,7
PS78/209-3	17.08.11	13:51	RAMSES	hoisting	86° 59.14' N	58° 32.70' E	4637,2
PS78/209-3	17.08.11	13:57	RAMSES	at surface	86° 59.13' N	58° 33.04' E	4700,4
PS78/209-3	17.08.11	13:58	RAMSES	on deck	86° 59.13' N	58° 33.10' E	4702,4
PS78/209-4	17.08.11	14:18	CTD	in the water	86° 59.10' N	58° 34.27' E	4682
PS78/209-4	17.08.11	16:00	CTD	on ground/ max depth	86° 58.96' N	58° 40.77' E	4606,4
PS78/209-4	17.08.11	16:01	CTD	hoisting	86° 58.96' N	58° 40.83' E	4591
PS78/209-4	17.08.11	17:31	CTD	at surface	86° 58.89' N	58° 47.05' E	4587,5
PS78/209-4	17.08.11	17:33	CTD	on deck	86° 58.89' N	58° 47.21' E	4595,6

A.4 Stationsliste / station list PS 78

Station	Date	Time	Gear	Action	Position Lat	Position Lon	Water Depth [m]
PS78/209-5	17.08.11	17:42	GF PUMPE	in the water	86° 58.89' N	58° 47.90' E	4580,8
PS78/209-5	17.08.11	17:42	GF PUMPE	profile start	86° 58.89' N	58° 47.90' E	4580,8
PS78/209-5	17.08.11	17:54	GF PUMPE	on ground/ max depth	86° 58.89' N	58° 48.90' E	4584,4
PS78/209-5	17.08.11	19:15	GF PUMPE	on ground/ max depth	86° 58.92' N	58° 56.68' E	4600,2
PS78/209-5	17.08.11	19:26	GF PUMPE	profile end	86° 58.93' N	58° 57.92' E	4636,7
PS78/209-5	17.08.11	19:27	GF PUMPE	on deck	86° 58.93' N	58° 58.03' E	4625,3
PS78/209-6	17.08.11	19:31	MUWS	in the water	86° 58.93' N	58° 58.49' E	4636,4
PS78/209-6	17.08.11	19:31	MUWS	profile start	86° 58.93' N	58° 58.49' E	4636,4
PS78/209-6	17.08.11	19:39	MUWS	on ground/ max depth	86° 58.94' N	58° 59.40' E	4625,4
PS78/209-6	17.08.11	19:39	MUWS	hoisting	86° 58.94' N	58° 59.40' E	4625,4
PS78/209-1	17.08.11	19:46	ICE	on ground/ max depth	86° 58.95' N	59° 0.20' E	4621,1
PS78/209-1	17.08.11	19:46	ICE	on deck	86° 58.95' N	59° 0.20' E	4621,1
PS78/209-6	17.08.11	19:48	MUWS	profile end	86° 58.95' N	59° 0.43' E	4617,4
PS78/209-6	17.08.11	19:48	MUWS	on deck	86° 58.95' N	59° 0.43' E	4617,4
PS78/209-7	17.08.11	22:02	XCTD	in the water	87° 7.85' N	59° 52.63' E	3561,6
PS78/209-7	17.08.11	22:02	XCTD	on ground/ max depth	87° 7.85' N	59° 52.63' E	3561,6
PS78/209-8	17.08.11	22:06	XCTD	in the water	87° 8.09' N	59° 57.68' E	3518,1
PS78/209-8	17.08.11	22:06	XCTD	on ground/ max depth	87° 8.09' N	59° 57.68' E	3518,1
PS78/210-1	18.08.11	01:35	CTD/RO	in the water	87° 17.63' N	59° 47.73' E	4064,4
PS78/210-1	18.08.11	01:59	CTD/RO	on ground/ max depth	87° 17.57' N	59° 49.21' E	4079,7
PS78/210-1	18.08.11	02:12	CTD/RO	at surface	87° 17.54' N	59° 49.78' E	4078,4
PS78/210-1	18.08.11	02:13	CTD/RO	on deck	87° 17.53' N	59° 49.82' E	4080,3
PS78/210-5	18.08.11	03:49	CTD/RO	in the water	87° 17.09' N	59° 50.13' E	4071,8
PS78/210-5	18.08.11	03:52	CTD/RO	lowering	87° 17.09' N	59° 50.18' E	4071,5
PS78/210-5	18.08.11	05:10	CTD/RO	on ground/ max depth	87° 16.99' N	59° 51.86' E	4072,1
PS78/210-5	18.08.11	05:11	CTD/RO	hoisting	87° 16.99' N	59° 51.88' E	4071,8
PS78/210-5	18.08.11	06:29	CTD/RO	on deck	87° 16.99' N	59° 54.84' E	4076,3
PS78/210-2	18.08.11	06:31	BONGO	in the water	87° 16.99' N	59° 54.93' E	4073,6
PS78/210-2	18.08.11	06:47	BONGO	on ground/ max depth	87° 17.00' N	59° 55.73' E	4070
PS78/210-2	18.08.11	06:47	BONGO	hoisting	87° 17.00' N	59° 55.73' E	4070
PS78/210-2	18.08.11	07:00	BONGO	on deck	87° 17.01' N	59° 56.49' E	4070,9
PS78/210-3	18.08.11	07:10	MN	in the water	87° 17.01' N	59° 56.94' E	4071,6
PS78/210-3	18.08.11	09:34	MN	on ground/ max depth	87° 17.00' N	60° 3.77' E	4073,9
PS78/210-3	18.08.11	09:35	MN	hoisting	87° 17.00' N	60° 3.83' E	4068,6
PS78/210-3	18.08.11	12:09	MN	on deck	87° 16.89' N	60° 10.05' E	4071

A.4 Stationsliste / station list PS 78

Station	Date	Time	Gear	Action	Position Lat	Position Lon	Water Depth [m]
PS78/210-4	18.08.11	15:21	XCTD	in the water	87° 26.91' N	59° 58.93' E	3460,4
PS78/210-4	18.08.11	15:24	XCTD	information	87° 27.10' N	59° 59.17' E	3423,4
PS78/210-4	18.08.11	15:28	XCTD	in the water	87° 27.44' N	60° 0.53' E	3535,8
PS78/210-4	18.08.11	15:30	XCTD	on ground/ max depth	87° 27.60' N	60° 2.09' E	3304,8
PS78/210-4	18.08.11	15:31	XCTD	on deck	87° 27.66' N	60° 2.81' E	3615,7
PS78/211-1	18.08.11	18:03	MUC	in the water	87° 35.97' N	61° 1.96' E	4022,2
PS78/211-1	18.08.11	18:59	MUC	on ground/ max depth	87° 36.04' N	61° 3.23' E	4026
PS78/211-1	18.08.11	19:00	MUC	hoisting	87° 36.04' N	61° 3.25' E	4022,4
PS78/211-1	18.08.11	19:48	MUC	on deck	87° 36.11' N	61° 4.77' E	4007,5
PS78/211-2	18.08.11	20:13	CTD/RO	in the water	87° 36.16' N	61° 5.79' E	4004,7
PS78/211-2	18.08.11	21:35	CTD/RO	on ground/ max depth	87° 36.29' N	61° 9.09' E	3993,7
PS78/211-2	18.08.11	21:35	CTD/RO	hoisting	87° 36.29' N	61° 9.09' E	3993,7
PS78/211-2	18.08.11	22:57	CTD/RO	on deck	87° 36.37' N	61° 13.01' E	3978
PS78/211-3	19.08.11	01:47	XCTD	in the water	87° 47.51' N	60° 31.17' E	4080,9
PS78/211-3	19.08.11	01:47	XCTD	on ground/ max depth	87° 47.51' N	60° 31.17' E	4080,9
PS78/211-4	19.08.11	01:52	XCTD	in the water	87° 47.78' N	60° 34.25' E	4330,5
PS78/211-4	19.08.11	01:52	XCTD	on ground/ max depth	87° 47.78' N	60° 34.25' E	4330,5
PS78/212-1	19.08.11	09:42	ICE	in the water	88° 1.11' N	59° 58.53' E	4261,7
PS78/212-2	19.08.11	10:44	CTD/RO	in the water	88° 1.10' N	59° 57.42' E	4260
PS78/212-2	19.08.11	10:55	CTD/RO	on ground/ max depth	88° 1.10' N	59° 57.15' E	4265,8
PS78/212-2	19.08.11	10:56	CTD/RO	hoisting	88° 1.10' N	59° 57.13' E	4261,5
PS78/212-2	19.08.11	11:06	CTD/RO	on deck	88° 1.09' N	59° 56.85' E	4261,6
PS78/212-3	19.08.11	11:11	RAMSES	in the water	88° 1.09' N	59° 56.70' E	4259,9
PS78/212-3	19.08.11	11:31	RAMSES	on ground/ max depth	88° 1.08' N	59° 56.07' E	4260,5
PS78/212-3	19.08.11	11:32	RAMSES	hoisting	88° 1.08' N	59° 56.03' E	4261
PS78/212-3	19.08.11	11:38	RAMSES	on deck	88° 1.08' N	59° 55.82' E	4260,2
PS78/212-4	19.08.11	11:42	GF PUMPE	in the water	88° 1.08' N	59° 55.67' E	4263,1
PS78/212-4	19.08.11	11:42	GF PUMPE	profile start	88° 1.08' N	59° 55.67' E	4263,1
PS78/212-4	19.08.11	11:49	GF PUMPE	on ground/ max depth	88° 1.07' N	59° 55.40' E	4259,5
PS78/212-4	19.08.11	13:18	GF PUMPE	on deck	88° 1.00' N	59° 50.75' E	4261,3
PS78/212-4	19.08.11	13:18	GF PUMPE	profile end	88° 1.00' N	59° 50.75' E	4261,3
PS78/212-5	19.08.11	13:20	CTD/RO	in the water	88° 1.00' N	59° 50.63' E	4259,9
PS78/212-5	19.08.11	14:44	CTD/RO	on ground/ max depth	88° 0.96' N	59° 44.79' E	4258,2
PS78/212-5	19.08.11	14:44	CTD/RO	hoisting	88° 0.96' N	59° 44.79' E	4258,2
PS78/212-5	19.08.11	16:03	CTD/RO	on deck	88° 0.95' N	59° 39.19' E	4263,6
PS78/212-6	19.08.11	16:09	BONGO	in the water	88° 0.96' N	59° 38.73' E	4261,4

A.4 Stationsliste / station list PS 78

Station	Date	Time	Gear	Action	Position Lat	Position Lon	Water Depth [m]
PS78/212-6	19.08.11	16:22	BONGO	on ground/ max depth	88° 0.96' N	59° 37.87' E	4259,4
PS78/212-6	19.08.11	16:22	BONGO	hoisting	88° 0.96' N	59° 37.87' E	4259,4
PS78/212-6	19.08.11	16:34	BONGO	at surface	88° 0.96' N	59° 37.08' E	4259,8
PS78/212-6	19.08.11	16:36	BONGO	on deck	88° 0.97' N	59° 36.95' E	4260
PS78/212-7	19.08.11	16:50	MN	in the water	88° 0.97' N	59° 36.07' E	4261
PS78/212-7	19.08.11	18:47	MN	on ground/ max depth	88° 1.11' N	59° 30.41' E	4265,3
PS78/212-7	19.08.11	18:47	MN	hoisting	88° 1.11' N	59° 30.41' E	4265,3
PS78/212-1	19.08.11	20:55	ICE	on ground/ max depth	88° 1.30' N	59° 27.15' E	4259,6
PS78/212-7	19.08.11	21:28	MN	on deck	88° 1.35' N	59° 26.72' E	4260
PS78/212-8	19.08.11	21:34	MUWS	in the water	88° 1.35' N	59° 26.64' E	4262,4
PS78/212-8	19.08.11	21:34	MUWS	profile start	88° 1.35' N	59° 26.64' E	4262,4
PS78/212-8	19.08.11	21:42	MUWS	on ground/ max depth	88° 1.36' N	59° 26.54' E	4258,7
PS78/212-8	19.08.11	21:42	MUWS	hoisting	88° 1.36' N	59° 26.54' E	4258,7
PS78/212-8	19.08.11	21:50	MUWS	profile end	88° 1.37' N	59° 26.48' E	4260,1
PS78/212-8	19.08.11	21:51	MUWS	on deck	88° 1.37' N	59° 26.45' E	4259,7
PS78/212-9	19.08.11	22:01	MUWS	in the water	88° 1.38' N	59° 26.36' E	4260
PS78/212-9	19.08.11	22:01	MUWS	profile start	88° 1.38' N	59° 26.36' E	4260
PS78/212-9	19.08.11	22:02	MUWS	on ground/ max depth	88° 1.38' N	59° 26.34' E	4259,3
PS78/212-9	19.08.11	22:03	MUWS	hoisting	88° 1.38' N	59° 26.33' E	4258,8
PS78/212-9	19.08.11	22:08	MUWS	on deck	88° 1.39' N	59° 26.25' E	4260,3
PS78/212-9	19.08.11	22:08	MUWS	profile end	88° 1.39' N	59° 26.25' E	4260,3
PS78/212-10	19.08.11	22:23	MN	in the water	88° 1.40' N	59° 26.30' E	4261,8
PS78/212-10	19.08.11	22:47	MN	on ground/ max depth	88° 1.42' N	59° 25.81' E	4261,1
PS78/212-10	19.08.11	22:47	MN	hoisting	88° 1.42' N	59° 25.81' E	4261,1
PS78/212-10	19.08.11	23:20	MN	on deck	88° 1.46' N	59° 24.89' E	4267,7
PS78/213-1	20.08.11	03:57	CTD	in the water	88° 22.85' N	59° 8.10' E	4256,7
PS78/213-1	20.08.11	05:21	CTD	on ground/ max depth	88° 23.13' N	59° 8.28' E	4257,4
PS78/213-1	20.08.11	05:23	CTD	hoisting	88° 23.13' N	59° 8.31' E	4258,4
PS78/213-1	20.08.11	06:43	CTD	on deck	88° 23.46' N	59° 11.25' E	4256,9
PS78/214-1	20.08.11	12:52	CTD	in the water	88° 47.61' N	60° 5.07' E	4250,7
PS78/214-1	20.08.11	14:21	CTD	on ground/ max depth	88° 47.64' N	60° 12.90' E	4249,7
PS78/214-1	20.08.11	14:22	CTD	hoisting	88° 47.64' N	60° 13.00' E	4247,2
PS78/214-1	20.08.11	15:37	CTD	at surface	88° 47.65' N	60° 20.09' E	4249,8
PS78/214-1	20.08.11	15:38	CTD	on deck	88° 47.65' N	60° 20.18' E	4250
PS78/214-2	20.08.11	15:44	RAMSES	in the water	88° 47.65' N	60° 20.77' E	4251,5

A.4 Stationsliste / station list PS 78

Station	Date	Time	Gear	Action	Position Lat	Position Lon	Water Depth [m]
PS78/214-2	20.08.11	15:45	RAMSES	lowering	88° 47.65' N	60° 20.86' E	4249,6
PS78/214-2	20.08.11	16:02	RAMSES	on ground/ max depth	88° 47.65' N	60° 22.44' E	4250,5
PS78/214-2	20.08.11	16:11	RAMSES	on deck	88° 47.65' N	60° 23.31' E	4250,5
PS78/215-1	20.08.11	21:24	CTD/RO	in the water	89° 11.57' N	60° 29.12' E	4221,4
PS78/215-1	20.08.11	22:56	CTD/RO	on ground/ max depth	89° 11.51' N	60° 48.31' E	4223,6
PS78/215-1	20.08.11	22:56	CTD/RO	hoisting	89° 11.51' N	60° 48.31' E	4223,6
PS78/215-1	21.08.11	00:09	CTD/RO	on deck	89° 11.39' N	61° 1.26' E	4228,7
PS78/215-2	21.08.11	00:11	BONGO	in the water	89° 11.39' N	61° 1.58' E	4222,8
PS78/215-2	21.08.11	00:26	BONGO	on ground/ max depth	89° 11.37' N	61° 3.83' E	4223,6
PS78/215-2	21.08.11	00:27	BONGO	hoisting	89° 11.37' N	61° 4.00' E	4222,1
PS78/215-2	21.08.11	00:39	BONGO	on deck	89° 11.34' N	61° 5.60' E	4224,8
PS78/215-3	21.08.11	00:48	MN	in the water	89° 11.34' N	61° 7.06' E	4224
PS78/215-3	21.08.11	03:10	MN	on ground/ max depth	89° 11.03' N	61° 15.50' E	4224,4
PS78/215-3	21.08.11	03:10	MN	hoisting	89° 11.03' N	61° 15.50' E	4224,4
PS78/215-3	21.08.11	06:00	MN	at surface	89° 10.69' N	61° 18.83' E	4218,6
PS78/215-3	21.08.11	06:08	MN	on deck	89° 10.70' N	61° 19.62' E	4225,6
PS78/216-1	21.08.11	13:24	CTD/RO	in the water	89° 36.01' N	60° 43.10' E	4177,4
PS78/216-1	21.08.11	13:36	CTD/RO	on ground/ max depth	89° 35.98' N	60° 44.79' E	4178,5
PS78/216-1	21.08.11	13:38	CTD/RO	hoisting	89° 35.98' N	60° 44.83' E	4177,9
PS78/216-1	21.08.11	13:50	CTD/RO	on deck	89° 35.94' N	60° 42.75' E	4178,6
PS78/216-2	21.08.11	13:58	RAMSES	in the water	89° 35.92' N	60° 42.32' E	4178,5
PS78/216-2	21.08.11	14:19	RAMSES	on ground/ max depth	89° 35.87' N	60° 44.26' E	4178,7
PS78/216-2	21.08.11	14:19	RAMSES	hoisting	89° 35.87' N	60° 44.26' E	4178,7
PS78/216-2	21.08.11	14:26	RAMSES	at surface	89° 35.86' N	60° 44.39' E	4179,1
PS78/216-2	21.08.11	14:27	RAMSES	on deck	89° 35.85' N	60° 44.44' E	4178,6
PS78/216-3	21.08.11	14:41	CTD	in the water	89° 35.82' N	60° 44.92' E	4178,8
PS78/216-3	21.08.11	16:09	CTD	on ground/ max depth	89° 35.67' N	60° 46.06' E	4179,9
PS78/216-3	21.08.11	17:24	CTD	at surface	89° 35.57' N	60° 50.52' E	4180,8
PS78/216-3	21.08.11	17:27	CTD	on deck	89° 35.57' N	60° 50.83' E	4178,1
PS78/216-4	21.08.11	17:32	TEST	in the water	89° 35.56' N	60° 51.37' E	4179,4
PS78/216-4	21.08.11	18:32	TEST	on ground/ max depth	89° 35.50' N	60° 58.74' E	4180,9
PS78/216-4	21.08.11	18:41	TEST	hoisting	89° 35.49' N	60° 59.84' E	4179,4
PS78/216-4	21.08.11	20:00	TEST	on deck	89° 35.38' N	61° 11.14' E	4181,1
PS78/217-1	22.08.11	04:59	MUC	in the water	89° 57.75' N	103° 43.36' E	4120,9
PS78/217-1	22.08.11	05:00	MUC	lowering	89° 57.74' N	103° 36.14' E	4121,5
PS78/217-1	22.08.11	05:52	MUC	on ground/ max depth	89° 57.73' N	97° 41.59' E	4121,9

A.4 Stationsliste / station list PS 78

Station	Date	Time	Gear	Action	Position Lat	Position Lon	Water Depth [m]
PS78/217-1	22.08.11	05:53	MUC	hoisting	89° 57.72' N	97° 35.10' E	4121,4
PS78/217-1	22.08.11	06:44	MUC	on deck	89° 57.67' N	92° 34.85' E	4122,5
PS78/218-1	22.08.11	11:13	ICE	in the water	89° 57.84' N	150° 49.07' E	4118,7
PS78/218-2	22.08.11	11:32	CTD/RO	in the water	89° 57.86' N	148° 6.72' E	4118,3
PS78/218-2	22.08.11	11:42	CTD/RO	on ground/ max depth	89° 57.87' N	146° 37.87' E	4117,9
PS78/218-2	22.08.11	11:44	CTD/RO	hoisting	89° 57.87' N	146° 19.33' E	4119,4
PS78/218-2	22.08.11	11:54	CTD/RO	on deck	89° 57.88' N	144° 45.13' E	4118,2
PS78/218-3	22.08.11	12:00	RAMSES	in the water	89° 57.89' N	143° 46.93' E	4133,4
PS78/218-3	22.08.11	12:20	RAMSES	on ground/ max depth	89° 57.90' N	140° 26.27' E	4119,3
PS78/218-3	22.08.11	12:21	RAMSES	hoisting	89° 57.90' N	140° 16.08' E	4120,3
PS78/218-3	22.08.11	12:39	RAMSES	on deck	89° 57.91' N	137° 6.29' E	4118,9
PS78/218-4	22.08.11	12:41	CTD/RO	in the water	89° 57.91' N	136° 44.58' E	4132,2
PS78/218-4	22.08.11	12:53	CTD/RO	on ground/ max depth	89° 57.92' N	134° 36.37' E	4165,2
PS78/218-4	22.08.11	12:54	CTD/RO	hoisting	89° 57.92' N	134° 25.57' E	4054
PS78/218-4	22.08.11	13:04	CTD/RO	on deck	89° 57.92' N	132° 35.91' E	4120,7
PS78/218-5	22.08.11	13:16	MUWS	in the water	89° 57.92' N	130° 24.64' E	4120,8
PS78/218-5	22.08.11	13:16	MUWS	profile start	89° 57.92' N	130° 24.64' E	4120,8
PS78/218-5	22.08.11	13:19	MUWS	on ground/ max depth	89° 57.92' N	129° 51.56' E	4122,3
PS78/218-5	22.08.11	13:20	MUWS	hoisting	89° 57.92' N	129° 40.68' E	4136,9
PS78/218-5	22.08.11	13:25	MUWS	on deck	89° 57.92' N	128° 46.08' E	4121,8
PS78/218-5	22.08.11	13:25	MUWS	profile end	89° 57.92' N	128° 46.08' E	4121,8
PS78/218-6	22.08.11	13:40	GF PUMPE	in the water	89° 57.92' N	126° 0.79' E	4124,5
PS78/218-6	22.08.11	13:42	GF PUMPE	profile start	89° 57.92' N	125° 38.50' E	4125,8
PS78/218-6	22.08.11	15:20	GF PUMPE	profile end	89° 57.90' N	107° 18.81' E	4117
PS78/218-6	22.08.11	15:22	GF PUMPE	on deck	89° 57.90' N	106° 56.44' E	4121
PS78/218-7	23.08.11	04:59	CTD	in the water	89° 54.20' N	56° 42.06' E	4141,9
PS78/218-7	23.08.11	06:26	CTD	on ground/ max depth	89° 53.66' N	55° 1.93' E	4140,6
PS78/218-7	23.08.11	06:26	CTD	hoisting	89° 53.66' N	55° 1.93' E	4140,6
PS78/218-7	23.08.11	07:43	CTD	on deck	89° 53.21' N	54° 12.51' E	4138,1
PS78/218-8	23.08.11	07:49	BONGO	in the water	89° 53.18' N	54° 10.07' E	4139,4
PS78/218-8	23.08.11	08:02	BONGO	on ground/ max depth	89° 53.11' N	54° 5.29' E	4137,9
PS78/218-8	23.08.11	08:02	BONGO	hoisting	89° 53.11' N	54° 5.29' E	4137,9
PS78/218-8	23.08.11	08:12	BONGO	on deck	89° 53.05' N	54° 2.71' E	4137
PS78/218-9	23.08.11	08:28	MN	in the water	89° 52.96' N	53° 58.74' E	4142,6
PS78/218-9	23.08.11	10:39	MN	on ground/ max depth	89° 52.23' N	54° 50.78' E	4145,2
PS78/218-9	23.08.11	10:40	MN	hoisting	89° 52.22' N	54° 51.63' E	4149,7
PS78/218-9	23.08.11	13:12	MN	on deck	89° 51.20' N	55° 47.01' E	4150

A.4 Stationsliste / station list PS 78

Station	Date	Time	Gear	Action	Position Lat	Position Lon	Water Depth [m]
PS78/218-1	23.08.11	13:37	ICE	on ground/ max depth	89° 51.00' N	55° 47.98' E	4151,1
PS78/218-1	23.08.11	13:38	ICE	on deck	89° 51.00' N	55° 50.51' E	4147,5
PS78/219-1	23.08.11	22:08	CTD/RO	in the water	89° 36.45' N	115° 6.72' W	4088,8
PS78/219-1	23.08.11	23:32	CTD/RO	on ground/ max depth	89° 36.92' N	115° 13.65' W	4089
PS78/219-1	23.08.11	23:33	CTD/RO	hoisting	89° 36.93' N	115° 13.68' W	4088
PS78/219-1	24.08.11	00:54	CTD/RO	on deck	89° 37.45' N	115° 15.58' W	4088,6
PS78/219-2	24.08.11	03:01	XCTD	in the water	89° 29.84' N	118° 47.70' W	3391,2
PS78/219-2	24.08.11	03:03	XCTD	action	89° 29.69' N	118° 34.73' W	3822,9
PS78/219-2	24.08.11	03:11	XCTD	action	89° 29.14' N	118° 2.78' W	3301,7
PS78/219-2	24.08.11	03:12	XCTD	on ground/ max depth	89° 29.15' N	118° 2.56' W	3323
PS78/219-2	24.08.11	03:12	XCTD	on deck	89° 29.15' N	118° 2.56' W	3323
PS78/219-3	24.08.11	05:02	XCTD	in the water	89° 22.30' N	117° 24.04' W	2648,4
PS78/219-3	24.08.11	05:03	XCTD	action	89° 22.28' N	117° 22.01' W	2298,4
PS78/219-3	24.08.11	05:09	XCTD	in the water	89° 22.30' N	117° 19.86' W	2087,1
PS78/219-3	24.08.11	05:11	XCTD	on ground/ max depth	89° 22.27' N	117° 15.04' W	2111,8
PS78/219-3	24.08.11	05:11	XCTD	on deck	89° 22.27' N	117° 15.04' W	2111,8
PS78/220-1	24.08.11	07:50	CTD/RO	in the water	89° 14.93' N	116° 44.36' W	1708,6
PS78/220-1	24.08.11	08:01	CTD/RO	on ground/ max depth	89° 14.97' N	116° 43.97' W	1717,4
PS78/220-1	24.08.11	08:02	CTD/RO	hoisting	89° 14.97' N	116° 43.78' W	1717,7
PS78/220-1	24.08.11	08:12	CTD/RO	on deck	89° 14.98' N	116° 42.34' W	1719,8
PS78/220-2	24.08.11	08:22	RAMSES	in the water	89° 15.00' N	116° 42.01' W	1731,1
PS78/220-2	24.08.11	08:45	RAMSES	on ground/ max depth	89° 15.10' N	116° 42.70' W	1761,3
PS78/220-2	24.08.11	08:46	RAMSES	hoisting	89° 15.11' N	116° 42.48' W	1770,3
PS78/220-2	24.08.11	08:53	RAMSES	on deck	89° 15.14' N	116° 42.75' W	1790,1
PS78/220-3	24.08.11	09:03	BONGO	in the water	89° 15.18' N	116° 42.61' W	1807,2
PS78/220-3	24.08.11	09:15	BONGO	on ground/ max depth	89° 15.23' N	116° 44.68' W	1822
PS78/220-3	24.08.11	09:16	BONGO	hoisting	89° 15.23' N	116° 44.07' W	1830,1
PS78/220-3	24.08.11	09:25	BONGO	on deck	89° 15.25' N	116° 43.71' W	1841,7

A.4 Stationsliste / station list PS 78

Station	Date	Time	Gear	Action	Position Lat	Position Lon	Water Depth [m]
PS78/220-4	24.08.11	09:34	CTD/RO	action	89° 15.28' N	116° 43.70' W	1855,3
PS78/220-4	24.08.11	10:19	CTD/RO	on ground/ max depth	89° 15.44' N	116° 45.25' W	1920,7
PS78/220-4	24.08.11	10:21	CTD/RO	hoisting	89° 15.45' N	116° 45.43' W	1910,7
PS78/220-4	24.08.11	11:10	CTD/RO	on deck	89° 15.67' N	116° 50.64' W	1971,5
PS78/220-5	24.08.11	11:25	MN	in the water	89° 15.65' N	117° 0.67' W	1973
PS78/220-5	24.08.11	12:30	MN	on ground/ max depth	89° 15.99' N	117° 8.28' W	2102,2
PS78/220-5	24.08.11	12:30	MN	hoisting	89° 15.99' N	117° 8.28' W	2102,2
PS78/220-5	24.08.11	13:47	MN	on deck	89° 16.45' N	117° 7.19' W	2233,8
PS78/220-6	24.08.11	18:04	MUC	in the water	89° 14.58' N	115° 26.85' W	1601,9
PS78/220-6	24.08.11	18:29	MUC	on ground/ max depth	89° 14.67' N	115° 20.83' W	1616
PS78/220-6	24.08.11	18:30	MUC	hoisting	89° 14.67' N	115° 20.83' W	1619,1
PS78/220-6	24.08.11	18:54	MUC	on deck	89° 14.67' N	115° 12.90' W	1627,7
PS78/220-7	24.08.11	19:34	GC	in the water	89° 14.81' N	115° 11.97' W	1653,9
PS78/220-7	24.08.11	19:54	GC	on ground/ max depth	89° 14.86' N	115° 11.34' W	1667,7
PS78/220-7	24.08.11	19:55	GC	hoisting	89° 14.86' N	115° 11.29' W	1673,2
PS78/220-7	24.08.11	20:24	GC	on deck	89° 14.93' N	115° 12.19' W	1677,8
PS78/221-1	25.08.11	13:34	CTD/RO	in the water	88° 55.42' N	116° 12.46' W	2009,1
PS78/221-1	25.08.11	14:18	CTD/RO	on ground/ max depth	88° 55.57' N	116° 10.80' W	1947,4
PS78/221-1	25.08.11	14:19	CTD/RO	hoisting	88° 55.58' N	116° 10.75' W	1963,7
PS78/221-1	25.08.11	14:59	CTD/RO	at surface	88° 55.70' N	116° 8.65' W	1921,3
PS78/221-1	25.08.11	15:00	CTD/RO	on deck	88° 55.70' N	116° 8.58' W	1920,4
PS78/221-2	25.08.11	15:06	RAMSES	in the water	88° 55.72' N	116° 8.21' W	1917,2
PS78/221-2	25.08.11	15:06	RAMSES	lowering	88° 55.72' N	116° 8.21' W	1917,2
PS78/221-2	25.08.11	15:36	RAMSES	on ground/ max depth	88° 55.80' N	116° 6.23' W	1904,6
PS78/221-2	25.08.11	15:36	RAMSES	hoisting	88° 55.80' N	116° 6.23' W	1904,6
PS78/221-2	25.08.11	15:44	RAMSES	at surface	88° 55.82' N	116° 5.71' W	1901,3
PS78/221-2	25.08.11	15:44	RAMSES	on deck	88° 55.82' N	116° 5.71' W	1901,3
PS78/221-3	25.08.11	15:59	MUC	in the water	88° 55.86' N	116° 4.79' W	1895,6
PS78/221-3	25.08.11	15:59	MUC	lowering	88° 55.86' N	116° 4.79' W	1895,6
PS78/221-3	25.08.11	16:27	MUC	on ground/ max depth	88° 55.92' N	116° 2.89' W	1884
PS78/221-3	25.08.11	16:27	MUC	hoisting	88° 55.92' N	116° 2.89' W	1884
PS78/221-3	25.08.11	16:49	MUC	at surface	88° 55.96' N	116° 1.55' W	1876,1

A.4 Stationsliste / station list PS 78

Station	Date	Time	Gear	Action	Position Lat	Position Lon	Water Depth [m]
PS78/221-3	25.08.11	16:52	MUC	on deck	88° 55.97' N	116° 1.39' W	1875,2
PS78/221-4	25.08.11	17:11	GC	in the water	88° 56.01' N	116° 0.36' W	1866,3
PS78/221-4	25.08.11	17:12	GC	lowering	88° 56.01' N	116° 0.31' W	1866,8
PS78/221-4	25.08.11	17:35	GC	on ground/ max depth	88° 56.05' N	115° 59.28' W	1858,5
PS78/221-4	25.08.11	17:35	GC	hoisting	88° 56.05' N	115° 59.28' W	1858,5
PS78/221-4	25.08.11	18:04	GC	on deck	88° 56.10' N	115° 58.31' W	1849,9
PS78/221-5	25.08.11	18:20	BC	in the water	88° 56.13' N	115° 57.93' W	1846,1
PS78/221-5	25.08.11	18:48	BC	on ground/ max depth	88° 56.18' N	115° 57.49' W	1840,1
PS78/221-5	25.08.11	18:49	BC	hoisting	88° 56.18' N	115° 57.48' W	1840,1
PS78/221-5	25.08.11	19:16	BC	on deck	88° 56.22' N	115° 57.40' W	1834,7
PS78/222-1	26.08.11	07:26	ICE	in the water	88° 44.14' N	128° 14.92' W	3853,8
PS78/222-1	26.08.11	07:27	ICE	on ground/ max depth	0° 0.00' N	0° 0.00' E	3852,3
PS78/222-2	26.08.11	07:27	CTD/RO	in the water	88° 44.14' N	128° 14.93' W	3853,3
PS78/222-2	26.08.11	07:36	CTD/RO	on ground/ max depth	88° 44.15' N	128° 14.96' W	3852,1
PS78/222-2	26.08.11	07:37	CTD/RO	hoisting	88° 44.15' N	128° 14.96' W	3852
PS78/222-2	26.08.11	07:47	CTD/RO	on deck	88° 44.16' N	128° 15.01' W	3852,4
PS78/222-2	26.08.11	07:52	RAMSES	in the water	88° 44.16' N	128° 15.03' W	3851,8
PS78/222-2	26.08.11	08:22	RAMSES	on ground/ max depth	88° 44.19' N	128° 15.36' W	3852,7
PS78/222-2	26.08.11	08:22	RAMSES	hoisting	88° 44.19' N	128° 15.36' W	3852,7
PS78/222-2	26.08.11	08:29	RAMSES	on deck	88° 44.20' N	128° 15.48' W	3853,4
PS78/222-4	26.08.11	08:35	BONGO	in the water	88° 44.20' N	128° 15.59' W	3852,6
PS78/222-4	26.08.11	08:48	BONGO	on ground/ max depth	88° 44.22' N	128° 15.81' W	3851,5
PS78/222-4	26.08.11	08:48	BONGO	hoisting	88° 44.22' N	128° 15.81' W	3851,5
PS78/222-4	26.08.11	09:00	BONGO	on deck	88° 44.23' N	128° 16.05' W	3851,9
PS78/222-5	26.08.11	09:10	CTD/RO	in the water	88° 44.24' N	128° 16.24' W	3854,6
PS78/222-6	26.08.11	09:15	GF PUMPE	in the water	88° 44.24' N	128° 16.35' W	3853,2
PS78/222-6	26.08.11	09:15	GF PUMPE	profile start	88° 44.24' N	128° 16.35' W	3853,2
PS78/222-5	26.08.11	10:29	CTD/RO	on ground/ max depth	88° 44.34' N	128° 17.97' W	3851,2

A.4 Stationsliste / station list PS 78

Station	Date	Time	Gear	Action	Position Lat	Position Lon	Water Depth [m]
PS78/222-5	26.08.11	10:30	CTD/RO	hoisting	88° 44.34' N	128° 17.99' W	3850,7
PS78/222-5	26.08.11	11:47	CTD/RO	on deck	88° 44.45' N	128° 19.33' W	3852,1
PS78/222-6	26.08.11	11:53	GF PUMPE	profile end	88° 44.46' N	128° 19.40' W	3852,3
PS78/222-7	26.08.11	11:54	MUWS	in the water	88° 44.46' N	128° 19.41' W	3851,8
PS78/222-6	26.08.11	11:54	GF PUMPE	on deck	88° 44.46' N	128° 19.41' W	3851,8
PS78/222-7	26.08.11	11:54	MUWS	profile start	88° 44.46' N	128° 19.41' W	3851,8
PS78/222-7	26.08.11	11:56	MUWS	on ground/ max depth	88° 44.47' N	128° 19.42' W	3852,3
PS78/222-7	26.08.11	11:56	MUWS	hoisting	88° 44.47' N	128° 19.42' W	3852,3
PS78/222-7	26.08.11	12:02	MUWS	on deck	88° 44.48' N	128° 19.48' W	3851,2
PS78/222-7	26.08.11	12:02	MUWS	profile end	88° 44.48' N	128° 19.48' W	3851,2
PS78/222-8	26.08.11	12:18	MN	in the water	88° 44.50' N	128° 19.59' W	3852
PS78/222-8	26.08.11	14:18	MN	on ground/ max depth	88° 44.68' N	128° 18.99' W	3851,7
PS78/222-8	26.08.11	16:20	MN	at surface	88° 44.81' N	128° 16.54' W	3850
PS78/222-8	26.08.11	16:30	MN	on deck	88° 44.82' N	128° 16.38' W	3850
PS78/222-1	26.08.11	16:43	ICE	on deck	88° 44.80' N	128° 16.59' W	3852,9
PS78/223-1	27.08.11	01:00	CTD/RO	in the water	88° 27.09' N	141° 8.71' W	3108,9
PS78/223-1	27.08.11	02:05	CTD/RO	on ground/ max depth	88° 27.12' N	141° 10.24' W	3098,2
PS78/223-1	27.08.11	02:06	CTD/RO	hoisting	88° 27.12' N	141° 10.25' W	3103,1
PS78/223-1	27.08.11	02:59	CTD/RO	at surface	88° 27.14' N	141° 10.74' W	3090,5
PS78/223-1	27.08.11	03:01	CTD/RO	on deck	88° 27.14' N	141° 10.78' W	3091,1
PS78/224-1	27.08.11	15:04	CTD/RO	in the water	88° 3.63' N	152° 1.49' W	3320,1
PS78/224-2	27.08.11	15:19	GF PUMPE	in the water	88° 3.63' N	152° 1.73' W	3356,5
PS78/224-2	27.08.11	15:33	GF PUMPE	profile start	88° 3.62' N	152° 2.30' W	3338,2
PS78/224-2	27.08.11	15:33	GF PUMPE	profile end	88° 3.62' N	152° 2.30' W	3338,2
PS78/224-2	27.08.11	15:34	GF PUMPE	on deck	88° 3.62' N	152° 2.32' W	3356
PS78/224-1	27.08.11	16:30	CTD/RO	on ground/ max depth	88° 3.60' N	152° 3.25' W	3356,6
PS78/224-1	27.08.11	16:31	CTD/RO	hoisting	88° 3.60' N	152° 3.27' W	3356,3
PS78/224-1	27.08.11	17:43	CTD/RO	at surface	88° 3.55' N	152° 4.53' W	3352,5
PS78/224-1	27.08.11	17:44	CTD/RO	on deck	88° 3.55' N	152° 4.55' W	3355,7
PS78/224-3	27.08.11	17:49	RAMSES	in the water	88° 3.54' N	152° 4.66' W	3353,3

A.4 Stationsliste / station list PS 78

Station	Date	Time	Gear	Action	Position Lat	Position Lon	Water Depth [m]
PS78/224-3	27.08.11	18:16	RAMSES	on ground/ max depth	88° 3.52' N	152° 5.20' W	3350,4
PS78/224-3	27.08.11	18:17	RAMSES	hoisting	88° 3.52' N	152° 5.22' W	3353,9
PS78/224-3	27.08.11	18:26	RAMSES	at surface	88° 3.51' N	152° 5.50' W	3351,4
PS78/224-3	27.08.11	18:27	RAMSES	on deck	88° 3.51' N	152° 5.51' W	3352,7
PS78/225-1	28.08.11	02:12	CTD/RO	in the water	87° 39.42' N	157° 32.10' W	2346,6
PS78/225-1	28.08.11	03:00	CTD/RO	on ground/ max depth	87° 39.38' N	157° 33.85' W	2343,4
PS78/225-1	28.08.11	03:01	CTD/RO	hoisting	87° 39.38' N	157° 33.89' W	2350,5
PS78/225-1	28.08.11	03:46	CTD/RO	at surface	87° 39.35' N	157° 35.41' W	2339,8
PS78/225-1	28.08.11	03:46	CTD/RO	on deck	87° 39.35' N	157° 35.41' W	2339,8
PS78/225-2	28.08.11	03:55	MN	in the water	87° 39.34' N	157° 35.70' W	2339,2
PS78/225-2	28.08.11	05:16	MN	on ground/ max depth	87° 39.26' N	157° 38.11' W	2332,2
PS78/225-2	28.08.11	05:16	MN	hoisting	87° 39.26' N	157° 38.11' W	2332,2
PS78/225-2	28.08.11	06:39	MN	on deck	87° 39.16' N	157° 40.90' W	2320,7
PS78/225-3	28.08.11	06:49	BONGO	in the water	87° 39.15' N	157° 41.29' W	2334,9
PS78/225-3	28.08.11	07:01	BONGO	on ground/ max depth	87° 39.13' N	157° 41.74' W	2319,1
PS78/225-3	28.08.11	07:01	BONGO	hoisting	87° 39.13' N	157° 41.74' W	2319,1
PS78/225-3	28.08.11	07:13	BONGO	on deck	87° 39.12' N	157° 42.21' W	2316,4
PS78/225-4	28.08.11	07:18	MUC	in the water	87° 39.11' N	157° 42.39' W	2315,9
PS78/225-4	28.08.11	07:48	MUC	on ground/ max depth	87° 39.09' N	157° 43.61' W	2313,9
PS78/225-4	28.08.11	07:49	MUC	hoisting	87° 39.09' N	157° 43.65' W	2312
PS78/225-4	28.08.11	08:18	MUC	on deck	87° 39.07' N	157° 44.85' W	2308,6
PS78/226-1	28.08.11	15:43	CTD/RO	in the water	87° 17.07' N	165° 15.97' W	3807,9
PS78/226-1	28.08.11	15:55	CTD/RO	on ground/ max depth	87° 17.07' N	165° 16.16' W	3811,8
PS78/226-1	28.08.11	16:08	CTD/RO	on deck	87° 17.07' N	165° 16.38' W	3813,7
PS78/226-2	28.08.11	16:13	RAMSES	in the water	87° 17.07' N	165° 16.45' W	3814,5
PS78/226-2	28.08.11	16:43	RAMSES	on ground/ max depth	87° 17.06' N	165° 16.86' W	3813
PS78/226-2	28.08.11	16:51	RAMSES	on deck	87° 17.06' N	165° 16.97' W	3814,5
PS78/226-3	28.08.11	16:57	CTD/RO	in the water	87° 17.06' N	165° 17.05' W	3815,1

A.4 Stationsliste / station list PS 78

Station	Date	Time	Gear	Action	Position Lat	Position Lon	Water Depth [m]
PS78/226-3	28.08.11	18:13	CTD/RO	on ground/ max depth	87° 17.06' N	165° 18.36' W	3816,6
PS78/226-3	28.08.11	18:13	CTD/RO	hoisting	87° 17.06' N	165° 18.36' W	3816,6
PS78/226-3	28.08.11	19:26	CTD/RO	on deck	87° 17.04' N	165° 19.80' W	3809,7
PS78/227-2	29.08.11	07:26	CTD/RO	in the water	86° 51.65' N	155° 2.54' W	3782,3
PS78/227-2	29.08.11	07:37	CTD/RO	on ground/ max depth	86° 51.64' N	155° 2.68' W	3780,5
PS78/227-2	29.08.11	07:38	CTD/RO	hoisting	86° 51.64' N	155° 2.69' W	3780,9
PS78/227-1	29.08.11	07:41	ICE	in the water	86° 51.64' N	155° 2.72' W	3780,6
PS78/227-1	29.08.11	07:42	ICE	on ground/ max depth	86° 51.64' N	155° 2.73' W	3781,9
PS78/227-2	29.08.11	07:50	CTD/RO	on deck	86° 51.64' N	155° 2.82' W	3780,4
PS78/227-3	29.08.11	07:56	RAMSES	in the water	86° 51.64' N	155° 2.85' W	3781,6
PS78/227-3	29.08.11	08:25	RAMSES	on ground/ max depth	86° 51.63' N	155° 3.19' W	3782
PS78/227-3	29.08.11	08:25	RAMSES	hoisting	86° 51.63' N	155° 3.19' W	3782
PS78/227-3	29.08.11	08:31	RAMSES	on deck	86° 51.63' N	155° 3.30' W	3782,9
PS78/227-4	29.08.11	08:35	GF PUMPE	in the water	86° 51.63' N	155° 3.34' W	3783
PS78/227-4	29.08.11	08:36	GF PUMPE	profile start	86° 51.63' N	155° 3.35' W	3782,8
PS78/227-5	29.08.11	08:47	CTD/RO	in the water	86° 51.63' N	155° 3.51' W	3782,1
PS78/227-5	29.08.11	10:03	CTD/RO	on ground/ max depth	86° 51.64' N	155° 4.66' W	3786,2
PS78/227-5	29.08.11	10:05	CTD/RO	hoisting	86° 51.64' N	155° 4.69' W	3792,4
PS78/227-4	29.08.11	10:18	GF PUMPE	profile end	86° 51.64' N	155° 4.90' W	3795,6
PS78/227-4	29.08.11	10:18	GF PUMPE	hoisting	86° 51.64' N	155° 4.90' W	3795,6
PS78/227-4	29.08.11	10:18	GF PUMPE	on deck	86° 51.64' N	155° 4.90' W	3795,6
PS78/227-5	29.08.11	11:22	CTD/RO	on deck	86° 51.68' N	155° 5.79' W	3784,3
PS78/227-6	29.08.11	11:28	MUWS	in the water	86° 51.69' N	155° 5.86' W	3785,5
PS78/227-6	29.08.11	11:28	MUWS	profile start	86° 51.69' N	155° 5.86' W	3785,5
PS78/227-6	29.08.11	11:32	MUWS	on ground/ max depth	86° 51.69' N	155° 5.91' W	3793,3
PS78/227-6	29.08.11	11:32	MUWS	hoisting	86° 51.69' N	155° 5.91' W	3793,3
PS78/227-6	29.08.11	11:32	MUWS	profile end	86° 51.69' N	155° 5.91' W	3793,3
PS78/227-6	29.08.11	11:40	MUWS	on deck	86° 51.69' N	155° 6.01' W	3786,8
PS78/227-7	29.08.11	11:46	BONGO	in the water	86° 51.70' N	155° 6.08' W	3786,1
PS78/227-7	29.08.11	11:57	BONGO	on ground/ max depth	86° 51.71' N	155° 6.16' W	3786,4
PS78/227-7	29.08.11	11:58	BONGO	hoisting	86° 51.71' N	155° 6.18' W	3785,8
PS78/227-7	29.08.11	12:07	BONGO	on deck	86° 51.72' N	155° 6.25' W	3785,1
PS78/227-8	29.08.11	12:19	MN	in the water	86° 51.73' N	155° 6.34' W	3785
PS78/227-8	29.08.11	14:29	MN	on ground/ max depth	86° 51.80' N	155° 6.43' W	3783,6
PS78/227-8	29.08.11	14:29	MN	hoisting	86° 51.80' N	155° 6.43' W	3783,6

A.4 Stationsliste / station list PS 78

Station	Date	Time	Gear	Action	Position Lat	Position Lon	Water Depth [m]
PS78/227-1	29.08.11	15:40	ICE	on deck	86° 51.82' N	155° 6.02' W	3780,4
PS78/227-8	29.08.11	16:31	MN	at surface	86° 51.82' N	155° 5.67' W	3778,1
PS78/227-8	29.08.11	16:37	MN	on deck	86° 51.82' N	155° 5.60' W	3781,4
PS78/228-1	30.08.11	04:05	CTD	in the water	86° 17.53' N	146° 41.28' W	2581,2
PS78/228-1	30.08.11	04:08	CTD	lowering	86° 17.54' N	146° 41.22' W	2582,4
PS78/228-1	30.08.11	05:00	CTD	on ground/ max depth	86° 17.54' N	146° 40.14' W	2578,4
PS78/228-1	30.08.11	05:01	CTD	hoisting	86° 17.54' N	146° 39.97' W	2577,5
PS78/228-1	30.08.11	05:49	CTD	at surface	86° 17.54' N	146° 39.15' W	2574,8
PS78/228-1	30.08.11	05:51	CTD	on deck	86° 17.54' N	146° 39.11' W	2572,4
PS78/228-2	30.08.11	05:56	DUMMY	in the water	86° 17.54' N	146° 39.01' W	2574,5
PS78/228-2	30.08.11	05:56	DUMMY	profile start	86° 17.54' N	146° 39.01' W	2574,5
PS78/228-2	30.08.11	06:35	DUMMY	on ground/ max depth	86° 17.54' N	146° 38.41' W	2573,8
PS78/228-2	30.08.11	07:32	DUMMY	profile end	86° 17.54' N	146° 37.53' W	2567,7
PS78/228-2	30.08.11	07:33	DUMMY	on deck	86° 17.54' N	146° 37.52' W	2569,2
PS78/229-1	31.08.11	00:37	CTD/RO	in the water	85° 43.91' N	140° 53.53' W	2264,4
PS78/229-1	31.08.11	01:28	CTD/RO	on ground/ max depth	85° 44.20' N	140° 52.04' W	2268,7
PS78/229-1	31.08.11	01:30	CTD/RO	hoisting	85° 44.21' N	140° 51.98' W	2269,2
PS78/229-1	31.08.11	02:20	CTD/RO	at surface	85° 44.47' N	140° 50.05' W	2265
PS78/229-1	31.08.11	02:22	CTD/RO	on deck	85° 44.48' N	140° 49.97' W	2270,9
PS78/230-1	31.08.11	18:25	ICE	in the water	85° 3.50' N	137° 21.39' W	1835,9
PS78/230-2	31.08.11	18:46	CTD/RO	in the water	85° 3.54' N	137° 20.45' W	1820,7
PS78/230-2	31.08.11	18:57	CTD/RO	on ground/ max depth	85° 3.56' N	137° 19.97' W	1803,2
PS78/230-2	31.08.11	18:57	CTD/RO	hoisting	85° 3.56' N	137° 19.97' W	1803,2
PS78/230-2	31.08.11	19:08	CTD/RO	action	85° 3.58' N	137° 19.48' W	1814,1
PS78/230-2	31.08.11	19:08	CTD/RO	on deck	85° 3.58' N	137° 19.48' W	1814,1
PS78/230-3	31.08.11	19:14	RAMSES	in the water	85° 3.59' N	137° 19.21' W	1818,4
PS78/230-3	31.08.11	19:46	RAMSES	on ground/ max depth	85° 3.66' N	137° 17.80' W	1817,8
PS78/230-3	31.08.11	19:46	RAMSES	hoisting	85° 3.66' N	137° 17.80' W	1817,8

A.4 Stationsliste / station list PS 78

Station	Date	Time	Gear	Action	Position Lat	Position Lon	Water Depth [m]
PS78/230-3	31.08.11	20:00	RAMSES	on deck	85° 3.68' N	137° 17.19' W	1817
PS78/230-4	31.08.11	20:05	MUWS	in the water	85° 3.69' N	137° 16.97' W	1845,4
PS78/230-4	31.08.11	20:06	MUWS	profile start	85° 3.70' N	137° 16.93' W	1838,2
PS78/230-4	31.08.11	20:10	MUWS	on ground/ max depth	85° 3.70' N	137° 16.75' W	1844
PS78/230-4	31.08.11	20:11	MUWS	hoisting	85° 3.71' N	137° 16.70' W	1844,6
PS78/230-4	31.08.11	20:17	MUWS	profile end	85° 3.72' N	137° 16.44' W	1849,3
PS78/230-4	31.08.11	20:17	MUWS	on deck	85° 3.72' N	137° 16.44' W	1849,3
PS78/230-5	31.08.11	20:26	CTD/RO	in the water	85° 3.74' N	137° 16.04' W	1853,3
PS78/230-6	31.08.11	20:33	GF PUMPE	in the water	85° 3.75' N	137° 15.73' W	1855
PS78/230-6	31.08.11	20:35	GF PUMPE	profile start	85° 3.75' N	137° 15.64' W	1854,3
PS78/230-6	31.08.11	20:39	GF PUMPE	on ground/ max depth	85° 3.76' N	137° 15.47' W	1857,1
PS78/230-5	31.08.11	21:10	CTD/RO	on ground/ max depth	85° 3.83' N	137° 14.09' W	1864,8
PS78/230-5	31.08.11	21:10	CTD/RO	hoisting	85° 3.83' N	137° 14.09' W	1864,8
PS78/230-5	31.08.11	21:59	CTD/RO	on deck	85° 3.94' N	137° 11.80' W	1857,9
PS78/230-7	31.08.11	22:05	BONGO	in the water	85° 3.96' N	137° 11.50' W	1858,1
PS78/230-6	31.08.11	22:07	GF PUMPE	hoisting	85° 3.96' N	137° 11.40' W	1860,4
PS78/230-7	31.08.11	22:19	BONGO	on ground/ max depth	85° 3.99' N	137° 10.79' W	1863,9
PS78/230-7	31.08.11	22:20	BONGO	hoisting	85° 3.99' N	137° 10.74' W	1864
PS78/230-7	31.08.11	22:29	BONGO	on deck	85° 4.02' N	137° 10.27' W	1863,3
PS78/230-6	31.08.11	22:33	GF PUMPE	profile end	85° 4.02' N	137° 10.06' W	1871,8
PS78/230-6	31.08.11	22:33	GF PUMPE	on deck	85° 4.02' N	137° 10.06' W	1871,8
PS78/230-8	31.08.11	23:25	MN	in the water	85° 4.14' N	137° 7.15' W	1867,4
PS78/230-1	31.08.11	23:44	ICE	on ground/ max depth	85° 4.18' N	137° 6.05' W	1866,4
PS78/230-1	31.08.11	23:45	ICE	on deck	85° 4.19' N	137° 6.00' W	1870,4
PS78/230-8	01.09.11	00:29	MN	on ground/ max depth	85° 4.27' N	137° 3.33' W	1873,8
PS78/230-8	01.09.11	00:29	MN	hoisting	85° 4.27' N	137° 3.33' W	1873,8
PS78/230-8	01.09.11	01:30	MN	on deck	85° 4.36' N	136° 59.39' W	1871,5
PS78/231-1	01.09.11	05:38	MUC	in the water	84° 54.33' N	137° 49.84' W	1590,1

A.4 Stationsliste / station list PS 78

Station	Date	Time	Gear	Action	Position Lat	Position Lon	Water Depth [m]
PS78/231-1	01.09.11	06:01	MUC	on ground/ max depth	84° 54.32' N	137° 48.54' W	1594
PS78/231-1	01.09.11	06:01	MUC	hoisting	84° 54.32' N	137° 48.54' W	1594
PS78/231-1	01.09.11	06:23	MUC	on deck	84° 54.31' N	137° 47.31' W	1595,4
PS78/231-2	01.09.11	06:45	GC	in the water	84° 54.30' N	137° 46.06' W	1612,2
PS78/231-2	01.09.11	07:04	GC	on ground/ max depth	84° 54.29' N	137° 45.00' W	1617,9
PS78/231-2	01.09.11	07:05	GC	hoisting	84° 54.29' N	137° 44.94' W	1618,3
PS78/231-2	01.09.11	07:28	GC	on deck	84° 54.29' N	137° 43.60' W	1627,4
PS78/231-3	01.09.11	07:44	BC	in the water	84° 54.29' N	137° 42.67' W	1633,3
PS78/231-3	01.09.11	08:09	BC	on ground/ max depth	84° 54.29' N	137° 41.20' W	1646,3
PS78/231-3	01.09.11	08:09	BC	hoisting	84° 54.29' N	137° 41.20' W	1646,3
PS78/231-3	01.09.11	08:35	BC	on deck	84° 54.30' N	137° 39.68' W	1659,7
PS78/231-4	01.09.11	13:44	XCTD	in the water	84° 37.64' N	135° 22.18' W	2274,4
PS78/231-4	01.09.11	13:46	XCTD	on ground/ max depth	84° 37.67' N	135° 21.77' W	2276,1
PS78/232-1	01.09.11	15:52	CTD/RO	in the water	84° 30.83' N	134° 32.57' W	2441
PS78/232-2	01.09.11	16:07	GF PUMPE	in the water	84° 30.81' N	134° 31.81' W	2439,6
PS78/232-2	01.09.11	16:07	GF PUMPE	profile start	84° 30.81' N	134° 31.81' W	2439,6
PS78/232-2	01.09.11	16:21	GF PUMPE	profile end	84° 30.78' N	134° 31.10' W	2438,4
PS78/232-2	01.09.11	16:22	GF PUMPE	on deck	84° 30.78' N	134° 31.05' W	2466,8
PS78/232-1	01.09.11	16:46	CTD/RO	on ground/ max depth	84° 30.73' N	134° 29.88' W	2399,3
PS78/232-1	01.09.11	16:47	CTD/RO	hoisting	84° 30.73' N	134° 29.84' W	2412,2
PS78/232-1	01.09.11	17:36	CTD/RO	at surface	84° 30.62' N	134° 27.58' W	2425,3
PS78/232-1	01.09.11	17:38	CTD/RO	on deck	84° 30.61' N	134° 27.49' W	2414,6
PS78/232-3	01.09.11	21:45	XCTD	in the water	84° 12.16' N	133° 32.15' W	2270,2
PS78/232-3	01.09.11	21:46	XCTD	on ground/ max depth	84° 12.14' N	133° 32.25' W	2272
PS78/233-1	02.09.11	01:55	CTD/RO	in the water	83° 56.06' N	132° 25.57' W	3160,4
PS78/233-2	02.09.11	02:00	GF PUMPE	in the water	83° 56.05' N	132° 25.34' W	3159,9
PS78/233-2	02.09.11	02:01	GF PUMPE	profile start	83° 56.05' N	132° 25.29' W	3159,7

A.4 Stationsliste / station list PS 78

Station	Date	Time	Gear	Action	Position Lat	Position Lon	Water Depth [m]
PS78/233-2	02.09.11	02:13	GF PUMPE	profile end	83° 56.05' N	132° 24.95' W	3160,1
PS78/233-2	02.09.11	02:14	GF PUMPE	on deck	83° 56.05' N	132° 24.91' W	3159,8
PS78/233-1	02.09.11	03:01	CTD/RO	on ground/ max depth	83° 56.01' N	132° 23.50' W	3163
PS78/233-1	02.09.11	03:03	CTD/RO	hoisting	83° 56.01' N	132° 23.44' W	3163,3
PS78/233-1	02.09.11	04:04	CTD/RO	at surface	83° 55.95' N	132° 21.61' W	3155,1
PS78/233-1	02.09.11	04:05	CTD/RO	on deck	83° 55.95' N	132° 21.58' W	3161,6
PS78/233-3	02.09.11	08:36	XCTD	in the water	83° 36.63' N	131° 36.47' W	3300,7
PS78/233-3	02.09.11	08:40	XCTD	on ground/ max depth	83° 36.56' N	131° 35.86' W	3302,9
PS78/233-3	02.09.11	08:40	XCTD	on deck	83° 36.56' N	131° 35.86' W	3302,9
PS78/234-1	02.09.11	12:16	CTD/RO	in the water	83° 22.75' N	131° 1.23' W	3351,3
PS78/234-2	02.09.11	12:24	GF PUMPE	in the water	83° 22.75' N	131° 1.13' W	3351,1
PS78/234-2	02.09.11	12:27	GF PUMPE	on ground/ max depth	83° 22.75' N	131° 1.10' W	3351,2
PS78/234-2	02.09.11	12:27	GF PUMPE	profile start	83° 22.75' N	131° 1.10' W	3351,2
PS78/234-2	02.09.11	12:43	GF PUMPE	profile end	83° 22.74' N	131° 0.89' W	3351,2
PS78/234-2	02.09.11	12:44	GF PUMPE	on deck	83° 22.74' N	131° 0.88' W	3351,2
PS78/234-1	02.09.11	13:27	CTD/RO	on ground/ max depth	83° 22.73' N	131° 0.26' W	3350,9
PS78/234-1	02.09.11	13:28	CTD/RO	hoisting	83° 22.73' N	131° 0.25' W	3351,2
PS78/234-1	02.09.11	14:34	CTD/RO	at surface	83° 22.70' N	130° 59.40' W	3350,9
PS78/234-1	02.09.11	14:35	CTD/RO	on deck	83° 22.70' N	130° 59.39' W	3352
PS78/235-1	02.09.11	21:03	ICE	in the water	83° 1.80' N	130° 2.34' W	3380
PS78/235-2	02.09.11	21:41	CTD/RO	in the water	83° 1.75' N	130° 2.14' W	3381,8
PS78/235-2	02.09.11	21:51	CTD/RO	on ground/ max depth	83° 1.74' N	130° 2.08' W	3383,2
PS78/235-2	02.09.11	21:53	CTD/RO	hoisting	83° 1.73' N	130° 2.07' W	3354,1
PS78/235-2	02.09.11	22:04	CTD/RO	on deck	83° 1.72' N	130° 2.00' W	3382,1
PS78/235-3	02.09.11	22:10	RAMSES	in the water	83° 1.71' N	130° 1.97' W	3382,7
PS78/235-3	02.09.11	22:30	RAMSES	on ground/ max depth	83° 1.68' N	130° 1.83' W	3382,2
PS78/235-3	02.09.11	22:31	RAMSES	hoisting	83° 1.68' N	130° 1.82' W	3382,1
PS78/235-3	02.09.11	22:39	RAMSES	on deck	83° 1.67' N	130° 1.76' W	3382,8
PS78/235-4	02.09.11	22:53	CTD/RO	in the water	83° 1.65' N	130° 1.65' W	3378,7
PS78/235-4	02.09.11	22:59	CTD/RO	on ground/ max depth	83° 1.65' N	130° 1.61' W	3382,1
PS78/235-4	02.09.11	23:00	CTD/RO	hoisting	83° 1.64' N	130° 1.60' W	3381,4
PS78/235-4	02.09.11	23:05	CTD/RO	on deck	83° 1.64' N	130° 1.56' W	3382,6
PS78/235-5	02.09.11	23:12	MUWS	in the water	83° 1.63' N	130° 1.49' W	3382,2

A.4 Stationsliste / station list PS 78

Station	Date	Time	Gear	Action	Position Lat	Position Lon	Water Depth [m]
PS78/235-5	02.09.11	23:12	MUWS	profile start	83° 1.63' N	130° 1.49' W	3382,2
PS78/235-5	02.09.11	23:17	MUWS	on ground/ max depth	83° 1.63' N	130° 1.45' W	3382,2
PS78/235-5	02.09.11	23:18	MUWS	hoisting	83° 1.63' N	130° 1.44' W	3375,5
PS78/235-5	02.09.11	23:24	MUWS	on deck	83° 1.62' N	130° 1.39' W	3382,5
PS78/235-5	02.09.11	23:24	MUWS	profile end	83° 1.62' N	130° 1.39' W	3382,5
PS78/235-6	02.09.11	23:37	CTD/RO	in the water	83° 1.61' N	130° 1.27' W	3382,7
PS78/235-7	02.09.11	23:41	GF PUMPE	in the water	83° 1.60' N	130° 1.23' W	3382,6
PS78/235-7	02.09.11	23:41	GF PUMPE	profile start	83° 1.60' N	130° 1.23' W	3382,6
PS78/235-7	02.09.11	23:47	GF PUMPE	on ground/ max depth	83° 1.60' N	130° 1.17' W	3382,5
PS78/235-6	03.09.11	00:46	CTD/RO	on ground/ max depth	83° 1.56' N	130° 0.50' W	3383,4
PS78/235-6	03.09.11	00:47	CTD/RO	hoisting	83° 1.56' N	130° 0.49' W	3382,3
PS78/235-7	03.09.11	01:12	GF PUMPE	profile end	83° 1.54' N	130° 0.15' W	3381,5
PS78/235-7	03.09.11	01:12	GF PUMPE	on deck	83° 1.54' N	130° 0.15' W	3381,5
PS78/235-6	03.09.11	02:03	CTD/RO	at surface	83° 1.52' N	129° 59.36' W	3381,9
PS78/235-6	03.09.11	02:04	CTD/RO	on deck	83° 1.52' N	129° 59.34' W	3381,6
PS78/235-8	03.09.11	02:22	MN	in the water	83° 1.51' N	129° 59.04' W	3382,2
PS78/235-8	03.09.11	04:12	MN	on ground/ max depth	83° 1.44' N	129° 56.97' W	3380,7
PS78/235-8	03.09.11	04:12	MN	hoisting	83° 1.44' N	129° 56.97' W	3380,7
PS78/235-8	03.09.11	06:09	MN	on deck	83° 1.34' N	129° 54.62' W	3381,8
PS78/235-8	03.09.11	06:25	BONGO	in the water	83° 1.32' N	129° 54.33' W	3381,5
PS78/235-1	03.09.11	06:31	ICE	on ground/ max depth	83° 1.32' N	129° 54.22' W	3381,2
PS78/235-8	03.09.11	06:38	BONGO	on ground/ max depth	83° 1.31' N	129° 54.08' W	3380
PS78/235-8	03.09.11	06:38	BONGO	hoisting	83° 1.31' N	129° 54.08' W	3380
PS78/235-8	03.09.11	06:53	BONGO	on deck	83° 1.30' N	129° 53.81' W	3380,7
PS78/236-1	04.09.11	11:12	CTD/RO	in the water	83° 30.33' N	145° 57.53' W	2941,9
PS78/236-2	04.09.11	11:17	GF PUMPE	in the water	83° 30.35' N	145° 57.61' W	2941,1
PS78/236-2	04.09.11	11:19	GF PUMPE	on ground/ max depth	83° 30.35' N	145° 57.61' W	2941,6
PS78/236-2	04.09.11	11:19	GF PUMPE	profile start	83° 30.35' N	145° 57.61' W	2941,6
PS78/236-1	04.09.11	11:29	CTD/RO	on ground/ max depth	83° 30.38' N	145° 57.72' W	2940,6
PS78/236-2	04.09.11	11:30	GF PUMPE	profile end	83° 30.39' N	145° 57.73' W	2939,8

A.4 Stationsliste / station list PS 78

Station	Date	Time	Gear	Action	Position Lat	Position Lon	Water Depth [m]
PS78/236-2	04.09.11	11:30	GF PUMPE	hoisting	83° 30.39' N	145° 57.73' W	2939,8
PS78/236-2	04.09.11	11:32	GF PUMPE	on deck	83° 30.39' N	145° 57.77' W	2940,9
PS78/236-1	04.09.11	11:49	CTD/RO	on deck	83° 30.45' N	145° 57.97' W	2940,1
PS78/236-3	04.09.11	11:56	RAMSES	in the water	83° 30.47' N	145° 58.03' W	2939,9
PS78/236-3	04.09.11	12:21	RAMSES	on ground/ max depth	83° 30.54' N	145° 58.24' W	2940,6
PS78/236-3	04.09.11	12:21	RAMSES	hoisting	83° 30.54' N	145° 58.24' W	2940,6
PS78/236-3	04.09.11	12:31	RAMSES	on deck	83° 30.56' N	145° 58.35' W	2938,8
PS78/237-1	05.09.11	03:11	MUC	in the water	83° 44.54' N	154° 24.59' W	2366,2
PS78/237-2	05.09.11	03:15	GF PUMPE	in the water	83° 44.55' N	154° 24.62' W	2365,9
PS78/237-2	05.09.11	03:16	GF PUMPE	profile start	83° 44.56' N	154° 24.63' W	2367,2
PS78/237-2	05.09.11	03:27	GF PUMPE	profile end	83° 44.59' N	154° 24.75' W	2370,4
PS78/237-2	05.09.11	03:28	GF PUMPE	on deck	83° 44.60' N	154° 24.76' W	2377
PS78/237-1	05.09.11	03:43	MUC	on ground/ max depth	83° 44.65' N	154° 24.88' W	2377,8
PS78/237-1	05.09.11	03:45	MUC	hoisting	83° 44.65' N	154° 24.90' W	2370,3
PS78/237-1	05.09.11	04:13	MUC	at surface	83° 44.74' N	154° 25.16' W	2370
PS78/237-1	05.09.11	04:15	MUC	on deck	83° 44.75' N	154° 25.19' W	2371
PS78/237-3	05.09.11	04:31	GC	in the water	83° 44.79' N	154° 25.35' W	2370,3
PS78/237-3	05.09.11	04:33	GC	lowering	83° 44.79' N	154° 25.38' W	2378,1
PS78/237-3	05.09.11	04:58	GC	on ground/ max depth	83° 44.85' N	154° 25.64' W	2369
PS78/237-3	05.09.11	04:59	GC	hoisting	83° 44.85' N	154° 25.65' W	2368,9
PS78/237-3	05.09.11	05:30	GC	on deck	83° 44.91' N	154° 25.94' W	2371,3
PS78/238-1	05.09.11	16:03	GC	in the water	83° 55.01' N	162° 45.68' W	2651,5
PS78/238-1	05.09.11	16:34	GC	on ground/ max depth	83° 55.02' N	162° 45.90' W	2649,4
PS78/238-1	05.09.11	16:34	GC	hoisting	83° 55.02' N	162° 45.90' W	2649,4
PS78/238-1	05.09.11	17:07	GC	at surface	83° 55.02' N	162° 46.23' W	2649,9
PS78/238-1	05.09.11	17:11	GC	on deck	83° 55.02' N	162° 46.25' W	2649,5
PS78/238-2	05.09.11	17:26	BC	in the water	83° 55.01' N	162° 46.36' W	2650,5

A.4 Stationsliste / station list PS 78

Station	Date	Time	Gear	Action	Position Lat	Position Lon	Water Depth [m]
PS78/238-2	05.09.11	18:04	BC	on ground/ max depth	83° 54.98' N	162° 46.67' W	2649,8
PS78/238-2	05.09.11	18:05	BC	hoisting	83° 54.98' N	162° 46.68' W	2646,1
PS78/238-2	05.09.11	18:41	BC	on deck	83° 54.95' N	162° 47.09' W	2644,2
PS78/239-1	05.09.11	22:20	ICE	in the water	84° 4.40' N	164° 11.55' W	2019,6
PS78/239-2	05.09.11	22:48	CTD/RO	in the water	84° 4.41' N	164° 11.98' W	2003
PS78/239-2	05.09.11	22:58	CTD/RO	on ground/ max depth	84° 4.41' N	164° 12.13' W	1997,7
PS78/239-2	05.09.11	23:00	CTD/RO	hoisting	84° 4.41' N	164° 12.16' W	2000,6
PS78/239-2	05.09.11	23:12	CTD/RO	action	84° 4.42' N	164° 12.34' W	1994,1
PS78/239-2	05.09.11	23:13	CTD/RO	on deck	84° 4.42' N	164° 12.36' W	1995,9
PS78/239-3	05.09.11	23:19	RAMSES	in the water	84° 4.42' N	164° 12.44' W	1990,8
PS78/239-3	05.09.11	23:44	RAMSES	on ground/ max depth	84° 4.42' N	164° 12.77' W	1983,4
PS78/239-3	05.09.11	23:44	RAMSES	hoisting	84° 4.42' N	164° 12.77' W	1983,4
PS78/239-3	05.09.11	23:50	RAMSES	on deck	84° 4.43' N	164° 12.84' W	1984,2
PS78/239-4	05.09.11	23:58	MUWS	in the water	84° 4.43' N	164° 12.94' W	1980,1
PS78/239-4	05.09.11	23:58	MUWS	profile start	84° 4.43' N	164° 12.94' W	1980,1
PS78/239-4	06.09.11	00:02	MUWS	on ground/ max depth	84° 4.43' N	164° 12.98' W	1980,2
PS78/239-4	06.09.11	00:03	MUWS	hoisting	84° 4.44' N	164° 12.99' W	1980,3
PS78/239-4	06.09.11	00:09	MUWS	profile end	84° 4.44' N	164° 13.06' W	1985
PS78/239-5	06.09.11	00:16	CTD/RO	in the water	84° 4.44' N	164° 13.13' W	1978,5
PS78/239-6	06.09.11	00:21	GF PUMPE	in the water	84° 4.45' N	164° 13.18' W	1978,7
PS78/239-6	06.09.11	00:27	GF PUMPE	on ground/ max depth	84° 4.45' N	164° 13.24' W	1977,6
PS78/239-6	06.09.11	00:27	GF PUMPE	profile start	84° 4.45' N	164° 13.24' W	1977,6
PS78/239-5	06.09.11	01:00	CTD/RO	on ground/ max depth	84° 4.48' N	164° 13.50' W	1973,4
PS78/239-5	06.09.11	01:02	CTD/RO	hoisting	84° 4.49' N	164° 13.51' W	1972,3
PS78/239-5	06.09.11	01:48	CTD/RO	on deck	84° 4.54' N	164° 13.67' W	1968,5
PS78/239-6	06.09.11	01:53	GF PUMPE	profile end	84° 4.54' N	164° 13.67' W	1963,8
PS78/239-6	06.09.11	02:03	GF PUMPE	hoisting	84° 4.56' N	164° 13.67' W	1963,6

A.4 Stationsliste / station list PS 78

Station	Date	Time	Gear	Action	Position Lat	Position Lon	Water Depth [m]
PS78/239-7	06.09.11	02:07	MN	in the water	84° 4.56' N	164° 13.67' W	1965,7
PS78/239-6	06.09.11	02:12	GF PUMPE	on deck	84° 4.57' N	164° 13.66' W	1964,8
PS78/239-7	06.09.11	03:11	MN	on ground/ max depth	84° 4.63' N	164° 13.43' W	1958,8
PS78/239-7	06.09.11	03:12	MN	hoisting	84° 4.63' N	164° 13.43' W	1960,4
PS78/239-7	06.09.11	04:16	MN	at surface	84° 4.67' N	164° 12.83' W	1959,1
PS78/239-7	06.09.11	04:21	MN	on deck	84° 4.67' N	164° 12.78' W	1959,5
PS78/239-8	06.09.11	04:30	BONGO	in the water	84° 4.67' N	164° 12.68' W	1958,4
PS78/239-8	06.09.11	04:43	BONGO	on ground/ max depth	84° 4.68' N	164° 12.53' W	1962
PS78/239-8	06.09.11	04:52	BONGO	at surface	84° 4.68' N	164° 12.42' W	1962,5
PS78/239-8	06.09.11	04:55	BONGO	on deck	84° 4.68' N	164° 12.39' W	1962,1
PS78/239-1	06.09.11	12:45	ICE	on ground/ max depth	84° 4.33' N	164° 11.14' W	2052,8
PS78/239-1	06.09.11	12:45	ICE	on deck	84° 4.33' N	164° 11.14' W	2052,8
PS78/240-1	06.09.11	20:07	CTD/RO	in the water	84° 10.99' N	168° 20.04' W	2490,8
PS78/240-1	06.09.11	21:02	CTD/RO	on ground/ max depth	84° 10.83' N	168° 20.33' W	2489,4
PS78/240-1	06.09.11	21:02	CTD/RO	hoisting	84° 10.83' N	168° 20.33' W	2489,4
PS78/240-1	06.09.11	22:01	CTD/RO	on deck	84° 10.65' N	168° 20.69' W	2487,6
PS78/240-2	07.09.11	01:14	XCTD	in the water	84° 17.02' N	170° 28.82' W	1652,2
PS78/240-2	07.09.11	01:16	XCTD	on ground/ max depth	84° 17.01' N	170° 28.80' W	1653,1
PS78/240-3	07.09.11	01:18	XCTD	in the water	84° 17.01' N	170° 28.78' W	1652,3
PS78/240-3	07.09.11	01:23	XCTD	on ground/ max depth	84° 17.00' N	170° 28.73' W	1652,7
PS78/241-1	07.09.11	05:49	CTD	in the water	84° 23.11' N	172° 21.37' W	1657,9
PS78/241-2	07.09.11	06:02	GF PUMPE	in the water	84° 23.07' N	172° 20.94' W	1651,4
PS78/241-2	07.09.11	06:16	GF PUMPE	profile start	84° 23.02' N	172° 20.47' W	1648,4
PS78/241-2	07.09.11	06:17	GF PUMPE	profile end	84° 23.02' N	172° 20.44' W	1648,1
PS78/241-2	07.09.11	06:17	GF PUMPE	on deck	84° 23.02' N	172° 20.44' W	1648,1
PS78/241-1	07.09.11	06:25	CTD	on ground/ max depth	84° 22.98' N	172° 20.15' W	1643,1
PS78/241-1	07.09.11	07:04	CTD	on deck	84° 22.83' N	172° 18.86' W	1633

A.4 Stationsliste / station list PS 78

Station	Date	Time	Gear	Action	Position Lat	Position Lon	Water Depth [m]
PS78/241-3	07.09.11	07:15	GC	in the water	84° 22.78' N	172° 18.53' W	1631,9
PS78/241-3	07.09.11	07:37	GC	on ground/ max depth	84° 22.69' N	172° 17.90' W	1625,3
PS78/241-3	07.09.11	07:38	GC	hoisting	84° 22.69' N	172° 17.88' W	1624,6
PS78/241-3	07.09.11	08:03	GC	on deck	84° 22.59' N	172° 17.21' W	1619,8
PS78/241-4	07.09.11	08:16	BC	in the water	84° 22.53' N	172° 16.89' W	1613
PS78/241-4	07.09.11	08:41	BC	on ground/ max depth	84° 22.44' N	172° 16.31' W	1602,9
PS78/241-4	07.09.11	08:42	BC	hoisting	84° 22.43' N	172° 16.29' W	1604,6
PS78/241-4	07.09.11	09:06	BC	on deck	84° 22.34' N	172° 15.78' W	1594
PS78/241-5	07.09.11	11:43	XCTD	in the water	84° 25.81' N	174° 0.28' W	2025,7
PS78/241-5	07.09.11	11:45	XCTD	on ground/ max depth	84° 25.80' N	174° 0.21' W	2023,9
PS78/241-6	07.09.11	11:46	XCTD	in the water	84° 25.80' N	174° 0.18' W	2026,5
PS78/241-6	07.09.11	11:49	XCTD	on ground/ max depth	84° 25.79' N	174° 0.09' W	2026,2
PS78/242-1	07.09.11	16:54	CTD/RO	in the water	84° 33.84' N	177° 30.32' W	1873,3
PS78/242-2	07.09.11	17:03	RAMSES	in the water	84° 33.81' N	177° 29.75' W	1873,4
PS78/242-1	07.09.11	17:34	CTD/RO	on ground/ max depth	84° 33.71' N	177° 28.09' W	1872,8
PS78/242-1	07.09.11	17:36	CTD/RO	hoisting	84° 33.71' N	177° 27.98' W	1872,7
PS78/242-2	07.09.11	17:39	RAMSES	on ground/ max depth	84° 33.70' N	177° 27.81' W	1872,9
PS78/242-2	07.09.11	17:40	RAMSES	hoisting	84° 33.70' N	177° 27.76' W	1871,6
PS78/242-2	07.09.11	17:45	RAMSES	at surface	84° 33.68' N	177° 27.48' W	1872,6
PS78/242-2	07.09.11	17:46	RAMSES	on deck	84° 33.68' N	177° 27.43' W	1873,3
PS78/242-3	07.09.11	17:51	GF PUMPE	in the water	84° 33.66' N	177° 27.15' W	1873,4
PS78/242-3	07.09.11	17:52	GF PUMPE	profile start	84° 33.66' N	177° 27.09' W	1873,7
PS78/242-3	07.09.11	18:03	GF PUMPE	profile end	84° 33.62' N	177° 26.50' W	1872,3
PS78/242-3	07.09.11	18:03	GF PUMPE	on deck	84° 33.62' N	177° 26.50' W	1872,3
PS78/242-1	07.09.11	18:22	CTD/RO	on deck	84° 33.57' N	177° 25.50' W	1873,1
PS78/242-4	07.09.11	21:34	XCTD	in the water	84° 37.07' N	179° 39.25' W	2177,3
PS78/242-4	07.09.11	21:38	XCTD	on ground/ max depth	84° 37.10' N	179° 39.47' W	2177,3
PS78/243-1	08.09.11	00:53	CTD/RO	in the water	84° 42.28' N	177° 19.11' E	2462,6

A.4 Stationsliste / station list PS 78

Station	Date	Time	Gear	Action	Position Lat	Position Lon	Water Depth [m]
PS78/243-2	08.09.11	00:57	GF PUMPE	in the water	84° 42.28' N	177° 19.41' E	2457,6
PS78/243-2	08.09.11	00:57	GF PUMPE	profile start	84° 42.28' N	177° 19.41' E	2457,6
PS78/243-2	08.09.11	01:09	GF PUMPE	profile end	84° 42.26' N	177° 20.22' E	2454,1
PS78/243-2	08.09.11	01:10	GF PUMPE	on deck	84° 42.26' N	177° 20.29' E	2452,8
PS78/243-1	08.09.11	01:12	CTD/RO	on ground/ max depth	84° 42.26' N	177° 20.42' E	2451,5
PS78/243-1	08.09.11	01:26	CTD/RO	on deck	84° 42.23' N	177° 21.44' E	2444,2
PS78/243-4	08.09.11	01:57	CTD/RO	in the water	84° 42.17' N	177° 23.03' E	2436,4
PS78/243-4	08.09.11	02:49	CTD/RO	on ground/ max depth	84° 42.11' N	177° 26.93' E	2410,5
PS78/243-4	08.09.11	02:50	CTD/RO	hoisting	84° 42.11' N	177° 27.00' E	2409,8
PS78/243-4	08.09.11	03:39	CTD/RO	at surface	84° 42.08' N	177° 30.83' E	2385,2
PS78/243-4	08.09.11	03:40	CTD/RO	on deck	84° 42.07' N	177° 30.90' E	2385,5
PS78/243-3	08.09.11	07:42	XCTD	in the water	84° 45.44' N	174° 0.88' E	3032,2
PS78/243-3	08.09.11	07:47	XCTD	on ground/ max depth	84° 45.52' N	174° 0.71' E	3028,3
PS78/244-1	08.09.11	10:08	CTD/RO	in the water	84° 46.80' N	172° 38.78' E	3231,8
PS78/244-2	08.09.11	10:33	GF PUMPE	in the water	84° 46.78' N	172° 41.06' E	3231,1
PS78/244-2	08.09.11	10:35	GF PUMPE	on ground/ max depth	84° 46.78' N	172° 41.24' E	3230,6
PS78/244-2	08.09.11	10:35	GF PUMPE	profile start	84° 46.78' N	172° 41.24' E	3230,6
PS78/244-2	08.09.11	10:48	GF PUMPE	profile end	84° 46.77' N	172° 42.42' E	3225,2
PS78/244-2	08.09.11	10:48	GF PUMPE	on deck	84° 46.77' N	172° 42.42' E	3225,2
PS78/244-1	08.09.11	11:14	CTD/RO	on ground/ max depth	84° 46.74' N	172° 44.81' E	3224,4
PS78/244-1	08.09.11	11:15	CTD/RO	hoisting	84° 46.74' N	172° 44.90' E	3227,6
PS78/244-1	08.09.11	12:24	CTD/RO	on deck	84° 46.69' N	172° 51.36' E	3179,2
PS78/244-3	08.09.11	18:48	XCTD	in the water	84° 49.10' N	168° 26.08' E	3381,5
PS78/244-3	08.09.11	18:54	XCTD	on ground/ max depth	84° 49.06' N	168° 25.86' E	3382,3
PS78/245-1	08.09.11	21:45	ICE	in the water	84° 47.68' N	166° 25.46' E	3373,8
PS78/245-2	08.09.11	22:04	CTD/RO	in the water	84° 47.67' N	166° 25.07' E	3373,8
PS78/245-2	08.09.11	22:15	CTD/RO	on ground/ max depth	84° 47.67' N	166° 24.88' E	3376,1
PS78/245-2	08.09.11	22:16	CTD/RO	hoisting	84° 47.67' N	166° 24.86' E	3377,7
PS78/245-2	08.09.11	22:27	CTD/RO	on deck	84° 47.68' N	166° 24.69' E	3379,1
PS78/245-3	08.09.11	22:38	MUWS	in the water	84° 47.69' N	166° 24.54' E	3377,4
PS78/245-3	08.09.11	22:40	MUWS	on ground/ max depth	84° 47.70' N	166° 24.52' E	3379,1
PS78/245-3	08.09.11	22:40	MUWS	profile start	84° 47.70' N	166° 24.52' E	3379,1
PS78/245-3	08.09.11	22:41	MUWS	hoisting	84° 47.70' N	166° 24.51' E	3379,4
PS78/245-3	08.09.11	22:48	MUWS	profile end	84° 47.71' N	166° 24.44' E	3377,1
PS78/245-3	08.09.11	22:49	MUWS	on deck	84° 47.71' N	166° 24.43' E	3378,3
PS78/245-4	08.09.11	22:56	RAMSES	in the water	84° 47.72' N	166° 24.38' E	3375

A.4 Stationsliste / station list PS 78

Station	Date	Time	Gear	Action	Position Lat	Position Lon	Water Depth [m]
PS78/245-4	08.09.11	23:27	RAMSES	on ground/ max depth	84° 47.79' N	166° 24.39' E	3374,8
PS78/245-4	08.09.11	23:27	RAMSES	hoisting	84° 47.79' N	166° 24.39' E	3374,8
PS78/245-4	08.09.11	23:28	RAMSES	off ground	84° 47.79' N	166° 24.40' E	3374,4
PS78/245-4	08.09.11	23:37	RAMSES	on deck	84° 47.81' N	166° 24.48' E	3373,1
PS78/245-6	08.09.11	23:51	GF PUMPE	in the water	84° 47.84' N	166° 24.66' E	3372,8
PS78/245-6	08.09.11	23:55	GF PUMPE	on ground/ max depth	84° 47.85' N	166° 24.74' E	3373,1
PS78/245-6	08.09.11	23:55	GF PUMPE	profile start	84° 47.85' N	166° 24.74' E	3373,1
PS78/245-5	09.09.11	00:04	CTD/RO	in the water	84° 47.87' N	166° 24.92' E	3372,4
PS78/245-6	09.09.11	01:07	GF PUMPE	profile end	84° 47.99' N	166° 26.77' E	3372,7
PS78/245-6	09.09.11	01:07	GF PUMPE	hoisting	84° 47.99' N	166° 26.77' E	3372,7
PS78/245-6	09.09.11	01:19	GF PUMPE	on deck	84° 48.00' N	166° 27.21' E	3373,7
PS78/245-5	09.09.11	01:44	CTD/RO	on ground/ max depth	84° 48.01' N	166° 28.07' E	3377,7
PS78/245-5	09.09.11	01:45	CTD/RO	hoisting	84° 48.01' N	166° 28.10' E	3374,9
PS78/245-5	09.09.11	02:54	CTD/RO	at surface	84° 48.02' N	166° 29.82' E	3376,6
PS78/245-5	09.09.11	02:56	CTD/RO	on deck	84° 48.02' N	166° 29.88' E	3374,5
PS78/245-7	09.09.11	03:08	MN	in the water	84° 48.03' N	166° 30.18' E	3372,6
PS78/245-7	09.09.11	05:02	MN	on ground/ max depth	84° 48.11' N	166° 31.22' E	3375,5
PS78/245-7	09.09.11	05:02	MN	hoisting	84° 48.11' N	166° 31.22' E	3375,5
PS78/245-7	09.09.11	06:55	MN	on deck	84° 48.32' N	166° 28.17' E	3372,9
PS78/245-8	09.09.11	07:02	BONGO	in the water	84° 48.33' N	166° 27.82' E	3375,1
PS78/245-8	09.09.11	07:18	BONGO	on ground/ max depth	84° 48.36' N	166° 26.95' E	3370,7
PS78/245-8	09.09.11	07:23	BONGO	hoisting	84° 48.36' N	166° 26.66' E	3371,8
PS78/245-8	09.09.11	07:41	BONGO	on deck	84° 48.40' N	166° 25.58' E	3376,1
PS78/245-9	09.09.11	07:48	MUWS	in the water	84° 48.41' N	166° 25.14' E	3371,2
PS78/245-9	09.09.11	07:49	MUWS	profile start	84° 48.41' N	166° 25.08' E	3373,2
PS78/245-9	09.09.11	07:54	MUWS	profile end	84° 48.42' N	166° 24.76' E	3374,7
PS78/245-9	09.09.11	07:55	MUWS	on deck	84° 48.42' N	166° 24.70' E	3372,2
PS78/245-10	09.09.11	08:31	RAMSES	in the water	84° 48.51' N	166° 22.30' E	3374,2
PS78/245-10	09.09.11	09:00	RAMSES	on ground/ max depth	84° 48.59' N	166° 20.19' E	3370,9
PS78/245-10	09.09.11	09:01	RAMSES	hoisting	84° 48.59' N	166° 20.11' E	3372,9
PS78/245-10	09.09.11	09:08	RAMSES	on deck	84° 48.61' N	166° 19.58' E	3369,9
PS78/245-1	09.09.11	10:31	ICE	on ground/ max depth	84° 48.80' N	166° 12.99' E	3369,7
PS78/245-1	09.09.11	10:31	ICE	on deck	84° 48.80' N	166° 12.99' E	3369,7
PS78/246-1	09.09.11	17:31	CTD	in the water	84° 49.37' N	161° 2.22' E	3497,7
PS78/246-2	09.09.11	17:34	GF PUMPE	in the water	84° 49.35' N	161° 2.11' E	3496,7

A.4 Stationsliste / station list PS 78

Station	Date	Time	Gear	Action	Position Lat	Position Lon	Water Depth [m]
PS78/246-2	09.09.11	17:35	GF PUMPE	profile start	84° 49.34' N	161° 2.07' E	3497,1
PS78/246-2	09.09.11	17:49	GF PUMPE	profile end	84° 49.24' N	161° 1.56' E	3500,2
PS78/246-2	09.09.11	17:50	GF PUMPE	on deck	84° 49.23' N	161° 1.53' E	3499,3
PS78/246-1	09.09.11	18:40	CTD	on ground/ max depth	84° 48.83' N	160° 59.77' E	3496,6
PS78/246-1	09.09.11	18:40	CTD	hoisting	84° 48.83' N	160° 59.77' E	3496,6
PS78/246-1	09.09.11	19:52	CTD	on deck	84° 48.23' N	160° 57.57' E	3498,6
PS78/246-3	09.09.11	22:30	XCTD	in the water	84° 49.89' N	158° 29.45' E	2870,2
PS78/246-3	09.09.11	22:33	XCTD	on ground/ max depth	84° 49.86' N	158° 29.37' E	2883,4
PS78/247-1	10.09.11	01:39	CTD/RO	in the water	84° 46.39' N	155° 42.97' E	2376,5
PS78/247-2	10.09.11	01:42	GF PUMPE	in the water	84° 46.36' N	155° 42.96' E	2374,3
PS78/247-2	10.09.11	01:43	GF PUMPE	profile start	84° 46.35' N	155° 42.94' E	2372,4
PS78/247-2	10.09.11	01:57	GF PUMPE	profile end	84° 46.22' N	155° 42.57' E	2370,9
PS78/247-2	10.09.11	01:58	GF PUMPE	on deck	84° 46.21' N	155° 42.54' E	2367,4
PS78/247-1	10.09.11	02:28	CTD/RO	on ground/ max depth	84° 45.93' N	155° 41.70' E	2353,2
PS78/247-1	10.09.11	02:30	CTD/RO	hoisting	84° 45.91' N	155° 41.65' E	2351,2
PS78/247-1	10.09.11	03:17	CTD/RO	at surface	84° 45.45' N	155° 40.33' E	2322,5
PS78/247-1	10.09.11	03:18	CTD/RO	on deck	84° 45.44' N	155° 40.30' E	2322
PS78/247-3	10.09.11	03:36	MN	in the water	84° 45.26' N	155° 39.81' E	2312,9
PS78/247-3	10.09.11	04:48	MN	on ground/ max depth	84° 44.52' N	155° 36.71' E	2212,3
PS78/247-3	10.09.11	04:48	MN	hoisting	84° 44.52' N	155° 36.71' E	2212,3
PS78/247-3	10.09.11	06:02	MN	on deck	84° 43.75' N	155° 31.57' E	2179,8
PS78/247-4	10.09.11	09:01	XCTD	in the water	84° 42.44' N	152° 54.41' E	1932,9
PS78/247-4	10.09.11	09:12	XCTD	on ground/ max depth	84° 42.41' N	152° 50.49' E	1929,4
PS78/247-5	10.09.11	12:04	BUOY	information	84° 41.51' N	150° 12.40' E	1616,9
PS78/247-5	10.09.11	12:13	BUOY	information	84° 41.44' N	150° 11.48' E	1616,8
PS78/247-5	10.09.11	12:18	BUOY	on ground/ max depth	84° 41.39' N	150° 10.98' E	1615,6
PS78/247-5	10.09.11	12:18	BUOY	on deck	84° 41.39' N	150° 10.98' E	1615,6
PS78/248-1	10.09.11	12:56	CTD/RO	in the water	84° 41.55' N	150° 10.00' E	1616,7
PS78/248-2	10.09.11	13:12	RAMSES	in the water	84° 41.40' N	150° 8.53' E	1616
PS78/248-1	10.09.11	13:33	CTD/RO	on ground/ max depth	84° 41.28' N	150° 6.39' E	1609,9
PS78/248-2	10.09.11	13:34	RAMSES	on ground/ max depth	84° 41.27' N	150° 6.29' E	1612,3
PS78/248-1	10.09.11	13:35	CTD/RO	hoisting	84° 41.26' N	150° 6.20' E	1610,9
PS78/248-2	10.09.11	13:40	RAMSES	on deck	84° 41.23' N	150° 5.76' E	1609,3
PS78/248-3	10.09.11	13:49	GF PUMPE	in the water	84° 41.15' N	150° 4.98' E	1607,7
PS78/248-3	10.09.11	13:52	GF PUMPE	profile start	84° 41.14' N	150° 4.69' E	1608
PS78/248-3	10.09.11	13:52	GF PUMPE	on ground/ max depth	84° 41.14' N	150° 4.69' E	1608

A.4 Stationsliste / station list PS 78

Station	Date	Time	Gear	Action	Position Lat	Position Lon	Water Depth [m]
PS78/248-3	10.09.11	14:02	GF PUMPE	profile end	84° 41.07' N	150° 3.78' E	1605,8
PS78/248-3	10.09.11	14:02	GF PUMPE	hoisting	84° 41.07' N	150° 3.78' E	1605,8
PS78/248-3	10.09.11	14:02	GF PUMPE	on deck	84° 41.07' N	150° 3.78' E	1605,8
PS78/248-1	10.09.11	14:13	CTD/RO	at surface	84° 40.99' N	150° 2.80' E	1606,9
PS78/248-1	10.09.11	14:14	CTD/RO	on deck	84° 40.98' N	150° 2.71' E	1606,8
PS78/248-4	10.09.11	14:20	MUC	in the water	84° 40.94' N	150° 2.18' E	1607,3
PS78/248-4	10.09.11	14:51	MUC	on ground/ max depth	84° 40.75' N	149° 59.41' E	1611,4
PS78/248-4	10.09.11	14:52	MUC	hoisting	84° 40.75' N	149° 59.33' E	1610,5
PS78/248-4	10.09.11	15:11	MUC	at surface	84° 40.64' N	149° 57.66' E	1614,5
PS78/248-4	10.09.11	15:15	MUC	on deck	84° 40.62' N	149° 57.32' E	1613,8
PS78/248-5	10.09.11	15:26	MUC	in the water	84° 40.57' N	149° 56.33' E	1611,8
PS78/248-5	10.09.11	15:50	MUC	on ground/ max depth	84° 40.49' N	149° 53.98' E	1606,2
PS78/248-5	10.09.11	15:51	MUC	hoisting	84° 40.48' N	149° 53.88' E	1607,4
PS78/248-5	10.09.11	16:11	MUC	on deck	84° 40.44' N	149° 51.90' E	1606,4
PS78/248-6	10.09.11	16:37	GC	in the water	84° 40.39' N	149° 49.48' E	1613,6
PS78/248-6	10.09.11	16:57	GC	on ground/ max depth	84° 40.37' N	149° 47.79' E	1619,8
PS78/248-6	10.09.11	16:57	GC	hoisting	84° 40.37' N	149° 47.79' E	1619,8
PS78/248-6	10.09.11	17:17	GC	at surface	84° 40.36' N	149° 46.05' E	1626
PS78/248-6	10.09.11	17:20	GC	on deck	84° 40.37' N	149° 45.81' E	1625,1
PS78/248-7	10.09.11	20:10	XCTD	in the water	84° 35.87' N	147° 40.08' E	2522,4
PS78/248-7	10.09.11	20:15	XCTD	on ground/ max depth	84° 35.83' N	147° 37.47' E	2528,6
PS78/249-1	10.09.11	23:00	CTD/RO	in the water	84° 32.28' N	145° 1.61' E	2046,1
PS78/249-2	10.09.11	23:05	GF PUMPE	in the water	84° 32.24' N	145° 1.05' E	2029,6
PS78/249-2	10.09.11	23:13	GF PUMPE	on ground/ max depth	84° 32.18' N	144° 59.87' E	1913
PS78/249-2	10.09.11	23:14	GF PUMPE	profile start	84° 32.17' N	144° 59.64' E	1903
PS78/249-2	10.09.11	23:21	GF PUMPE	hoisting	84° 32.14' N	144° 58.72' E	1848,7
PS78/249-2	10.09.11	23:21	GF PUMPE	profile end	84° 32.14' N	144° 58.72' E	1848,7
PS78/249-2	10.09.11	23:21	GF PUMPE	on deck	84° 32.14' N	144° 58.72' E	1848,7
PS78/249-1	10.09.11	23:42	CTD/RO	on ground/ max depth	84° 31.96' N	144° 57.01' E	1818,8
PS78/249-1	10.09.11	23:42	CTD/RO	hoisting	84° 31.96' N	144° 57.01' E	1818,8
PS78/249-1	11.09.11	00:29	CTD/RO	on deck	84° 31.67' N	144° 52.73' E	1944,6
PS78/249-3	11.09.11	00:38	MN	in the water	84° 31.58' N	144° 52.25' E	1977,3
PS78/249-3	11.09.11	01:39	MN	on ground/ max depth	84° 31.22' N	144° 46.96' E	2049
PS78/249-3	11.09.11	01:39	MN	hoisting	84° 31.22' N	144° 46.96' E	2049
PS78/249-3	11.09.11	02:43	MN	at surface	84° 30.98' N	144° 43.25' E	2170,2
PS78/249-3	11.09.11	02:47	MN	on deck	84° 30.94' N	144° 43.11' E	2182,4
PS78/249-4	11.09.11	04:59	XCTD	in the water	84° 26.64' N	143° 2.34' E	2978,4

A.4 Stationsliste / station list PS 78

Station	Date	Time	Gear	Action	Position Lat	Position Lon	Water Depth [m]
PS78/249-4	11.09.11	05:00	XCTD	on ground/ max depth	84° 26.61' N	143° 1.60' E	3007,4
PS78/249-4	11.09.11	05:04	XCTD	on deck	84° 26.50' N	142° 59.03' E	2993,6
PS78/250-1	11.09.11	10:00	ICE	in the water	84° 23.61' N	139° 56.04' E	3674,3
PS78/250-2	11.09.11	10:39	CTD/RO	in the water	84° 23.18' N	139° 54.75' E	3674,3
PS78/250-2	11.09.11	10:48	CTD/RO	on ground/ max depth	84° 23.10' N	139° 54.60' E	3674,1
PS78/250-3	11.09.11	10:48	RAMSES	in the water	84° 23.10' N	139° 54.60' E	3674,1
PS78/250-2	11.09.11	10:49	CTD/RO	hoisting	84° 23.09' N	139° 54.59' E	3675,3
PS78/250-2	11.09.11	11:01	CTD/RO	on deck	84° 22.96' N	139° 54.35' E	3676,6
PS78/250-3	11.09.11	11:21	RAMSES	on ground/ max depth	84° 22.82' N	139° 53.59' E	3674,2
PS78/250-3	11.09.11	11:21	RAMSES	hoisting	84° 22.82' N	139° 53.59' E	3674,2
PS78/250-3	11.09.11	11:26	RAMSES	on deck	84° 22.79' N	139° 53.34' E	3673,7
PS78/250-4	11.09.11	11:41	MUWS	in the water	84° 22.71' N	139° 52.80' E	3678,4
PS78/250-4	11.09.11	11:41	MUWS	profile start	84° 22.71' N	139° 52.80' E	3678,4
PS78/250-4	11.09.11	11:49	MUWS	on ground/ max depth	84° 22.66' N	139° 52.62' E	3675,4
PS78/250-4	11.09.11	11:49	MUWS	hoisting	84° 22.66' N	139° 52.62' E	3675,4
PS78/250-4	11.09.11	11:54	MUWS	on deck	84° 22.63' N	139° 52.51' E	3674,5
PS78/250-4	11.09.11	11:54	MUWS	profile end	84° 22.63' N	139° 52.51' E	3674,5
PS78/250-5	11.09.11	12:36	CTD/RO	in the water	84° 22.48' N	139° 50.85' E	3674,3
PS78/250-6	11.09.11	12:45	GF PUMPE	in the water	84° 22.46' N	139° 50.37' E	3673,3
PS78/250-6	11.09.11	12:47	GF PUMPE	on ground/ max depth	84° 22.45' N	139° 50.27' E	3672,8
PS78/250-6	11.09.11	12:47	GF PUMPE	profile start	84° 22.45' N	139° 50.27' E	3672,8
PS78/250-6	11.09.11	12:57	GF PUMPE	profile end	84° 22.43' N	139° 49.71' E	3673
PS78/250-6	11.09.11	12:57	GF PUMPE	hoisting	84° 22.43' N	139° 49.71' E	3673
PS78/250-6	11.09.11	12:57	GF PUMPE	on deck	84° 22.43' N	139° 49.71' E	3673
PS78/250-5	11.09.11	13:50	CTD/RO	on ground/ max depth	84° 22.33' N	139° 47.20' E	3672,2
PS78/250-5	11.09.11	13:51	CTD/RO	hoisting	84° 22.33' N	139° 47.17' E	3670,8
PS78/250-5	11.09.11	15:04	CTD/RO	at surface	84° 22.32' N	139° 46.72' E	3673,1
PS78/250-5	11.09.11	15:07	CTD/RO	on deck	84° 22.32' N	139° 46.76' E	3673,7
PS78/250-7	11.09.11	15:18	MN	in the water	84° 22.33' N	139° 46.93' E	3671,7
PS78/250-7	11.09.11	17:15	MN	on ground/ max depth	84° 22.21' N	139° 49.73' E	3674,5
PS78/250-7	11.09.11	17:16	MN	hoisting	84° 22.20' N	139° 49.77' E	3675,8
PS78/250-1	11.09.11	18:25	ICE	on ground/ max depth	84° 21.95' N	139° 52.59' E	3681,8
PS78/250-7	11.09.11	19:22	MN	on deck	84° 21.74' N	139° 55.63' E	3686,9
PS78/250-8	11.09.11	22:12	XCTD	in the water	84° 14.55' N	138° 25.23' E	3934,6
PS78/250-8	11.09.11	22:18	XCTD	on ground/ max depth	84° 14.52' N	138° 25.03' E	3933
PS78/251-1	12.09.11	02:17	CTD/RO	in the water	84° 8.93' N	135° 53.09' E	4224,1

A.4 Stationsliste / station list PS 78

Station	Date	Time	Gear	Action	Position Lat	Position Lon	Water Depth [m]
PS78/251-2	12.09.11	02:20	GF PUMPE	in the water	84° 8.95' N	135° 53.05' E	4223
PS78/251-2	12.09.11	02:21	GF PUMPE	profile start	84° 8.95' N	135° 53.04' E	4222,6
PS78/251-2	12.09.11	02:32	GF PUMPE	profile end	84° 8.99' N	135° 52.88' E	4224,8
PS78/251-2	12.09.11	02:33	GF PUMPE	on deck	84° 8.99' N	135° 52.87' E	4221,1
PS78/251-1	12.09.11	03:37	CTD/RO	on ground/ max depth	84° 9.25' N	135° 52.93' E	4221,3
PS78/251-1	12.09.11	03:39	CTD/RO	hoisting	84° 9.25' N	135° 52.96' E	4226
PS78/251-1	12.09.11	04:50	CTD/RO	at surface	84° 9.48' N	135° 54.66' E	4230,7
PS78/251-1	12.09.11	04:51	CTD/RO	on deck	84° 9.49' N	135° 54.69' E	4224,8
PS78/251-3	12.09.11	08:11	XCTD	in the water	84° 0.61' N	133° 37.26' E	4248,9
PS78/251-3	12.09.11	08:17	XCTD	on ground/ max depth	84° 0.55' N	133° 37.46' E	4251
PS78/252-1	12.09.11	10:31	CTD/RO	in the water	83° 53.94' N	131° 48.19' E	4255,6
PS78/252-2	12.09.11	10:50	GF PUMPE	in the water	83° 53.66' N	131° 47.51' E	4259,8
PS78/252-2	12.09.11	10:50	GF PUMPE	profile start	83° 53.66' N	131° 47.51' E	4259,8
PS78/252-2	12.09.11	11:04	GF PUMPE	profile end	83° 53.46' N	131° 46.65' E	4257,7
PS78/252-2	12.09.11	11:04	GF PUMPE	on deck	83° 53.46' N	131° 46.65' E	4257,7
PS78/252-3	12.09.11	11:37	RAMSES	in the water	83° 53.01' N	131° 43.96' E	4261,1
PS78/252-1	12.09.11	11:59	CTD/RO	on ground/ max depth	83° 52.72' N	131° 41.76' E	4256,7
PS78/252-1	12.09.11	12:00	CTD/RO	hoisting	83° 52.71' N	131° 41.63' E	4258,7
PS78/252-3	12.09.11	12:00	RAMSES	on ground/ max depth	83° 52.71' N	131° 41.63' E	4258,7
PS78/252-3	12.09.11	12:06	RAMSES	on deck	83° 52.64' N	131° 40.89' E	4257,3
PS78/252-1	12.09.11	13:28	CTD/RO	on deck	83° 52.13' N	131° 29.77' E	4259,6
PS78/252-4	12.09.11	13:40	BUOY	information	83° 52.21' N	131° 28.71' E	4260
PS78/252-4	12.09.11	13:42	BUOY	on ground/ max depth	83° 52.22' N	131° 28.49' E	4260,1
PS78/252-4	12.09.11	13:42	BUOY	on deck	83° 52.22' N	131° 28.49' E	4260,1
PS78/253-1	12.09.11	18:05	CTD/RO	in the water	53° 37.21' N	128° 11.06' E	4261,8
PS78/253-2	12.09.11	18:18	GF PUMPE	in the water	83° 37.30' N	128° 11.99' E	4260,8
PS78/253-2	12.09.11	18:19	GF PUMPE	profile start	83° 37.31' N	128° 12.06' E	4257,6
PS78/253-2	12.09.11	18:32	GF PUMPE	on deck	83° 37.38' N	128° 13.04' E	4258,4
PS78/253-2	12.09.11	18:33	GF PUMPE	profile end	83° 37.39' N	128° 13.12' E	4257,5
PS78/253-1	12.09.11	19:29	CTD/RO	on ground/ max depth	83° 37.54' N	128° 17.70' E	4256,4
PS78/253-1	12.09.11	19:29	CTD/RO	hoisting	83° 37.54' N	128° 17.70' E	4256,4
PS78/253-3	12.09.11	20:55	TEST	in the water	83° 37.23' N	128° 23.85' E	4256
PS78/253-1	12.09.11	21:02	CTD/RO	on deck	83° 37.18' N	128° 24.16' E	4253,1
PS78/253-3	12.09.11	21:11	TEST	hoisting	83° 37.11' N	128° 24.51' E	4254,4
PS78/253-3	12.09.11	21:13	TEST	on ground/ max depth	83° 37.09' N	128° 24.58' E	4253,5
PS78/253-3	12.09.11	21:13	TEST	on deck	83° 37.09' N	128° 24.58' E	4253,5
PS78/253-4	12.09.11	23:03	XCTD	in the water	83° 29.73' N	127° 2.05' E	4251,6

A.4 Stationsliste / station list PS 78

Station	Date	Time	Gear	Action	Position Lat	Position Lon	Water Depth [m]
PS78/253-4	12.09.11	23:08	XCTD	on ground/ max depth	83° 29.47' N	126° 59.75' E	4247,2
PS78/254-1	13.09.11	01:55	CTD/RO	in the water	83° 19.25' N	125° 9.99' E	4243,4
PS78/254-1	13.09.11	03:19	CTD/RO	on ground/ max depth	83° 19.72' N	125° 5.32' E	4242,8
PS78/254-1	13.09.11	03:21	CTD/RO	hoisting	83° 19.74' N	125° 5.23' E	4246,1
PS78/254-1	13.09.11	04:35	CTD/RO	at surface	83° 20.50' N	125° 4.53' E	4245,8
PS78/254-1	13.09.11	04:36	CTD/RO	on deck	83° 20.52' N	125° 4.55' E	4245,7
PS78/254-2	13.09.11	04:44	MOR	in the water	83° 20.62' N	125° 4.77' E	4246,9
PS78/254-2	13.09.11	05:22	MOR	in the water	83° 21.10' N	125° 5.96' E	4249,8
PS78/254-2	13.09.11	06:02	MOR	in the water	83° 21.58' N	125° 7.65' E	4248,6
PS78/254-2	13.09.11	07:37	MOR	in the water	83° 22.11' N	125° 13.48' E	4248,5
PS78/254-2	13.09.11	07:53	MOR	in the water	83° 22.11' N	125° 14.31' E	4249,3
PS78/254-2	13.09.11	08:09	MOR	in the water	83° 22.10' N	125° 15.13' E	4248,9
PS78/254-2	13.09.11	08:12	MOR	in the water	83° 22.11' N	125° 15.30' E	4250,9
PS78/254-2	13.09.11	08:21	MOR	in the water	83° 22.11' N	125° 15.72' E	4250,1
PS78/254-2	13.09.11	08:22	MOR	lowering	83° 22.10' N	125° 15.78' E	4249,5
PS78/254-2	13.09.11	08:25	MOR	on ground/ max depth	83° 22.10' N	125° 15.87' E	4250,6
PS78/255-1	13.09.11	09:56	MOR	in the water	83° 16.78' N	125° 0.89' E	4245,2
PS78/255-1	13.09.11	10:07	MOR	in the water	83° 16.73' N	125° 0.57' E	4239,8
PS78/255-1	13.09.11	10:11	MOR	in the water	83° 16.71' N	125° 0.48' E	4241,9
PS78/255-1	13.09.11	10:19	MOR	in the water	83° 16.67' N	125° 0.31' E	4244,2
PS78/255-1	13.09.11	10:20	MOR	lowering	83° 16.66' N	125° 0.27' E	4241,9
PS78/255-1	13.09.11	11:13	MOR	in the water	83° 16.42' N	124° 57.54' E	4248,1
PS78/255-1	13.09.11	11:56	MOR	in the water	83° 16.27' N	124° 54.19' E	4249
PS78/255-1	13.09.11	11:59	MOR	in the water	83° 16.26' N	124° 53.90' E	4248,4
PS78/255-1	13.09.11	12:31	MOR	in the water	83° 16.18' N	124° 50.73' E	4250,5
PS78/255-1	13.09.11	12:37	MOR	in the water	83° 16.17' N	124° 50.07' E	4254,2
PS78/255-1	13.09.11	12:41	MOR	in the water	83° 16.16' N	124° 49.63' E	4251,3
PS78/255-1	13.09.11	12:56	MOR	in the water	83° 16.16' N	124° 48.07' E	4252,7
PS78/255-1	13.09.11	13:08	MOR	in the water	83° 16.17' N	124° 46.97' E	4256,1
PS78/255-1	13.09.11	13:11	MOR	lowering	83° 16.20' N	124° 46.73' E	4255,8
PS78/255-1	13.09.11	13:13	MOR	on ground/ max depth	83° 16.22' N	124° 46.47' E	4257,8
PS78/255-1	13.09.11	13:13	MOR	information	83° 16.22' N	124° 46.47' E	4257,8
PS78/256-1	13.09.11	14:05	MOR	in the water	83° 16.58' N	124° 41.40' E	4259,9
PS78/256-1	13.09.11	14:14	MOR	in the water	83° 16.61' N	124° 40.25' E	4259,3
PS78/256-1	13.09.11	14:39	MOR	in the water	83° 16.73' N	124° 36.91' E	4271,3
PS78/256-1	13.09.11	15:56	MOR	in the water	83° 17.33' N	124° 28.68' E	4267,9
PS78/256-1	13.09.11	16:09	MOR	in the water	83° 17.47' N	124° 28.07' E	4266,1
PS78/256-1	13.09.11	16:13	MOR	in the water	83° 17.49' N	124° 27.81' E	4266,8

A.4 Stationsliste / station list PS 78

Station	Date	Time	Gear	Action	Position Lat	Position Lon	Water Depth [m]
PS78/256-1	13.09.11	16:14	MOR	on ground/ max depth	83° 17.49' N	124° 27.74' E	4263,3
PS78/256-1	13.09.11	16:15	MOR	on deck	83° 17.50' N	124° 27.67' E	4266,3
PS78/257-1	13.09.11	17:16	CTD/RO	in the water	83° 20.09' N	124° 54.54' E	4238,4
PS78/257-2	13.09.11	17:23	GF PUMPE	in the water	83° 20.17' N	124° 54.45' E	4226,1
PS78/257-1	13.09.11	17:25	CTD/RO	on ground/ max depth	83° 20.17' N	124° 54.28' E	4226,1
PS78/257-2	13.09.11	17:25	GF PUMPE	on ground/ max depth	83° 20.17' N	124° 54.28' E	4226,1
PS78/257-2	13.09.11	17:25	GF PUMPE	profile start	83° 20.17' N	124° 54.28' E	4226,1
PS78/257-1	13.09.11	17:27	CTD/RO	hoisting	83° 20.17' N	124° 54.09' E	4224,7
PS78/257-1	13.09.11	17:37	CTD/RO	at surface	83° 20.17' N	124° 53.30' E	4231,9
PS78/257-1	13.09.11	17:39	CTD/RO	on deck	83° 20.17' N	124° 53.19' E	4231,4
PS78/257-2	13.09.11	17:41	GF PUMPE	hoisting	83° 20.17' N	124° 53.08' E	4235,1
PS78/257-2	13.09.11	17:41	GF PUMPE	profile end	83° 20.17' N	124° 53.08' E	4235,1
PS78/257-2	13.09.11	17:43	GF PUMPE	on deck	83° 20.18' N	124° 52.98' E	4228,6
PS78/257-3	13.09.11	17:50	MUWS	in the water	83° 20.23' N	124° 52.91' E	4219,9
PS78/257-3	13.09.11	17:53	MUWS	on ground/ max depth	83° 20.26' N	124° 52.88' E	4227
PS78/257-3	13.09.11	17:53	MUWS	hoisting	83° 20.26' N	124° 52.88' E	4227
PS78/257-3	13.09.11	18:01	MUWS	profile end	83° 20.32' N	124° 52.77' E	4217,8
PS78/257-3	13.09.11	18:01	MUWS	profile start	83° 20.32' N	124° 52.77' E	4217,8
PS78/257-3	13.09.11	18:02	MUWS	on deck	83° 20.33' N	124° 52.80' E	4222,5
PS78/257-4	13.09.11	18:09	RAMSES	in the water	83° 20.36' N	124° 52.79' E	4213,7
PS78/257-4	13.09.11	18:42	RAMSES	hoisting	83° 20.47' N	124° 52.20' E	4213,4
PS78/257-4	13.09.11	18:51	RAMSES	on ground/ max depth	83° 20.48' N	124° 52.04' E	4214,3
PS78/257-4	13.09.11	18:51	RAMSES	on deck	83° 20.48' N	124° 52.04' E	4214,3
PS78/257-5	13.09.11	19:01	CTD/RO	in the water	83° 20.45' N	124° 52.16' E	4213,3
PS78/257-5	13.09.11	19:15	CTD/RO	on ground/ max depth	83° 20.48' N	124° 51.98' E	4218,8
PS78/257-5	13.09.11	19:16	CTD/RO	hoisting	83° 20.48' N	124° 51.96' E	4210,4
PS78/257-5	13.09.11	19:34	CTD/RO	on deck	83° 20.47' N	124° 51.61' E	4220,3
PS78/258-1	13.09.11	23:28	CTD/RO	in the water	83° 14.80' N	121° 32.23' E	3200,1
PS78/258-1	14.09.11	00:46	CTD/RO	on ground/ max depth	83° 14.22' N	121° 21.56' E	3618,2
PS78/258-1	14.09.11	00:47	CTD/RO	hoisting	83° 14.22' N	121° 21.42' E	3618,8
PS78/258-1	14.09.11	02:01	CTD/RO	at surface	83° 13.96' N	121° 10.47' E	3721,7
PS78/258-1	14.09.11	02:03	CTD/RO	on deck	83° 13.96' N	121° 10.20' E	3721,2
PS78/259-1	14.09.11	06:01	CTD/RO	in the water	83° 8.92' N	117° 59.57' E	3849,3
PS78/259-2	14.09.11	07:21	RAMSES	in the water	83° 9.02' N	117° 56.78' E	3836,8
PS78/259-1	14.09.11	07:23	CTD/RO	on ground/ max depth	83° 9.01' N	117° 56.78' E	3836,7
PS78/259-1	14.09.11	07:23	CTD/RO	hoisting	83° 9.01' N	117° 56.78' E	3836,7

A.4 Stationsliste / station list PS 78

Station	Date	Time	Gear	Action	Position Lat	Position Lon	Water Depth [m]
PS78/259-2	14.09.11	07:52	RAMSES	on ground/ max depth	83° 8.98' N	117° 56.19' E	3818
PS78/259-2	14.09.11	07:52	RAMSES	on deck	83° 8.98' N	117° 56.19' E	3818
PS78/259-3	14.09.11	07:57	GF PUMPE	in the water	83° 8.98' N	117° 56.10' E	3813,4
PS78/259-3	14.09.11	08:10	GF PUMPE	profile start	83° 8.96' N	117° 55.91' E	3803,8
PS78/259-3	14.09.11	08:11	GF PUMPE	profile end	83° 8.96' N	117° 55.91' E	3808,2
PS78/259-3	14.09.11	08:12	GF PUMPE	on deck	83° 8.95' N	117° 55.92' E	3809,7
PS78/259-4	14.09.11	08:17	ADCP	action	83° 8.92' N	117° 55.91' E	3798,5
PS78/259-4	14.09.11	08:24	ADCP	profile start	83° 8.87' N	117° 55.90' E	3796,9
PS78/259-4	14.09.11	08:24	ADCP	profile end	83° 8.87' N	117° 55.90' E	3796,9
PS78/259-1	14.09.11	08:40	CTD/RO	on deck	83° 8.76' N	117° 55.61' E	3770,5
PS78/260-1	14.09.11	13:21	CTD/RO	in the water	82° 59.64' N	114° 42.96' E	0
PS78/260-1	14.09.11	14:27	CTD/RO	on ground/ max depth	82° 59.62' N	114° 39.54' E	3318
PS78/260-1	14.09.11	14:28	CTD/RO	hoisting	82° 59.61' N	114° 39.51' E	3326,9
PS78/260-1	14.09.11	15:20	CTD/RO	at surface	82° 59.76' N	114° 37.82' E	3332,7
PS78/260-1	14.09.11	15:22	CTD/RO	on deck	82° 59.77' N	114° 37.78' E	3332,1
PS78/261-1	14.09.11	19:34	CTD/RO	in the water	82° 49.99' N	111° 47.07' E	0
PS78/261-1	14.09.11	20:47	CTD/RO	on ground/ max depth	82° 49.71' N	111° 48.57' E	0
PS78/261-1	14.09.11	20:47	CTD/RO	hoisting	82° 49.71' N	111° 48.57' E	0
PS78/261-1	14.09.11	21:50	CTD/RO	on deck	82° 49.42' N	111° 49.38' E	3500
PS78/262-1	15.09.11	01:55	CTD/RO	in the water	82° 39.25' N	108° 53.47' E	0
PS78/262-1	15.09.11	03:06	CTD/RO	on ground/ max depth	82° 39.49' N	108° 53.09' E	3598
PS78/262-1	15.09.11	03:09	CTD/RO	hoisting	82° 39.51' N	108° 53.10' E	0
PS78/262-2	15.09.11	03:25	RAMSES	in the water	82° 39.60' N	108° 53.11' E	0
PS78/262-2	15.09.11	03:55	RAMSES	on ground/ max depth	82° 39.72' N	108° 53.34' E	0
PS78/262-1	15.09.11	04:10	CTD/RO	at surface	82° 39.82' N	108° 53.52' E	0
PS78/262-1	15.09.11	04:12	CTD/RO	on deck	82° 39.83' N	108° 53.61' E	3598
PS78/262-2	15.09.11	04:16	RAMSES	on deck	82° 39.86' N	108° 53.73' E	3598
PS78/262-3	15.09.11	05:01	MOR	in the water	82° 38.11' N	108° 55.26' E	0
PS78/262-3	15.09.11	05:18	MOR	in the water	82° 38.20' N	108° 55.74' E	0
PS78/262-3	15.09.11	05:23	MOR	in the water	82° 38.23' N	108° 55.88' E	0
PS78/262-3	15.09.11	06:00	MOR	in the water	82° 38.40' N	108° 56.95' E	0
PS78/262-3	15.09.11	06:46	MOR	in the water	82° 38.60' N	108° 58.50' E	0
PS78/262-3	15.09.11	07:08	MOR	in the water	82° 38.65' N	108° 59.48' E	0
PS78/262-3	15.09.11	07:15	MOR	in the water	82° 38.67' N	108° 59.78' E	0
PS78/262-3	15.09.11	07:24	MOR	in the water	82° 38.69' N	109° 0.19' E	0
PS78/262-3	15.09.11	07:40	MOR	in the water	82° 38.73' N	109° 0.92' E	3581,1
PS78/262-3	15.09.11	07:42	MOR	lowering	82° 38.73' N	109° 1.01' E	3578,6

A.4 Stationsliste / station list PS 78

Station	Date	Time	Gear	Action	Position Lat	Position Lon	Water Depth [m]
PS78/262-3	15.09.11	07:45	MOR	on ground/ max depth	82° 38.73' N	109° 1.14' E	3578
PS78/263-1	15.09.11	10:20	MOR	in the water	82° 37.72' N	108° 26.92' E	3547,7
PS78/263-1	15.09.11	10:22	MOR	lowering	82° 37.73' N	108° 26.94' E	3552,4
PS78/263-1	15.09.11	11:39	MOR	information	82° 37.94' N	108° 27.90' E	3552,9
PS78/263-1	15.09.11	11:50	MOR	information	82° 37.97' N	108° 27.94' E	3557
PS78/263-1	15.09.11	12:00	MOR	in the water	82° 38.01' N	108° 28.02' E	3554,9
PS78/263-1	15.09.11	12:02	MOR	in the water	82° 38.01' N	108° 28.04' E	3557,1
PS78/263-1	15.09.11	12:12	MOR	in the water	82° 38.06' N	108° 28.20' E	3553,3
PS78/263-1	15.09.11	12:13	MOR	lowering	82° 38.07' N	108° 28.22' E	3550,6
PS78/263-1	15.09.11	12:16	MOR	on ground/ max depth	82° 38.08' N	108° 28.26' E	3555,7
PS78/263-1	15.09.11	12:16	MOR	information	82° 38.08' N	108° 28.26' E	3555,7
PS78/263-2	15.09.11	13:00	MN	in the water	82° 35.97' N	108° 23.23' E	3555,6
PS78/263-2	15.09.11	14:56	MN	on ground/ max depth	82° 36.61' N	108° 23.69' E	3549
PS78/263-2	15.09.11	14:57	MN	hoisting	82° 36.62' N	108° 23.69' E	3554,2
PS78/263-2	15.09.11	16:43	MN	at surface	82° 37.37' N	108° 24.79' E	3552,5
PS78/263-2	15.09.11	16:50	MN	on deck	82° 37.42' N	108° 24.92' E	3553,2
PS78/264-1	15.09.11	20:39	CTD/RO	in the water	82° 21.79' N	106° 55.80' E	3470,1
PS78/264-1	15.09.11	22:06	CTD/RO	on ground/ max depth	82° 21.41' N	106° 59.18' E	3468,2
PS78/264-1	15.09.11	22:07	CTD/RO	hoisting	82° 21.41' N	106° 59.18' E	3471,1
PS78/264-1	15.09.11	23:05	CTD/RO	on deck	82° 21.48' N	106° 59.43' E	3472,9
PS78/265-1	16.09.11	04:05	CTD/RO	in the water	81° 58.23' N	105° 20.65' E	3330,7
PS78/265-2	16.09.11	04:51	RAMSES	in the water	81° 58.39' N	105° 22.14' E	3336,1
PS78/265-1	16.09.11	05:11	CTD/RO	on ground/ max depth	81° 58.45' N	105° 22.61' E	3335,2
PS78/265-1	16.09.11	05:12	CTD/RO	hoisting	81° 58.45' N	105° 22.63' E	3334,8
PS78/265-2	16.09.11	05:21	RAMSES	on ground/ max depth	81° 58.47' N	105° 22.82' E	3338
PS78/265-2	16.09.11	05:21	RAMSES	hoisting	81° 58.47' N	105° 22.82' E	3338
PS78/265-2	16.09.11	05:29	RAMSES	at surface	81° 58.46' N	105° 23.14' E	3334,4
PS78/265-2	16.09.11	05:30	RAMSES	on deck	81° 58.46' N	105° 23.17' E	3335,7
PS78/265-1	16.09.11	06:08	CTD/RO	on deck	81° 58.53' N	105° 24.00' E	3334,2
PS78/266-1	16.09.11	11:00	CTD/RO	in the water	81° 37.68' N	104° 0.29' E	3005
PS78/266-1	16.09.11	11:58	CTD/RO	on ground/ max depth	81° 37.98' N	103° 59.93' E	2997
PS78/266-1	16.09.11	12:00	CTD/RO	hoisting	81° 37.99' N	103° 59.92' E	2991,5
PS78/266-1	16.09.11	12:50	CTD/RO	on deck	81° 38.31' N	103° 59.84' E	2996,4
PS78/266-2	16.09.11	13:00	MN	in the water	81° 38.37' N	103° 59.95' E	2996,5
PS78/266-2	16.09.11	14:48	MN	on ground/ max depth	81° 39.23' N	104° 1.48' E	3012,9
PS78/266-2	16.09.11	14:49	MN	hoisting	81° 39.24' N	104° 1.51' E	3010,7

A.4 Stationsliste / station list PS 78

Station	Date	Time	Gear	Action	Position Lat	Position Lon	Water Depth [m]
PS78/266-2	16.09.11	16:27	MN	at surface	81° 39.92' N	104° 4.77' E	3033,8
PS78/266-2	16.09.11	16:30	MN	on deck	81° 39.94' N	104° 4.88' E	3038,7
PS78/267-1	16.09.11	23:00	ICE	in the water	81° 26.86' N	103° 12.55' E	2580,7
PS78/267-2	16.09.11	23:37	CTD/RO	in the water	81° 26.95' N	103° 11.17' E	2574,8
PS78/267-2	17.09.11	00:31	CTD/RO	on ground/ max depth	81° 27.22' N	103° 9.27' E	2578,1
PS78/267-2	17.09.11	00:33	CTD/RO	hoisting	81° 27.23' N	103° 9.22' E	2582,5
PS78/267-2	17.09.11	01:24	CTD/RO	on deck	81° 27.59' N	103° 8.19' E	2571,3
PS78/267-3	17.09.11	02:40	MN	in the water	81° 28.24' N	103° 7.49' E	2564,4
PS78/267-3	17.09.11	04:10	MN	action	81° 28.83' N	103° 8.58' E	2560,2
PS78/267-3	17.09.11	04:41	MN	lowering	81° 28.93' N	103° 9.59' E	2565,6
PS78/267-3	17.09.11	05:12	MN	on ground/ max depth	81° 29.02' N	103° 10.38' E	2569,9
PS78/267-3	17.09.11	05:13	MN	hoisting	81° 29.02' N	103° 10.40' E	2568,3
PS78/267-3	17.09.11	06:36	MN	on deck	81° 29.18' N	103° 11.64' E	2583,8
PS78/267-4	17.09.11	06:52	DUMMY	in the water	81° 29.23' N	103° 11.79' E	2586,4
PS78/267-5	17.09.11	07:01	RAMSES	in the water	81° 29.26' N	103° 11.87' E	2584
PS78/267-5	17.09.11	07:35	RAMSES	on ground/ max depth	81° 29.34' N	103° 12.12' E	2584,7
PS78/267-5	17.09.11	07:35	RAMSES	hoisting	81° 29.34' N	103° 12.12' E	2584,7
PS78/267-5	17.09.11	07:41	RAMSES	on deck	81° 29.35' N	103° 12.15' E	2588,9
PS78/267-4	17.09.11	07:42	DUMMY	on ground/ max depth	81° 29.35' N	103° 12.16' E	2585,4
PS78/267-4	17.09.11	07:43	DUMMY	hoisting	81° 29.35' N	103° 12.16' E	2584,9
PS78/267-4	17.09.11	08:43	DUMMY	profile start	81° 29.45' N	103° 12.18' E	2586,8
PS78/267-4	17.09.11	08:43	DUMMY	profile end	81° 29.45' N	103° 12.18' E	2586,8
PS78/267-4	17.09.11	08:43	DUMMY	on deck	81° 29.45' N	103° 12.18' E	2586,8
PS78/267-1	17.09.11	09:00	ICE	on ground/ max depth	81° 29.56' N	103° 12.37' E	2586
PS78/267-1	17.09.11	09:00	ICE	on deck	81° 29.56' N	103° 12.37' E	2586
PS78/268-1	17.09.11	13:02	CTD/RO	in the water	81° 15.62' N	102° 41.36' E	2193,6
PS78/268-1	17.09.11	13:50	CTD/RO	on ground/ max depth	81° 15.82' N	102° 40.31' E	2199,3
PS78/268-1	17.09.11	13:51	CTD/RO	hoisting	81° 15.83' N	102° 40.30' E	2200,4
PS78/268-1	17.09.11	14:27	CTD/RO	at surface	81° 16.00' N	102° 39.62' E	2205,6
PS78/268-1	17.09.11	14:30	CTD/RO	on deck	81° 16.02' N	102° 39.57' E	2205,1
PS78/268-2	17.09.11	14:38	MN	in the water	81° 16.06' N	102° 39.44' E	2205,3
PS78/268-2	17.09.11	15:46	MN	on ground/ max depth	81° 16.48' N	102° 38.98' E	2205,6
PS78/268-2	17.09.11	15:46	MN	hoisting	81° 16.48' N	102° 38.98' E	2205,6
PS78/268-2	17.09.11	16:57	MN	at surface	81° 16.97' N	102° 39.74' E	2215,4
PS78/268-2	17.09.11	17:05	MN	on deck	81° 17.03' N	102° 39.90' E	2218
PS78/269-1	17.09.11	19:01	CTD/RO	in the water	81° 6.64' N	102° 12.81' E	1400,7

A.4 Stationsliste / station list PS 78

Station	Date	Time	Gear	Action	Position Lat	Position Lon	Water Depth [m]
PS78/269-1	17.09.11	19:37	CTD/RO	on ground/ max depth	81° 6.64' N	102° 13.22' E	1404,8
PS78/269-1	17.09.11	19:37	CTD/RO	hoisting	81° 6.64' N	102° 13.22' E	1404,8
PS78/269-1	17.09.11	19:59	CTD/RO	on deck	81° 6.64' N	102° 13.50' E	1409,8
PS78/269-2	17.09.11	20:09	MN	in the water	81° 6.68' N	102° 13.53' E	1409,2
PS78/269-2	17.09.11	20:52	MN	on ground/ max depth	81° 6.66' N	102° 14.60' E	1428,4
PS78/269-2	17.09.11	20:52	MN	hoisting	81° 6.66' N	102° 14.60' E	1428,4
PS78/269-2	17.09.11	21:46	MN	on deck	81° 6.65' N	102° 14.87' E	1431,3
PS78/270-1	17.09.11	23:42	CTD	in the water	80° 57.89' N	101° 50.92' E	395
PS78/270-1	17.09.11	23:57	CTD	on ground/ max depth	80° 57.91' N	101° 51.12' E	395
PS78/270-1	18.09.11	00:09	CTD	on deck	80° 57.91' N	101° 51.08' E	395
PS78/270-2	18.09.11	00:24	MN	in the water	80° 57.97' N	101° 51.17' E	396
PS78/270-2	18.09.11	00:35	MN	on ground/ max depth	80° 57.94' N	101° 51.05' E	395
PS78/270-2	18.09.11	00:36	MN	hoisting	80° 57.94' N	101° 51.06' E	395
PS78/270-2	18.09.11	00:56	MN	on deck	80° 57.97' N	101° 51.06' E	396
PS78/271-1	19.09.11	01:38	CTD/RO	in the water	82° 9.86' N	119° 8.93' E	4330,8
PS78/271-2	19.09.11	01:50	GF PUMPE	in the water	82° 9.86' N	119° 8.99' E	4328
PS78/271-2	19.09.11	01:53	GF PUMPE	on ground/ max depth	82° 9.86' N	119° 9.00' E	4334,1
PS78/271-2	19.09.11	01:54	GF PUMPE	profile start	82° 9.87' N	119° 9.01' E	4328,4
PS78/271-2	19.09.11	02:02	GF PUMPE	profile end	82° 9.89' N	119° 9.03' E	4326,4
PS78/271-2	19.09.11	02:02	GF PUMPE	on deck	82° 9.89' N	119° 9.03' E	4326,4
PS78/271-1	19.09.11	03:05	CTD/RO	on ground/ max depth	82° 9.69' N	119° 9.47' E	4335,5
PS78/271-1	19.09.11	03:07	CTD/RO	hoisting	82° 9.70' N	119° 9.48' E	4335,8
PS78/271-1	19.09.11	04:25	CTD/RO	at surface	82° 9.89' N	119° 10.74' E	4334,1
PS78/271-1	19.09.11	04:27	CTD/RO	on deck	82° 9.90' N	119° 10.73' E	4332,5
PS78/271-3	19.09.11	04:33	MUWS	in the water	82° 9.89' N	119° 10.84' E	4337
PS78/271-3	19.09.11	04:37	MUWS	on ground/ max depth	82° 9.87' N	119° 10.95' E	4334,1
PS78/271-3	19.09.11	04:37	MUWS	hoisting	82° 9.87' N	119° 10.95' E	4334,1
PS78/271-3	19.09.11	04:37	MUWS	profile start	82° 9.87' N	119° 10.95' E	4334,1
PS78/271-3	19.09.11	04:43	MUWS	profile end	82° 9.83' N	119° 11.05' E	4336,4
PS78/271-3	19.09.11	04:43	MUWS	at surface	82° 9.83' N	119° 11.05' E	4336,4
PS78/271-3	19.09.11	04:44	MUWS	on deck	82° 9.83' N	119° 11.03' E	4336,8
PS78/271-4	19.09.11	06:49	XCTD	in the water	81° 57.06' N	119° 36.23' E	3287
PS78/271-4	19.09.11	06:55	XCTD	on ground/ max depth	81° 56.69' N	119° 36.53' E	3376,4
PS78/272-1	19.09.11	08:33	RAMSES	in the water	81° 46.54' N	119° 58.16' E	4994,5
PS78/272-2	19.09.11	08:42	CTD/RO	in the water	81° 46.50' N	119° 58.14' E	5001,4
PS78/272-2	19.09.11	08:52	CTD/RO	on ground/ max depth	81° 46.44' N	119° 58.36' E	4999,7

A.4 Stationsliste / station list PS 78

Station	Date	Time	Gear	Action	Position Lat	Position Lon	Water Depth [m]
PS78/272-2	19.09.11	08:53	CTD/RO	hoisting	81° 46.44' N	119° 58.39' E	4997,5
PS78/272-2	19.09.11	09:03	CTD/RO	on deck	81° 46.39' N	119° 58.65' E	4986,6
PS78/272-1	19.09.11	09:08	RAMSES	on ground/ max depth	81° 46.37' N	119° 58.79' E	4988,9
PS78/272-1	19.09.11	09:08	RAMSES	hoisting	81° 46.37' N	119° 58.79' E	4988,9
PS78/272-1	19.09.11	09:17	RAMSES	on deck	81° 46.35' N	119° 59.10' E	4976,8
PS78/272-3	19.09.11	09:53	CTD/RO	in the water	81° 46.35' N	120° 0.22' E	4932
PS78/272-4	19.09.11	09:57	GF PUMPE	in the water	81° 46.35' N	120° 0.32' E	4926,6
PS78/272-4	19.09.11	10:00	GF PUMPE	on ground/ max depth	81° 46.35' N	120° 0.40' E	4919,7
PS78/272-4	19.09.11	10:00	GF PUMPE	profile start	81° 46.35' N	120° 0.40' E	4919,7
PS78/272-4	19.09.11	10:10	GF PUMPE	profile end	81° 46.36' N	120° 0.66' E	4909,4
PS78/272-4	19.09.11	10:10	GF PUMPE	hoisting	81° 46.36' N	120° 0.66' E	4909,4
PS78/272-4	19.09.11	10:10	GF PUMPE	on deck	81° 46.36' N	120° 0.66' E	4909,4
PS78/272-3	19.09.11	11:32	CTD/RO	on ground/ max depth	81° 46.34' N	120° 2.07' E	4837,8
PS78/272-3	19.09.11	11:33	CTD/RO	hoisting	81° 46.34' N	120° 2.08' E	4834,3
PS78/272-3	19.09.11	13:12	CTD/RO	on deck	81° 46.32' N	120° 4.65' E	4740,3
PS78/272-5	19.09.11	15:20	XCTD	in the water	81° 34.09' N	120° 20.77' E	5036,7
PS78/272-5	19.09.11	15:24	XCTD	on ground/ max depth	81° 33.68' N	120° 20.52' E	5050,6
PS78/272-5	19.09.11	15:25	XCTD	on deck	81° 33.63' N	120° 20.31' E	5056,1
PS78/273-1	19.09.11	17:40	CTD/RO	in the water	81° 21.48' N	120° 43.28' E	5267,5
PS78/273-2	19.09.11	17:45	GF PUMPE	in the water	81° 21.51' N	120° 43.44' E	5268,9
PS78/273-2	19.09.11	17:45	GF PUMPE	profile start	81° 21.51' N	120° 43.44' E	5268,9
PS78/273-2	19.09.11	17:58	GF PUMPE	profile end	81° 21.61' N	120° 43.57' E	5263,9
PS78/273-2	19.09.11	17:58	GF PUMPE	on deck	81° 21.61' N	120° 43.57' E	5263,9
PS78/273-1	19.09.11	19:29	CTD/RO	on ground/ max depth	81° 21.59' N	120° 45.63' E	5218
PS78/273-1	19.09.11	19:29	CTD/RO	hoisting	81° 21.59' N	120° 45.63' E	5218
PS78/273-1	19.09.11	21:07	CTD/RO	on deck	81° 21.48' N	120° 47.68' E	5149,8
PS78/273-1	19.09.11	21:13	MUWS	in the water	81° 21.48' N	120° 47.77' E	5145,2
PS78/273-1	19.09.11	21:15	MUWS	on ground/ max depth	81° 21.49' N	120° 47.80' E	5142,5
PS78/273-1	19.09.11	21:15	MUWS	profile start	81° 21.49' N	120° 47.80' E	5142,5
PS78/273-1	19.09.11	21:20	MUWS	profile end	81° 21.52' N	120° 47.84' E	5133,9
PS78/273-1	19.09.11	21:20	MUWS	on deck	81° 21.52' N	120° 47.84' E	5133,9
PS78/273-3	19.09.11	22:39	XCTD	in the water	81° 9.50' N	120° 42.02' E	3950
PS78/273-3	19.09.11	22:47	XCTD	on ground/ max depth	81° 7.81' N	120° 41.38' E	3359,1
PS78/274-1	19.09.11	23:42	CTD/RO	in the water	80° 58.03' N	120° 36.56' E	3313
PS78/274-2	19.09.11	23:48	GF PUMPE	in the water	80° 58.01' N	120° 36.49' E	3316,3
PS78/274-2	19.09.11	23:50	GF PUMPE	on ground/ max depth	80° 58.02' N	120° 36.44' E	3313,3

A.4 Stationsliste / station list PS 78

Station	Date	Time	Gear	Action	Position Lat	Position Lon	Water Depth [m]
PS78/274-2	19.09.11	23:50	GF PUMPE	profile start	80° 58.02' N	120° 36.44' E	3313,3
PS78/274-2	20.09.11	00:00	GF PUMPE	profile end	80° 58.07' N	120° 35.96' E	3316,6
PS78/274-2	20.09.11	00:00	GF PUMPE	hoisting	80° 58.07' N	120° 35.96' E	3316,6
PS78/274-2	20.09.11	00:00	GF PUMPE	on deck	80° 58.07' N	120° 35.96' E	3316,6
PS78/274-1	20.09.11	00:51	CTD/RO	on ground/ max depth	80° 57.99' N	120° 35.39' E	3331,8
PS78/274-1	20.09.11	00:51	CTD/RO	hoisting	80° 57.99' N	120° 35.39' E	3331,8
PS78/274-1	20.09.11	02:02	CTD/RO	at surface	80° 58.08' N	120° 33.95' E	3350,2
PS78/274-1	20.09.11	02:04	CTD/RO	on deck	80° 58.08' N	120° 33.89' E	3351,3
PS78/275-1	20.09.11	03:18	MUC	in the water	80° 49.17' N	120° 57.89' E	3532,1
PS78/275-2	20.09.11	03:58	XCTD	in the water	80° 49.15' N	120° 58.14' E	3524,7
PS78/275-1	20.09.11	04:04	MUC	on ground/ max depth	80° 49.13' N	120° 58.26' E	3527,1
PS78/275-2	20.09.11	04:04	XCTD	on ground/ max depth	80° 49.13' N	120° 58.26' E	3527,1
PS78/275-2	20.09.11	04:04	XCTD	on deck	80° 49.13' N	120° 58.26' E	3527,1
PS78/275-1	20.09.11	04:06	MUC	hoisting	80° 49.13' N	120° 58.31' E	3527,9
PS78/275-1	20.09.11	04:46	MUC	at surface	80° 49.15' N	120° 59.20' E	3527,9
PS78/275-1	20.09.11	04:49	MUC	on deck	80° 49.16' N	120° 59.29' E	3527,2
PS78/276-1	20.09.11	06:05	CTD/RO	in the water	80° 38.63' N	121° 19.46' E	3487,3
PS78/276-2	20.09.11	06:09	RAMSES	in the water	80° 38.64' N	121° 19.52' E	3492,5
PS78/276-1	20.09.11	06:15	CTD/RO	on ground/ max depth	80° 38.62' N	121° 19.65' E	3489,8
PS78/276-1	20.09.11	06:16	CTD/RO	hoisting	80° 38.62' N	121° 19.66' E	3491,6
PS78/276-1	20.09.11	06:27	CTD/RO	on deck	80° 38.61' N	121° 19.76' E	3497
PS78/276-2	20.09.11	06:37	RAMSES	on ground/ max depth	80° 38.60' N	121° 19.82' E	3495,3
PS78/276-2	20.09.11	06:37	RAMSES	hoisting	80° 38.60' N	121° 19.82' E	3495,3
PS78/276-2	20.09.11	06:44	RAMSES	on deck	80° 38.60' N	121° 19.90' E	3492
PS78/276-3	20.09.11	06:45	MUWS	in the water	80° 38.59' N	121° 19.91' E	3496,8
PS78/276-3	20.09.11	06:46	MUWS	profile start	80° 38.59' N	121° 19.93' E	3494,8
PS78/276-3	20.09.11	06:55	MUWS	profile end	80° 38.58' N	121° 20.05' E	3491,1
PS78/276-3	20.09.11	06:55	MUWS	on deck	80° 38.58' N	121° 20.05' E	3491,1
PS78/276-4	20.09.11	07:10	CTD/RO	in the water	80° 38.35' N	121° 20.33' E	3489,1
PS78/276-4	20.09.11	07:17	CTD/RO	at surface	80° 38.32' N	121° 20.28' E	3487,4
PS78/276-4	20.09.11	07:18	CTD/RO	lowering	80° 38.32' N	121° 20.28' E	3487,6
PS78/276-5	20.09.11	07:31	GF PUMPE	in the water	80° 38.31' N	121° 20.33' E	3485,5
PS78/276-5	20.09.11	07:31	GF PUMPE	profile start	80° 38.31' N	121° 20.33' E	3485,5
PS78/276-5	20.09.11	07:43	GF PUMPE	hoisting	80° 38.32' N	121° 20.23' E	3491,7
PS78/276-5	20.09.11	07:43	GF PUMPE	profile end	80° 38.32' N	121° 20.23' E	3491,7
PS78/276-5	20.09.11	07:45	GF PUMPE	on deck	80° 38.31' N	121° 20.24' E	3489,5
PS78/276-4	20.09.11	08:30	CTD/RO	on ground/ max depth	80° 38.13' N	121° 19.83' E	3489

A.4 Stationsliste / station list PS 78

Station	Date	Time	Gear	Action	Position Lat	Position Lon	Water Depth [m]
PS78/276-4	20.09.11	08:31	CTD/RO	hoisting	80° 38.13' N	121° 19.81' E	3490,1
PS78/276-4	20.09.11	09:54	CTD/RO	on deck	80° 37.60' N	121° 17.00' E	3471,4
PS78/276-6	20.09.11	09:59	MUC	in the water	80° 37.58' N	121° 16.74' E	3463,9
PS78/276-6	20.09.11	10:47	MUC	on ground/ max depth	80° 37.56' N	121° 16.04' E	3467,3
PS78/276-6	20.09.11	10:49	MUC	hoisting	80° 37.56' N	121° 16.04' E	3466,5
PS78/276-6	20.09.11	11:30	MUC	on deck	80° 37.55' N	121° 15.23' E	3458,4
PS78/276-7	20.09.11	12:28	XCTD	in the water	80° 29.08' N	121° 34.05' E	3469,1
PS78/276-7	20.09.11	12:32	XCTD	on ground/ max depth	80° 28.33' N	121° 35.83' E	3470,6
PS78/276-8	20.09.11	12:41	XCTD	in the water	80° 26.62' N	121° 39.76' E	3229,1
PS78/276-8	20.09.11	12:42	XCTD	on ground/ max depth	80° 26.43' N	121° 40.21' E	3235,7
PS78/277-1	20.09.11	13:31	CTD/RO	in the water	80° 18.40' N	121° 58.36' E	3222,9
PS78/277-1	20.09.11	14:42	CTD/RO	on ground/ max depth	80° 18.39' N	121° 57.35' E	3238,1
PS78/277-1	20.09.11	14:43	CTD/RO	hoisting	80° 18.39' N	121° 57.34' E	3234,2
PS78/277-1	20.09.11	15:54	CTD/RO	at surface	80° 18.48' N	121° 57.52' E	3229,4
PS78/277-1	20.09.11	15:56	CTD/RO	on deck	80° 18.47' N	121° 57.49' E	3230,5
PS78/277-2	20.09.11	16:43	MUC	in the water	80° 12.65' N	122° 12.19' E	3361,9
PS78/277-2	20.09.11	17:27	MUC	on ground/ max depth	80° 12.54' N	122° 12.20' E	3358,9
PS78/277-2	20.09.11	17:28	MUC	hoisting	80° 12.54' N	122° 12.22' E	3356,6
PS78/277-2	20.09.11	18:10	MUC	on deck	80° 12.38' N	122° 12.48' E	3353
PS78/277-3	20.09.11	19:08	XCTD	in the water	80° 5.38' N	122° 27.41' E	3353,9
PS78/277-3	20.09.11	19:21	XCTD	on ground/ max depth	80° 2.89' N	122° 33.06' E	3428,6
PS78/278-1	20.09.11	20:16	CTD/RO	in the water	79° 54.59' N	122° 50.87' E	3449,9
PS78/278-2	20.09.11	20:22	GF PUMPE	in the water	79° 54.60' N	122° 50.40' E	3447
PS78/278-2	20.09.11	21:16	GF PUMPE	profile end	79° 54.59' N	122° 48.98' E	3443
PS78/278-2	20.09.11	21:16	GF PUMPE	profile start	79° 54.59' N	122° 48.98' E	3443
PS78/278-2	20.09.11	21:16	GF PUMPE	on deck	79° 54.59' N	122° 48.98' E	3443
PS78/278-1	20.09.11	21:32	CTD/RO	on ground/ max depth	79° 54.62' N	122° 48.62' E	3440,6
PS78/278-1	20.09.11	21:32	CTD/RO	hoisting	79° 54.62' N	122° 48.62' E	3440,6
PS78/278-1	20.09.11	22:46	CTD/RO	on deck	79° 54.68' N	122° 47.35' E	3440,7
PS78/278-3	21.09.11	00:03	XCTD	in the water	79° 42.13' N	123° 19.65' E	3396
PS78/278-3	21.09.11	00:07	XCTD	on ground/ max depth	79° 41.38' N	123° 21.33' E	3402,5
PS78/279-1	21.09.11	01:12	CTD/RO	in the water	79° 30.53' N	123° 45.38' E	3475,6
PS78/279-1	21.09.11	02:22	CTD/RO	on ground/ max depth	79° 30.57' N	123° 45.82' E	3474,5
PS78/279-1	21.09.11	02:23	CTD/RO	hoisting	79° 30.57' N	123° 45.82' E	3472,6
PS78/279-1	21.09.11	03:25	CTD/RO	at surface	79° 30.46' N	123° 46.01' E	3474,6
PS78/279-1	21.09.11	03:27	CTD/RO	on deck	79° 30.44' N	123° 46.04' E	3473,6

A.4 Stationsliste / station list PS 78

Station	Date	Time	Gear	Action	Position Lat	Position Lon	Water Depth [m]
PS78/279-2	21.09.11	04:35	XCTD	in the water	79° 19.25' N	123° 57.19' E	3167,1
PS78/279-2	21.09.11	04:38	XCTD	action	79° 18.90' N	123° 57.52' E	3167,9
PS78/279-2	21.09.11	04:43	XCTD	in the water	79° 18.52' N	123° 57.96' E	3182,5
PS78/279-2	21.09.11	04:48	XCTD	on ground/ max depth	79° 18.22' N	123° 58.21' E	3185,9
PS78/279-2	21.09.11	04:49	XCTD	on deck	79° 18.16' N	123° 58.27' E	3185,2
PS78/280-1	21.09.11	05:49	CTD/RO	in the water	79° 8.83' N	124° 7.75' E	3121,8
PS78/280-1	21.09.11	05:59	CTD/RO	on ground/ max depth	79° 8.84' N	124° 7.59' E	3120,9
PS78/280-1	21.09.11	05:59	CTD/RO	hoisting	79° 8.84' N	124° 7.59' E	3120,9
PS78/280-1	21.09.11	06:09	CTD/RO	on deck	79° 8.86' N	124° 7.47' E	3116,9
PS78/280-2	21.09.11	06:14	RAMSES	in the water	79° 8.85' N	124° 7.41' E	3121,9
PS78/280-3	21.09.11	06:38	MUWS	in the water	79° 8.86' N	124° 6.84' E	3122,9
PS78/280-2	21.09.11	06:43	RAMSES	on ground/ max depth	79° 8.87' N	124° 6.74' E	3123,9
PS78/280-2	21.09.11	06:44	RAMSES	hoisting	79° 8.87' N	124° 6.72' E	3123,7
PS78/280-3	21.09.11	06:50	MUWS	profile start	79° 8.87' N	124° 6.56' E	3124,9
PS78/280-3	21.09.11	06:50	MUWS	profile end	79° 8.87' N	124° 6.56' E	3124,9
PS78/280-3	21.09.11	06:50	MUWS	on deck	79° 8.87' N	124° 6.56' E	3124,9
PS78/280-2	21.09.11	06:51	RAMSES	on deck	79° 8.87' N	124° 6.52' E	3125,6
PS78/280-4	21.09.11	07:03	CTD/RO	in the water	79° 8.88' N	124° 6.15' E	3127,7
PS78/280-5	21.09.11	07:26	GF PUMPE	in the water	79° 8.89' N	124° 5.52' E	3122,3
PS78/280-5	21.09.11	07:40	GF PUMPE	profile start	79° 8.92' N	124° 5.17' E	3117,4
PS78/280-5	21.09.11	07:40	GF PUMPE	profile end	79° 8.92' N	124° 5.17' E	3117,4
PS78/280-5	21.09.11	07:40	GF PUMPE	on deck	79° 8.92' N	124° 5.17' E	3117,4
PS78/280-4	21.09.11	08:08	CTD/RO	on ground/ max depth	79° 8.92' N	124° 4.54' E	3097,5
PS78/280-4	21.09.11	08:10	CTD/RO	hoisting	79° 8.92' N	124° 4.49' E	3094,7
PS78/280-4	21.09.11	09:14	CTD/RO	on deck	79° 8.92' N	124° 3.11' E	3075
PS78/280-6	21.09.11	09:31	MUC	in the water	79° 8.98' N	124° 2.62' E	3077,9
PS78/280-6	21.09.11	10:12	MUC	on ground/ max depth	79° 8.97' N	124° 2.11' E	3077,4
PS78/280-6	21.09.11	10:14	MUC	hoisting	79° 8.97' N	124° 2.10' E	3075,4
PS78/280-6	21.09.11	10:52	MUC	on deck	79° 9.02' N	124° 2.10' E	3075,9
PS78/280-7	21.09.11	12:18	XCTD	in the water	78° 53.05' N	124° 36.29' E	3011,7
PS78/280-7	21.09.11	12:22	XCTD	on ground/ max depth	78° 52.27' N	124° 37.83' E	3000,3
PS78/280-8	21.09.11	13:38	XCTD	in the water	78° 35.11' N	125° 9.55' E	2682,2
PS78/280-8	21.09.11	13:42	XCTD	on ground/ max depth	78° 34.19' N	125° 11.20' E	2653,5
PS78/281-1	21.09.11	14:35	MOR	action	78° 25.74' N	125° 28.18' E	2700,7
PS78/281-1	21.09.11	14:36	MOR	in the water	78° 25.74' N	125° 28.14' E	2692,9
PS78/281-1	21.09.11	14:44	MOR	on deck	78° 25.66' N	125° 27.91' E	2677,9
PS78/281-1	21.09.11	14:45	MOR	in the water	78° 25.66' N	125° 27.92' E	2680,9

A.4 Stationsliste / station list PS 78

Station	Date	Time	Gear	Action	Position Lat	Position Lon	Water Depth [m]
PS78/281-1	21.09.11	14:53	MOR	information	78° 25.68' N	125° 27.75' E	2680
PS78/281-1	21.09.11	15:14	MOR	in the water	78° 25.74' N	125° 29.04' E	2680
PS78/281-1	21.09.11	15:31	MOR	on deck	78° 25.72' N	125° 28.98' E	2680
PS78/281-1	21.09.11	15:36	MOR	in the water	78° 25.72' N	125° 28.82' E	2680
PS78/281-1	21.09.11	15:42	MOR	action	78° 25.72' N	125° 28.59' E	2680
PS78/281-1	21.09.11	15:45	MOR	on deck	78° 25.73' N	125° 28.50' E	2680
PS78/281-1	21.09.11	15:46	MOR	action	78° 25.73' N	125° 28.48' E	2680
PS78/281-1	21.09.11	17:40	MOR	on ground/ max depth	78° 25.72' N	125° 28.35' E	2680
PS78/281-1	21.09.11	17:43	MOR	on deck	78° 25.70' N	125° 28.40' E	2680
PS78/282-1	21.09.11	18:28	MOR	information	78° 29.68' N	125° 49.54' E	0
PS78/282-1	21.09.11	18:39	MOR	information	78° 29.66' N	125° 49.85' E	0
PS78/282-1	21.09.11	19:20	MOR	on ground/ max depth	78° 29.58' N	125° 48.95' E	2600
PS78/283-1	21.09.11	20:11	CTD/RO	in the water	78° 33.06' N	125° 22.54' E	2908,3
PS78/283-2	21.09.11	20:26	GF PUMPE	in the water	78° 32.85' N	125° 22.61' E	2902,4
PS78/283-2	21.09.11	20:39	GF PUMPE	profile start	78° 32.71' N	125° 22.28' E	2903,9
PS78/283-2	21.09.11	20:39	GF PUMPE	profile end	78° 32.71' N	125° 22.28' E	2903,9
PS78/283-2	21.09.11	20:39	GF PUMPE	on deck	78° 32.71' N	125° 22.28' E	2903,9
PS78/283-1	21.09.11	21:17	CTD/RO	on ground/ max depth	78° 32.26' N	125° 21.69' E	2863,4
PS78/283-1	21.09.11	21:17	CTD/RO	hoisting	78° 32.26' N	125° 21.69' E	2863,4
PS78/283-1	21.09.11	22:20	CTD/RO	on deck	78° 31.51' N	125° 21.05' E	2831,9
PS78/283-3	21.09.11	22:23	MUC	in the water	78° 31.51' N	125° 21.03' E	2832,5
PS78/283-3	21.09.11	23:00	MUC	on ground/ max depth	78° 31.49' N	125° 20.98' E	2829,2
PS78/283-3	21.09.11	23:01	MUC	hoisting	78° 31.49' N	125° 20.98' E	2831,2
PS78/283-3	21.09.11	23:02	MUC	off ground	78° 31.49' N	125° 20.98' E	2829,5
PS78/283-3	21.09.11	23:35	MUC	on deck	78° 31.50' N	125° 20.95' E	2833
PS78/284-1	22.09.11	00:57	MOR	action	78° 29.57' N	125° 49.05' E	2762,6
PS78/284-1	22.09.11	01:23	MOR	in the water	78° 29.47' N	125° 49.29' E	2759,9
PS78/284-1	22.09.11	01:28	MOR	in the water	78° 29.48' N	125° 49.29' E	2759,2
PS78/284-1	22.09.11	01:49	MOR	in the water	78° 29.61' N	125° 48.20' E	2769
PS78/284-1	22.09.11	01:58	MOR	in the water	78° 29.61' N	125° 48.19' E	2768,4
PS78/284-1	22.09.11	02:03	MOR	action	78° 29.62' N	125° 48.18' E	2767,7
PS78/284-1	22.09.11	02:41	MOR	information	78° 29.36' N	125° 48.99' E	2762,5
PS78/284-1	22.09.11	03:05	MOR	action	78° 29.51' N	125° 49.49' E	2760,7
PS78/284-1	22.09.11	03:05	MOR	on ground/ max depth	78° 29.51' N	125° 49.49' E	2760,7
PS78/284-1	22.09.11	03:25	MOR	action	78° 29.56' N	125° 48.04' E	2758,3
PS78/284-1	22.09.11	03:28	MOR	on deck	78° 29.59' N	125° 47.99' E	2760,8
PS78/284-1	22.09.11	03:40	MOR	hoisting	78° 29.77' N	125° 47.62' E	2779,3
PS78/284-1	22.09.11	03:48	MOR	in the water	78° 29.75' N	125° 47.26' E	2776,9

A.4 Stationsliste / station list PS 78

Station	Date	Time	Gear	Action	Position Lat	Position Lon	Water Depth [m]
PS78/284-1	22.09.11	03:57	MOR	at surface	78° 29.79' N	125° 46.80' E	2779,4
PS78/284-1	22.09.11	03:59	MOR	on deck	78° 29.80' N	125° 46.68' E	2780
PS78/284-1	22.09.11	04:07	MOR	action	78° 29.73' N	125° 46.43' E	2776,9
PS78/284-1	22.09.11	04:08	MOR	on deck	78° 29.73' N	125° 46.41' E	2774,4
PS78/284-1	22.09.11	04:46	MOR	on deck	78° 29.46' N	125° 45.71' E	2764,6
PS78/284-1	22.09.11	05:19	MOR	on deck	78° 29.50' N	125° 45.16' E	2765,6
PS78/285-1	22.09.11	06:27	MOR	information	78° 25.54' N	125° 27.76' E	2591,8
PS78/285-1	22.09.11	06:27	MOR	on ground/ max depth	78° 25.54' N	125° 27.76' E	2591,8
PS78/285-1	22.09.11	07:09	MOR	action	78° 25.48' N	125° 28.56' E	2617,6
PS78/285-1	22.09.11	07:10	MOR	in the water	78° 25.48' N	125° 28.71' E	2623,5
PS78/285-1	22.09.11	07:29	MOR	in the water	78° 25.53' N	125° 28.47' E	2637,7
PS78/285-1	22.09.11	07:39	MOR	in the water	78° 25.62' N	125° 28.15' E	2610,2
PS78/285-1	22.09.11	07:50	MOR	in the water	78° 25.69' N	125° 27.92' E	2606,3
PS78/285-1	22.09.11	08:56	MOR	action	78° 25.70' N	125° 29.37' E	2676
PS78/285-1	22.09.11	08:59	MOR	on deck	78° 25.68' N	125° 29.48' E	2682
PS78/285-1	22.09.11	09:02	MOR	hoisting	78° 25.63' N	125° 29.57' E	2684
PS78/285-1	22.09.11	09:06	MOR	action	78° 25.55' N	125° 29.44' E	2666,5
PS78/285-1	22.09.11	09:13	MOR	hoisting	78° 25.55' N	125° 28.91' E	0
PS78/285-1	22.09.11	09:21	MOR	information	78° 25.56' N	125° 28.49' E	0
PS78/285-1	22.09.11	09:41	MOR	on deck	78° 25.51' N	125° 27.98' E	2595
PS78/285-1	22.09.11	09:45	MOR	at surface	78° 25.49' N	125° 27.78' E	0
PS78/285-1	22.09.11	09:56	MOR	on deck	78° 25.44' N	125° 27.27' E	0
PS78/285-1	22.09.11	10:20	MOR	on deck	78° 25.30' N	125° 26.23' E	0
PS78/285-1	22.09.11	10:39	MOR	on deck	78° 25.12' N	125° 25.56' E	0
PS78/285-1	22.09.11	10:53	MOR	in the water	78° 25.00' N	125° 25.01' E	0
PS78/285-1	22.09.11	10:56	MOR	information	78° 24.96' N	125° 24.86' E	2467,4
PS78/285-1	22.09.11	10:56	MOR	on deck	78° 24.96' N	125° 24.86' E	2467,4
PS78/285-1	22.09.11	11:21	MOR	on deck	78° 24.74' N	125° 23.85' E	2466,4
PS78/285-1	22.09.11	11:29	MOR	on deck	78° 24.64' N	125° 23.35' E	2470,2
PS78/285-1	22.09.11	11:32	MOR	on deck	78° 24.60' N	125° 23.22' E	0
PS78/285-2	22.09.11	13:05	CTD/RO	in the water	78° 29.61' N	125° 48.47' E	2767,1
PS78/285-2	22.09.11	13:14	CTD/RO	on ground/ max depth	78° 29.59' N	125° 48.13' E	2763,7
PS78/285-2	22.09.11	13:16	CTD/RO	hoisting	78° 29.59' N	125° 48.06' E	2762
PS78/285-2	22.09.11	13:27	CTD/RO	on deck	78° 29.60' N	125° 47.54' E	2766,2
PS78/285-3	22.09.11	13:37	MUWS	in the water	78° 29.60' N	125° 47.16' E	2761,8
PS78/285-3	22.09.11	13:39	MUWS	on ground/ max depth	78° 29.61' N	125° 47.05' E	2764,3
PS78/285-3	22.09.11	13:39	MUWS	profile start	78° 29.61' N	125° 47.05' E	2764,3
PS78/285-3	22.09.11	13:41	MUWS	hoisting	78° 29.61' N	125° 47.00' E	2763,5
PS78/285-3	22.09.11	13:41	MUWS	profile end	78° 29.61' N	125° 47.00' E	2763,5

A.4 Stationsliste / station list PS 78

Station	Date	Time	Gear	Action	Position Lat	Position Lon	Water Depth [m]
PS78/285-3	22.09.11	13:46	MUWS	on deck	78° 29.61' N	125° 46.78' E	2767,9
PS78/285-4	22.09.11	14:03	CTD/RO	in the water	78° 29.68' N	125° 46.13' E	2771,8
PS78/285-5	22.09.11	14:09	GF PUMPE	in the water	78° 29.67' N	125° 46.02' E	2776,6
PS78/285-5	22.09.11	14:10	GF PUMPE	profile start	78° 29.67' N	125° 45.99' E	2772,3
PS78/285-5	22.09.11	14:21	GF PUMPE	profile end	78° 29.67' N	125° 45.63' E	2772,5
PS78/285-5	22.09.11	14:22	GF PUMPE	on deck	78° 29.67' N	125° 45.59' E	2775,3
PS78/285-4	22.09.11	15:00	CTD/RO	on ground/ max depth	78° 29.65' N	125° 44.81' E	2774,4
PS78/285-4	22.09.11	15:02	CTD/RO	hoisting	78° 29.65' N	125° 44.74' E	2774,7
PS78/285-4	22.09.11	15:57	CTD/RO	on deck	78° 29.80' N	125° 43.94' E	2789,1
PS78/285-6	22.09.11	16:06	MUC	in the water	78° 29.84' N	125° 43.90' E	2794,5
PS78/285-6	22.09.11	16:44	MUC	on ground/ max depth	78° 29.97' N	125° 42.94' E	2805,3
PS78/285-6	22.09.11	16:44	MUC	hoisting	78° 29.97' N	125° 42.94' E	2805,3
PS78/285-6	22.09.11	17:16	MUC	at surface	78° 30.11' N	125° 42.76' E	2804,7
PS78/285-6	22.09.11	17:19	MUC	on deck	78° 30.11' N	125° 42.79' E	2806,8
PS78/285-7	22.09.11	18:53	XCTD	in the water	78° 16.05' N	126° 10.45' E	2613,8
PS78/285-7	22.09.11	18:58	XCTD	on ground/ max depth	78° 15.14' N	126° 12.17' E	2592,3
PS78/286-1	22.09.11	19:49	CTD/RO	in the water	78° 6.48' N	126° 26.69' E	2406,9
PS78/286-1	22.09.11	20:41	CTD/RO	on ground/ max depth	78° 6.52' N	126° 26.10' E	2408,3
PS78/286-1	22.09.11	20:41	CTD/RO	hoisting	78° 6.52' N	126° 26.10' E	2408,3
PS78/286-1	22.09.11	21:20	CTD/RO	on deck	78° 6.55' N	126° 25.27' E	2415,8
PS78/286-2	22.09.11	22:16	XCTD	in the water	77° 58.80' N	126° 40.17' E	2187,6
PS78/286-2	22.09.11	22:23	XCTD	on ground/ max depth	77° 57.53' N	126° 42.43' E	2188,6
PS78/287-1	22.09.11	23:10	CTD/RO	in the water	77° 50.86' N	126° 55.98' E	2045,1
PS78/287-1	22.09.11	23:54	CTD/RO	on ground/ max depth	77° 51.07' N	126° 55.09' E	2055,3
PS78/287-1	22.09.11	23:56	CTD/RO	hoisting	77° 51.08' N	126° 55.05' E	2054,7
PS78/287-1	23.09.11	00:29	CTD/RO	on deck	77° 51.12' N	126° 54.06' E	2058,9
PS78/287-2	23.09.11	01:15	XCTD	in the water	77° 43.78' N	127° 7.22' E	1929,4
PS78/287-2	23.09.11	01:20	XCTD	on ground/ max depth	77° 42.76' N	127° 9.03' E	1888,8
PS78/288-1	23.09.11	01:47	CTD/RO	in the water	77° 38.44' N	127° 17.39' E	1602,3
PS78/288-1	23.09.11	02:22	CTD/RO	on ground/ max depth	77° 38.46' N	127° 17.37' E	1605,6
PS78/288-1	23.09.11	02:22	CTD/RO	hoisting	77° 38.46' N	127° 17.37' E	1605,6
PS78/288-1	23.09.11	02:47	CTD/RO	at surface	77° 38.48' N	127° 17.46' E	1604,3
PS78/288-1	23.09.11	02:48	CTD/RO	on deck	77° 38.48' N	127° 17.46' E	1607
PS78/288-2	23.09.11	03:24	XCTD	in the water	77° 32.77' N	127° 28.33' E	1215,9
PS78/288-2	23.09.11	03:29	XCTD	on ground/ max depth	77° 32.35' N	127° 29.03' E	1156,7
PS78/288-2	23.09.11	03:30	XCTD	on deck	77° 32.27' N	127° 29.17' E	1152,3

A.4 Stationsliste / station list PS 78

Station	Date	Time	Gear	Action	Position Lat	Position Lon	Water Depth [m]
PS78/289-1	23.09.11	04:05	CTD/RO	in the water	77° 27.38' N	127° 36.25' E	972,8
PS78/289-1	23.09.11	04:29	CTD/RO	on ground/ max depth	77° 27.39' N	127° 36.57' E	962,3
PS78/289-1	23.09.11	04:29	CTD/RO	action	77° 27.39' N	127° 36.57' E	962,3
PS78/289-1	23.09.11	04:47	CTD/RO	at surface	77° 27.43' N	127° 36.94' E	959,2
PS78/289-1	23.09.11	04:49	CTD/RO	on deck	77° 27.43' N	127° 36.97' E	959,7
PS78/289-2	23.09.11	06:01	XCTD	in the water	77° 14.82' N	127° 56.87' E	100,2
PS78/289-2	23.09.11	06:02	XCTD	on ground/ max depth	77° 14.62' N	127° 57.20' E	97,8
PS78/290-1	23.09.11	06:46	CTD/RO	in the water	77° 7.63' N	128° 9.11' E	83,9
PS78/290-1	23.09.11	06:51	CTD/RO	on ground/ max depth	77° 7.59' N	128° 9.41' E	83,8
PS78/290-1	23.09.11	06:52	CTD/RO	hoisting	77° 7.58' N	128° 9.49' E	82,9
PS78/290-1	23.09.11	06:56	CTD/RO	on deck	77° 7.57' N	128° 9.73' E	84,2
PS78/290-2	23.09.11	07:05	RAMSES	in the water	77° 7.52' N	128° 10.35' E	84
PS78/290-2	23.09.11	07:30	RAMSES	on ground/ max depth	77° 7.42' N	128° 11.56' E	82,8
PS78/290-2	23.09.11	07:32	RAMSES	hoisting	77° 7.41' N	128° 11.53' E	83,5
PS78/290-2	23.09.11	07:35	RAMSES	on deck	77° 7.39' N	128° 11.47' E	83,3
PS78/291-1	23.09.11	23:18	CTD/RO	in the water	76° 10.65' N	115° 30.34' E	32,2
PS78/291-1	23.09.11	23:21	CTD/RO	on ground/ max depth	76° 10.62' N	115° 30.34' E	32,1
PS78/291-1	23.09.11	23:22	CTD/RO	hoisting	76° 10.60' N	115° 30.34' E	32
PS78/291-1	23.09.11	23:27	CTD/RO	on deck	76° 10.52' N	115° 30.28' E	31,6
PS78/291-2	23.09.11	23:33	BONGO	in the water	76° 10.46' N	115° 30.23' E	32,3
PS78/291-2	23.09.11	23:36	BONGO	on ground/ max depth	76° 10.44' N	115° 30.26' E	32,1
PS78/291-2	23.09.11	23:39	BONGO	action	76° 10.42' N	115° 30.23' E	32,1
PS78/291-2	23.09.11	23:39	BONGO	hoisting	76° 10.42' N	115° 30.23' E	32,1
PS78/291-2	23.09.11	23:42	BONGO	at surface	76° 10.45' N	115° 30.16' E	32,2
PS78/291-2	23.09.11	23:43	BONGO	on deck	76° 10.45' N	115° 30.15' E	32,1
PS78/292-1	24.09.11	01:01	CTD/RO	in the water	76° 20.66' N	116° 4.66' E	40,5
PS78/292-1	24.09.11	01:05	CTD/RO	on ground/ max depth	76° 20.65' N	116° 4.57' E	40,4
PS78/292-1	24.09.11	01:05	CTD/RO	hoisting	76° 20.65' N	116° 4.57' E	40,4
PS78/292-1	24.09.11	01:07	CTD/RO	at surface	76° 20.65' N	116° 4.53' E	40,4
PS78/292-1	24.09.11	01:08	CTD/RO	on deck	76° 20.65' N	116° 4.51' E	40,6
PS78/293-1	24.09.11	02:32	CTD/RO	in the water	76° 34.04' N	116° 38.60' E	2,6
PS78/293-1	24.09.11	02:36	CTD/RO	on ground/ max depth	76° 34.02' N	116° 38.57' E	42,8
PS78/293-1	24.09.11	02:37	CTD/RO	at surface	76° 34.02' N	116° 38.56' E	43,3
PS78/293-1	24.09.11	02:38	CTD/RO	on deck	76° 34.01' N	116° 38.54' E	43,6
PS78/294-1	24.09.11	04:36	CTD/RO	in the water	76° 50.94' N	117° 35.56' E	39,3
PS78/294-1	24.09.11	04:41	CTD/RO	on ground/ max depth	76° 50.92' N	117° 35.57' E	38,3

A.4 Stationsliste / station list PS 78

Station	Date	Time	Gear	Action	Position Lat	Position Lon	Water Depth [m]
PS78/294-1	24.09.11	04:41	CTD/RO	hoisting	76° 50.92' N	117° 35.57' E	38,3
PS78/294-1	24.09.11	04:42	CTD/RO	at surface	76° 50.92' N	117° 35.58' E	38,3
PS78/294-1	24.09.11	04:43	CTD/RO	on deck	76° 50.91' N	117° 35.59' E	38,2
PS78/295-1	24.09.11	06:26	CTD/RO	in the water	77° 7.93' N	118° 22.93' E	64,2
PS78/295-1	24.09.11	06:32	CTD/RO	on ground/ max depth	77° 7.95' N	118° 22.96' E	64,3
PS78/295-1	24.09.11	06:32	CTD/RO	hoisting	77° 7.95' N	118° 22.96' E	64,3
PS78/295-1	24.09.11	06:37	CTD/RO	on deck	77° 7.97' N	118° 22.97' E	64,3
PS78/295-2	24.09.11	06:44	RAMSES	in the water	77° 8.00' N	118° 23.04' E	65
PS78/295-2	24.09.11	07:04	RAMSES	on ground/ max depth	77° 8.05' N	118° 23.15' E	65,6
PS78/295-2	24.09.11	07:04	RAMSES	hoisting	77° 8.05' N	118° 23.15' E	65,6
PS78/295-2	24.09.11	07:09	RAMSES	on deck	77° 8.06' N	118° 23.20' E	65,6
PS78/295-3	24.09.11	07:48	XCTD	in the water	77° 14.43' N	118° 41.82' E	178
PS78/295-3	24.09.11	07:51	XCTD	on ground/ max depth	77° 14.97' N	118° 43.45' E	195
PS78/296-1	24.09.11	08:12	CTD/RO	in the water	77° 17.52' N	118° 50.35' E	296
PS78/296-1	24.09.11	08:25	CTD/RO	on ground/ max depth	77° 17.54' N	118° 50.35' E	297
PS78/296-1	24.09.11	08:25	CTD/RO	hoisting	77° 17.54' N	118° 50.35' E	297
PS78/296-1	24.09.11	08:34	CTD/RO	on deck	77° 17.55' N	118° 50.40' E	298
PS78/296-2	24.09.11	09:22	XCTD	in the water	77° 24.84' N	119° 14.80' E	763,4
PS78/296-2	24.09.11	09:25	XCTD	on ground/ max depth	77° 25.33' N	119° 16.58' E	789,4
PS78/297-1	24.09.11	10:00	CTD/RO	in the water	77° 29.64' N	119° 31.19' E	1001,8
PS78/297-1	24.09.11	10:21	CTD/RO	on ground/ max depth	77° 29.60' N	119° 31.22' E	1000,7
PS78/297-1	24.09.11	10:22	CTD/RO	hoisting	77° 29.59' N	119° 31.21' E	998,1
PS78/297-1	24.09.11	10:42	CTD/RO	on deck	77° 29.52' N	119° 31.11' E	994,7
PS78/297-2	24.09.11	11:33	XCTD	in the water	77° 36.82' N	119° 57.49' E	1276,6
PS78/297-2	24.09.11	11:39	XCTD	on ground/ max depth	77° 37.75' N	120° 0.97' E	1316,5
PS78/297-3	24.09.11	12:24	XCTD	in the water	77° 45.37' N	120° 26.43' E	1594,2
PS78/297-3	24.09.11	12:30	XCTD	on ground/ max depth	77° 46.34' N	120° 29.71' E	1629,2
PS78/298-1	24.09.11	13:12	CTD/RO	in the water	77° 51.83' N	120° 49.61' E	1800,2
PS78/298-1	24.09.11	13:53	CTD/RO	on ground/ max depth	77° 51.79' N	120° 50.09' E	1797,5
PS78/298-1	24.09.11	13:54	CTD/RO	hoisting	77° 51.78' N	120° 50.10' E	1797,8
PS78/298-1	24.09.11	14:25	CTD/RO	at surface	77° 51.79' N	120° 50.28' E	1795,9
PS78/298-1	24.09.11	14:26	CTD/RO	on deck	77° 51.79' N	120° 50.28' E	1798,9
PS78/299-1	25.09.11	01:19	CTD/RO	in the water	79° 40.20' N	114° 57.33' E	3108
PS78/299-1	25.09.11	02:25	CTD/RO	on ground/ max depth	79° 40.28' N	114° 57.45' E	3111,1
PS78/299-1	25.09.11	02:26	CTD/RO	hoisting	79° 40.28' N	114° 57.45' E	3109,1

A.4 Stationsliste / station list PS 78

Station	Date	Time	Gear	Action	Position Lat	Position Lon	Water Depth [m]
PS78/299-1	25.09.11	03:17	CTD/RO	at surface	79° 40.35' N	114° 57.86' E	3106,6
PS78/299-1	25.09.11	03:18	CTD/RO	on deck	79° 40.35' N	114° 57.87' E	3105
PS78/299-2	25.09.11	04:23	XCTD	in the water	79° 33.13' N	114° 19.55' E	3049,7
PS78/299-2	25.09.11	04:29	XCTD	on ground/ max depth	79° 32.65' N	114° 17.05' E	3046,7
PS78/299-2	25.09.11	04:29	XCTD	on deck	79° 32.65' N	114° 17.05' E	3046,7
PS78/300-1	25.09.11	05:26	CTD/RO	in the water	79° 25.47' N	113° 39.67' E	2985,1
PS78/300-2	25.09.11	06:11	RAMSES	in the water	79° 25.34' N	113° 39.14' E	2983,7
PS78/300-1	25.09.11	06:30	CTD/RO	on ground/ max depth	79° 25.24' N	113° 39.01' E	2984,9
PS78/300-1	25.09.11	06:30	CTD/RO	hoisting	79° 25.24' N	113° 39.01' E	2984,9
PS78/300-2	25.09.11	06:45	RAMSES	on ground/ max depth	79° 25.17' N	113° 38.88' E	2979,7
PS78/300-2	25.09.11	06:45	RAMSES	hoisting	79° 25.17' N	113° 38.88' E	2979,7
PS78/300-2	25.09.11	06:49	RAMSES	on deck	79° 25.15' N	113° 38.85' E	2981,3
PS78/300-1	25.09.11	07:28	CTD/RO	on deck	79° 24.96' N	113° 38.35' E	2978,1
PS78/300-3	25.09.11	08:46	XCTD	in the water	79° 17.02' N	112° 56.21' E	2861,5
PS78/300-3	25.09.11	08:50	XCTD	on ground/ max depth	79° 16.46' N	112° 52.93' E	2846,7
PS78/301-1	25.09.11	09:36	CTD/RO	in the water	79° 10.35' N	112° 18.82' E	2571,7
PS78/301-1	25.09.11	10:32	CTD/RO	on ground/ max depth	79° 10.21' N	112° 16.89' E	2557,1
PS78/301-1	25.09.11	10:33	CTD/RO	hoisting	79° 10.20' N	112° 16.86' E	2554
PS78/301-1	25.09.11	11:16	CTD/RO	on deck	79° 10.17' N	112° 15.32' E	2544,5
PS78/301-2	25.09.11	12:15	XCTD	in the water	79° 2.79' N	111° 37.35' E	1856,9
PS78/301-2	25.09.11	12:21	XCTD	on ground/ max depth	79° 1.86' N	111° 33.01' E	1750,2
PS78/302-1	25.09.11	13:11	CTD/RO	in the water	78° 55.04' N	111° 0.78' E	812,9
PS78/302-1	25.09.11	13:35	CTD/RO	on ground/ max depth	78° 55.03' N	111° 0.77' E	810,4
PS78/302-1	25.09.11	13:36	CTD/RO	hoisting	78° 55.03' N	111° 0.76' E	809,9
PS78/302-1	25.09.11	13:51	CTD/RO	on deck	78° 55.02' N	111° 0.77' E	808,9
PS78/302-2	25.09.11	14:19	XCTD	in the water	78° 52.92' N	110° 48.57' E	445,3
PS78/302-2	25.09.11	14:21	XCTD	on ground/ max depth	78° 52.77' N	110° 47.72' E	440,1
PS78/302-2	25.09.11	14:22	XCTD	on deck	78° 52.69' N	110° 47.27' E	434,9
PS78/302-3	25.09.11	14:53	XCTD	in the water	78° 48.55' N	110° 24.08' E	290,2
PS78/302-3	25.09.11	14:55	XCTD	on ground/ max depth	78° 48.28' N	110° 22.54' E	275,6
PS78/302-3	25.09.11	14:55	XCTD	on deck	78° 48.28' N	110° 22.54' E	275,6
PS78/303-1	25.09.11	16:05	CTD/RO	in the water	78° 39.51' N	109° 34.18' E	137,8
PS78/303-1	25.09.11	16:14	CTD/RO	on ground/ max depth	78° 39.57' N	109° 34.36' E	134,7
PS78/303-1	25.09.11	16:16	CTD/RO	on deck	78° 39.58' N	109° 34.42' E	133,6
PS78/304-1	25.09.11	18:07	CTD/RO	in the water	78° 22.25' N	110° 17.03' E	62

A.4 Stationsliste / station list PS 78

Station	Date	Time	Gear	Action	Position Lat	Position Lon	Water Depth [m]
PS78/304-1	25.09.11	18:11	CTD/RO	on ground/ max depth	78° 22.28' N	110° 17.00' E	61,7
PS78/304-1	25.09.11	18:12	CTD/RO	hoisting	78° 22.28' N	110° 16.99' E	61,9
PS78/304-1	25.09.11	18:15	CTD/RO	on deck	78° 22.28' N	110° 17.06' E	61,8
PS78/305-1	25.09.11	20:00	CTD/RO	in the water	78° 4.62' N	110° 59.09' E	310,2
PS78/305-1	25.09.11	20:17	CTD/RO	on ground/ max depth	78° 4.70' N	110° 59.13' E	310,6
PS78/305-1	25.09.11	20:18	CTD/RO	hoisting	78° 4.69' N	110° 59.13' E	310,5
PS78/305-1	25.09.11	20:24	CTD/RO	on deck	78° 4.64' N	110° 59.07' E	310,5
PS78/306-1	25.09.11	22:09	CTD	in the water	77° 47.01' N	111° 38.95' E	278,1
PS78/306-1	25.09.11	22:23	CTD	on ground/ max depth	77° 46.89' N	111° 39.73' E	275,4
PS78/306-1	25.09.11	22:24	CTD	hoisting	77° 46.88' N	111° 39.80' E	277,9
PS78/306-1	25.09.11	22:33	CTD	on deck	77° 46.88' N	111° 40.09' E	278
PS78/307-1	26.09.11	00:10	CTD/RO	in the water	77° 29.53' N	112° 15.70' E	59,8
PS78/307-1	26.09.11	00:16	CTD/RO	on ground/ max depth	77° 29.40' N	112° 15.83' E	59,8
PS78/307-1	26.09.11	00:17	CTD/RO	hoisting	77° 29.39' N	112° 15.87' E	59,3
PS78/307-1	26.09.11	00:20	CTD/RO	on deck	77° 29.37' N	112° 15.94' E	61,6
PS78/308-1	26.09.11	02:06	CTD/RO	in the water	77° 11.76' N	112° 51.68' E	54,3
PS78/308-1	26.09.11	02:11	CTD/RO	on ground/ max depth	77° 11.73' N	112° 51.61' E	53,8
PS78/308-1	26.09.11	02:12	CTD/RO	hoisting	77° 11.72' N	112° 51.58' E	54,1
PS78/308-1	26.09.11	02:16	CTD/RO	at surface	77° 11.70' N	112° 51.45' E	54,5
PS78/308-1	26.09.11	02:18	CTD/RO	on deck	77° 11.69' N	112° 51.40' E	54
PS78/308-2	26.09.11	02:28	BONGO	in the water	77° 11.71' N	112° 51.20' E	54,2
PS78/308-2	26.09.11	02:33	BONGO	on ground/ max depth	77° 11.70' N	112° 50.88' E	54,2
PS78/308-2	26.09.11	02:33	BONGO	hoisting	77° 11.70' N	112° 50.88' E	54,2
PS78/308-2	26.09.11	02:37	BONGO	at surface	77° 11.69' N	112° 50.66' E	53,8
PS78/308-2	26.09.11	02:38	BONGO	on deck	77° 11.69' N	112° 50.61' E	53,6
PS78/309-1	01.10.11	11:17	FLOAT	in the water	70° 0.11' N	14° 7.44' E	2564,9
PS78/309-1	01.10.11	11,17	FLOAT	on ground/ max depth	70° 0.11' N	14° 7.44' E	2564,9
PS78/310-1	01.10.11	13:54	FLOAT	in the water	69° 50.09' N	13° 27.06' E	2699,2
PS78/310-1	01.10.11	13:54	FLOAT	on ground/ max depth	69° 50.09' N	13° 27.06' E	2699,2
PS78/311-1	01.10.11	15:17	FLOAT	in the water	69° 43.11' N	12° 53.79' E	2779,1
PS78/311-1	01.10.11	15:17	FLOAT	on ground/ max depth	69° 43.11' N	12° 53.79' E	2779,1

Gear Abbreviations:

CTD/RO	Conductivity/Temperature/Depth System and Rosette Water Sampler
MN	Multinet
Bongo	Bong
Cal	Calibration
RAMSES	RAMSES-Spectrometer
MOR	Mooring deployment/recovery
ROV	Remote Operating Vehicle
ICE	Ice station
MUWS	Multiple Water Sampler
MUC	Multicorer
GF PUMP	Grundfoss Pump
XCTD	expendable CTD
GC	Gravity Corer
BC	Box Corer

Die "**Berichte zur Polar- und Meeresforschung**" (ISSN 1866-3192) werden beginnend mit dem Heft Nr. 569 (2008) als Open-Access-Publikation herausgegeben. Ein Verzeichnis aller Hefte einschließlich der Druckausgaben (Heft 377-568) sowie der früheren "**Berichte zur Polarforschung**" (Heft 1-376, von 1981 bis 2000) befindet sich im open access institutional repository for publications and presentations (**ePIC**) des AWI unter der URL <http://epic.awi.de>. Durch Auswahl "Reports on Polar- and Marine Research" (via "browse"/"type") wird eine Liste der Publikationen sortiert nach Heftnummer innerhalb der absteigenden chronologischen Reihenfolge der Jahrgänge erzeugt.

To generate a list of all Reports past issues, use the following URL: <http://epic.awi.de> and select "browse"/"type" to browse "Reports on Polar and Marine Research". A chronological list in declining order, issues chronological, will be produced, and pdf-icons shown for open access download.

Verzeichnis der zuletzt erschienenen Hefte:

Heft-Nr. 638/2011 — "Long-term evolution of (millennial-scale) climate variability in the North Atlantic over the last four million years - Results from Integrated Ocean Drilling Project Site U1313", by Bernhard David Adriaan Naafs

Heft-Nr. 639/2011 — "The Expedition of the Research Vessel 'Polarstern' to the Antarctic in 2011 (ANT-XXVII/4)", edited by Saad El Nagger

Heft-Nr. 640/2012 — "ARCTIC MARINE BIOLOGY - A workshop celebrating two decades of cooperation between Murmansk Marine Biological Institute and Alfred Wegener Institute for Polar and Marine Research", edited by Gotthilf Hempel, Karin Lochte, Gennady Matishov

Heft-Nr. 641/2012 — "The Expedition of the Research Vessel 'Maria S. Merian' to the South Atlantic in 2011 (MSM 19/2)", edited by Gabriele Uenzelmann-Neben

Heft-Nr. 642/2012 — "Russian-German Cooperation SYSTEM LAPTEV SEA: The Expedition LENA 2008", edited by Dirk Wagner, Paul Overduin, Mikhail N. Grigoriev, Christian Knoblauch, and Dimitry Yu. Bolshiyarov

Heft-Nr. 643/2012 — "The Expedition of the Research Vessel 'Sonne' to the subpolar North Pacific and the Bering Sea in 2009 (SO202-INOPEX)", edited by Rainer Gersonde

Heft-Nr. 644/2012 — "The Expedition of the Research Vessel 'Polarstern' to the Antarctic in 2011 (ANT-XXVII/3)", edited by Rainer Knust, Dieter Gerdes and Katja Mintenbeck

Heft-Nr. 645/2012 — "The Expedition of the Research Vessel 'Polarstern' to the Arctic in 2011 (ARK-XXVI/2)", edited by Michael Klages

Heft-Nr. 646/2012 — "The Expedition of the Research Vessel 'Polarstern' to the Antarctic in 2011/12 (ANT-XXVIII/2)", edited by Gerhard Kattner

Heft-Nr. 647/2012 — "The Expedition of the Research Vessel 'Polarstern' to the Arctic in 2011 (ARK-XXVI/1)", edited by Agnieszka Beszczynska-Möller

Heft-Nr. 648/2012 — "Interannual and decadal variability of sea ice drift, concentration and thickness in the Weddell Sea", by Sandra Schwegmann

Heft-Nr. 649/2012 — "The Expedition of the Research Vessel 'Polarstern' to the Arctic in 2011 (ARK-XXVI/3 - TransArc)", edited by Ursula Schauer